



UNIVERSITAT DE BARCELONA



UNIVERSITAT DE BARCELONA
FACULTAT DE QUÍMICA
DEPARTAMENT D'ENGINYERIA QUÍMICA

***OPERATION AND MODEL DESCRIPTION OF ADVANCED
BIOLOGICAL NITROGEN REMOVAL TREATMENTS OF
HIGHLY AMMONIUM LOADED WASTEWATERS***

Doctoral Thesis directed by Joan Mata Álvarez

Joan Dosta Parras

Barcelona, Juliol 2007

Programa de doctorat d'Enginyeria del Medi Ambient i del Producte

Bienni 2003-2005



UNIVERSITAT DE BARCELONA



El Dr. **JOAN MATA ÁLVAREZ**, Catedràtic del Departament d'Enginyeria Química de la Universitat de Barcelona,

CERTIFICA QUE:

el treball d'investigació titulat '*OPERATION AND MODEL DESCRIPTION OF ADVANCED BIOLOGICAL NITROGEN REMOVAL TREATMENTS OF HIGHLY AMMONIUM LOADED WASTEWATERS*' constitueix la memòria que presenta l'Enginyer Químic **JOAN DOSTA PARRAS** per a aspirar al grau de Doctor per la Universitat de Barcelona. Aquesta tesi doctoral ha estat realitzada dins del programa de Doctorat "Enginyeria del Medi Ambient i del Producte", bienni 2003-2005, en el Departament d'Enginyeria Química de la Universitat de Barcelona.

I perquè així consti als efectes oportuns, signa el present certificat a Barcelona, en 5 de Juliol de 2007.

Dr. Joan Mata Álvarez
Director de la tesi doctoral

No podemos ocuparnos de todo. Reconocer nuestra limitación, aceptarla humildemente y hacer lo que podemos es una prueba de sabiduría.

José-Román Flecha Andrés

Moral de los refranes

Acknowledgements.

Molta gent ha col·laborat en aquest treball aportant els seus consells i idees, de manera que voldria expressar la meua gratitud envers ells en aquest punt.

En primer lloc, voldria agrair al Dr. Joan Mata, director d'aquest treball, l'oportunitat de prendre part del seu grup d'investigació per realitzar la tesi doctoral, així com els seus consells, recolzament i 'bon rotllo' durant el transcurs d'aquests anys.

M'agradaria també expressar el meu agraïment als professors del Departament d'Enginyeria Química de la Universitat de Barcelona, molt especialment al Dr. Ricard Torres, per la seva ajuda durant el decurs del doctorat, i al Dr. Joan Llorens i el Dr. David Curcó per orientar-me en el desenvolupament dels sistemes d'adquisició de dades dels dispositius experimentals emprats en aquest treball i la realització del programa de simulació.

Als companys del laboratori de Barcelona: Meritxell Minoves, Joan Rovira, Àlex Galí, Toufik Benabdallah El-Hadj, Sílvia López, Ramón Márquez, Sandra Macé, Pilar "Moy", Anna May, Sergi Astals i Ivan Lago pels vostres consells i suport. Tanmateix, a en Jordi Bonet, en Jordi Labanda, l'Andrea Guastali, la Pilar Marco, la Isabel Solè i la Marta Granollers pel vostre recolzament des del primer moment.



Amb el Dr. Joan Mata i els companys al laboratori de biotecnologia de la UB (Abril 2005)



Amb els companys del laboratori de biotecnologia de la UB (Juny 2005)



Amb l'Àlex Galí, l'Albert Magrí, l'Helio López i en Lluís Corominas a un congrés de Cracòvia. (Octubre 2005)

A la Dra. Aurora Seco i el Dr. José Ferrer, per l'oportunitat de fer una breu estada dins el seu grup d'investigació per aprendre aspectes de modelització de processos biològics i la utilització del programa DESASS. També voldria expressar la meua gratitud als altres doctors i doctorands de les universitats UV i UPV, especialment a en Josep Ribes, l'Alberto Bouzas i la Núria Martí, pels seus consells i el 'tour' pel casc antic de València.

A l'Albert Magrí i els altres companys del GIRO CT i la Universitat de Lleida i de Girona, per les útils converses sobre els nostres treballs d'investigació.

Finalmente, quixera agradecer aos doutores Ramón Méndez Pampín, Juan Lema, Anuska Mosquera e José Luis Campos a oportunidade de facer unha estancia dentro do seu grupo de biotecnología da Universidade de Santiago de Compostela. Grazas a todos: Rosiña, Isaac, Rosa Torres, Pastora, José Antonio, Rubén, Núria Montes, Jose, Mónica Figueroa, Sonia, Carmen, Álex, Rocío, Marisol, Beata, Sara, Mar, Miriam, Mónica, etc ... Con vós non só se aprende biotecnología, senón tamén a ser mellor persoa!!

Ja en el terreny personal, voldria agrair als meus pares, al meu germà Sergi i als amics "de sempre" (Georgina, Joan Ferré, Raquel, David, Fernando, Carol, Anna, Pili, Enric, Mercè, Rosa Ferràs, Carmen, Núria i Vane) el seu suport incondicional.



Amb els companys de la Universitat de València en la falla de l'Ajuntament durant les jornades tècniques META. (Febrer 2006)



Amb els companys de la Universitat de Santiago de Compostela. (Desembre 2006)



Amb els companys de la Universitat de Barcelona. (Abril 2007)

Table of Contents

SUMMARY.....	i
1 – INTRODUCTION.....	1
1.1 NITROGEN POLLUTION IN WASTEWATERS.....	3
1.2 NITROGEN ELIMINATION FROM WASTEWATERS.....	3
1.3 BIOLOGICAL NITROGEN REMOVAL.....	8
1.3.1 The nitrogen cycle.....	8
1.3.2 Biological nitrogen removal processes.....	9
1.3.2.1 Nitrification.....	10
1.3.2.1 Denitrification.....	18
1.3.2.2.1 Heterotrophic denitrification.....	18
1.3.2.2.1 Anammox.....	22
1.4 MODELLING OF BIOLOGICAL NITROGEN REMOVAL.....	27
1.4.1 IWA Activated Sludge Models.....	28
1.4.2 Stoichiometry and kinetics in Activated Sludge Models.....	28
1.4.3 Format and notation.....	30
1.4.4 Carbon and nitrogen components considered in Activated Sludge Models.....	33
1.4.5 Biological carbon and nitrogen removal processes considered in ASM2d.....	35
1.5 CASE STUDIES.....	41
1.5.1 Supernatant from AD of sewage sludge (sludge reject water).....	41
1.5.2 Supernatant from AD of the OFMSW.....	45
1.5.1 Supernatant from AD of piggery wastewater.....	48
1.6 BIOLOGICAL SYSTEMS TO TREAT HIGHLY AMMONIUM LOADED WASTEWATERS.....	51
1.6.1 SBR treatment.....	52
1.6.2 SHARON process.....	53
1.6.3 Anammox process.....	54
1.6.4 CANON process.....	55
1.6.5 BABE process.....	55

2 – OBJECTIVES AND THESIS STRUCTURE.....	57
2.1 MOTIVATION AND OBJECTIVES.....	59
2.2 THESIS STRUCTURE.....	61
3 – MATERIALS AND METHODS.....	65
3.1 BIOLOGICAL REACTORS.....	67
3.1.1 SBR for biological nitrogen removal over nitrite.....	67
3.1.2 SHARON chemostat reactor.....	68
3.1.3 Anammox SBR.....	69
3.2 CLOSED INTERMITTENT-FLOW RESPIROMETER.....	70
3.3 ANAMMOX ACTIVITY TESTS.....	75
3.4 JAR-TESTS.....	75
3.5 SIMULATION OF BIOLOGICAL PROCESSES.....	76
3.6 SUBSTRATE AND INOCULUM.....	77
3.7 ANALYTICAL METHODS.....	78
3.7.1 Solids content.....	79
3.7.2 Chemical Oxygen Demand (COD) and Biological Oxygen Demand (BOD).....	80
3.7.3 Total Ammonium Nitrogen.....	81
3.7.4 Nitrites, Nitrates and Phosphates.....	82
3.7.5 Volatile Fatty Acids (VFA).....	83
3.7.6 Alkalinity.....	83
3.7.7 Sludge Volumetric Index (SVI).....	84
4 – OPERATION AND MODEL DESCRIPTION OF A SEQUENCING BATCH REACTOR TREATING REJECT WATER FOR BIOLOGICAL NITROGEN REMOVAL OVER NITRITE	85
4.1 INTRODUCTION.....	87
4.2 RESULTS AND DISCUSSION.....	89
4.2.1 Reject water characterisation.....	89
4.2.2 Start-up of the SBR.....	90
4.2.3 Reject water treatment in a SBR.....	91
4.2.4 Four-step nitrogen removal model.....	92
4.2.5 Calibration of the model.....	96
4.2.5.1 Stoichiometric parameters assessment.....	98
4.2.5.2 Kinetic parameters assessment.....	103

4.2.5.3 Influence of pH and temperature.....	118
4.2.6 Simulation of experimental results.....	122
4.3 CONCLUSIONS.....	124
5 – MODELLING OF A SEQUENCING BATCH REACTOR TO TREAT THE SUPERNATANT FROM ANAEROBIC DIGESTION OF THE ORGANIC FRACTION OF MUNICIPAL SOLID WASTE.....	127
5.1 INTRODUCTION.....	128
5.2 RESULTS AND DISCUSSION.....	131
5.2.1 Wastewater characterisation.....	131
5.2.2 Optimum SBR operation.....	132
5.2.3 Activated Sludge Model extended for nitrite route description.....	133
5.2.4 Model calibration.....	140
5.2.5 Modelling of the SBR performance.....	143
5.3 CONCLUSIONS.....	145
6 – COD AND NITROGEN REMOVAL OF SUPERNATANT OF ANAEROBICALLY DIGESTED PIGGERY WASTEWATER IN A BIOLOGICAL SBR WITH A COAGULATION/FLOCCULATION STEP.....	147
6.1 INTRODUCTION.....	149
6.2 RESULTS AND DISCUSSION.....	151
6.2.1 Wastewater characterisation.....	151
6.2.2 Sequencing Batch Reactor operation.....	153
6.2.3 Optimisation study of the Coagulation/Flocculation step.....	157
6.2.4 Introduction of the Coagulation/Flocculation step in the SBR cycle.....	159
6.2.5 Influence of experimental conditions of the SBR on Nitrogen removal.....	162
6.3 CONCLUSIONS.....	169
7 – OPERATION OF THE SHARON-DENITRIFICATION PROCESS TO TREAT SLUDGE REJECT WATER USING HYDROLYSED PRIMARY SLUDGE TO DENITRIFY.....	171
7.1 INTRODUCTION.....	173
7.2 RESULTS AND DISCUSSION.....	175
7.2.1 Reject water composition.....	175
7.2.2 SHARON/Denitrification using methanol to denitrify.....	176
7.2.3 Selection of an internal flow of the WWTP to denitrify.....	179

7.2.4 SHARON/Denitrification using supernatant of hydrolysed primary sludge.....	184
7.3 CONCLUSIONS.....	187
8 – MODELLING OF PARTIAL NITRIFICATION IN A SHARON CHEMOSTAT AND IN A SEQUENCING BATCH REACTOR TO ACHIEVE A SUITED INFLUENT TO THE ANAMMOX PROCESS.....	189
8.1 INTRODUCTION.....	191
8.2 RESULTS AND DISCUSSION.....	192
8.2.1 Extended ASM model.....	192
8.2.2 Reject water characterisation.....	193
8.2.3 Partial nitrification in a SBR.....	194
8.2.4 Partial nitrification in a SHARON process.....	199
8.2.5 Comparison of the partial nitrification in a SBR and in a SHARON chemostat....	202
8.3 CONCLUSIONS.....	204
9 – OPERATION OF AN ANAMMOX REACTOR TO TREAT HIGHLY AMMONIUM LOADED WASTEWATERS AT LOW TEMPERATURES.....	205
9.1 INTRODUCTION.....	207
9.2 RESULTS AND DISCUSSION.....	209
9.2.1 Temperature influence on Anammox activity.....	209
9.2.2 Reactor performance at reduced temperatures.....	213
9.2.3 Biomass properties.....	219
9.3 CONCLUSIONS.....	220
10 – GENERAL CONCLUSIONS AND RECOMMENDATIONS.....	223
10.1 GENERAL CONCLUSIONS.....	223
10.2 RECOMMENDATIONS.....	229
11 – REFERENCES.....	233
12 – NOTATION.....	249
13 – PUBLICATIONS.....	257
14 – RESUM EN CATALÀ.....	259

14.1 INTRODUCCIÓ.....	261
14.1.1 Eliminació biològica de nitrogen.....	262
14.1.2 Nitrificació.....	262
14.1.3 Desnitrificació.....	264
14.1.3.1 Desnitrificació heterotròfica.....	265
14.1.3.2 Anammox.....	266
14.1.4 Modelització de tractaments biològics. Respirometria.....	268
14.1.5 Problemàtica dels sobrenedants de digestió anaeròbica de residus orgànics.....	268
14.1.6 Tractaments d'eliminació biològica de nitrogen en els sobrenedants de digestió anaeròbica.....	269
14.2 JUSTIFICACIÓ I OBJECTIUS.....	271
14.3 MATERIALS I MÈTODES.....	272
14.3.1 Reactors biològics a escala de laboratori.....	272
14.3.2 Respiròmetre tancat seqüencial.....	272
14.3.3 Test d'activitat Anammox.....	274
14.3.4 Jar tests.....	274
14.3.5 Modelització de processos biològics.....	274
14.3.6 Substrat i inòcul.....	275
14.3.7 Mètodes analítics.....	275
14.4 DISCUSSIÓ DE RESULTATS I CONCLUSIONS.....	276
14.4.1 Eliminació biològica de nitrogen via nitrit en un reactor SBR.....	276
14.4.2 Eliminació biològica de nitrogen via nitrit en un reactor SHARON/DN.....	279
14.4.3 Nitrificació parcial en un reactor SBR i en un reactor SHARON.....	280
14.4.4 Eliminació biològica de nitrogen en un reactor Anammox.....	281
14.5 RECOMANACIONS.....	283
14.6 REFERÈNCIES.....	285
14.7 NOMENCLATURA.....	287

List of Tables

TABLES OF CHAPTER 1

Table 1.1 – Characterisation of highly ammonium loaded wastewaters.....	6
Table 1.2 – Industrial Anammox plants.....	26
Table 1.3 – Process kinetics and stoichiometry for aerobic heterotrophic growth.....	31
Table 1.4 – Composition matrix for COD.....	32
Table 1.5 – Composition matrix of the ASM2d.....	35
Table 1.6 – Process rate equations for ASM2d.....	36
Table 1.7 – Petersen Matrix of ASM2d.....	37

TABLES OF CHAPTER 3

Table 3.1 – Relationship between SVI and Activated Sludge settling characteristics.....	84
---	----

TABLES OF CHAPTER 4

Table 4.1 – Average composition of the centrifuged sludge effluent during 2004.....	89
Table 4.2 – Kinetic equations of the considered processes.....	94
Table 4.3 – Petersen Matrix of the proposed Activated Sludge Model.....	95
Table 4.4 – Coefficients used in this study for the application of continuity functions.....	96
Table 4.5 – Average values of model parameters for the case studied.....	97
Table 4.6 – Petersen matrix for the consumption of S_S by heterotrophic biomass.....	100
Table 4.7 – Petersen matrix for the consumption of NH_4^+ -N and NO_2^- -N by autotrophic biomass...	103
Table 4.8 – Petersen matrix for the decay process of heterotrophic biomass.....	104
Table 4.9 – Petersen matrix for the maximum heterotrophic growth rate assessment.....	106
Table 4.10 – Petersen matrix for the correction factor of heterotrophic anoxic growth assessment..	111
Table 4.11 – Petersen matrix for $\mu_{m,AOB}$ assessment.....	112
Table 4.12 – Comparison of the $K_{O,AOB}$ and $K_{O,NOB}$ obtained with other values from literature.....	117
Table 4.13 – Parameters obtained for pH dependency modelling.....	120
Table 4.14 – Temperature dependency parameters obtained for AOB and heterotrophic biomass...	122

TABLES OF CHAPTER 5

Table 5.1 – Average composition of the supernatant tested and other similar wastewaters.....	131
Table 5.2 – Main characteristics of the optimum SBR operating strategy.....	132

Table 5.3 – Composition matrix of the proposed model.....	135
Table 5.4 – Conversion factors for C and N content in biomass and inert matter.....	135
Table 5.5 – Dissociation constants and temperature dependency coefficients considered.....	136
Table 5.6 – Petersen Matrix of the proposed Activated Sludge Model.....	138
Table 5.7 – Kinetic equations of the considered processes.....	139
Table 5.8 – Average values of kinetic and stoichiometric parameters obtained by respirometry.....	141

TABLES OF CHAPTER 6

Table 6.1 – Composition of the piggery reject water tested in this study.....	151
Table 6.2 – Summary of the main parameters obtained in the studied cycles.....	153
Table 6.3 – Main characteristics of the SBR operating strategy.....	155
Table 6.4 – Effluent qualities obtained with and without the Coagulation/Flocculation step.....	160

TABLES OF CHAPTER 7

Table 7.1 – Average composition of the reject water tested in this study.....	176
Table 7.2 – Main characteristics of the operating strategies of the SHARON/DN process.....	177
Table 7.3 – Qualities of the effluent of the SHARON/DN process when using methanol and supernatant from hydrolysed primary sludge as electron donor to denitrify.....	179
Table 7.4 – Average composition of several internal flows of the WWTP.....	182
Table 7.5 – Composition of the supernatant of the pre-treated hydrolysed primary sludge.....	183

TABLES OF CHAPTER 8

Table 8.1– Processes and Kinetic equations used to model the partial nitrification process in a SBR and a SHARON chemostat.....	193
Table 8.2 – Average composition of the reject water tested in this study.....	194
Table 8.3 – Model parameters (average values) for Partial Nitrification in a SBR and SHARON...	196
Table 8.4 – Main operational characteristics in the SBR and in the SHARON chemostat.....	203

TABLES OF CHAPTER 9

Table 9.1 – Feeding and trace solution composition.....	214
Table 9.2 – Main operational characteristics of the Anammox SBR.....	215
Table 9.3 – Experimental periods in the Anammox SBR.....	216
Table 9.4 – Ratio of substrate consumption and nitrate production at 30 and 18 °C.....	219
Table 9.5 – Physical properties of the Anammox biomass tested in this study.....	220

List of Figures

FIGURES OF CHAPTER 1

Figure 1.1 – Cost comparison between chemical-physical sludge water treatment and biological treatment process after an extensive pilot-plant test.....	5
Figure 1.2 – Scheme of the nitrogen cycle.....	8
Figure 1.3 – Effect of temperature on the activity of <i>Nitrosomonas</i> and <i>Nitrobacter</i>	12
Figure 1.4 – Growth rate of <i>Nitrosomonas</i> and <i>Nitrobacter</i> as a function of temperature and SRT..	13
Figure 1.5 – Effect of relatively low $\text{NH}_3\text{-N}$ concentrations on the percentage of OUR related to nitrification kinetics at 35°C	14
Figure 1.6 – Influence of free ammonia and nitrous acid concentrations on AOB and NOB activity.....	15
Figure 1.7 – Effect of DO concentration on nitrification and denitrification kinetics.....	16
Figure 1.8 – Effect of pH on the activity of isolated <i>Nitrosomonas</i> and <i>Nitrobacter</i> cultures.....	17
Figure 1.9 – Influence of the quality of biodegradable COD and temperature on denitrification.....	18
Figure 1.10 – Influence of temperature on the activity of Anammox biomass.....	24
Figure 1.11 – Influence of pH on the activity of Anammox biomass.....	24
Figure 1.12 – Influence of $\text{NO}_2^- \text{-N}$, $\text{NH}_4^+ \text{-N}$ and $\text{NO}_3^- \text{-N}$ concentrations on Anammox activity...	25
Figure 1.13 – Plot of the switching function versus substrate concentration.....	29
Figure 1.14 – Process diagram of the anaerobic digestion of organic matter.....	43
Figure 1.15 – Flow diagram of the studied zone of the municipal WWTP.....	44
Figure 1.16 – Installed capacity per million of inhabitant to treat MSW by AD in Europe in 2004..	46
Figure 1.17 – Distribution and capacity of full-scale AD plants treating OFMSW in Spain.....	46
Figure 1.18 – Schematic diagram of the treatment of mixed MSW in the Ecoparc of Barcelona.....	47
Figure 1.19 – Schematic diagram of the VALPUREN process where supernatant of anaerobically digested piggyery wastewater was collected.....	50
Figure 1.20 – Schematic diagram of SBR performance for biological nitrogen removal.....	53
Figure 1.21 – Methanol, $\text{NH}_4^+ \text{-N}$, $\text{NO}_2^- \text{-N}$ and pH patterns in a SHARON/Denitrification process..	54
Figure 1.22 – Schematic diagram of a combined SHARON – Anammox process.....	55
Figure 1.23 – Schematic diagram of the BABE process.....	56

FIGURES OF CHAPTER 3

Figure 3.1 – Schematic diagram of the SBR tested in this work.....	67
Figure 3.2 – Lab-scale SBR used in this study with its accessories and data acquisition system.....	68

Figure 3.3 – Lab-scale SHARON reactor (4L) used in this study.....	69
Figure 3.4 – Anammox SBR of 1L tested in this work.....	69
Figure 3.5 – Closed Intermittent-Flow respirometer constructed in this study.....	71
Figure 3.6 – Scheme of the acquisition data system for the closed intermittent-flow respirometer...	72
Figure 3.7 – Flow diagram and output graphics of the Advantech Genie programme.....	74
Figure 3.8 – DO profile monitored by the Advantech Genie programme during a respirometric batch test and its corresponding respirogram.....	74
Figure 3.9 – Jar-test device used in this study.....	76
Figure 3.10 – Initial menu of the programme written in Mathematica 4.1 for this study.....	77
Figure 3.11 – Apparatus used to perform the analysis of COD.....	81
Figure 3.12 – CE device and electropherogram of a patron with nitrites and nitrates.....	82
Figure 3.13 – Gas chromatograph and a typical chromatogram of a VFA standard mixture.....	83
Figure 3.14 – Titrator used to perform alkalinity measurements.....	84

FIGURES OF CHAPTER 4

Figure 4.1 – Respirogram obtained for the determination of BOD _{ST} of reject water under study without nitrification inhibition and with 12 mg L ⁻¹ of ATU.....	90
Figure 4.2 – sAUR evolution during the enrichment of secondary activated sludge on nitrifiers....	91
Figure 4.3 – Experimental pH and DO profiles during consecutive cycles inside the SBR under steady state conditions.....	92
Figure 4.4 – Experimental and modelled profiles of NH ₄ ⁺ -N, NO ₂ ⁻ -N, NO ₃ ⁻ -N, pH and DO.....	93
Figure 4.5 – Scheme of the heterotrophic yield coefficient.....	98
Figure 4.6 – Experimental assessment of Y _H	99
Figure 4.7 – Scheme of the AOB and NOB yield coefficients.....	101
Figure 4.8 – Experimental assessment of Y _{AOB}	102
Figure 4.9 – Experimental assessment of lineal decay constant, b _H	104
Figure 4.10 – Experimental assessment of μ _{mH} according to the test of Kappeler and Gujer (1992)..	108
Figure 4.11 – Experimental assessment of the combination μ _{mH} X _{BH} according to the S ₁₀ /X ₁₀ =1/200 experiment (Spanjers and Vanrolleghem, 1995).....	109
Figure 4.12 – Experimental determination of anoxic correction factors for heterotrophic growth....	110
Figure 4.13 – Experimental assessment of the maximum autotrophic growth rate (μ _{mAOB}) according to the methodology established by Kappeler and Gujer (1992).....	113
Figure 4.14 – Experimental assessment of the combined parameters μ _{m,AOB} X _{AOB} and μ _{m,NOB} X _{NOB} ..	114
Figure 4.15 – Experimental device used to assess substrate half-affinity constants.....	115
Figure 4.16 – Assessment of K _S and K _{NH}	116
Figure 4.17 – K _{OH} , K _{O,AOB} and K _{O,NOB} assessment.....	118
Figure 4.18 - Relative activity versus pH for heterotrophic and autotrophic biomass (32 °C).....	119

Figure 4.19 – Relative activity of heterotrophic and autotrophic biomass versus temperature.....	121
Figure 4.20 – Experimental assessment of $K_L a$	123

FIGURES OF CHAPTER 5

Figure 5.1 – Schematic flow-diagram of the treatment of mixed MSW in the Ecoparc-1.....	129
Figure 5.2 – Respirogram obtained for the determination of BOD_{ST} of supernatant from AD of the OFMSW under study without nitrification inhibition and with 12 mg L^{-1} of ATU.....	132
Figure 5.3 – Scheme of the model structure.....	140
Figure 5.4 – Experimental assessment and simulation of Y_H , Y_{AOB} , K_S , K_{NH} , K_{OH} and $K_{O,AOB}$ for the biomass to treat supernatant from AD of the OFMSW.....	142
Figure 5.5 – pH influence on nitrifying activity.....	143
Figure 5.6 – Main parameters in a working cycle under steady state conditions.....	144

FIGURES OF CHAPTER 6

Figure 6.1 – Distribution of pig slurry production in the European Union and Spain.....	149
Figure 6.2 – Representative respirogram obtained for the determination of BOD_{ST} of supernatant of anaerobically digested piggery wastewater of Period 2.....	152
Figure 6.3 – pH and DO profiles during 12 consecutive optimized SBR operating cycles under stationary state conditions.....	154
Figure 6.4 – Experimental concentrations of NH_4^+ -N, NO_2^- -N, NO_3^- -N, Alkalinity, pH and DO along the SBR cycle.....	156
Figure 6.5 – COD removal yields and effluent pH during the Jar-Test using several $FeCl_3$ doses and relative activity of nitrifying biomass with several $FeCl_3$ doses.....	158
Figure 6.6 – Coloration of the treated effluents after coagulation/flocculation.....	158
Figure 6.7 – pH and DO profiles during 8 consecutive optimized SBR operating cycles with a Coagulation/Flocculation step under stationary state conditions.....	160
Figure 6.8 – Experimental concentrations of NH_4^+ -N, NO_2^- -N, NO_3^- -N, Alkalinity, pH and DO inside the SBR with a Coagulation/Flocculation step.....	161
Figure 6.9 – Experimental assessment of Y_H and Y_{AOB}	162
Figure 6.10 – Experimental assessment of K_S and K_{NH3}	163
Figure 6.11 – Experimental assessment of K_{OH} and $K_{O,AOB}$	163
Figure 6.12 – Respirometric analysis for the assessment of the inhibition by total ammonium nitrogen and free ammonia on AOB.....	164
Figure 6.13 – Respirometric analysis for the assessment of the inhibition by total nitrite concentration and HNO_2 on AOB.....	166
Figure 6.14 – Experimental relative activity of AOB versus pH.....	167

FIGURES OF CHAPTER 7

Figure 7.1 – Experimental DO and pH profiles of 24 consecutive SHARON-Denitrification cycles (using methanol to denitrify) under steady-state operation of Period 2..... 178

Figure 7.2 – Experimental profiles of effluent $\text{NH}_4^+\text{-N}$ and $\text{NO}_2^-\text{-N}$ during 3 months of steady-state operation in the SHARON-Denitrification process using methanol to denitrify..... 178

Figure 7.3 – WWTP flow diagram and flow-rates (average values of 2004)..... 181

Figure 7.4 – Repirogram of the hydrolysed primary sludge..... 183

Figure 7.5 – Experimental DO and pH profiles of 24 consecutive SHARON-Denitrification cycles (using supernatant of hydrolysed primary sludge to denitrify) under steady-state operation.. 185

Figure 7.6 – Experimental profiles of effluent $\text{NH}_4^+\text{-N}$, $\text{NO}_2^-\text{-N}$ and pH range (minimum and maximum) during 15 days of steady-state operation in the SHARON-Denitrification process using supernatant of hydrolysed primary sludge to denitrify..... 186

FIGURES OF CHAPTER 8

Figure 8.1 – Experimental profiles of DO and pH during 6 consecutive SBR cycles working under steady-state conditions..... 195

Figure 8.2 – Experimental and modelled profiles during the SBR cycle..... 195

Figure 8.3 – Assessment of Y_{AOB} , $\mu_{\text{mAOB}}X_{\text{AOB}}$, $K_{\text{O, AOB}}$ and K_{NH_3} for the biomass developed in a SBR for partial nitrification of sludge reject water..... 197

Figure 8.4 – pH dependency of AOB in the SBR treatment of reject water to obtain a suited influent to the Anammox process..... 198

Figure 8.5 – Experimental profiles of DO and pH during 1 day of steady state operation of the SHARON process..... 199

Figure 8.6 – Assessment of Y_{AOB} , $\mu_{\text{mAOB}}X_{\text{AOB}}$, $K_{\text{O, AOB}}$, and K_{NH_3} for the biomass developed in a SHARON chemostat for partial nitrification of sludge reject water..... 200

Figure 8.7 – Experimental and modelled profiles during the SHARON operation under steady-state conditions..... 201

FIGURES OF CHAPTER 9

Figure 9.1 – Temperature dependency profiles on Anammox biomass..... 210

Figure 9.2 – Aspect of the Anammox biomass and the supernatant after the second injection of the Specific Anammox Activity (SAA) test at 40 °C and 45 °C..... 212

Figure 9.3 – Absorbance profiles of supernatant of the SAA Tests at 35, 40 and 45 °C..... 213

Figure 9.4 – Time distribution in the Anammox SBR cycle..... 215

Figure 9.5 – Experimental profiles of $\text{NH}_4^+\text{-N}$ and $\text{NO}_2^-\text{-N}$ in the effluent, nitrogen loading rate and maximum nitrogen removal rate during the operation of the Anammox SBR..... 217

Figure 9.6 – Photographs of the biomass aggregates from the Anammox SBR working at 18°C..... 220

Summary

In the last years, stricter effluent standards have been implemented by legislation in order to reduce the nutrients evacuation to receiving waters. The reduction of the nitrogen present in wastewaters to an environmentally supportable level is essential, since it could lead to several environmental and health risks, such as eutrophication.

The supernatants from anaerobic digestion of protein rich organic materials are typical wastewaters with high content in ammonium (in the range of 0.5 - 4.0 g $\text{NH}_4^+\text{-N L}^{-1}$). For the treatment of these kind of wastewaters, Biological Nitrogen Removal (BNR) is preferred in front of other chemical or physic-chemical processes (MAP process, air stripping, steam stripping, ...) based on cost aspects, chemical and energy requirements, operation experience, process reliability and environmental impact.

The conventional BNR process consists on the oxidation of ammonia to nitrate (nitrification) and the subsequent reduction of nitrate to nitrogen gas (denitrification) using biodegradable COD as electron donor. If this BNR process is carried out over nitrite, it is obtained a saving of 25% of the aeration costs and 40% of the external carbon source needed during denitrification, as well as a reduction in the amount of sludge produced. Another feasible treatment of highly ammonium loaded wastewaters is the combination of partial nitrification (oxidation of the 50% of $\text{NH}_4^+\text{-N}$ to $\text{NO}_2^-\text{-N}$) with Anammox (denitrification of $\text{NO}_2^-\text{-N}$ to N_2 using $\text{NH}_4^+\text{-N}$ as electron donor). When compared with conventional BNR, this process avoids the requirement of organic carbon source to denitrify, allows saving over 65% of the oxygen supply and produces little sludge. The slow growth rate of Anammox biomass, its high inhibition by nitrite concentrations and the need of high operating temperatures are the main disadvantages of this process.

In this study, several biological processes have been tested to remove the nitrogen present in three types of wastewaters widely generated in Catalonia: supernatant from Anaerobic Digestion (AD) of municipal sewage sludge (sludge reject water), supernatant from AD of the Organic Fraction of Municipal Solid Waste (OFMSW) and supernatant from AD of piggery wastewater.

For these three wastewaters, the Sequencing Batch Reactor (SBR) technology was tested, operating with 3 cycles per day and SRT 11-12 days. Temperature was maintained at 30-32 °C, considering that these wastewaters come from mesophilic anaerobic digestion. An external carbon source (methanol, acetate or acetic acid) was used to denitrify, since the wastewaters tested had very low BOD concentrations. The free ammonia concentration at the beginning of each cycle was sufficiently high to inhibit the oxidation of nitrite to nitrate. Moreover, dissolved oxygen was maintained below 1 mg O₂ L⁻¹ to promote the nitrite route. The operating nitrogen loading rates were 0.87, 0.85 and 0.37 kg N m⁻³ day⁻¹, for the treatment of sludge reject water, supernatant from AD of piggery wastewater and supernatant from AD of the OFMSW, respectively. Moreover, for the SBR treatment of supernatant from AD of piggery wastewater, a coagulation/flocculation step inside the operating SBR cycle was introduced in order to reduce the effluent COD concentration below the effluent standards established in legislation. The SBR operation resulted very flexible, compact and efficient to treat these highly ammonium loaded wastewaters.

Moreover, the SBR operation for the three wastewaters tested was modelled by means of an Activated Sludge Model extended to describe the biological nitrogen removal over nitrite. This model (implemented in the software Mathematica 4.1) includes the inhibition of nitrification by unionised ammonia and nitrous acid concentrations, the pH dependency of both autotrophic and heterotrophic biomass, pH calculation and the oxygen supply and stripping of CO₂ and NH₃. In order to calibrate the model, a closed intermittent flow respirometer with both pH and temperature control was set up. A methodology based on respirometric batch tests reported in literature was also proposed and applied to reproduce the experimental data obtained in the laboratory. Once calibrated by respirometry, the proposed model showed very good agreement between experimental and simulated data of the three studied SBR treatments. In these biological treatments, free ammonia concentration and dissolved oxygen were identified as the responsible of the nitrite route.

Another efficient biological treatment was studied to treat sludge reject water: the SHARON-Denitrification process. This biological process takes place in a continuous reactor where aerobic/anoxic periods are alternated under specific HRT and temperature conditions that favours ammonium oxidizers growth and assures the total wash-out of nitrite oxidizers, achieving the biological nitrogen removal over nitrite. An optimized

performance of this process was obtained using methanol and working at HRT 2.1 days, 33 °C and a cycle length of 2 hours. The operating nitrogen loading rate achieved with this strategy was 0.33 kg N m⁻³ day⁻¹.

The use of supernatant of hydrolysed primary sludge as the organic carbon source to denitrify in the SHARON/Denitrification process was also tested. Since the BOD concentration was not extremely high in the primary sludge, the fluid dynamics of the system were changed with respect to the strategy with methanol but maintaining the reject water influent flow-rate. Due to this reason, the HRT was reduced from 2.1 days to 1.4 days. The use of hydrolysed primary sludge improved the process efficiency since its alkalinity content buffered the process until an optimum pH range. Considering the ammonium present in hydrolysed primary sludge, the operating nitrogen loading rate of this reactor was 0.38 kg N m⁻³ day⁻¹.

Furthermore, two biological nitrogen removal treatments for partial nitrification of sludge reject water were operated at lab-scale conditions to achieve an appropriate influent for the Anammox process. These two processes were the SHARON process and the partial nitrification in a Sequencing Batch Reactor (SBR). Both processes showed a good performance in the generation of an effluent with a NH₄⁺-N to NO₂⁻-N on molar basis of approximately 1. However, the SBR was capable to partially oxidize 2.2 kg NH₄⁺-N (m³ day)⁻¹, while the SHARON reactor treated an ammonium loading rate of 0.7 kg NH₄⁺-N (m³ day)⁻¹. Both processes were also modelled by means of an Activated Sludge Model extended for nitrite route description and pH calculation. The calibrated model provided a good match between experimental and simulated data, and quantified the inhibitions that lead to the nitrite route. For the partial nitrification in an SBR, the key factor responsible of the inhibition of nitrite oxidizers was the working free ammonia concentration. However, for the SHARON process the key factor was the implemented SRT at the operating temperature.

Finally, an Anammox lab-scale SBR was operated to treat a highly ammonium loaded synthetic wastewater, that represented the effluent obtained in the aforementioned partial nitrification units (SHARON and SBR). Since the Anammox process has been usually presented as a biological process that requires heating (usually at 35 °C) to achieve proper removal efficiencies, the feasibility of the Anammox process at different temperature conditions (namely, 30, 25, 23, 20, 18 and 15 °C) has been tested. As an initial approach

to assess the temperature influence at short time on Anammox biomass, several batch activity tests were run at controlled temperature conditions. These results were adjusted to the Arrhenius model and were taken as the basis to decide the biomass concentration needed to manage a previously defined nitrogen loading rate in a lab-scale Anammox Sequencing Batch Reactor (SBR) when the operating temperature range was reduced. At 18 °C, a steady state operation was achieved treating $0.30 \text{ kg N (L day)}^{-1}$, with a stoichiometry slightly different from that obtained under 30 °C. As predicted by the model, the system accumulated nitrite when the operating temperature was reduced to 15 °C, so a very slow adaptation of Anammox biomass to low temperatures was observed.

1. Introduction

ABSTRACT

The reduction of the nitrogen present in wastewaters to an environmentally supportable level is essential, since an excess of nitrogen to receiving waters would lead to several environmental and health risks. The supernatant from anaerobic digestion of protein rich organic materials, such as sewage sludge, piggery wastewater or organic fraction of municipal solid waste (OFMSW) is a typical highly ammonium loaded wastewater that needs to be treated. For the treatment of these kind of wastewaters, biological nitrogen removal is preferred in front of other chemical or physico-chemical processes (MAP process, air stripping, steam stripping, ...) based on cost aspects, chemical and energy requirements, operation experience, process reliability and environmental impact.

The conventional biological nitrogen removal (BNR) process consists on the oxidation of ammonia to nitrate (nitrification) and the subsequent reduction of nitrate to nitrogen gas (denitrification) using biodegradable COD as electron donor. If this BNR process is carried out over nitrite, it is obtained a saving of 25% of the aeration costs and 40% of the external carbon source needed during denitrification, as well as a reduction in the amount of sludge produced. Several strategies can be performed to stop the oxidation of nitrite to nitrate: working at high free ammonia and/or nitrous acid concentrations capable to inhibit Nitrite Oxidizing Biomass (NOB) but not Ammonium Oxidizing Biomass (AOB); using a reduced dissolved oxygen concentration to favour AOB over NOB; and working at low sludge retention times (SRT) and high operating temperatures (35°C) to enable the proliferation of AOB and the total wash-out of NOB (SHARON process). Another feasible treatment of these kind of effluents is the combination of a stable partial nitrification in a first aerobic reactor, with anaerobic ammonium oxidation (Anammox) in a second tank. When compared with conventional BNR, this autotrophic process avoids the requirement of organic carbon source to denitrify, allows saving over 65% of the oxygen supply and produces little sludge. The slow growth rate of Anammox biomass, its high inhibition by nitrite concentrations and the need of high operating temperatures are the main disadvantages of using this process.

1.1 NITROGEN POLLUTION IN WASTEWATERS

During the last century, activated sludge systems have been successfully used to treat municipal wastewaters for biological carbon removal. In the past decades, activated sludge nutrient removal processes have been investigated and widely introduced. Nowadays, water for consume is a good that starts to be scarce due to the increase of population and its low availability. This makes a growing public concern for environmental protection and leads to the implementation of stricter effluent standards. This, in turn, impelles efforts to achieve better effluent quality, especially regarding nitrogen removal (van Loosdrecht and Salem, 2006).

The reduction of the nitrogen present in wastewaters to an environmentally supportable level is essential, since an excess of nitrogen to receiving waters would lead to several environmental and health risks. Ammonia is an indispensable plant nutrient and, after nitrification to nitrate, it is responsible of eutrophication (uncontrolled blooming of algae and other photosynthetic organisms) and/or the total depletion of Dissolved Oxygen (DO) present in natural waters. Aquatic plants influence the DO and pH of the surrounding water and if an overgrowth of these plants is promoted, great fluctuations in pH and DO levels could occur, with the consequent disease or death of aquatic organisms. Moreover, Ammonia (NH_3) and nitrous acid (HNO_2) are also toxic for aquatic organisms at very low concentrations. Nitrites in drinking water can also lead to oxygen shortage of newly borns. During chlorination of drinking water, nitrite can interact with compounds containing organic nitrogen and form carcinogenic nitrosamines. Finally, its important to highlight that nitrate can be partly reduced to toxic nitrite inside the human body and thus, in high concentrations, cause health problems.

Consequently, nitrogen compounds need to be removed from wastewaters. Several biological and chemical processes are available to carry out this nitrogen removal (Siegrist, 1996; Hans *et al.*, 1997; Hellinga *et al.*, 1999).

1.2 NITROGEN ELIMINATION FROM WASTEWATERS

Several ways to remove nitrogen from wastewaters have been reported in literature. The most relevant treatments are listed below:

The MAP process is a physico-chemical process that consists on the precipitation of ammonia in the form of MgNH_4PO_4 (MAP) through the addition of phosphoric acid and magnesium oxide. For this treatment it is necessary to control the pH in the range 8.5-10 to favour the precipitation of MAP, which can be used as a fertilizer in agriculture. Nitrogen removal efficiencies around 90% have been reported for this treatment (Siegrist, 1996).

The Air stripping process is a physico-chemical process that recovers the NH_4^+ -N present in wastewater in the form of free ammonia (NH_3) by transferring this volatile compound into an air stream. To this purpose, the pH of the wastewater is regulated to a value of 10 to convert NH_4^+ to NH_3 . Subsequently, an air stream is passed through the wastewater to capture free ammonia. Finally, ammonia is absorbed in a solution containing sulphuric acid to form $(\text{NH}_4)_2\text{SO}_4$. Siegrist (1996) reported nitrogen removal efficiencies above 97% when working with this process at temperatures between 10-22°C.

The Steam stripping process is a method similar to the Air stripping process but using water steam instead of air for the desorption in order to recover ammonia by condensation (Teichgraber and Stein, 1994; Siegrist, 1996).

Finally, there are a wide variety of Biological nitrogen removal processes to convert ammonia to dinitrogen gas. These processes will be explained in detail in section 1.3. They are based on the capacity of microorganisms to assimilate nitrogen to create new cells, oxidize ammonium to nitrite or nitrate and to reduce nitrite/nitrate to nitrogen gas. Moreover, the biological reactor configuration will also depend on the biological nitrogen removal process selected.

For specific application, the available alternatives must be evaluated based on costs aspects, chemical and energy requirements, operation experience, process reliability and environmental impact.

According to Mulder (2003), the selection of a biological or a physico-chemical method is determined by the nitrogen concentration of the wastewater. This author reported that low ammonium loaded wastewaters ($0\text{-}100 \text{ mg NH}_4^+\text{-N L}^{-1}$), such as influent wastewater of municipal wastewater treatment plants (WWTP), must be treated by biological nitrogen removal processes based on cost-effectiveness. For highly ammonium loaded

wastewaters ($100\text{-}5,000 \text{ mg NH}_4^+\text{-N L}^{-1}$) intensive biological treatment is to be preferred (Janus and van der Roest, 1997; Macé and Mata-Álvarez, 2002). Although ammonia stripping and producing MgNH_4PO_4 were identified as interesting alternatives for resource recovery, these options are not cost-effective (Siegrist, 1996; Janus and van der Roest, 1997). For this kind of wastewaters, van Loosdrecht and Salem (2006) recently performed an economic study and concluded that the cost of a biological nitrogen removal process (namely, the SHARON-Denitrification process which will be discussed further in detail) was $0.9\text{-}1.4 \text{ euro kg}^{-1} \text{ N removed}$, while other physical or chemical processes were almost 5-9 times higher. Figure 1.1 shows the cost comparison between physical-chemical and biological processes. Finally, Mulder (2003) justified that physico-chemical methods, such as steam stripping, are technically and economically feasible to treat extremely highly ammonium loaded wastewaters (higher than $5,000 \text{ mg NH}_4^+\text{-N L}^{-1}$).

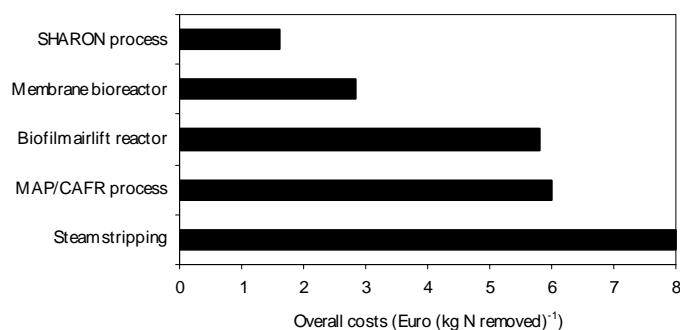


Figure 1.1 – Cost comparison between physico-chemical sludge water treatment and biological treatment process after an extensive pilot-plant test (STOWA, 1996; van Loosdrecht and Salem, 2006)

This study is focussed on the treatment of highly ammonium loaded wastewaters ($100\text{-}5,000 \text{ mg NH}_4^+\text{-N L}^{-1}$), where biological nitrogen removal treatment is clearly preferred in front of other physico-chemical treatments. Table 1.1 shows an overview of wastewaters containing high ammonium loads. Most of these wastewaters come from anaerobic digestion of protein-rich sludge (such as sludge reject water or supernatant from anaerobically digested sewage sludge from a municipal WWTP, anaerobically digested pig slurry, anaerobically digested Organic Fraction of Municipal Solid Waste (OFMSW), anaerobically digested slaughter house waste). Untreated thin fraction of piggery manure, landfill leachates and other industrial wastewaters (such as meat processing effluents, effluents from starch production or pectine industry wastewaters) are also characterised by high ammonium concentrations.

Table 1.1 – Characterisation of highly ammonium loaded wastewaters (after Donckels (2004) and Van Hulle (2004))

Type of wastewater	COD (mg COD L ⁻¹)	BOD ₅ (mg O ₂ L ⁻¹)	Total nitrogen (mg N L ⁻¹)	Phosphorous (mg P L ⁻¹)	Reference
Reject water					
	710	-	610 (NH ₄ ⁺ -N) 670 (TKN) 0 (NO _x ⁻ -N)	-	Teichgraber and Stein (1994)
	700 – 1,000	-	1,250 – 1,700 (NH ₄ ⁺ -N)	-	Wett <i>et al.</i> (1998)
	810	230	1,000 (NH ₄ ⁺ -N) 1,053 (TKN)	27	Hellingsa <i>et al.</i> (1999)
	1,411	-	244 (NH ₄ ⁺ -N) 305 (TKN)	34 (PO ₄ ³⁻ -P)	Ghyoot <i>et al.</i> (1999)
	453 ± 272	109 ± 44	668 ± 133 (NH ₄ ⁺ -N) 794 ± 251 (TKN)	53 ± 22 (total P) 32 ± 8 (PO ₄ ³⁻ -P)	Vandaele <i>et al.</i> (2000)
	-	-	1,180 ± 140 (NH ₄ ⁺ -N) 0 (NO _x ⁻ -N)	-	Van Dongen <i>et al.</i> (2001)
	-	-	657 ± 56 (NH ₄ ⁺ -N) 0.4 ± 0.7 (NO ₂ ⁻ -N) 0.2 ± 0.7 (NO ₃ ⁻ -N)	7.3 ± 5.0 (PO ₄ ³⁻ -P)	Fux <i>et al.</i> (2002) (Werdhoelzli WWTP)
	-	-	619 ± 21 (NH ₄ ⁺ -N) 4.7 ± 6.2 (NO ₂ ⁻ -N) 0.2 ± 0.2 (NO ₃ ⁻ -N)	0.6 ± 0.8 (PO ₄ ³⁻ -P)	Fux <i>et al.</i> (2002) (Au WWTP)
	610	140	910	-	Wyffels <i>et al.</i> (2003)
	1,044 ± 855	-	840 ± 99 (NH ₄ ⁺ -N) 1,177 ± 163 (TKN)	-	Fux <i>et al.</i> (2003)
	232 – 12,587	81 - 750	260 - 958	33 - 207	Gil and Choi (2004)
	390 – 2,720	-	943 - 1513	-	Jenicek <i>et al.</i> (2004)
	119 - 530	9.5 – 86.7	403 – 997 (NH ₄ ⁺ -N) 0 – 2.25 (NO ₂ ⁻ -N) 0 – 0.2 (NO ₃ ⁻ -N)	41 – 92 (PO ₄ ³⁻ -P)	Caffaz <i>et al.</i> (2005)
Piggery wastewater (Thin fraction pig slurry)					
	2,940 ± 1,100	-	970 ± 50	93 ± 26 (total P) 53 ± 8 (PO ₄ ³⁻ -P)	Hwang <i>et al.</i> (2005)
	-	2,912	707	55	Chen <i>et al.</i> (2004)
	3,969	1,730	1650 (NH ₄ ⁺ -N) 1,700 (TKN)	171	Obaja <i>et al.</i> (2003) *
	9,000-13,000	-	3,100-4,300	20-40	Poo <i>et al.</i> (2004)
	6,456	-	695	91.8	Tilche <i>et al.</i> (1999)
	18,408 – 19,117	-	1,582 – 1,680 (NH ₄ ⁺ -N) 2,636 – 2,694 (TKN)	824 – 1,271 (total P) 140 - 271 (PO ₄ ³⁻ -P)	Magri and Flotats (2000)

Type of wastewater	COD (mg COD L ⁻¹)	BOD ₅ (mg O ₂ L ⁻¹)	Total nitrogen (mg N L ⁻¹)	Phosphorous (mg P L ⁻¹)	Reference
Anaerobically digested Organic Fraction of Municipal Solid Waste (OFMSW)					
	3,000-23,800	700-10,000	229 – 963 (NH ₄ ⁺ -N) 305 – 1,558 (TKN)	-	Kautz and Nelles (1995)
	7,300-28,300	1,650 – 7,100	510 – 2,600 (NH ₄ ⁺ -N)	-	Kübler (1996)
	2,300 – 36,200	660 – 13,700	565 – 1,490 (NH ₄ ⁺ -N)	4.8 – 20 (PO ₄ ³⁻ -P)	Loll (1998)
	3,000-15,000	1,000 – 15,000	500 – 2,500 (NH ₄ ⁺ -N)	-	Müller (1999)
	3,000-24,000	700 – 3,500	200 – 1,800 (NH ₄ ⁺ -N)	30 – 150 (PO ₄ ³⁻ -P)	Bidlingmaier (2000)
Landfill leachate					
	-	45	310	-	Ilies and Mavinic (2001)
	1,300 - 1,600	-	160 - 270	-	Jokela <i>et al.</i> (2002)
	2,000 - 5,000	1,500-4,000	500 - 1,000	20-50	Chung <i>et al.</i> (2003)
	9,660 – 20,560	-	780 - 1,080	20-51	Kalyuzhnyi and Gladchenko (2004)
	3,200 – 6,100	136 – 1,059	1,150 – 3,223 (NH ₄ ⁺ -N) 1,690.8 – 3,594 (TKN) 0 – 18.4 (NO ₂ ⁻ -N) 0 – 11.83 (NO ₃ ⁻ -N)	-	Canigué <i>et al.</i> (2007)
	14,600 – 70,800	-	1,275 – 5,500 (NH ₄ ⁺ -N)	-	Vilar <i>et al.</i> (2007)
Tannery wastewater					
	300 – 1,400	-	160 - 270	-	Carucci <i>et al.</i> (1999)
	1,940 – 2,700	-	123 - 185	-	Murat <i>et al.</i> (2003)
Slaughter house waste processing					
	1,400 – 2,400	-	170 - 200	35 - 55	Keller <i>et al.</i> (1997)
	2,380-3,480	-	173-222 (NH ₄ ⁺ -N) 228-278 (TKN)	37-42 (total P) 31-39 (PO ₄ ³⁻ -P)	Keller (2005)
Meat processing effluents					
	3,600 – 13,000	-	500 – 1,200	-	Mosquera-Corral <i>et al.</i> (2003)
	1,735	1,595	101.8	-	Thayalakumaran <i>et al.</i> (2003)
Wastewater from laboratories for analysis of dairy products					
	500 – 3,000	300 – 1,500	50 - 200	-	Arrojo <i>et al.</i> (2004)
Starch production					
	3,000	990	1,060	210	Abeling and Seyfried (1992)
	5,000 – 10,000	2,000 – 5,000	800 – 1,100	170 - 230	Abeling and Seyfried (1993)
Pectine industry wastewater					
	15,000 – 22,000	-	1,280 – 2,990	-	Austermann-Haun <i>et al.</i> (1999)
	8,100	-	1,600	11	Deng Petersen <i>et al.</i> (2003)

* After anaerobic digestion

1.3 BIOLOGICAL NITROGEN REMOVAL

1.3.1 The nitrogen cycle

Nitrogen naturally exists in various compounds with a valence ranging from -3 to +5. The various forms of nitrogen in the nature, and pathways by which these forms are transformed, are schematically depicted in Figure 1.2. Nitrogen oxidation state is changed by different kind of microorganisms, that carry out catabolic reactions (nitritation, nitrataion, denitrification, dissimilatory nitrate reduction and anaerobic ammonium oxidation), anabolic reactions (ammonium uptake, assimilatory nitrate reduction and nitrogen fixation) and ammonification (Brock *et al.*, 1997).

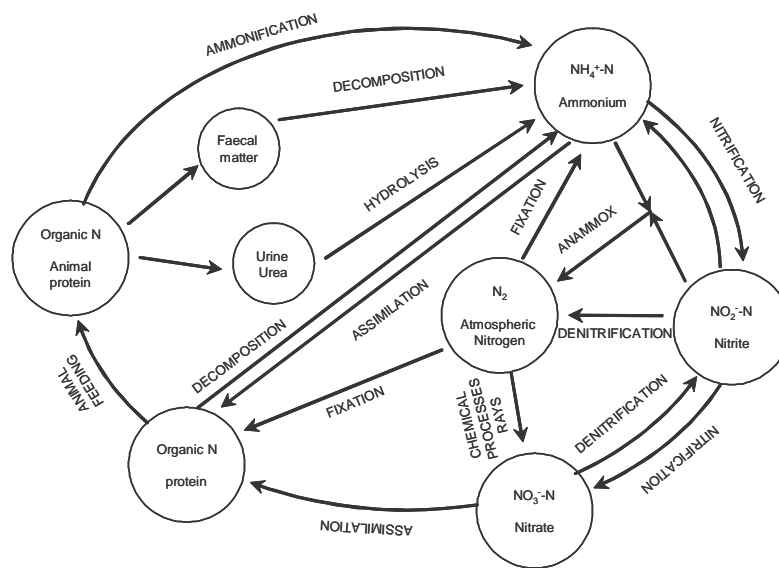


Figure 1.2 - Scheme of the nitrogen cycle. (Dapena-Mora, 2007)

Traditionally the nitrogen cycle is described by nitrification (ammonia is oxidized to nitrite and further on to nitrate by autotrophic biomass), denitrification (conversion of nitrate or nitrite to nitrogen gas by heterotrophic biomass), nitrogen fixation (conversion of molecular nitrogen to organic nitrogen), ammonification (death and cellular decomposition) and assimilation of ammonia to form new cells.

However, the detection of new organisms is making the nitrogen cycle increasingly complicated (see Figure 1.2). Recently it was found that “aerobic” ammonium oxidizers

could do other processes as well. When oxygen is limiting (micro-aerophilic conditions) nitrosomonas can combine hydroxylamine with nitrite to give dinitrogen oxide gas (Bock *et al.*, 1995). This process was referred to as aerobic deammonification (Hippen *et al.*, 1997). Moreover, in the presence of NO_2 the organisms can convert ammonium with NO_2 to NO gas (Schmidt *et al.*, 2002). Both conversions lead to the removal of ammonium from the water phase, but are clearly not wanted. Furthermore, a completely new microbial group has been discovered: the Anaerobic Ammonium Oxidisers (Anammox), which can oxidize ammonia to dinitrogen gas using nitrite as electron acceptor under anaerobic conditions. Schmid *et al.* (2003) reported that this process is an important contributor to nitrogen losses in natural systems, particularly in marine systems. The anaerobic oxidation of ammonia proceeds via hydrazine (N_2H_4), a volatile and toxic intermediate (Schalk *et al.*, 2000) which is further oxidized to dinitrogen gas.

1.3.2. Biological nitrogen removal processes

Four major forms of nitrogen are defined to depict nitrogen in wastewater discharges and receiving waters (Orhon and Artan, 1994; Henze *et al.*, 2000): organic nitrogen (N_{org}), ammonia nitrogen ($\text{NH}_4^+\text{-N}$), nitrite nitrogen ($\text{NO}_2^-\text{-N}$) and nitrate nitrogen ($\text{NO}_3^-\text{-N}$). As observed in Table 1.1, only the first two forms of nitrogen are significant for wastewaters, with the exception of a few specific industrial discharges.

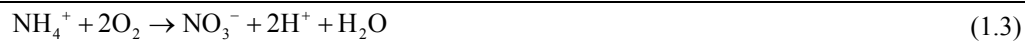
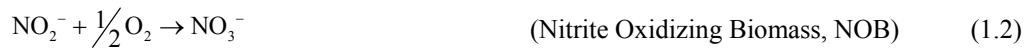
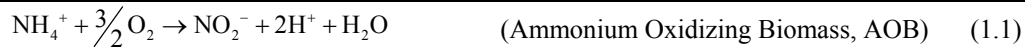
An important common feature of organic nitrogen and ammonia nitrogen is that they are the most reduced forms with the same oxidation state, corresponding to a valence of -3. Nitrogenous organic compounds may be involved in degradation reactions by bacterial action (hydrolysis), under both aerobic and anaerobic conditions, which release ammonia to the medium.

Ammonia nitrogen in aqueous solution exists as two different compounds: free ammonia (NH_3) and ammonium ion (NH_4^+). The ratio of the molar concentrations of these forms varies depending on the pH and temperature of the solution. Free ammonia is assimilated by both heterotrophic and autotrophic biomass to synthesise new cells. However, this biological process is not enough to remove ammonia present in wastewaters from Table 1.1 to an acceptable level. Therefore, the biological nitrification/denitrification process is usually used to remove high nitrogen loads.

Nitrification is the first step in a biological nitrogen removal system. This reaction oxidizes ammonia to nitrite and further on to nitrate. Subsequently, the formed nitrite or nitrate are reduced to nitrogen gas using biodegradable COD (conventional heterotrophic denitrification) or ammonia (autotrophic denitrification, Anammox) as electron acceptors (see Figure 1.2). These nitrification and denitrification processes are widely explained above. The influence of several operating parameters on nitrification/denitrification processes is also discussed.

1.3.2.1 Nitrification

Nitrification is the biological oxidation of ammonium first to nitrite (nitritation) and then to nitrate (nitrataion). The stoichiometry of both reactions is detailed in Equation 1.1 and 1.2 (Hellings *et al.*, 1999; Grady *et al.*, 1999). The pioneering work of Winogradsky (1890) established that nitrification is associated with the metabolism of a group of chemoautotrophic bacteria. Species of the genus *Nitrosomonas* were observed to derive their energy from the oxidation of ammonia to nitrite, and *Nitrobacter* species were found to depend on nitrite oxidation as their energy source. However, several other groups of chemoautotrophic bacteria (*Nitrosococcus*, *Nitrosospira*, *Nitrocystis*, ...) are also identified, although less frequently, as being capable of carrying out nitrification. Therefore, it is considered that nitritation and nitrataion are carried out by Ammonium Oxidizing Biomass (AOB) and Nitrite Oxidizing Biomass (NOB), respectively.



Assuming that the chemical composition of microorganisms is $\text{C}_5\text{H}_7\text{NO}_2$ (Hoover and Porges, 1952), when autotrophic cell synthesis is considered the global reaction of nitrification is the one shown in Equation 1.4 (Orhon and Artan, 1994).



Equation 1.3 shows that for each gram of nitrogen used as electron donor, 4.57 g of O₂ is required without any consideration of biomass formation. On the other hand, the stoichiometry of nitrification is usually based on the observation that 4.33 g of O₂ is consumed for each gram of NO₃⁻-N formed, as stipulated by Equation 1.4. Consequently, the O₂ equivalent of biomass generation under observed conditions is 0.24 g cell COD g⁻¹ N.

It should be noted that nitrification generates protons as indicated by Equation 1.3. Consequently, the process consumes alkalinity equivalent to the amount of protons released. Furthermore, there is an additional alkalinity reduction corresponding to the ammonia which is used as a nitrogen source in biosynthesis and converted into organic nitrogen in cellular constituents. The overall Equation (Equation 1.4) predicts that 1.98 moles of HCO₃⁻ are consumed per mole of NH₄⁺-N, which is equivalent to 7.07 g CaCO₃ g⁻¹ NH₄⁺-N.

A number of factors are found to affect the kinetics of nitrification. These factors may, at times, play a decisive role on the rate of nitrification, since autotrophic microorganisms are very sensitive to changes in environmental conditions. On the other hand, some authors (Abeling and Seyfreid, 1992; Hellinga *et al.*, 1999; Wett and Rauch, 2003) have discussed the beneficial effects of performing the biological nitrogen process oxidizing ammonia to nitrite instead of nitrate, since it suggests a saving of 25% of the aeration costs and 40% of the external carbon source needed during the subsequent denitrification process, as well as a reduction in the amount of sludge produced. The different influence of factors affecting nitrification on nitrification and nitrification are the key to avoid the oxidation of nitrite to nitrate. The main *factors affecting nitrification kinetics* are discussed below:

Effect of Temperature and Sludge Retention Time (SRT)

As in most biochemical reactions, nitrification kinetics are generally influenced by temperature. The most pronounced effect of temperature is commonly observed on the maximum specific growth rate ($\mu_{m,A}$). Experimental observations suggest that the effect of temperature on $\mu_{m,A}$ can be modelled by an Arrhenius type equation (see Equation 1.5), in the range of 7-30°C (Orhon and Artan, 1994; Henze *et al.*, 2000; Hao *et al.*, 2002; Hellinga *et al.*, 2004). In Equation 1.5, T is the actual temperature, $\mu_{m,A}(T)$ is the

maximum specific growth rate of autotrophic biomass at T, $\mu_{m,A}(20^{\circ}\text{C})$ is the maximum specific growth rate at 20°C and θ is the temperature coefficient. Several values are reported in literature for θ between 1.08 and 1.23 (Ekama and Marais, 1984; Henze *et al.*, 2000; Ferrer and Seco, 2003).

$$\mu_{m,A}(T) = \mu_{m,A}(20^{\circ}\text{C}) \theta^{(T-20^{\circ}\text{C})} \quad (1.5)$$

Grunditz and Dalhammar (2001) studied the effect of temperature on the activity of isolated AOB (Nitrosomonas) and NOB (Nitrobacter) cultures. Figure 1.3 shows their results, where it is observed an exponential growth until approximately 40°C , and then a sudden drop of the maximum activity with increasing temperatures. The highest activity was found at 35°C for Nitrosomonas and 38°C for Nitrobacter.

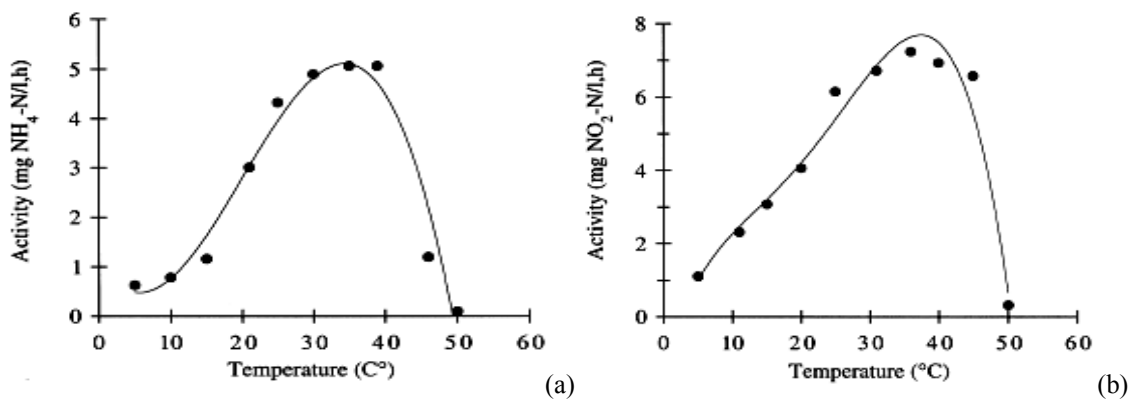


Figure 1.3 – Effect of temperature on the activity of Nitrosomonas (a) and Nitrobacter (b) (Grunditz and Dalhammar, 2001)

On the other hand, Hellinga *et al.* (1999) encountered that at high temperatures, Nitrosomonas have a distinctly lower growth rate than Nitrosomonas. This is depicted in Figure 1.4, where the minimum Sludge Retention Time (SRT) for AOB and NOB depending on temperature is represented, based on the activation energies reported by Hunik (1993): 65 kJ mole^{-1} for AOB and 45 kJ mole^{-1} for NOB).

Since SRT is inversely proportional to the maximum biological growth rate, in Figure 1.4 it is demonstrated that AOB grows faster than NOB for temperatures above 13°C . For this reason, in biological treatment of municipal wastewaters, nitrite accumulation is not

frequently encountered, since at the usual operating temperatures (10-20°C) and in absence of inhibitors, the maximum growth rate for NOB is higher (or similar) than for AOB (Wett and Rauch, 2003). However, if a low SRT and a high operating temperature (35°C) is carefully selected, the proliferation of AOB and the total wash-out of NOB can be easily achieved. This is the basis of the continuous SHARON process (Hellinga *et al.*, 1999).

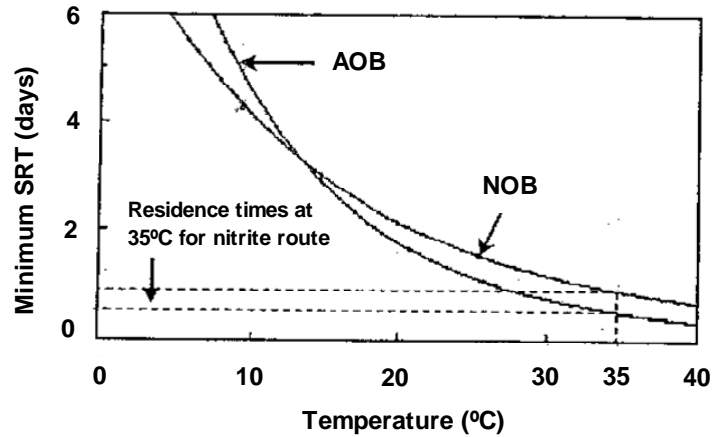


Figure 1.4 – Growth rate of *Nitrosomonas* and *Nitrobacter* as a function of temperature and residence time. The higher the temperature, the higher the growth rate and the lower the minimum residence time needed to avoid wash-out of biomass (Hellinga *et al.*, 1999)

Effect of ammonia (NH₃) and nitrous acid (HNO₂) concentrations

The relationship between the growth rate of nitrifying biomass and the concentration of energy yielding substrates (NH₄⁺-N and NO₂⁻-N for AOB and NOB, respectively) has been formulated most widely by a Monod type rate expression. Equations 1.5 and 1.6 show the Monod expressions to describe the growth rate of AOB and NOB, respectively. However, several studies have demonstrated that NH₃ rather than NH₄⁺ and HNO₂ rather than NO₂⁻ are the actual substrates in nitrification reactions (Hellinga *et al.*, 1999; Van Hulle *et al.*, 2004).

$$\mu_{AOB} = \mu_{m,AOB} \frac{S_{NH}}{K_{NH} + S_{NH}} \quad (1.5)$$

$$\mu_{NOB} = \mu_{m,NOB} \frac{S_{NO_2}}{K_{NO_2} + S_{NO_2}} \quad (1.6)$$

In this equations, μ_{AOB} and μ_{NOB} are the actual specific growth rate of AOB and NOB, respectively; $\mu_{m,AOB}$ and $\mu_{m,NOB}$ are the maximum specific growth rate of AOB and NOB, respectively; S_{NH} and S_{NO_2} are the NH_4^+ -N and NO_2^- -N concentrations in the growth medium; and K_{NH} and K_{NO_2} are the NH_4^+ -N and NO_2^- -N half-saturation constants, respectively. Figure 1.5 shows the dependency of the percentage of Oxygen Uptake Rate (OUR) related to nitrification kinetics (equivalent to $\mu_{AOB}/\mu_{m,AOB}$) on the concentration of NH_3 registered by Van Hulle *et al.* (2004). A K_{NH_3} value of $0.75 \text{ mg } NH_3\text{-N } L^{-1}$ was detected, corresponding to the NH_3 -N concentration at which the actual μ_A is 0.5 times the $\mu_{m,A}$ value.

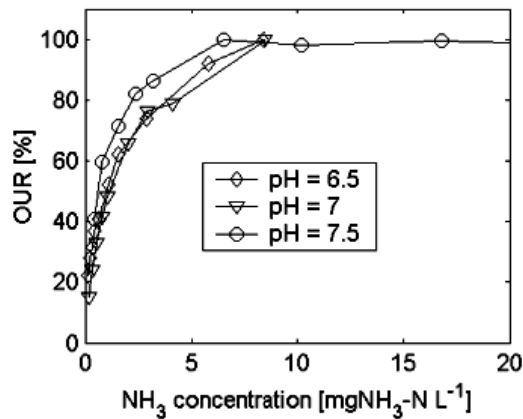


Figure 1.5 – Effect of relatively low NH_3 -N concentrations on the percentage of OUR related to nitrification kinetics at $35^\circ C$. (Van Hulle *et al.*, 2004)

On the other hand, experimental studies attribute high inhibitory effects on AOB and NOB activity in the presence of free ammonia and undissociated nitrous acid concentrations. Anthonisen *et al.* (1976) determined the effect of ammonia (NH_3) and nitrous acid (HNO_2) concentration upon the ammonium oxidation and the nitrite oxidation kinetics. These authors demonstrated that NOB is inhibited at concentrations higher than $0.2\text{-}2.8 \text{ mg } HNO_2 \text{ } L^{-1}$ and/or $0.1\text{-}1.0 \text{ mg } NH_3 \text{ } L^{-1}$, while AOB is inhibited by unionised ammonia concentrations higher than $10\text{-}150 \text{ mg } NH_3 \text{ } L^{-1}$. Figure 1.6 shows the different zones of inhibition of ammonia and nitrite oxidation depending on the pH value and the concentrations of NH_3 and HNO_2 . In this Figure, two zones can be distinguished in which nitrite accumulation is to be expected, since inhibition of NOB but not to AOB is detected.

Wett and Rauch (2003) corroborated these experimental results and experienced a partial inhibition of nitrite oxidizers in a SBR treating extremely ammonium loaded landfill leachate and reject water. Van Hulle *et al.* (2004) also evaluated the influence of free ammonia and nitrous acid concentrations in nitrifying biomass from a continuous SHARON reactor.

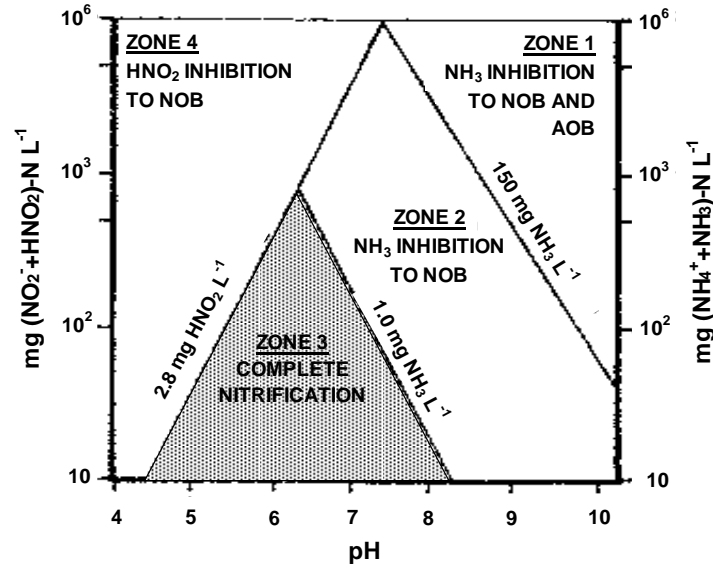


Figure 1.6 – Influence of free ammonia and undissociated nitrous acid concentrations on the activity of ammonium oxidizers and nitrite oxidizers (Anthonisen *et al.*, 1976)

Effect of Dissolved Oxygen (DO) concentration

Dissolved oxygen is an essential nutrient for nitrification. It is generally accepted that as dissolved oxygen decreases it becomes the growth limiting substrate. This is expressed by a double Monod switching function relating the rate of autotrophic biomass growth to $\text{NH}_4^+\text{-N}$ and DO as shown in Equation 1.7. In this Equation, r_{XA} is the autotrophic growth rate, S_O is the DO concentration and K_{OA} is the oxygen affinity constant for autotrophic biomass and X_{BA} is the autotrophic biomass concentration.

$$r_{X,A} = \mu_{m,A} \frac{S_{NH}}{K_{NH} + S_{NH}} \frac{S_O}{K_{O,A} + S_O} X_{B,A} \quad (1.7)$$

There is no consensus for the level of K_{OA} to be incorporated in the rate equation. The reported values range from 0.002 mg $\text{O}_2 \text{ L}^{-1}$ (Dold and Marais, 1986) to 2.0 mg $\text{O}_2 \text{ L}^{-1}$

(EPA, 1975). The wide range of K_{O_A} may be attributed to the fact that DO concentration inside the floc where the oxygen consumption takes place, is not necessarily the same as in the bulk liquid. Actually, the DO concentration inside the floc is likely to be less than the bulk DO depending on the physical properties of the floc, and will be greatly affected by the degree of mixing in the growth reactor. For model simulation purposes, a value of $0.5 \text{ mg O}_2 \text{ L}^{-1}$ is recommended (Henze *et al.*, 2000).

The two major steps of nitrification are reported to exhibit different responses to dissolved oxygen variations. NOB is somewhat more affected by low dissolved oxygen concentrations than AOB. The different impact of DO on nitrite and nitrate formation mechanisms may lead to nitrite accumulation at low dissolved concentrations. Several authors (Piciorneau *et al.*, 1997; Garrido *et al.*, 1997; Pollice *et al.*, 2002) have observed stable nitrite accumulation at reduced DO concentrations. Figure 1.7 shows the nitrite accumulation registered by Piciorneau *et al.* (1997) when working with a biofilm airlift suspension reactor working at low dissolved oxygen concentrations. As observed in this Figure, nitrite accumulation took place when working below $1.5 \text{ mg O}_2 \text{ L}^{-1}$. However, this strategy alone was not enough to completely avoid nitrate formation, which is in concordance with the observations of Van Loosdrecht and Salem (2005).

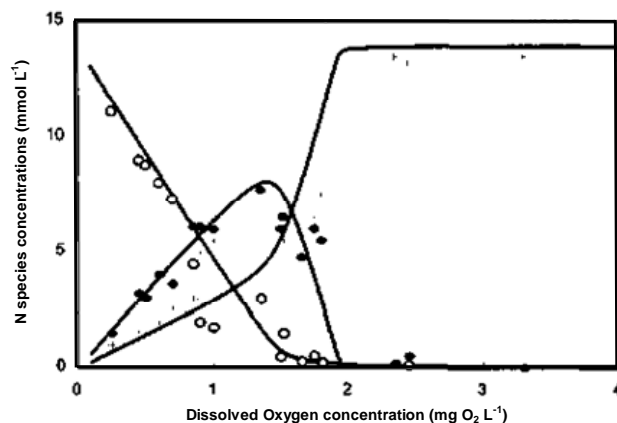


Figure 1.7 - Effect of DO concentration on nitrification and nitrification kinetics (Piciorneau *et al.*, 1997)

Effect of pH

The rate of nitrification is extremely sensitive to the pH of the medium for two main reasons (Orhon and Artan, 1994): there is a significant inhibitory action by both hydrogen

H^+ and hydroxyl OH^- ions on the growth rate of nitrifiers; and nitrification consumes the alkalinity of the medium, with a potential drop in pH. Grunditz and Dalhammar (2001) evaluated the effect of pH on the activity of isolated AOB (Nitrosomonas) and NOB (Nitrobacter) cultures. Figure 1.8 shows their results, that clearly show that there is an optimum pH range of 7.5 to 8.5 for the growth of nitrifiers. These experimental results were corroborated by Van Hulle *et al.* (2004). The efficiency of both nitrification declines as pH is lowered to the acid range. The adverse low pH effects can be reduced (not avoided) when biomass is acclimated to these conditions (Orhon and Artan, 1994). In the alkaline range, nitrification is not significantly impaired up to a pH of 9.5. In the results of Figure 1.8, NOB is more affected by basic pH than AOB.

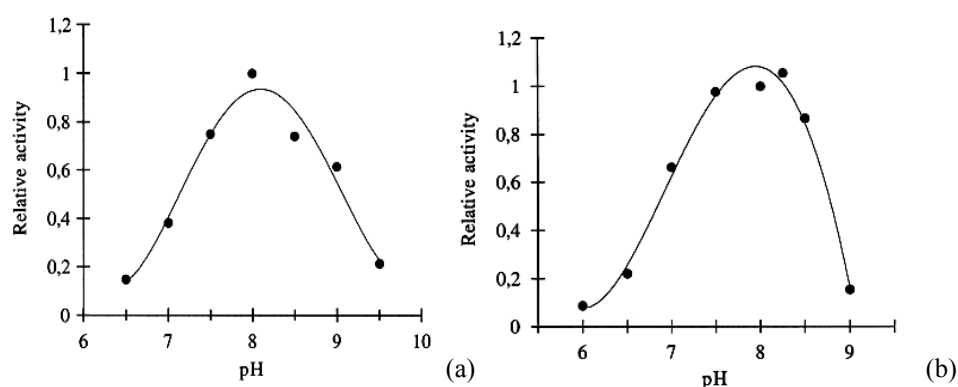


Figure 1.8 - Effect of pH on the activity of isolated Nitrosomonas (a) and Nitrobacter (b) cultures (Grunditz and Dalhammar, 2001)

Effect of inhibitors

Nitrifiers are affected by some organic and inorganic compounds which inhibit nitrification. Thiourea is a typical example of these compounds: it is the common inhibitor to block nitrification in the Standard BOD test.

Moreover, the presence of excess organic matter and heterotrophic microorganisms can lead to an indirect effect by reducing the DO concentration or modifying the pH which has an inhibitory effect on nitrification kinetics. If such environmental changes are controlled, no adverse effect on nitrification should be expected from the combined activity of heterotrophs and autotrophs (Orhon and Artan, 1994).

The actual tendency to treat highly ammonium loaded wastewaters by biological nitrogen removal (BNR) processes is to apply the nitrification/denitrification process over nitrite, taking advantage of the different influence of the aforementioned parameters on AOB and NOB. The BNR over nitrite suggests a saving of the 25% of the aeration costs and 40% of the external carbon source needed during denitrification, as well as a reduction in the amount of sludge produced. Moreover, if a combined SHARON/Anammox process (as detailed in section 1.3.2.2.2) is applied, it avoids the requirement of organic carbon source to denitrify, allows saving over 65% of the oxygen supply and produces little sludge (Fux *et al.*, 2002).

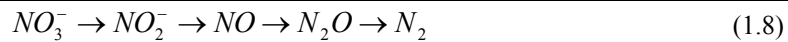
1.3.2.2 Denitrification

Denitrification (in combination with nitrification) is the most widely used nitrogen removal process for wastewaters. It is essentially a biochemical reaction which converts oxidized inorganic nitrogen to nitrogen gas (N₂). Denitrification converts soluble forms of nitrogen, which can harm the environment, into insoluble gaseous form, which have no significant effect on environmental quality.

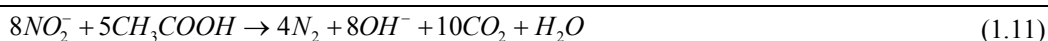
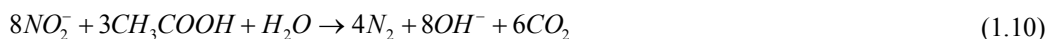
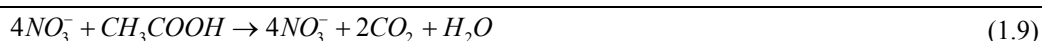
Basically there are two types of denitrification that take place under anoxic conditions: heterotrophic and autotrophic denitrification. Heterotrophic denitrification consumes organic matter, while autotrophic denitrification can use ammonia (Anammox) or sulphide (Kleerebezem and Méndez, 2002; Garbossa *et al.*, 2005). Conventional denitrification and Anammox, concomitantly with the environmental factors that can affect both processes, are detailed below.

1.3.2.2.1 Heterotrophic denitrification

Conventional denitrification is the reduction of NO₃⁻ to N₂ following the sequence indicated in Expression 1.8 (Metcalf & Eddy, 1991). Factors favouring the formation of a particular end product are not clearly identified. However, N₂ is generally observed as the major end product of denitrification in wastewater treatment (Orhon and Artan, 1994).

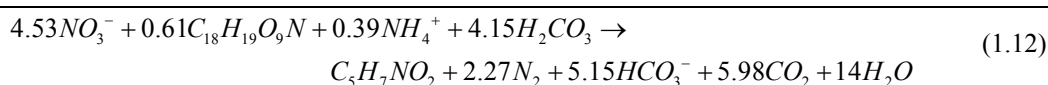


In a simplified context, denitrification is defined as a two-step process where NO_3^- is firstly reduced to NO_2^- (Equation 1.8) and further on to N_2 (Equation 1.9) by the catabolism of heterotrophic bacteria. This process is carried out in absence of molecular oxygen and with a biodegradable carbon source, such as acetic acid, as electron donor and nitrite or nitrate as the terminal electron acceptor. In Equation 1.11, it is observed that the overall denitrification process produces OH^- and, consequently, alkalinity and a pH rise in the growth medium.



As opposed to nitrification, a relatively broad range of heterotrophic bacteria can accomplish denitrification. Common denitrification bacteria include *Achromobacter*, *Bacillus*, *Aerobacter*, *Micrococcus*, *Alcaligenes*, *Flavobacterium* and *Proteus* (Christensen and Harremoes, 1977). They are all facultative and use the same pathways during both aerobic and anoxic respiration (Orhon and Artan, 1994). Anoxic growth of heterotrophs produces less sludge than when working under aerobic conditions. In other words, the yield coefficient of facultative heterotrophic biomass (g of cell COD produced per g of COD consumed) is lower when using nitrite and/or nitrate as final electron acceptor than when using molecular oxygen (Orhon *et al.*, 1996; Muller *et al.*, 2004).

Equation 1.12 shows the overall denitrification reaction considering the synthesis of new cells and assuming a chemical biomass composition of $\text{C}_5\text{H}_7\text{NO}_2$ (Hoover and Porges, 1952). From this Equation, it is deduced an alkalinity production of 4.94 mg of HCO_3^- per mg of N denitrified. Therefore, the denitrification process compensates in part the alkalinity loss during nitrification.



When oxygen is present in the growth medium, the synthesis of nitrate reducing enzymes are repressed and switches the metabolic activity to aerobic respiration. However, some

studies have reported denitrification at positive dissolved oxygen concentrations (Siegrist *et al.*, 1998). Denitrification under apparent aerobic conditions is usually attributed to the existence of an oxygen gradient within the bacterial floc (or granule), creating an interior region which is practically devoid of oxygen. This fact has led to the integration of nitrification and denitrification processes in a single aerated reactor with biomass in biofilm or granules, where denitrifying organisms are active in the internal layers of the biofilm or granule (Arrojo *et al.*, 2004; Van Loosdrecht and Salem, 2006).

The main *factors affecting denitrification kinetics* are detailed below:

Effect of Dissolved Oxygen (DO) concentration

As previously explained, the presence of oxygen is detrimental to denitrification. Provision of additional organic matter to act as electron donor is necessary to remove any dissolved oxygen which enters to the anoxic reactor. The inhibitory effect of DO concentration has been observed at DO concentrations as low as 0.13 mg O₂ L⁻¹ (Orhon and Artan, 1994).

To take into account the effect of DO concentration, the IWA Activated Sludge Models (Henze *et al.*, 2000) propose the insertion of a non-competitive inhibition switching function for DO as shown in Equation 1.13, where $\mu_{H, DN}$ is the actual growth rate of denitrifiers, $\mu_{max, H, DN}$ is the maximum growth rate of denitrifiers without considering DO effect, K_{OH} is the oxygen inhibition constant for heterotrophs and S_O is the DO concentration in the growing medium. A typical value for K_{OH} is 0.2 mg O₂ L⁻¹ (Henze *et al.*, 2000)

$$\mu_{H, DN} = \mu_{m, H, DN} \frac{K_{OH}}{K_{OH} + S_O} \quad (1.13)$$

Effect of substrate concentration: Organic substrate and NO_x⁻-N

The specific growth rate for denitrifiers is expressed in terms of double Monod-type function, and includes both organic matter and nitrate concentrations acting as carbon source and electron acceptors in denitrification. The specific growth rate of denitrifiers also includes the non-competitive inhibition term for DO concentration as expressed in

Equation 1.14. In this mathematical expression S_S is the concentration of the carbon source, S_{NO} is the NO_x^- -N concentration, K_S is the half-saturation constant for the carbon source, and K_{NO} is the half-saturation constant for the NO_x^- -N.

$$\mu_{H, DN} = \mu_{m, H, DN} \frac{S_S}{K_S + S_S} \frac{S_{NO}}{K_{NO} + S_{NO}} \frac{K_{OH}}{K_{OH} + S_O} \quad (1.14)$$

With this expression, NO_x^- -N is assumed to exert a similar effect to that of its counterpart, DO, on aerobic growth. Experimental values commonly associated to K_{NO} are in the range 0.1-0.5 mg NO_3^- -N L^{-1} (Orhon and Artan, 1994; Henze *et al.*, 2000). Therefore, denitrification kinetics are not affected for NO_3^- -N values higher than 1 mg NO_3^- -N L^{-1} .

On the other hand, the organic carbon used in the denitrification process must be biodegradable and could come from several sources: organic matter present in wastewater, organic matter produced due to the lysis of biomass, and/or a biodegradable external carbon source (methanol or acetic acid). However, specific growth rate for denitrifiers would depend on the quality of this biodegradable organic matter. Figure 1.9 shows the denitrification rate registered by Henze *et al.* (2002) when using several carbon sources to reduce NO_3^- -N to N_2 . As observed, the use of endogenous carbon coming from the lysis of biomass leads to a very reduced denitrification rate when compared with that obtained using carbon of raw wastewater or an external readily biodegradable substrate.

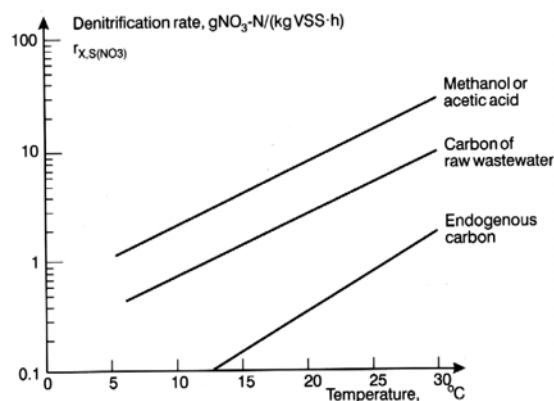


Figure 1.9 – Influence of the quality of biodegradable organic substrate and temperature on denitrification kinetics (Henze *et al.*, 2002)

Effect of Temperature

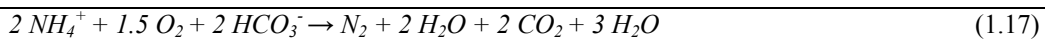
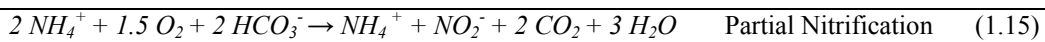
As in other biochemical reactions, rate constants of denitrification are affected by temperature as shown in Figure 1.9. The relationship between kinetic constants and temperature is generally described by Arrhenius expressions (see Equation 1.5). A temperature factor (θ) of 1.07 is commonly used in literature to take into account temperature influence on heterotrophic biomass (Henze *et al.*, 2000).

Effect of pH

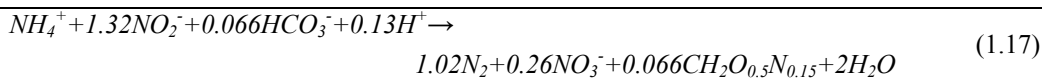
The rate of denitrification is generally observed to be depressed below pH 6.0 and above pH 8.0 (Orhon and Artan, 1994). In general, the highest rates are reported for a pH range of 7.0-7.5. Consequently, in nitrification/denitrification processes it is interesting to maintain the operating pH range near neutrality. This fact can be achieved by the addition of lime (Krishnamoorthy and Loer, 1989) or by inserting intermediate anoxic steps to denitrify the already produced NO_x^- -N (Hao and Kim, 1990). The second option is to be preferred, since it is more economic.

1.3.2.2.2 Anaerobic Ammonium Oxidation (Anammox)

The Anammox (ANAerobic AMMonium OXidation) process consists on the oxidation of ammonium with nitrite as the electron acceptor. This process need to be preceded by a partial nitrification unit, where total NH_4^+ -N should be oxidised for about 50% to NO_2^- -N by Ammonium Oxidizing Biomass (AOB) as presented in Equation 1.15. Subsequently, the Anammox process converts ammonium together with nitrite (electron acceptor) directly to dinitrogen gas under anoxic conditions in the absence of any organic carbon source, following the reaction in Equation 1.16. The overall reaction without considering biomass growth is shown in Equation 1.17. When compared with conventional nitrification/denitrification (see Equations 1.3 and 1.11), this completely autotrophic process avoids the requirement of organic carbon source to denitrify, allows saving over 65% of the oxygen supply and produces little sludge (Fux *et al.*, 2002).



If catabolism and anabolism of Anammox biomass are considered, the stoichiometric nitrite to ammonium ratio on molar basis is 1.32, as observed in Equation 1.18 (Jetten, 1999; van Dongen *et al.*, 2001; Mosquera-Corral *et al.*, 2005). Moreover, a small amount of alkalinity and nitrate are also produced.



Several Anammox organisms have been detected by PCR, phylogenetic analysis or FISH in both wastewater treatment and natural systems: *Candidatus* "Brocadia Anammoxidans", *Candidatus* "Kuenenia stuttgartiensis", *Candidatus* "Scalindua brodae", *Candidatus* "Scalindua wagneri" and *Candidatus* "Scalindua sorokinii" (Schmid *et al.*, 2003; Kuypers *et al.*, 2003).

The main factors affecting Anammox kinetics are discussed below:

Effect of Temperature

Similarly to nitrifiers and heterotrophic denitrifiers, Anammox rate constants are highly affected by temperature. Strous *et al.* (1999) studied the effect of temperature on Anammox biomass treating synthetic wastewater, obtaining an optimum removal of nitrite at 40 ± 3 °C (see Figure 1.10). These authors registered a null Anammox activity at 10°C and observed an Arrhenius type dependency (see Equation 1.5) between 20 and 37 °C. The results of Strous *et al.* (1999) are consistent with the results obtained by Egli *et al.* (2001), that situated the optimum Anammox activity at 37 °C for an enriched Anammox culture from a rotating disk contactor (minimum and maximum operating temperature: 10 and 43 °C, respectively). Yang *et al.* (2006) reported that the optimum temperature for Anammox biomass is between 30-35 °C. Toh *et al.* (2002) tried to select and enrich Anammox biomass at 37 and 55 °C, but thermophilic Anammox organisms could not be selected.

Moreover, Rysgaard *et al.* (2004) analyzed the Anammox activity in permanently cold (from -1.7 to 4 °C) sediments and reported an optimum temperature of 12 °C. These authors observed measurable Anammox activity between -2 and 30 °C. Dalsgaard and Thamdrup (2002) also studied the effect of temperature on Anammox activity in marine sediments, and reported an optimal ammonium removal rate at 15 °C and a sharply

decrease above 25°C. At 32°C the Anammox activity observed by these authors was almost zero. Consequently, it seems that in an Arctic environment, Anammox organisms are adapted to low temperatures.

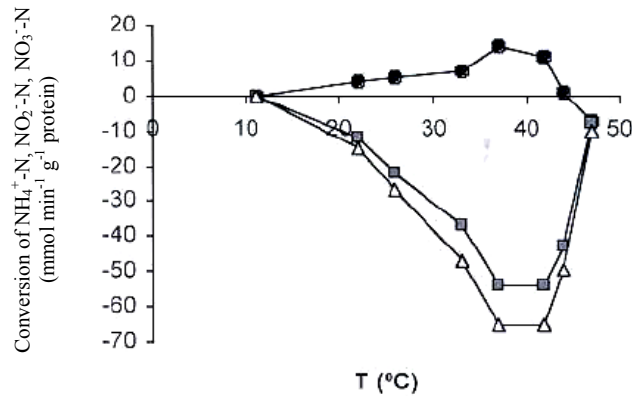


Figure 1.10 – Influence of temperature on the production of $\text{NO}_3^-\text{-N}$ (●) and removal of $\text{NH}_4^+\text{-N}$ (□) and $\text{NO}_2^-\text{-N}$ (▲) in Anammox biomass treating synthetic wastewater (Strous *et al.*, 1999)

Effect of pH

Strous (2000) analysed the pH influence on Anammox activity at 33 °C. This author detected a physiological pH range of 6.7 to 8.3, with an optimum at pH 8.0 (see Figure 1.11). Considering that the Anammox biomass analysed by Strous (2000) has been enriched for prolonged periods at pH 7.5 – 8.0 and 30°C, it was not surprising this pH dependency. However, if Anammox biomass is enriched and cultivated at different conditions (acid or alkaline pH), it could be able to cope with pH values outside this range.

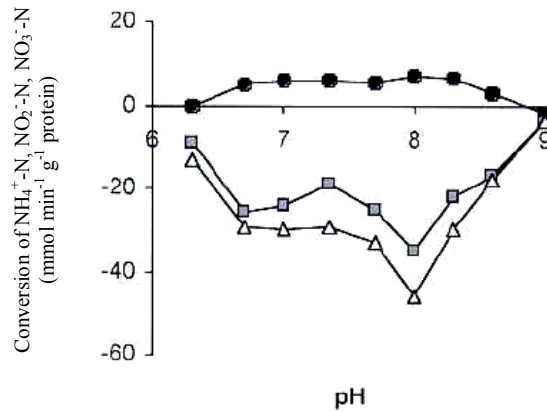


Figure 1.11 – Influence of pH on the production of $\text{NO}_3^-\text{-N}$ (●) and removal of $\text{NH}_4^+\text{-N}$ (□) and $\text{NO}_2^-\text{-N}$ (▲) in Anammox biomass treating synthetic wastewater at 33°C (Strous *et al.*, 1999)

Effect of substrates ($\text{NH}_4^+\text{-N}$ and $\text{NO}_2^-\text{-N}$) and products ($\text{NO}_3^-\text{-N}$)

According to Van Hulle (2005), the Anammox process is not inhibited by $\text{NH}_4^+\text{-N}$ or by the byproduct $\text{NO}_3^-\text{-N}$ up to concentrations of at least 1 g N L^{-1} . Strous *et al.* (2000) performed experiments in which Anammox biomass was exposed to high concentrations (up to 70 mM) in a Sequencing Batch Reactor during one week without observable inhibition to Anammox activity. However, Dapena-Mora *et al.* (2007a) performed denitrification batch assays to evaluate the effect at short time of both $\text{NH}_4^+\text{-N}$ and $\text{NO}_3^-\text{-N}$ on Anammox activity. As shown in Figure 1.12, the $\text{NH}_4^+\text{-N}$ and $\text{NO}_3^-\text{-N}$ concentrations encountered to achieve a 50 % of inhibition were 55 mM and 45 mM, respectively. Moreover, Fernández (2006) studied the $\text{NH}_4^+\text{-N}$ effect at long time on zeolite-attached Anammox biomass treating synthetic wastewater, obtaining that biomass activity began to be declined at free ammonia concentrations of $30,1 \text{ mg NH}_3\text{-N L}^{-1}$.

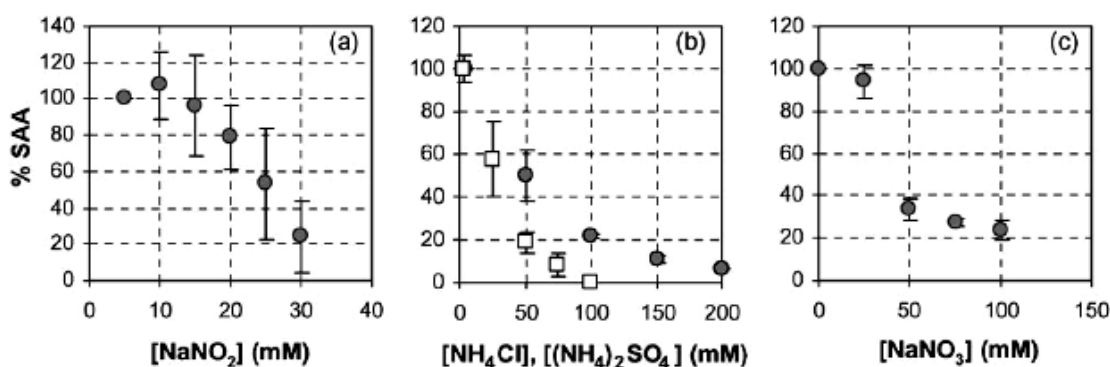


Figure 1.12 – Influence of $\text{NO}_2^-\text{-N}$ (a), $\text{NH}_4^+\text{-N}$ (b) and $\text{NO}_3^-\text{-N}$ (c) concentrations on the Anammox activity at short time. (Dapena-Mora *et al.*, 2007a)

On the other hand, the Anammox activity is very sensitive to $\text{NO}_2^-\text{-N}$ concentrations. Strous *et al.* (1999) found that the Anammox process was completely inhibited in the presence of more than $100 \text{ mg NO}_2^-\text{-N L}^{-1}$. Later, Egli *et al.* (2001) reported that the Anammox process was only inhibited at concentrations higher than $182 \text{ mg NO}_2^-\text{-N L}^{-1}$. Fux (2003) observed an inactivation of Anammox organisms when $40 \text{ mg NO}_2^-\text{-N L}^{-1}$ were maintained over a period of several days. Dapena-Mora *et al.* (2007a) determined the effect at short time of $\text{NO}_2^-\text{-N}$ on Anammox biomass and reported a 50% of inhibition on Anammox activity when working with 25 mM (see figure 1.12a).

Effect of dissolved oxygen

Van de Graaf *et al.* (1996) demonstrated in batch activity tests that dissolved oxygen completely inhibits the Anammox process at concentrations above $0.01 \text{ mg O}_2 \text{ L}^{-1}$. Strous *et al.* (1997) reported that Anammox activity is inhibited even under microaerobic conditions but this inhibition is reversible. In fact, this reversible inhibition makes partial nitrification and anammox possible in one reactor (Strous *et al.*, 1997).

Effect of organic matter and light

At prolonged periods, carbon sources (such as acetate, glucose and pyruvate) in the growing media of Anammox biomass have a negative impact, since they favour the growth of heterotrophic bacteria. However, in recent studies, it has been observed that the presence of some particular organic compounds, such as propionate, stimulates Anammox activity in continuous assays (Güven *et al.*, 2005). Van der Graaf *et al.* (1996) also detected that visible light provoked a decrease in activity of 30-50 %.

Table 1.2 – Industrial Anammox plants (Abma *et al.*, 2007)

Plant	Wastewater treated	Design capacity (kg N day ⁻¹)	Actual capacity (kg N day ⁻¹)	Start-up time
Rotterdam (The Netherlands)	Sludge reject water	490	750	3.5 years
IWL, Lichtenvoorde (The Netherlands)	Tannery wastewater	325	150	1 year
Waterstromen, Olburger (The Netherlands)	Potatoes Processing	1200	700	6 months
Semiconductor plant, Mie (Japan)	Wastewater from Semiconductor plant	220	220	2 months

Nowadays, there are only four industrial plants using the Anammox process: three in the Netherlands and the other in Japan (Abma *et al.*, 2007; Dapena-Mora *et al.*, 2007b). In Table 1.2, the type of wastewater treated, concomitantly with the actual nitrogen loading rate and time taken to start-up the process is shown. As observed, the Anammox process is used to treat several kind of wastewaters, which demonstrates the wide application of this technology. Moreover, its important to highlight that the time taken to start-up the plants has experienced a high decrease, since the inoculum availability and the practical

experience with this process has increased in the last years. Therefore, it is expected that the Anammox technology will have a widespread application in the immediate future.

1.4 MODELLING OF BIOLOGICAL NITROGEN REMOVAL

The need for a reliable basis for performance prediction in activated sludge systems led several investigators to propose mathematical models describing biological nutrient removal mechanisms. The use of mathematical models to design, enlarge or optimise wastewater treatment plants has provided excellent results (Copp *et al.*, 2002; Seco *et al.*, 2004). Some advantages of using models to design wastewater treatment units are :

- *Modelling leads to a better understanding of the real behaviour of a biological system.*
- *Mathematical models can be used to compare obtained results for different strategies or reactor configurations that could be feasible.*
- *Operating strategies and/or control systems can be designed on the basis of simulation.*

Biological treatment systems relies on the removal of pollutants from wastewaters through a series of complex biochemical reactions. To describe these biochemical processes, more accurate predictions will be obtained when more number of components and processes will be included in a mathematical model. However, a complicated model will also increase calculation efforts and the complexity of wastewater characterisation and model calibration. Consequently, a biological model is always an intermediate situation. On the one hand, enough components and processes must be considered to represent a wide range of operating conditions in a reliable way. On the other hand, the number of equations and parameters considered must be sufficiently reduced to apply the model without excessive complications.

Moreover, it is important to highlight that an increasing number of the parameters and processes considered in a model, usually leads to a reduction in the variability of parameters. Therefore, using similar values for model parameters, the model could reproduce a wide variety of situations. Consequently, the complexity of a model can sometimes avoid the necessity of calibrating several model parameters, which reduces calibration efforts.

1.4.1 IWA Activated Sludge Models

In the early 1980s, the International Water Association (IWA) formed a task group to develop a new model which incorporated biological carbon removal, nitrification and denitrification. This model was initially published in 1987 as the Activated Sludge Model No.1 (ASM1; Henze *et al.*, 1987) and considered two types of bacteria (heterotrophic and autotrophic) and 8 biological processes. In 1999, the Activated Sludge Model No.2d (ASM2d; Henze *et al.*, 1999) and the Activated Sludge Model No.3 (ASM3; Gujer *et al.*, 1999) were published as an extension of ASM1, considering biological phosphorous removal and intracellular accumulation of organic substrates, respectively.

Taking into account the objectives of this work, in the following paragraphs it is detailed the modelling of the biological removal of carbon and nitrogen as considered in the ASM models (Henze *et al.*, 2000).

1.4.2. Stoichiometry and Kinetics in Activated Sludge Models

The transformations carried out by microorganisms can be described as biochemical reactions defined by stoichiometric relations and kinetic equations.

Stoichiometry relates the quantity of reactives consumed with the quantity of products generated during a biochemical reaction. Since biological reactions are very complex, a component can be a reactive in one reaction, the product in other one, and inert in the rest. Consequently, the net production of a component is the sum of kinetic rates of the reactions in which it contributes multiplied by its corresponding stoichiometric coefficient (see Equation 1.18). In Equation 1.18, r_i is the transformation rate of a component “i”, $\nu_{i,j}$ is the stoichiometric coefficient of component “i” in reaction “j”, and r_j is the rate of reaction “j”. If r_i is positive, it means that the component “i” is generated in the overall process, but if it is negative, the component “i” is consumed in the whole process.

$$r_i = \sum_{j=1}^n \nu_{i,j} r_j \quad (1.18)$$

The kinetics of biological growth are usually represented by a first order kinetics as presented in Equation 1.19, where r_X is the biomass growth rate, μ is the specific growth rate and X is the biomass concentration.

$$r_X = \mu X \quad (1.19)$$

The effect of a limitant substrate or nutrient in microbial specific growth rate is commonly described by the Monod expression shown in Equation 1.20 (Monod, 1942), which was obtained in an empirical deduction from pure cultures studies. In Equation 1.20, μ_{max} is the maximum specific growth rate, S is the substrate concentration and K_S is the half-saturation constant for substrate. The term that corrects μ_{max} is commonly called Switching function and is of great importance in the modelling of biological treatment processes.

$$\mu = \mu_{max} \left(\frac{S}{K_S + S} \right) \quad (1.20)$$

Figure 1.13 shows the plot of a switching function ($S/(K_S+S)$) versus the limiting substrate (S). As observed, the value of the switching function is between 0 and 1. For substrate concentrations very higher than the K_S value, the switching function is close to 1. However, when substrate concentration is being consumed, the switching function is reduced and, therefore, the value of the actual specific growth rate decreases. In Figure 1, it is observed that the K_S value corresponds to the substrate concentration that yields a switching function value of 0.5.

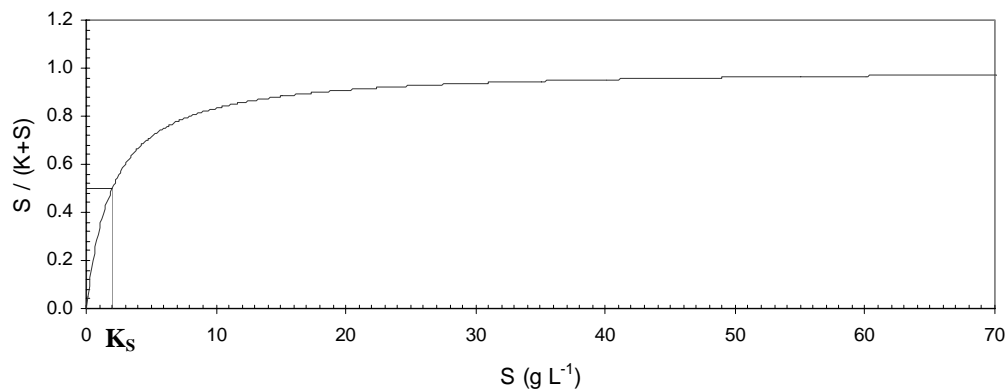


Figure 1.13 – Plot of the switching function versus substrate concentration.

The inclusion of switching functions in biological rate equations lets to include in a same model a lot of biological process without previously knowledge of which processes will occur inside the modelled system. If each kinetic equation includes switching functions of every substrate necessary to carry out the process, the model will predict the growth and development of those microorganisms without limitations.

If more than one substrate is necessary to perform a biological process, the ASM models consider their influence by including as much switching functions as more substrates are necessary (interactive model). Equation 1.21 shows this interactive model where S_1 and S_2 are the concentration of the limiting substrates, and $K_{S,1}$ and $K_{S,2}$ their correspondent half-saturation constants.

$$r_X = \mu_{\max} \left(\frac{S_1}{K_{S,1} + S_1} \right) \left(\frac{S_2}{K_{S,2} + S_2} \right) X \quad (1.21)$$

The substrate removal rate is correlated to the rate of biomass growth, since they obtain energy from the substrate oxidation. Considering the produced biomass per unit of substrate consumed (yield coefficient, Y), the correlation between the substrate removal rate (r_S) and the biomass growth rate (r_X) is the one presented in Equation 1.22.

$$r_S = \frac{1}{Y} r_X \quad (1.22)$$

Several processes can lead to a decrease in biomass concentration: predation, cellular maintenance and lysis. All these processes are usually agrupated in one overall process known as *decay*. For simulation purposes, the decay process is modelled as a first order kinetics as presented in Equation 1.23, where r_{DECAY} is the biomass decay rate, b is the specific decay rate and X is the biomass concentration.

$$r_{DECAY} = b X \quad (1.23)$$

1.4.3. Format and notation

The IWA Activated Sludge Models (Henze *et al.*, 2000) proposed a matrix format for a clear and structured presentation of reaction kinetics. This approach provides all the

necessary information about model components, processes and stoichiometric coefficients so that the observed conversion rate for each component is defined in a systematic way. To illustrate the use of the matrix format and the notation, a simple example is given below (from Orhon and Artan, 1994).

As previously mentioned, growth and decay are the two fundamental processes traditionally associated with organic matter removal in activated sludge. These two processes involve a minimum of 3 components: heterotrophic biomass (X_{BH}), substrate (S_S) and dissolved oxygen (S_O). As shown in Table 1.3, the matrix representation involves listing the two processes considered (j) down the left side of the table and the three components (i) across the top. The process rate expressions r_j are given in the right side of the matrix. The stoichiometric coefficients, v_{ij} , are included in the body of the matrix and relate the reaction rate of the constituent " i ", r_{ij} , to the process rate r_j . Then, the transformation rate of a component " i " (r_i) can be calculated by means of Equation 1.18.

Table 1.3 – Process kinetics and stoichiometry for heterotrophic bacterial growth in an aerobic environment.

Component $i \rightarrow$	Biomass (mg COD L ⁻¹)	DO (mg O ₂ L ⁻¹)	Substrate (mg COD L ⁻¹)	
Process $j \downarrow$	X_{BH}	S_O	S_S	\downarrow reaction rate, r_j
<i>Aerobic growth of heterotrophs on S_S</i>	1	$-\left(\frac{1-Y_H}{Y_H}\right)$	$-\left(\frac{1}{Y_H}\right)$	$\mu_{mH} \frac{S_S}{K_S + S_S} \frac{S_O}{K_{OH} + S_O} X_{BH}$
<i>Decay of heterotrophs</i>	-1	-1		$b_H X_{BH}$

For the particular case of carbon removal in aerobic conditions, in Table 1.3 the first line corresponds to the aerobic heterotrophic growth ($j=1$) and the second one to the decay of heterotrophs ($j=2$). For example, the observed biomass conversion rate (r_1) is the stoichiometric coefficient v_{11} (=1) multiplied by the reaction rate referred to aerobic heterotrophs (r_1) plus the stoichiometric coefficient v_{12} (= -1) multiplied by the reaction rate referred to heterotrophic decay (r_2). The conversion rates for heterotrophic biomass, dissolved oxygen and organic substrate can be checked in Equations 1.24, 1.25 and 1.26, respectively. In these equations, Y_H is the heterotrophic yield coefficient, $\mu_{max,H}$ is the heterotrophic maximum specific growth rate constant, b_H is the heterotrophic specific

decay rate constant and K_{OH} is the oxygen half-saturation constant for heterotrophic biomass.

$$r_1 = \frac{d X_{BH}}{dt} = \mu_{\max,H} \frac{S}{K_S + S} X_{BH} - b_H X_{BH} \quad (1.24)$$

$$r_2 = \frac{d S_O}{dt} = -\frac{(1 - Y_H)}{Y_H} \mu_{\max,H} \frac{S}{K_S + S} X_{BH} - b_H X_{BH} \quad (1.25)$$

$$r_3 = \frac{d S}{dt} = -\frac{1}{Y_H} \mu_{\max,H} \frac{S}{K_S + S} X_{BH} \quad (1.26)$$

Moreover, for each line in the matrix of Table 1.3 (corresponding to an isolated biochemical reaction, j) a continuity equation must be applied. These continuity equations are equivalent to mass and/or electric charge balances. Equation 1.27 shows the general mathematical expression of a continuity function for a biochemical reaction ' j ' and material ' c ' subject to conservation (namely, COD, Nitrogen, Phosphorous, carbon, ...). In Equation 1.27, ν_{ij} is the stoichiometric coefficient for component ' i ' in process ' j ' and $i_{c,i}$ is the content of ' c ' in the component ' i '.

$$\sum_{i=1}^n \nu_{i,j} i_{c,i} = 0 \quad (1.27)$$

Usually, the conversion factors are listed in a Table known as the composition matrix. For the case of carbon removal in aerobic conditions, the composition matrix for COD is presented as Table 1.4. Equation 1.28 shows the application of the continuity equation for COD ($c=COD$).

Table 1.4 – Composition matrix for COD

Component	Units	$[i_{COD,i}]$ (g COD)
S_O	(g O ₂)	-1
S_S	(g COD)	1
X_{BH}	(g COD)	1

$$\sum_{i=1}^n \nu_{i,j} i_{c,i} = 1 \cdot 1 - \left(\frac{1 - Y_H}{Y_H} \right) (-1) - \left(\frac{1}{Y_H} \right) 1 = 0 \quad (1.28)$$

1.4.4. Carbon and Nitrogen components considered in Activated Sludge Models

The IWA Activated Sludge Models (Henze *et al.*, 2000) distinguish two types of components: soluble and particulated. Soluble components are identified by an S with an indicative subindex and particulate components are identified by an X with an indicative subindex.

Suspended components are assumed to be associated to activated sludge and can be concentrated in a thickener and/or settler. However, soluble components are always transported in the wastewater. Soluble and particulated components are not necessarily differentiated by filtration through 0.45 μ membrane filters. Some of these components are defined by their interaction with the biomass and require bioassays for their analysis. All particulate model components must be electrically neutral (no ionic charges), while soluble components may carry ionic charge.

Both soluble and particulated components considered in the model ASM2d (Henze *et al.*, 1999) and related to biological carbon and nitrogen removal are described below.

Soluble components

S_A (mg COD L^{-1}) : Fermentation products. This carbon source comes from the fermentation of organic matter (process considered in the model). For all stoichiometric computations it is considered to be acetate, since it is the volatile fatty acid produced in major percentage during fermentation.

S_{ALK} (mol HCO_3^- L^{-1}) : Alkalinity of the wastewater. Alkalinity is introduced in the model to have an early indication of possible low pH conditions, which may inhibit some biological processes. For all stoichiometric computations it is assumed to be exclusively HCO_3^- .

S_F (mg COD L^{-1}) : Fermentable, readily biodegradable organic substrates. This soluble COD fraction is readily available for biodegradation by heterotrophic organisms. Since it is assumed that S_F can serve as substrate for fermentation, it is not computed as S_A .

S_I ($mg\ COD\ L^{-1}$): Soluble non-biodegradable organic matter. The main characteristic of this component is that it could not be further degraded by microorganisms. This component may be part of the influent wastewater and it can be generated during the hydrolysis of suspended organic matter.

S_{N_2} ($mg\ N_2-N\ L^{-1}$): gaseous nitrogen. The ASM2d model assumes that it is the only product of denitrification, since it is generally observed as the major end product of denitrification in wastewater treatment (Orhon and Artan, 1994). N_2 may be subject to gas exchange.

S_{NH} ($mg\ NH_4^+-N\ L^{-1}$): Ammonium plus ammonia nitrogen. For the balance of electrical charges, S_{NH} is assumed to be NH_4^+ .

S_{NO} ($mg\ NO_x^- -N\ L^{-1}$): Nitrite plus nitrate nitrogen ($NO_2^- -N + NO_3^- -N$). For all stoichiometric computations (COD continuity functions), S_{NO} is considered to be exclusively NO_3^- .

S_O ($mg\ O_2\ L^{-1}$): Dissolved Oxygen. This component may be subject to gas exchange and it is a substrate for aerobic organisms and an inhibitor to denitrification.

Suspended components

X_{BA} ($mg\ COD\ L^{-1}$): autotrophic nitrifying biomass. It is responsible of the nitrification process and it is strictly aerobic. Nitrifying organisms include AOB and NOB.

X_{BH} ($mg\ COD\ L^{-1}$): Heterotrophic biomass. These microorganisms are facultative. They can grow under both aerobic and anoxic conditions and are capable to fermentate S_F under anaerobic conditions. Moreover, they are responsible of the hydrolysis of suspended organic matter.

X_I ($mg\ COD\ L^{-1}$): inert particulated organic material. This material is not degraded within the biological systems and it is flocculated onto the activated sludge. X_I may be a fraction of the influent wastewater or may be produced during biomass decay.

X_S (mg COD L⁻¹): Slowly biodegradable substrate. It represents high molecular weighted, colloidal and particulated organic substrates that must be hydrolyzed before being assimilated by cell synthesis. Products derived of hydrolysis of X_S (S_F) may be fermented.

X_{TSS} (mg TSS L⁻¹): Total suspended solids.

As previously explained in section 1.4.3, continuity equations are applied to COD, nitrogen, TSS and charge. Table 1.5 shows the conversion factors obtained from chemical stoichiometry, based on the definition of the model components. Nitrogen content in biomass can be calculated based on the chemical formula C₅H₇NO₂ (Hoover and Porges, 1952). On the other hand, the nitrogen content in each fraction of organic matter present in influent wastewater should be experimentally assessed for every specific case.

Table 1.5 – Composition matrix of the ASM2d (Henze *et al.*, 1999)

Component	Units	COD	N	TSS	Charge
		[<i>i</i> _{COD,i}]	[<i>i</i> _{N,i}]	[<i>i</i> _{TSS,i}]	[<i>i</i> _{Charge,i}]
		(g COD)	(g N)	(g TSS)	(mole charge +)
S_O	(g O ₂)	-1			
S_F	(g COD)	1	$i_{N,SF}$		
S_A	(g COD)	1			-1/64
S_{NH}	(g NH ₄ ⁺ -N)		1		1/14
S_{NO}	(g NO ₃ ⁻ -N)	-64/14	1		-1/14
S_I	(g COD)	1	$i_{N,SI}$		
S_{ALK}	(mol HCO ₃ ⁻)				-1
S_{N2}	(g N ₂ -N)	-24/14	1		
X_I	(g COD)	1	$i_{N,XI}$	$i_{TSS,XI}$	
X_S	(g COD)	1	$i_{N,XS}$	$i_{TSS,XS}$	
X_{BH}	(g COD)	1	$i_{N,Bm}$	$i_{TSS,Bm}$	
X_{BA}	(g COD)	1	$i_{N,Bm}$	$i_{TSS,Bm}$	
X_{TSS}	(g TSS)			1	

1.4.5. Biological carbon and nitrogen removal processes considered in ASM2d

The biological carbon and nitrogen removal processes considered in the ASM2d are described below aggrupated in two sections: heterotrophic and autotrophic processes. Moreover, Table 1.6 shows the kinetic rate equations considered and Table 1.7 the model

in a matrix format. As it will be further discussed in following chapters, this Activated Sludge Model can be enlarged or reduced depending on the specific characteristics of the biological system under study. As it is observed in Table 1.7, some stoichiometric parameters are obtained by applying the continuity functions as described in section 1.4.3.

Table 1.6 – Process rate equations for ASM2d (Henze *et al.*, 1999)

j	Process	Process rate equation ($r_j > 0$)
Heterotrophic biomass		
(1)	<i>Aerobic growth on fermentable substrate</i>	$\mu_{mH} \frac{S_F}{K_F + S_F} \frac{S_F}{S_A + S_F} \frac{S_O}{K_{OH} + S_O} \frac{S_{NH}}{K_{NH} + S_{NH}} \frac{S_{ALK}}{K_{ALK} + S_{ALK}} X_{BH}$
(2)	<i>Aerobic growth on fermentation products</i>	$\mu_{mH} \frac{S_A}{K_A + S_A} \frac{S_A}{S_A + S_F} \frac{S_O}{K_{OH} + S_O} \frac{S_{NH}}{K_{NH} + S_{NH}} \frac{S_{ALK}}{K_{ALK} + S_{ALK}} X_{BH}$
(3)	<i>Denitrification on fermentable substrate</i>	$\eta_{NO_3} \mu_{mH} \frac{S_F}{K_F + S_F} \frac{S_F}{S_A + S_F} \frac{K_{OH}}{K_{OH} + S_O} \frac{S_{NO}}{K_{NO} + S_{NO}} \frac{S_{ALK}}{K_{ALK} + S_{ALK}} X_{BH}$
(4)	<i>Denitrification on fermentation products</i>	$\eta_{NO_3} \mu_{mH} \frac{S_A}{K_A + S_A} \frac{S_F}{S_A + S_F} \frac{K_{OH}}{K_{OH} + S_O} \frac{S_{NO}}{K_{NO} + S_{NO}} \frac{S_{ALK}}{K_{ALK} + S_{ALK}} X_{BH}$
(5)	<i>Fermentation</i>	$q_F \frac{K_{OH}}{K_{OH} + S_O} \frac{S_{NO}}{K_{NO} + S_{NO}} \frac{S_F}{K_F + S_F} \frac{S_{ALK}}{K_{ALK} + S_{ALK}} X_{BH}$
(6)	<i>Aerobic hydrolysis</i>	$k_h \frac{S_O}{K_{OH} + S_O} \frac{X_S/X_{BH}}{K_X + X_S/X_{BH}} X_{BH}$
(7)	<i>Anoxic hydrolysis</i>	$\eta_{NO_3} k_h \frac{K_{OH}}{K_{OH} + S_O} \frac{S_{NO}}{K_{NO} + S_{NO}} \frac{X_S/X_{BH}}{K_X + X_S/X_{BH}} X_{BH}$
(8)	<i>Anaerobic hydrolysis</i>	$\eta_{fc} k_h \frac{K_{OH}}{K_{OH} + S_O} \frac{K_{NO}}{K_{NO} + S_{NO}} \frac{X_S/X_{BH}}{K_X + X_S/X_{BH}} X_{BH}$
(9)	<i>Decay of heterotrophs</i>	$b_H X_{BH}$
Autotrophic biomass		
(10)	<i>Aerobic growth of autotrophs</i>	$\mu_{mA} \frac{S_{NH}}{K_{NH} + S_{NH}} \frac{S_{ALK}}{K_{ALK} + S_{ALK}} \frac{S_O}{K_{OA} + S_O} X_{BA}$
(11)	<i>Decay of autotrophs</i>	$b_A X_{BA}$

Table 1.7 – Petersen Matrix of ASM2d (Henze *et al.*, 1999)

	S_0	S_I	S_F	S_A	S_{NH}	S_{ND}	S_{N2}	S_{ALK}	X_I	X_S	X_{EH}	X_{BA}	X_{TSS}
<i>Aerobic growth on fermentable substrate</i>	$-\left(\frac{1-Y_{II}}{Y_{II}}\right)$		$-\left(\frac{1}{Y_{II}}\right)$		$-i_{XB}$			(*)			1		(*) (1)
<i>Aerobic growth on fermentation products</i>	$-\left(\frac{1-Y_{II}}{Y_{II}}\right)$			$-\left(\frac{1}{Y_{II}}\right)$	$-i_{XB}$			(*)			1		(*) (2)
<i>Denitrification on fermentable substrate</i>			$-\left(\frac{1}{Y_{II}}\right)$		$-i_{XB}$	$-\left(\frac{1-Y_{II}}{2.86 Y_{II}}\right)$	$\left(\frac{1-Y_{II}}{2.86 Y_{II}}\right)$	(*)			1		(*) (3)
<i>Denitrification on fermentation products</i>				$-\left(\frac{1}{Y_{II}}\right)$	$-i_{XB}$	$-\left(\frac{1-Y_{II}}{2.86 Y_{II}}\right)$	$\left(\frac{1-Y_{II}}{2.86 Y_{II}}\right)$	(*)			1		(*) (4)
<i>Fermentation</i>			-1	1	(*)			(*)					(*) (5)
<i>Aerobic hydrolysis</i>		f_{SI}	$(1-f_{SI})$		(*)			(*)		-1			(*) (6)
<i>Anoxic hydrolysis</i>		f_{SI}	$(1-f_{SI})$		(*)			(*)		-1			(*) (7)
<i>Anaerobic hydrolysis</i>		f_{SI}	$(1-f_{SI})$		(*)			(*)		-1			(*) (8)
<i>Decay of heterotrophs</i>					(*)			(*)	f_{XI}	$1-f_{XI}$	-1		(*) (9)
<i>Aerobic growth of autotrophs</i>	$-\left(\frac{4.57-Y}{Y_A}\right)$				$-i_{XB} - \left(\frac{1}{Y_A}\right)$	$\left(\frac{1}{Y_A}\right)$		(*)			1		(*) (10)
<i>Decay of autotrophs</i>					(*)			(*)	f_{XI}	$1-f_{XI}$	-1		(*) (11)

(*) Stoichiometric parameters calculated from continuity equations

Heterotrophic processes

The biological processes carried out by this biomass are detailed below:

- *Aerobic heterotrophic growth*: Heterotrophic bacteria can use both fermentable substrate (S_F) and fermentation products (S_A) to produce new cells. ASM2d considers these two processes as parallel reactions with the same yield coefficient (Y_H) and maximum heterotrophic specific growth constant (μ_{mH}).
- *Anoxic heterotrophic growth*: Similarly to the aerobic heterotrophic growth, heterotrophic bacteria can grow using both S_A and S_F under anoxic conditions. These processes are similar to those described under aerobic conditions but using nitrate as the final electron acceptor instead of oxygen. Stoichiometry for nitrate has been calculated assuming that the only product of denitrification is dinitrogen gas (S_{N_2}); therefore, 1 mg of NO_3^- -N is equivalent to 2.86 mg of oxygen.

Moreover, a correction factor under anoxic conditions (η_{NO_3}) is used to reflect changes in the rates of microbial growth and substrate utilization when the system is switched from aerobic conditions to anoxic conditions. Two explanations are usually offered to justify the decreased removal rates under anoxic conditions (Orhon and Artan, 1994):

- *The maximum specific growth rate of heterotrophs is reduced under anoxic conditions*
- *A portion of heterotrophic biomass cannot use nitrate as the terminal electron acceptor.*

The ASM models (Henze *et al.*, 2000) consider that the heterotrophic yield coefficient (Y_H) is exactly the same under aerobic and anoxic conditions. However, this assumption is not really applicable, since some studies (Orhon *et al.*, 1996; Muller *et al.*, 2004) have demonstrated that the heterotrophic yield under anoxic conditions is reduced relative to its aerobic value.

- *Fermentation*: The model ASM2d considers that under anaerobic conditions, heterotrophic biomass is capable to transform fermentable substrate (S_F) into volatile fatty acids (S_A). Although this process leads to an heterotrophic growth, ASM2d does not

consider it in order to simplify the model and prevent the introduction of more kinetic and stoichiometric parameters.

- Hydrolysis: Colloidal substrates with high molecular weight can not be degraded directly by microorganisms and they must be previously hydrolysed. Hydrolysis consists on the conversion of high molecular weighted organic molecules (slowly biodegradable COD) to more simple molecules (readily biodegradable COD). This process is an extracellular enzymatic reaction. The ASM models (Henze *et al.*, 2000) consider that hydrolysis products are available in the growing media to its subsequent degradation.

The hydrolysis process rate highly depends on the terminal electron acceptor. Therefore, three types of hydrolysis are considered in the ASM2d model: Anaerobic hydrolysis ($S_O=0$; $S_{NO}=0$), anoxic hydrolysis ($S_O=0$; $S_{NO}>0$) and aerobic hydrolysis ($S_O>0$).

As observed in the Petersen Matrix of Table 1.7, in the hydrolysis process, slowly biodegradable COD (X_S) is transformed into readily biodegradable COD (S_F) and a small fraction of inert COD (S_I). Stoichiometric parameters of NH_4^+ -N and alkalinity are obtained by applying the continuity equations for nitrogen and electric charge, respectively. These coefficients are usually positive, since the hydrolysis process produces NH_4^+ -N and increases the alkalinity of the growing medium.

Since hydrolysis is an enzymatic process limited by the available superficial area of microorganisms, kinetic expressions related to hydrolysis include the switching function presented as Equation 1.29. This function is based on the consideration that X_S/X_{BH} is directly proportional to the area of contact.

$$\text{Hydrolysis Switching Function} = \frac{X_S / X_{BH}}{K_x + X_S / X_{BH}} \quad (1.29)$$

In the ASM2d model it is considered that only heterotrophic biomass is capable to carry out the hydrolysis process and the biological rate of this process under anoxic and anaerobic conditions is lower than when working under aerobic conditions. Therefore,

kinetic equations for hydrolysis under anoxic and anaerobic conditions include the correction factors η_{NO_3} and η_{Fe} , respectively.

- Heterotrophic decay: ASM2d model considers the death regeneration model to evaluate the decay of biomass. This model is based on the assumption that decay of biomass leads to the generation of slowly biodegradable COD (X_S) and inert particulated biomass (X_I).

Autotrophic processes

Activated Sludge Models (Henze *et al.*, 2000) considers the nitrification process as a one-step reaction where ammonia is converted directly to nitrate by autotrophic biomass. In order to reduce the complexity of the model, nitrite is not considered as a model component. Therefore, these models only consider 2 processes related to autotrophic biomass: Aerobic growth and lysis.

- Aerobic growth of autotrophs: Autotrophic biomass is considered to be strictly aerobic, and it grows exclusively under aerobic conditions. They consume NH_4^+ -N and alkalinity to produce NO_3^- -N and new cells.

- Autotrophic decay: The autotrophic decay is equivalent to the one described for heterotrophs.

1.4.6. Model calibration. Respirometry

The biological nature of wastewater treatment processes implies that their model parameters must be determined (model calibration) according to the local situation (Vanrolleghem *et al.*, 1999). Respirometry is the most popular tool used for model calibration and it consists on the measurement and analysis of the biological oxygen consumption under well defined experimental conditions (Rozich and Gaudy, 1992; Spanjers *et al.*, 1998).

Using the relationship between substrate removal and biological oxygen uptake (respiration), important parameters, such as Biological Oxygen Demand (BOD) and substrate removal activity by several types of microorganisms, can be assessed by respirometry (Chudoba *et al.*, 1989). The rate of oxygen consumption also gives

information about the process kinetics (Spanjers and Klapwijk, 1990; Bernardes, 1996; Vanrolleghem *et al.*, 1999). Therefore, the respiration rate or Oxygen Uptake Rate (OUR) is the key variable that characterizes the process and the associated removal and degradation of biodegradable matter.

The equipment which measures the respiration rate is called respirometer, which consists on a respiration chamber and a device to assess the dissolved oxygen variation. Respirometers can be manometric or volumetric (Spanjers, 1993). Manometric meters evaluate differences in pressure in a constant volume system as oxygen is consumed. In volumetric meters, the pressure is constant and the variation in oxygen concentration is directly measured with an oxygen probe.

The development of more reliable oxygen sensors has made the use of volumetric respirometers more attractive (Spanjers, 1993). The respirometer set-up of this work will be presented in detail in Chapter 3.

1.5 CASE STUDIES

In this study, the biological nitrogen removal process has been applied to treat several wastewaters, namely supernatant from anaerobic digestion (AD) of sewage sludge (the so-called sludge reject water), supernatant from AD of the Organic Fraction of Municipal Solid Waste (OFMSW) and the supernatant from AD of piggery wastewater. They are all characterised by a high ammonium load and a low biodegradable carbon content, since they all came from the anaerobic digestion of protein-rich organic materials. The concrete origin and characteristics of these wastewaters are discussed below.

1.5.1 Supernatant from AD of sewage sludge (sludge reject water)

One of the wastewaters studied in this work was the supernatant from anaerobic digestion of sewage sludge (sludge reject water) from a municipal WWTP of the Barcelona Metropolitan Area (AMB).

Anaerobic digestion of sewage sludge. In municipal WWTP, the excess sludge (mixture of primary and secondary sludge) is usually treated by means of mesophilic anaerobic digestion. In this treatment, biological decomposition of organic matter in total absence of

oxygen takes place producing a combustible gas (biogas). This biogas usually contains an elevated methane (CH₄) content (approximately, 60%) and has a calorific value of approximately 5,500 kcal m⁻³.

The anaerobic digestion process implies, concomitantly with biogas production, a parallel removal or depuration of the organic load inserted into the digester. Consequently, anaerobic digestion is a process that has been used to treat a wide variety of residues with elevated biodegradable organic carbon content: agro wastes, industrial and municipal wastewaters, sewage sludge, piggery wastewater, Slaughter house wastes and OFMSW, among many others (Flotats, 2000; Mata-Álvarez, 2002).

Anaerobic digestion is characterised by the co-existence of four basic biological steps in the substrate degradation process, carried out by different bacterial groups (see Figure 1.14):

- Hydrolysis: In this step, the organic molecules present in the composite to be digested are broken down into simple sugars, amino acids and fatty acids.
- Acidogenesis: In this biological step, a further breakdown into simpler molecules, i.e., volatile fatty acids (e.g., acetic, propionic, butyric, valeric) occurs, producing ammonia, carbon dioxide and hydrogen sulfide as byproducts.
- Acetogenesis: the simple molecules from acidogenesis are further digested to produce carbon dioxide, hydrogen and acetic acid.
- Methanogenesis: This step consists on the conversion of the previously produced compounds to methane, carbon dioxide and water. Since methanogenic microorganisms are strict and have maximum growth rates 5 times lower than acidogenic bacteria, this reaction is usually the limiting step in the biomethanisation process. When the operating conditions inside the digester are not suitable to maintain a healthy growth of methanogenic microbial population (e.g., presence of inhibitors, high organic loading rates), a decrease of pH is registered due to an accumulation of VFA. Therefore, a sufficient buffer capacity inside the anaerobic digester is essential to assure the stability of the anaerobic digestion process.

When biogas is produced by anaerobic digestion of sewage sludge, the supernatant of the effluent stream is enriched in ammonia, which is produced during the acidogenesis. If

proper COD removal efficiencies are reached, the COD present in the resulting wastewater is mainly slowly biodegradable and/or refractory. The main parameters affecting biomethanisation efficiency are: the operating temperature, the pH, the organic loading rate and the hydraulic Retention Time (HRT).

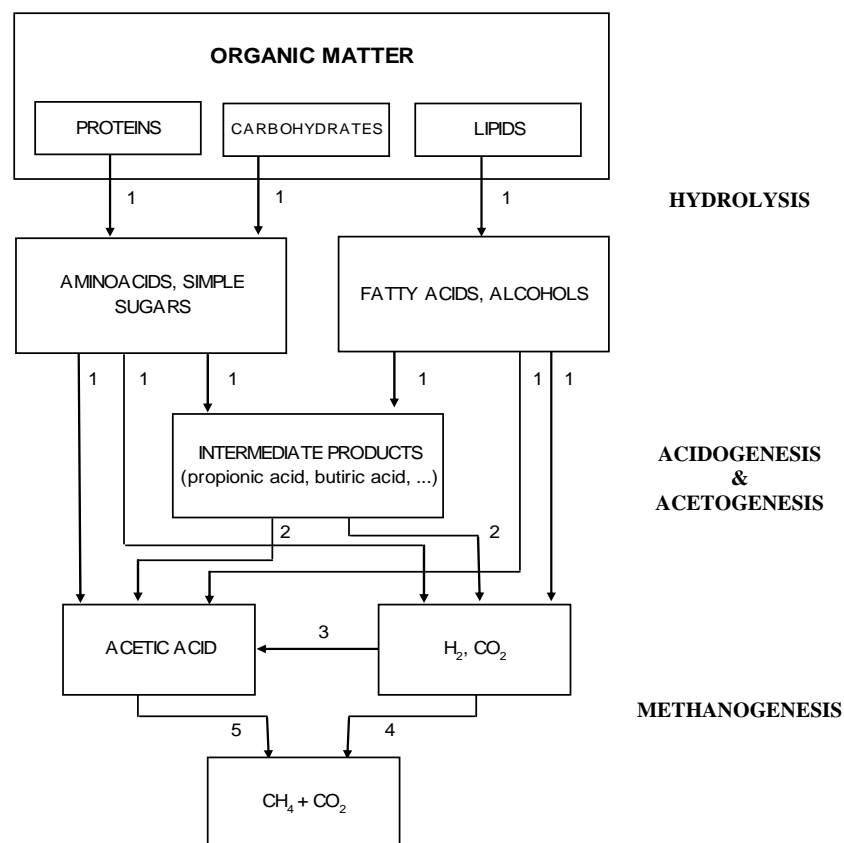


Figure 1.14 – Process diagram of the anaerobic digestion of organic matter and microbial populations responsible of the processes. (1 – Acid hydrolytic microorganisms; 2 - Acetogens; 3 - Homoacetogens; 4 – Hydrogen methanogens; 5 – Acetoclastic methanogens). (Flotats, 2000)

Requirements to treat sludge reject water. The stricter legislation requires upgrading existing municipal WWTPs to meet new standards. In order to improve the quality of the treated effluent and to avoid high space requirements, the actual strategy consists to treat internal flows highly concentrated with ammonia, so small tank volumes will be needed.

Reactor (SBR) technology is a good alternative due to its easy operation, low cost, flexibility and compactness. Nitrogen removal efficiencies of more than 95% have been reported in literature to treat sludge reject water by means of the SBR technology (Siegrist *et al.*, 1996, Vandaele *et al.*, 2000, Macé and Mata-Álvarez, 2002; Wett and Rauch, 2003; Keller, 2005). Moreover, other biological treatment strategies could be implemented, such as a partial nitrification combined with Anammox process. Both biological treatment strategies are discussed in detail in section 1.6.

1.5.2 Supernatant from AD of the OFMSW

Another wastewater tested in this work is the supernatant from anaerobic digestion of the Organic Fraction of Municipal Solid Waste (OFMSW). Similarly to sludge reject water, this supernatant comes from a mesophilic anaerobic digestion of protein rich organic matter and, consequently, it is highly ammonium loaded. In Table 1.1, the characterisation of several supernatants from AD of the OFMSW is presented. The actual situation of the treatment of OFMSW in Spain and the flow diagram of the studied plant are discussed below.

Treatment of the OFMSW in Spain. The present legislation for municipal solid waste in Europe forces the appearance of different ways of pre-selection or pre-treatment to recycle fractions such as plastics, paper, metals, etc. For the OFMSW, Anaerobic Digestion (AD) and composting seem to be the most appropriate technologies. Within this framework, incineration and landfilling are limited to the fractions that remain after some pre-selection and pre-treatment. For incineration the waste should have a significant heating value and for landfilling it has to be inert to biological activity in a high degree.

The first countries in implementing AD schemes into the MSW in a widespread basis were Germany and Austria, where a lot of experience has been gained during approximately the last 20 years. In fact, Germany is the EU country with the largest number of AD plants, with nearly 40 larger than 8000 t year⁻¹. However, Spain is the European Union country with major installed capacity per million of inhabitant to treat MSW by biomethanisation (see Figure 1.16).

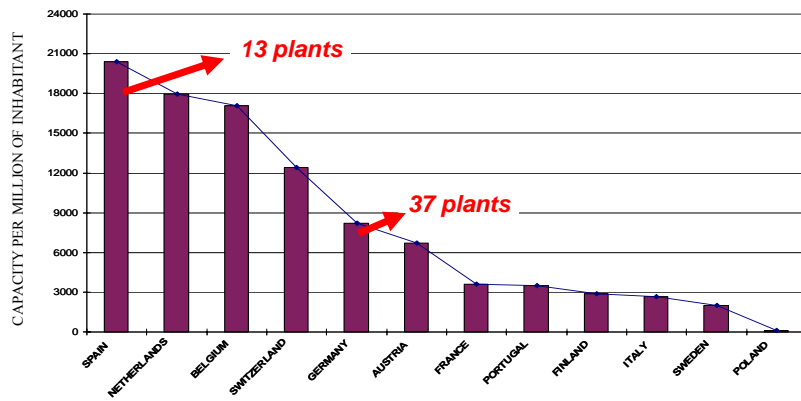


Figure 1.16 – Installed capacity per million of inhabitant to treat Municipal Solid Waste (MSW) by anaerobic digestion in Europe in 2004. (De Baere, 2004)

Spain has become the first country in installed capacity to treat the OFMSW by biomethanisation, with approximately 1,100,000 tons year⁻¹. This figure represents around 35% of the installed capacity in Europe (2,800,000 t year⁻¹) (de Baere, 2004). Figure 1.17 shows the distribution of full-scale anaerobic digestion (AD) plants for the treatment of OFMSW in Spain. In this Figure it is stated that the 30% of the total installed capacity is concentrated in the Barcelona Metropolitan Area, which is related to the Metropolitan Waste Management Program (PMGRM, Pla Metropolità de Residus Sòlids Municipals) of Barcelona. This program planned the construction of several treatment facilities (called Ecoparcs) for recovering recyclable materials and transforming organic waste into compost and biogas.

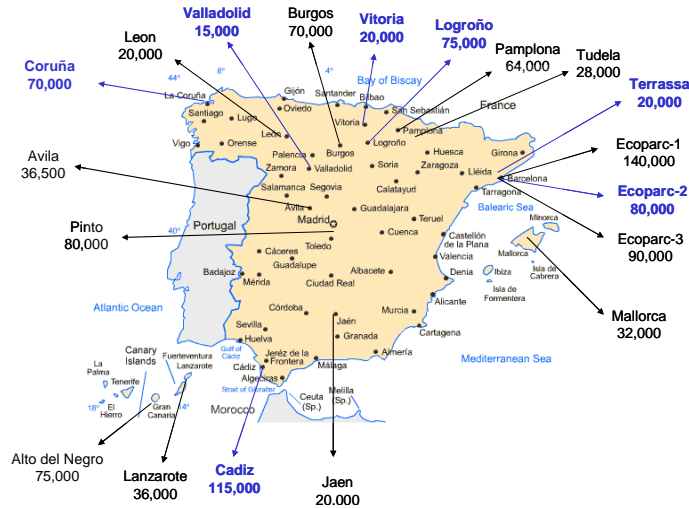


Figure 1.17 – Distribution and capacity in tonnes per year of full-scale anaerobic digestion (AD) plants for the treatment of OFMSW in Spain. (Blue: dry digestion; black: Wet digestion).

The Ecoparc of Barcelona. The Ecoparc of Barcelona are very large plants for anaerobic digestion and composting of the Organic Fraction of Municipal Solid Waste (OFMSW). The main objectives of these full-scale plants are to pre-select recyclable fractions still present in Municipal Solid Waste (MSW) (such as plastics, paper or metals) and to treat the OFMSW in order to produce biogas and compost of quality (Mata-Álvarez, 2002).

Figure 1.18 shows an scheme of the studied Ecoparc. There are basically two types of MSW that enters to this Ecoparc: source sorted OFMSW and mixed MSW. The source sorted OFMSW is integrated by green waste (GW), the remainders from pruning and cleaning of municipal parks and gardens, and OFMSW collected in special containers. The mixed MSW is the fraction of MSW collected in regular containers that still contains a proportion of organic matter and other recoverable materials.

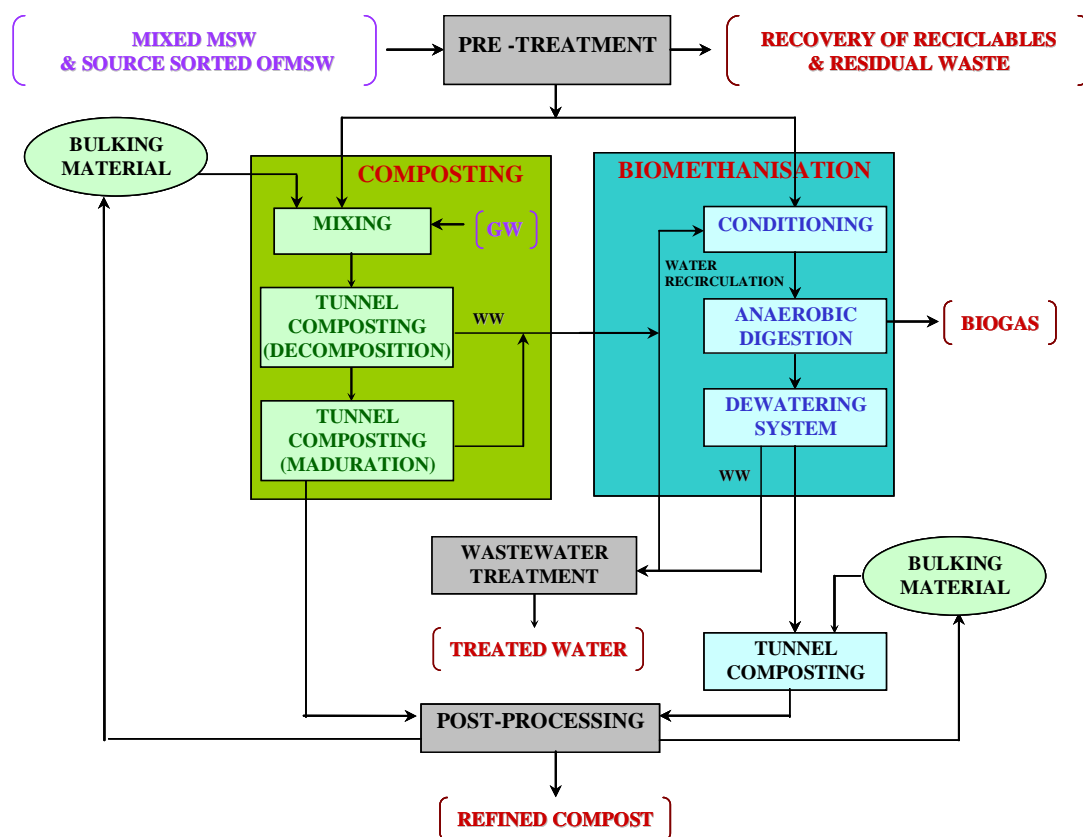


Figure 1.18- Schematic flow-diagram of the treatment of mixed MSW in the Ecoparc of Barcelona.

Mixed MSW and source sorted OFMSW are pre-treated in separated mechanical systems to recover valuable materials. Source sorted OFMSW (high quality) is pre-treated in a simple mechanical separation system and it is mixed with shredded green Waste (GW). The mixture OFMSW and GW (65-75 % and 25-35%, respectively) is conducted to tunnel composting (Haug, 1993). However, source sorted OFMSW is planned to be introduced into anaerobic digesters in the future (Macé *et al.*, 2005). The mixed MSW is pre-selected in a complex mechanical separation system (trommel, human separation, magnetic separation, Foucault inducers, ...) to obtain the OFMSW (low quality) without inappropriate materials. This fraction is treated by means of a wet mesophilic anaerobic digestion Linde-KCA technology (De Baere, 2004; Macé *et al.*, 2005), as depicted in Figure 1.18.

The digested effluent is conducted to a dewatering system where it is divided into two fractions: solid and liquid effluent. The dewatered solid material is treated by means of tunnel composting (Haug, 1993). The liquid effluent (supernatant of anaerobic digestion of the OFMSW) is treated in a wastewater treatment plant and used, in part, as process water to dilute the OFMSW before being fed to the anaerobic digester.

Similarly to the supernatant from anaerobic digestion of sewage sludge, this wastewater is characterised by a high ammonium concentration and an important content of slowly biodegradable and/or recalcitrant COD (see Table 1.1). Considering the possible treatments exposed in section 1.2 and the selection criteria, its treatment in a Sequencing Batch Reactor (SBR) or a partial nitrification/Anammox process for simultaneous COD and Nitrogen removal seems feasible. Both options are described in detail in section 1.6.

1.5.3 Supernatant from AD of piggery wastewater

Another highly ammonium loaded wastewater tested in this study was anaerobically digested piggery wastewater. The motivation of using this wastewater is that Spain is the European Union's second-largest pig meat producer behind Germany with 3% of the world output and 16% of the EU production (Lence, 2005). Moreover, the 28% of spanish pig production takes place in Catalonia, where more than 10,000,000 m³ year⁻¹ of animal slurry (mainly pig slurry) are produced.

The elevated water content of piggery wastewater (in the range of 95%), makes its transport really expensive and, consequently, the management of this wastewater needs to be performed near the place where it is produced. One of the main problems associated to the management of piggery wastewater is the actual tendency of separating factory farm exploitations from agricultural exploitations. This fact implies that the major part of pig factory farms does not dispose of enough agricultural superficial area to reutilize animal slurries, since the acceptance capacity of the medium is largely exceeded.

In Catalonia, pork producers in the areas with the heaviest concentration of production facilities are forming cooperatives to take advantage of EU subsidies for alternative sources of energy, by building waste-disposal plants that transform slurry into electricity and fertilizer (Lence, 2005). Anaerobic digestion has been applied in a variety of forms and scales to stabilize the organic matter in piggery wastes and produce electricity (Llabrés-Luengo and Mata-Álvarez, 1987; Chynoweth *et al.*, 1999; Flotats *et al.*, 2004). However, the conversion of organic nitrogen into ammonium during the anaerobic digestion treatment process (see section 1.5.1) makes that the effluent of AD of piggery wastewater is characterised by a high ammonium load that must be treated.

Some systems developed for the treatment of piggery wastewater that include anaerobic digestion are (Flotats *et al.*, 2004):

The Dansk Biogas Process. The Dansk Biogas has been implemented to digest (or co-digest with other organic waste) piggery wastewater by anaerobic digestion in small farms. After anaerobic digestion, the solid fraction is treated by composting. The liquid fraction is acidified to fix ammonia and partially evaporated under vacuum conditions at low temperatures.

The PROMEST process. This process is another system that include the anaerobic digestion of piggery wastewater. In this process, the liquid fraction is nitrified and then partially evaporated. The concentrated liquid from the evaporation unit (enriched in nitrate) is mixed with the solid fraction and the mixture is dried to form pellets used as agriculture fertilizer. The operation of this process needs the external supply of fuel gas. The PROMEST process was applied during two years but its use was then rejected, mainly due to the high cost of operation (especially for the drying unit) and the

difficulties related to commercialize the end product (Rulkens *et al.*, 1998; Wossink and Benson, 1999).

The MEMON process. This process is based on a complex combination of absorption/extraction processes using organic solvents, ammonium separation by stripping, evaporation and recovering of condensates, and anaerobic digestion of liquid effluents, with subsequent nitrification and pellet formation (Rulkens and Ten Have, 1994). The MEMON process has never been implemented in full-scale conditions due to its technological complexity and its lack of economical viability.

The VALPUREN process. In this process, the liquid effluent from anaerobic digestion of piggery wastewater is treated by vacuum evaporation with condensates recovering. The concentrated effluent is mixed with the solid fraction coming from anaerobic digestion, which is dried to produce pellets that can be applied to soil. Figure 1.19 shows a schematic flow-diagram of the VALPUREN process which has been implemented in some areas of Catalonia (Flotats *et al.*, 2004).

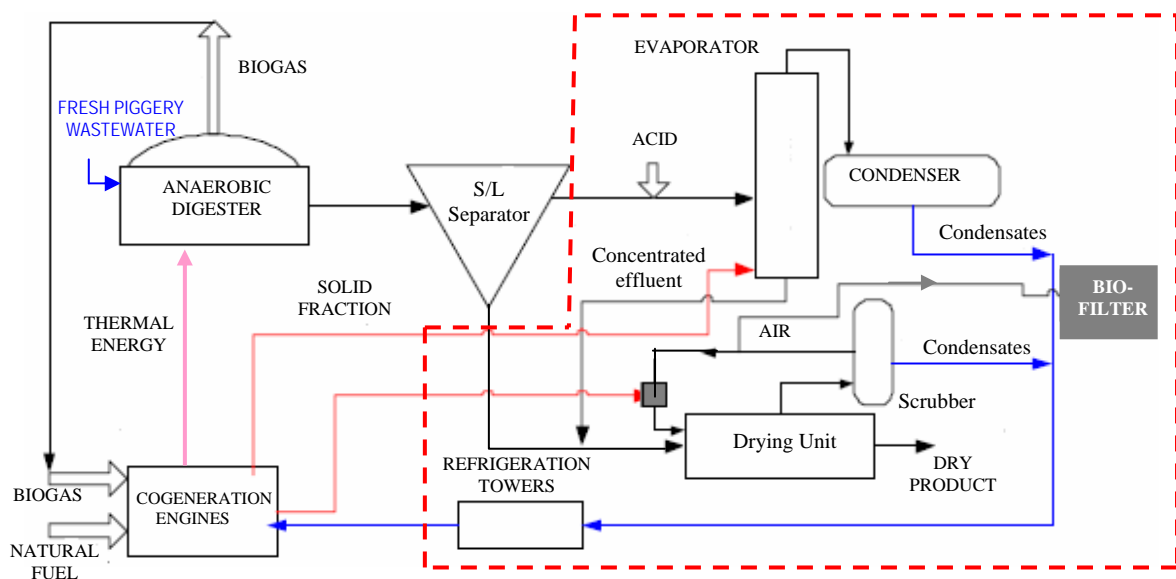


Figure 1.19- Schematic diagram of the VALPUREN process where supernatant of anaerobically digested piggery wastewater was collected. (---) Actual treatment of the effluent from anaerobic digestion (Flotats *et al.*, 2004).

As observed in this Figure, piggery wastewater is fed in an anaerobic digester at an hydraulic retention time (HRT) of typically 15-20 days. Although anaerobic digestion of piggery wastewater is feasible at both mesophilic and thermophilic conditions, under thermophilic conditions it can be highly inhibited by ammonia concentrations and lower biogas production rates are to be expected (Campos, 2001).

The effluent from anaerobic digestion is separated into two fractions: liquid and solid fraction. The liquid fraction is acidified with H_2SO_4 to avoid stripping of ammonia. Then, this liquid is conducted to a vacuum evaporation unit at low temperature, where it is enriched in $(NH_4)_2SO_4$. Subsequently, the effluent from this evaporation unit is mixed with the solid fraction previously separated. This mixture is inserted in a drying unit that is operated with gases coming from the cogeneration engines. The dried product is then converted into pellets that can be used as organic soil fertilizer.

The exhausted gases from the drying unit are filtered and washed in a Scrubber using acid agents to remove ammonia and other impurities. These gases are heated again in the cogeneration engines and returned to the drying unit.

As observed in Figure 1.19, this kind of plants consume all the biogas produced and need an external supply of fuel gas. In order to reduce the costs of the process, especially for small plants, and similarly to the effluents from anaerobic digestion of sewage sludge and OFMSW, the liquid effluent from anaerobically digested piggery wastewater could be treated by a biological treatment which is cheaper, easier to operate and more compact. The biological processes that could be applied for the wastewaters tested in this work are discussed in section 1.6.

1.6 BIOLOGICAL SYSTEMS TO TREAT HIGHLY AMMONIUM LOADED WASTEWATERS

As stated in section 1.5, the wastewaters tested in this study are highly ammonium loaded, in the range of $500 - 2,500 \text{ mg NH}_4^+ \text{-N L}^{-1}$. Moreover, the COD present in this wastewaters are mainly slowly biodegradable COD and/or refractory.

The biological system used to treat these wastewaters should be effective, compact and cheap. The main biological systems to be considered to treat this kind of wastewaters are discussed below.

1.6.1 SBR treatment

The biological nitrogen removal process can be performed by using a Sequencing Batch Reactor (SBR), which is an activated sludge system operating on a fill-and-draw (batch) basis. The SBR is essentially composed of a single tank or a number of tanks in parallel. The biological process inside the SBR consists of a semi-batch operation that combines biological conversion and settling in the same tank. The SBR process is a cyclic operation (see Figure 1.20) that includes 5 modes of operation or steps:

- 1) **Feeding:** The influent wastewater is fed under mixing and/or aeration conditions to begin the biological reaction.
- 2) **React:** The biological reactions initiated during the feeding step are performed during the react period. For the particular case of biological nitrogen removal, aerated and non-aerated periods must be alternated, since nitrification takes place under aerobic conditions (mixing and aeration) and denitrification takes place under anoxic conditions (mixing without air supply).
- 3) **Settle:** In this step, both mixing and aeration are stopped and microorganisms are separated from the treated wastewater by settle.
- 4) **Draw:** The discharge of the treated wastewater and the biomass generated during the operating cycle are performed in this step.
- 5) **Idle:** The SBR is left idle after discharging the treated effluent and before refilling.

In the last few years, high nitrogen efficiencies in the treatment of highly ammonium loaded wastewaters were recorded when using the SBR technology (Macé and Mata-Álvarez, 2002). The main features of the SBR for biological nitrogen removal are its flexibility of operation, effectiveness, compactness and low cost (Macé and Mata-Álvarez). Moreover, the SBR technology leads to an improvement of sludge settleability characteristics and, consequently, it can hold high microorganism concentrations.

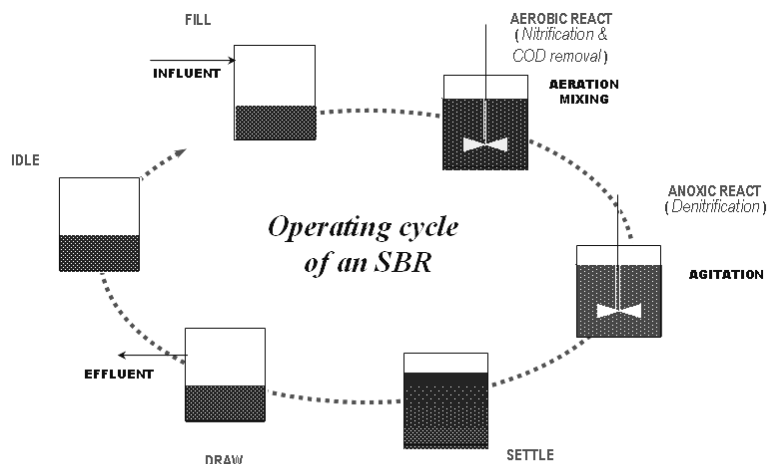


Figure 1.20- Schematic diagram of SBR performance for biological nitrogen removal

The actual tendency when using an SBR to treat highly ammonium loaded wastewaters is to perform the biological nitrogen removal over nitrite. If the biological nitrogen removal process is carried out over nitrite instead of over nitrate, it is obtained a saving of 25% of the aeration costs and 40% of the external carbon source needed during denitrification, as well as a reduction in the amount of sludge produced. The strategy to reach the nitrite route is to keep environmental conditions inside the SBR (such as dissolved oxygen concentration, pH, $\text{NH}_4^+\text{-N}$ concentration, ...) that favour AOB in front of NOB.

1.6.2 SHARON process

As stated in section 1.3.2.1, the SHARON process is based on the higher maximum specific growth rate of ammonia oxidizers (AOB) relative to the maximum specific growth rate of nitrite oxidizers (NOB) at higher temperatures. So there is a potential to use SRT (around 1 day) combined with relatively high temperatures (near the temperature range of mesophilic anaerobic digestion) to select the development of AOB and the total wash out of NOB in a completely mixed reactor.

By imposing intermittent aeration and adding biodegradable carbon source during non-aerated periods, both denitrification and concomitant pH control are possible. Figure 1.21 shows typical methanol, $\text{NH}_4^+\text{-N}$, $\text{NO}_2^-\text{-N}$ and pH patterns of this strategy, usually known

as SHARON/Denitrification process (Mulder and van Kempen, 1997; Verstraete and Philips, 1998; van Kempen *et al.*, 2001). Similarly to the biological nitrogen removal over nitrite in an SBR, this process allows savings in oxygen supply (25%) and reductant (40%) when compared with the biological nitrogen removal over nitrate.

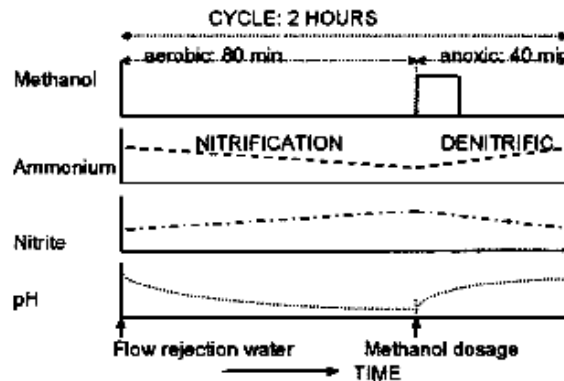


Figure 1.21- Methanol, $\text{NH}_4^+\text{-N}$, $\text{NO}_2^-\text{-N}$ and pH patterns in a SHARON/Denitrification process. Arrows indicate supply of wastewater and methanol. (van Kempen *et al.*, 2001).

The SHARON process is commonly used to oxidize only the 50% of $\text{NH}_4^+\text{-N}$ to $\text{NO}_2^-\text{-N}$ in a continuous reactor with HRT around 1 day, without sludge retention and pH around 6-6.7. For the particular case of sludge reject water, where usually the alkalinity to $\text{NH}_4^+\text{-N}$ ratio on molar basis is nearly 1.0, a mixture of 50% ammonium and 50% nitrite is obtained in the effluent of the SHARON reactor without controlling the pH. However, in wastewaters with other alkalinity to $\text{NH}_4^+\text{-N}$ ratios, pH control would be necessary to assure an effluent suitable to the Anammox process.

1.6.3 Anammox process

As previously explained in section 1.3.2.2.2, this process converts ammonium directly into dinitrogen gas under anaerobic conditions with nitrite as electron acceptor in absence of biodegradable COD. Therefore, it needs to be preceded by a first partial nitrification step (for example in a SHARON reactor) that converts 50% of the influent $\text{NH}_4^+\text{-N}$ into $\text{NO}_2^-\text{-N}$. The overall reaction of a partial nitrification and Anammox process (schematised in Figure 1.22) avoids the requirement of organic carbon source to denitrify, allows saving over 65% of the oxygen supply and produces little sludge (Fux *et al.*, 2002).

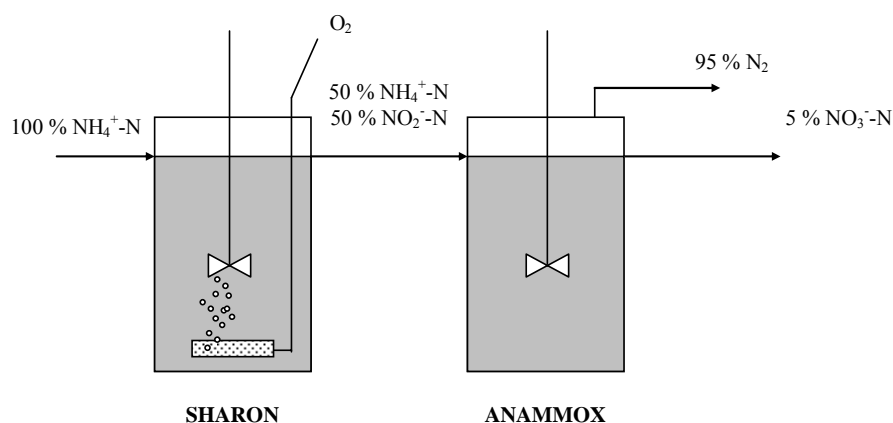


Figure 1.22- Schematic diagram of a combined SHARON – Anammox process.

The main problem of the Anammox microorganisms is that they have a very low specific growth rate (0.069 days^{-1} according to van de Graaf *et al.*, 1996). Therefore, this process must be carried out in a digester that assures high sludge retention and can assume high nitrogen loads. Several reactor configurations have been used to carry out the Anammox process, such as fixed and fluidized bed reactors (Strous *et al.*, 1997; Fux *et al.*, 2004), sequencing batch reactors (Strous *et al.*, 1998; Van Dongen *et al.*, 2001; Fux *et al.*, 2002; Dapena-Mora *et al.*, 2004a), gas lift reactors (Sliemers *et al.*, 2003, Dapena-Mora *et al.*, 2004a) or up flow bed reactors (Ahn *et al.*, 2004; Imajo *et al.*, 2004).

1.6.4 CANON process

Partial nitrification and Anammox can be combined in a single reactor commonly known as ‘Completely Autotrophic Nitrogen removal Over Nitrite’ or CANON process (Strous, 2000; Sliemers *et al.*, 2002). In this process, the autotrophic ammonium oxidation process is operated in a biofilm reactor under oxygen limitation such that approximately 50% of the ammonium can be oxidised. If the biofilm is stable, automatically an Anammox population will be developed in the deeper biofilm layers. Therefore, the completely autotrophic nitrogen removal can be carried out in one single biofilm reactor (van Loosdrecht and Salem, 2006).

1.6.5 BABE process

In municipal wastewater treatment plants (WWTP), high biological removal efficiencies can be achieved in the main line (secondary reactor) if bacteria that form the ‘natural’

population of the WWTP is bio-augmented. This bioaugmentation of nitrifying bacteria can reduce the aerobic (and thereby total) SRT of nutrient removal processes (van Loosdrecht and Salem, 2006).

This treatment strategy has been tested on full-scale conditions with excellent results (Salem *et al.*, 2004). It is named 'Biological Augmentation Batch Enhanced' or BABE process (Zilverentant, 1999). Figure 1.23 shows an schematic flow diagram of the BABE process. In this process, a limited amount of return sludge is conducted in a tank (BABE reactor) where sludge reject water is fed. Consequently, the autochthonous bacteria of the WWTP grows and it is augmented in the sludge. This strategy is a useful method for upgrading WWTP and obtaining better effluent qualities: for high loaded activated sludge systems the BABE process allows nitrification to take place below the minimal solid retention times; and for low loaded systems this novel process can be used to introduce extra denitrification space in low loaded systems. Salem *et al.* (2002) demonstrated, in a model-based evaluation for upgrading the Walcheren WWTP in the Netherlands, that there is a reduction of 50% in the area requirement if the BABE technology is used when compared to conventional upgrading (extending aerated and anoxic volumes).

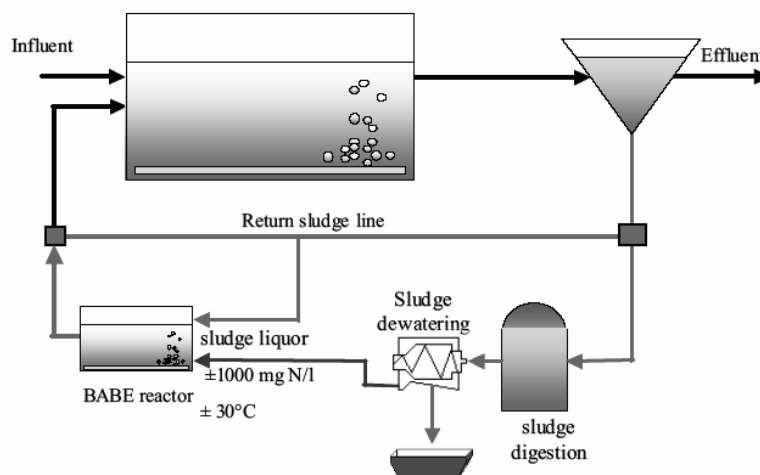


Figure 1.23- Schematic diagram of the BABE process (van Loosdrecht and Salem, 2006).

2. Objectives and Thesis Structure.

ABSTRACT

In this chapter, the objectives of this study are presented. Basically, the performance of three types of biological reactors to treat highly ammonium loaded wastewaters will be evaluated and modelled by means of an extended IWA Activated Sludge Model (Henze et al., 2000): an SBR, a SHARON chemostat and an Anammox reactor. To this purpose, the Activated Sludge Model has to be programmed (in this case, in the Software Mathematica 4.1) and a respirometric set-up needs to be constructed in order to assess the main kinetic and stoichiometric model parameters. Three kinds of wastewaters were tested in this work: sludge reject water, supernatant from anaerobic digestion of the OFMSW and anaerobically digested piggery wastewater. Finally, the structure of the thesis is detailed.

2.1. MOTIVATION AND OBJECTIVES.

As stated in Chapter 1, the reduction of the nitrogen present in wastewaters to an environmentally supportable level is essential, since an excess of nitrogen to receiving waters would lead to several environmental and health risks. This fact leads to the implementation of stricter effluent standards for nitrogen compounds.

Supernatants from anaerobic digestion of sewage sludge, OFMSW and piggery wastewater are characterised by a high ammonium load that must be effectively treated before being discharged in natural waters or public sewers. Some strategies can be used to treat this kind of wastewaters, but biological processes are preferred based on cost aspects, energy requirements, operation experience, process reliability and environmental impact. If the biological nitrogen removal process is carried out over nitrite, instead of nitrate, it is obtained a saving of 25% of the aeration costs and 40% of the external carbon source needed during denitrification, as well as a reduction in the amount of sludge produced. Moreover, the combination of a stable partial nitrification with Anammox allows saving over 65% of the oxygen supply and produces little sludge.

On the other hand, the IWA Activated Sludge Models were initially designed to simulate biological treatments for municipal wastewater (Henze *et al.*, 2000) and, consequently, they content some assumptions and simplifications that are often not applicable in biological treatments of other wastewaters. Limitations of these models to describe the biological nitrogen removal of highly ammonium loaded wastewaters have been reported in literature, specially when nitrite accumulation is obtained and/or pH becomes a limiting parameter (Wett and Rauch, 2003).

These considerations are the motivation of the present work, which deals with possible nitrogen removal strategies to treat highly ammonium loaded wastewaters (namely, SBR treatment, SHARON-Denitrification, and partial nitrification combined with Anammox) and the modelling of their performance to obtain an explanation of the processes and inhibitions that take place in the digesters. To reach this general objective, the following specific goals were proposed:

- ✓ To start-up an SBR for biological nitrogen removal over nitrite of sludge reject water.

- ✓ To reach an optimum SBR treatment for biological nitrogen removal over nitrite of sludge reject water, supernatant from anaerobic digestion of the OFMSW and liquid fraction of anaerobically digested piggery wastewater.
- ✓ To set-up a respirometer, including its data acquisition system, in order to assess by respirometric batch tests the main stoichiometric and kinetic parameters involved in biological nutrient removal processes.
- ✓ To enlarge IWA Activated Sludge Models to describe the biological nitrogen removal over nitrite, considering the effect of pH, temperature and other possible inhibitors.
- ✓ To implement the extended Activated Sludge Models to be used in this study in the Software Mathematica 4.1.
- ✓ To provide an easy and reliable methodology to assess kinetic and stoichiometric parameters of Activated Sludge Models.
- ✓ To incorporate a Coagulation/Flocculation step inside the SBR strategy for the treatment of anaerobically digested piggery wastewater to meet legal COD effluent standards.
- ✓ To model the biological nitrogen removal process of an SBR treating supernatants from anaerobic digestion of protein-rich materials.
- ✓ To evaluate the nitrogen removal efficiency of a SHARON/Denitrification process for the treatment of sludge reject water using methanol to denitrify.
- ✓ To substitute methanol by a biodegradable carbon source coming from an internal flow of the WWTP in the SHARON-Denitrification process.
- ✓ To model the performance of an SBR and a SHARON chemostat to generate a suited influent to the Anammox process (with $\text{NH}_4^+\text{-N}$ and $\text{NO}_2^-\text{-N}$ in an equimolar ratio).

- ✓ To assess and model the temperature influence at short time on the denitrifying activity of Anammox biomass.
- ✓ To run an Anammox SBR treating a highly ammonium loaded synthetic wastewater at several temperatures (namely, 30, 25, 23, 20, 18 and 15 °C).

2.2. THESIS STRUCTURE.

In Chapter 1, an introduction to the biological nitrogen removal processes is provided. Moreover, the origin and characteristics of the wastewaters to be analysed in this study, as well as the type of biological systems to be tested (namely, SBR, SHARON-Denitrification, SHARON and Anammox), are also introduced in Chapter 1.

In order to reach the objectives presented in section 2.1, the results obtained in this work are divided in the following chapters:

CHAPTER 3: Materials and Methods.

In this Chapter, the biological reactors and the techniques and analytical methods used to perform the experimental part of this thesis are detailed. Special attention is paid to the construction of a closed intermittent-flow respirometer to calibrate activated sludge models. Moreover, the implementation of extended Activated Sludge Models in the Software Mathematica 4.1 is also discussed.

CHAPTER 4: Operation and model description of an SBR treating sludge reject water for biological nitrogen removal over nitrite.

The start-up, operation and model description of an SBR for biological nitrogen removal from sludge reject water from a municipal WWTP is presented in this Chapter. The SBR strategy includes the control of oxygen supply and ammonia concentrations inside the digester to favour the biological nitrogen removal over nitrite, which makes the process more economical. Moreover, a four-step nitrogen removal model is also developed to describe the reactor's performance. This model enlarges the IWA activated sludge models for a more detailed description of the nitrogen elimination processes and their inhibitions. A respirometric procedure to assess the main stoichiometric and kinetic parameters of the

extended Activated Sludge Model is presented. Finally it is demonstrated that the calibrated model is capable to reproduce accurately experimental data.

CHAPTER 5: Modelling of an SBR to treat the supernatant from anaerobic digestion of the OFMSW.

Similarly to Chapter 4, in Chapter 5, an SBR is tested to remove COD and $\text{NH}_4^+\text{-N}$ from the supernatant of Anaerobic Digestion of the OFMSW. The optimum SBR operating sequence is modelled by the Activated Sludge Model developed in Chapter 4, but with some modifications to calculate pH evolution. The calibration of the model is then performed according to the respirometric procedure established in Chapter 4. The proposed model shows very good agreement between experimental and simulated $\text{NH}_4^+\text{-N}$, $\text{NO}_2^-\text{-N}$, $\text{NO}_3^-\text{-N}$ and pH profiles.

CHAPTER 6: COD and Nitrogen removal of supernatant of anaerobically digested piggery wastewater in a biological SBR with a Coagulation/Flocculation step.

In this Chapter, the SBR technology is used to treat the supernatant from mesophilic anaerobic digestion of piggery wastewater. The SBR treatment includes a similar strategy as the one proposed in chapters 4 and 5 to reach the biological nitrogen removal over nitrite, but including a final coagulation/flocculation step inside the SBR cycle to reach the legal COD effluent standards. Moreover, the influence of several operational parameters on the nitrifying-denitrifying biomass activity is also studied.

CHAPTER 7: Operation of the SHARON-Denitrification process to treat sludge reject water using hydrolysed primary sludge to denitrify.

In Chapter 7, an alternative treatment to the SBR, the SHARON-denitrification process, is analysed to treat sludge reject water. An optimized performance of this process is proposed using methanol and working at HRT 2 days, 33°C and cycle length 2 hours (1 hour aerobic and 1 hour anoxic). Moreover, the use of supernatant of hydrolysed primary sludge to denitrify during anoxic periods is also studied.

CHAPTER 8: Modelling of partial nitrification in a SHARON chemostat and in an SBR to achieve a suited influent to the Anammox process.

In this chapter, two biological nitrogen removal treatments of sludge reject water to achieve a suited influent to the Anammox process are tested and modelled. These two

processes are the SHARON process and the partial nitrification in a SBR. Both processes provide good performance in the generation of an effluent with $\text{NH}_4^+\text{-N}$ and $\text{NO}_2^-\text{-N}$ in equimolar ratios. The activated sludge models are calibrated by batch respirometric tests using activated sludge from the withdrawals of both reactors. The simulation was in accordance to the experimental data registered in the laboratory.

CHAPTER 9: Operation of an Anammox reactor to treat highly ammonium loaded wastewaters at low temperatures.

In Chapter 9, the Anammox process is operated at low temperatures to treat highly ammonium loaded wastewaters (such as the wastewaters tested in Chapters 4, 5 and 6) previously pretreated in a partial nitrification unit. As an initial approach to assess the temperature influence at short time on Anammox biomass, several batch activity tests are analysed and modelled at controlled temperature conditions. Subsequently, the operation of a lab-scale Anammox SBR at different temperature conditions (namely, 30, 25, 23, 20, 18 and 15 °C) is presented.

CHAPTER 10: General conclusions and recommendations.

In this Chapter, the general conclusions extracted from this work are compiled and discussed. Moreover, recommendations for further investigation are proposed.

3. Materials and methods.

ABSTRACT

In this chapter, the lab-scale digesters used in this study to develop several biological nitrogen removal treatments (such as nitrification/denitrification over nitrite in a SBR, SHARON, SHARON/Denitrification and Anammox) are presented.

Moreover, the design and construction of a closed intermittent-flow respirometer to assess the main stoichiometric and kinetic parameters of Activated Sludge Models is detailed. This experimental device was computer controlled and equipped with a data acquisition system (Advantech Genie Software). The methodology used to evaluate the denitrifying activity of Anammox biomass is also provided. Subsequently, the Jar test device used to carry out the coagulation/flocculation analysis on wastewaters with a high non-biodegradable COD concentration is presented.

Then, the implementation of the Activated Sludge Models (ASM) in the software Mathematica 4.1 is discussed. Finally, the substrate and inoculum, concomitantly with the experimental techniques and analytical procedures used in this study (solids content, COD, BOD₅, NH₄⁺-N, NO₂⁻-N, NO₃⁻-N, VFA, alkalinity and SVI) are detailed.

3.1. BIOLOGICAL REACTORS

In this study, basically 3 types of lab-scale reactors have been tested: an SBR for biological nitrogen removal over nitrite, a continuous chemostat reactor and an Anammox SBR. Due to the variety of operating strategies used in this study, the structure of the SBR operating cycles are detailed in the correspondent chapter.

3.1.1. SBR for biological nitrogen removal over nitrite.

The biological treatment of several wastewaters (sludge reject water, liquid fraction from anaerobically digested piggery wastewater and supernatant from anaerobic digestion of the organic fraction of municipal solid waste) was carried out in a lab-scale SBR reactor of 3L schematised in Figure 3.1. Operating temperature was maintained by means of a heating system (RM6 Lauda). Mixing was provided by means of a mechanical stirrer (Heidolph). Fill and draw stages were performed by two peristaltic pumps (Easy-Load Masterflex L/S, 7518/10; Easy-Load Masterflex, 7510/00). External carbon source was added through a peristaltic pump (EYELA Micro Tube Pump MP-3). The air flow inside the reactor was controlled by two air blowers (Rena Air 300) connected to a sparging system.

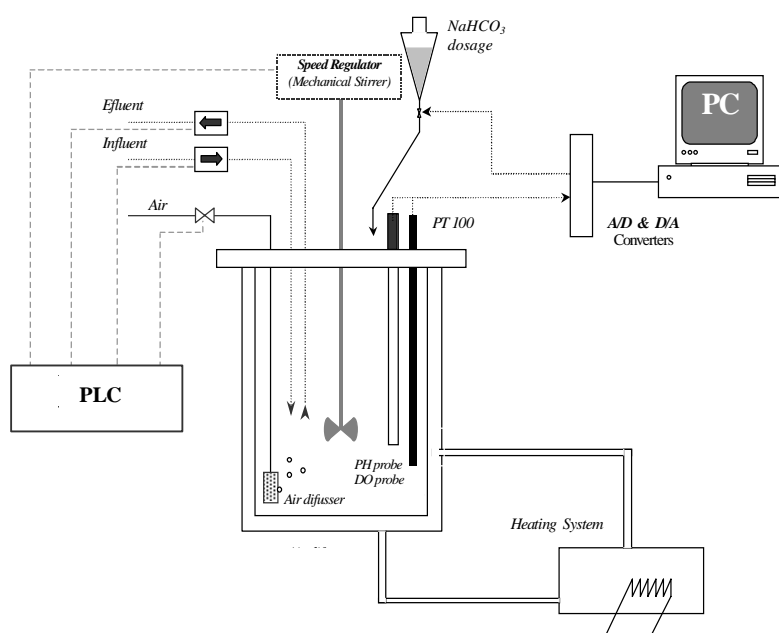


Figure 3.1 – Schematic diagram of the SBR tested in this work.

The SBR was also equipped with a pH electrode (Crison pH 28) and a Dissolved Oxygen (DO) probe (Oxi 340i, WTW). These parameters were monitored and registered in a computer with the Advantech Genie software (similar to the one described in section 3.2) that was built-up for this study. A Programmable Logic controller (PLC, LOGO SIEMENS 230RC) was used to temporize the different stages of the operating cycles. Figure 3.2 shows the SBR and details of the data acquisition system.

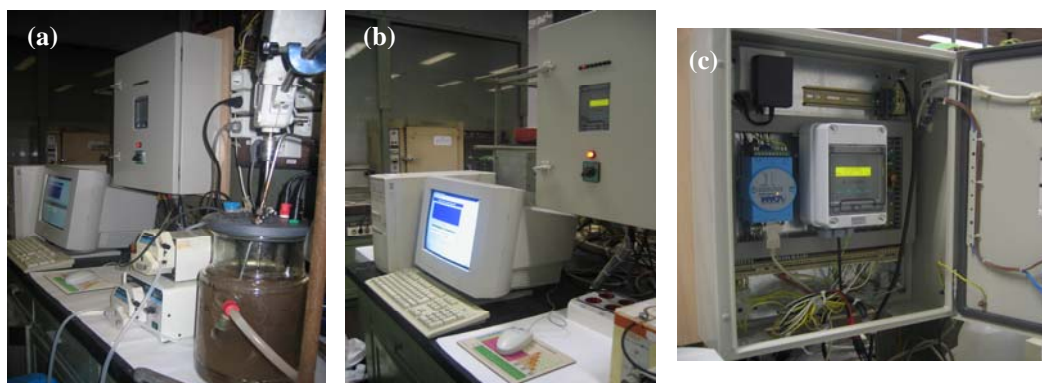


Figure 3.2 – Lab-scale SBR used in this study (a) with its accessories and details of the data acquisition system (b and c).

3.1.2. SHARON chemostat reactor.

A jacketed chemostat reactor (4L) was used to test the SHARON process at lab-scale conditions (see Figure 3.3). The operating temperature was maintained by a heating system (Termotronic, Selecta). Mixing was provided by a mechanical stirrer (Heidolph RZR1). Aeration was supplied by an air blower connected to a pumice stone system. A peristaltic pump (Ismatec REGLO) was used to perform the feeding of wastewater to the reactor. The withdrawn was carried out by means of an overflow system. Another peristaltic pump (Ismatec REGLO) performed the feeding of the electron donor used to denitrify. The digester was equipped with a Dissolved Oxygen (DO) probe (WTW Oxi 340i) and a pH electrode (Crison Rocon 18). Moreover, it was controlled and monitored by a Programmable Logic Controller (PLC, Logo Siemens) and a computer with a data acquisition card (PCL-812PG), a control box and an interphase card (PCL-743/745). The computer worked with Bioexpert Software (*version 1.1x*).



Figure 3.3 – Lab-scale SHARON reactor (4L) used in this study.



Figure 3.4 – Anammox SBR of 1L tested in this work.

3.1.3. Anammox SBR.

The Anammox process was carried out in a lab-scale SBR of 1 L (see Figure 3.4), since it has been reported that good mixing and high nitrogen elimination rates can be easily achieved in sequencing batch reactors with suspended (Fux *et al.*, 2002) or granulated biomass (Strous *et al.*, 1998). The biomass was attached in a zeolite (clinoptilolite) supplied by ZeoCat (94-96% of purity) previously sieved to select particles with 0.5-1.0 mm (Fernández *et al.*, 2006). The operating temperature was maintained by means of a temperature controller (PolyScience, USA). Mixing was provided by means of a mechanical stirrer (Ika Labortechnik) with a PTFE blade of 76 mm at 120 rpm. Fill and draw stages were performed by two peristaltic pumps (Masterflex Quick load, Cole-Parmer Instrument Company). The reactor was flushed with a mixture of 95% Ar/5% CO₂ to maintain anaerobic conditions. Norprene tubing and connections were used in order to minimize the diffusion of oxygen into the feeding. The operating cycles were controlled by a PLC (CPU224, Siemens).

3.2. CLOSED INTERMITTENT-FLOW RESPIROMETER

One of the objectives of this work was to set-up a respirometer in order to assess the kinetic and stoichiometric parameters of Activated Sludge systems for its subsequent modelling. A closed intermittent-flow respirometer was selected among the respirometric devices proposed in literature (Vanrolleghem *et al.*, 1998) due to its simplicity (it does not require the evaluation of the oxygen transfer from gas to liquid phase) and reliability (in this experimental device, the DO probe is located in a respiration chamber separated from the aeration vessel and, therefore, non-realistic DO values related to the adhesion of air bubbles in the DO probe are avoided). The promising results obtained by Marsilli-Libelli and Tabani (2002) and Gutiérrez (2003) also promote the selection of this type of respirometer.

The closed intermittent-flow respirometer used in this study is presented in Figure 3.5 and consisted of an aeration vessel (3 L) and a stirred watertight closed respiration chamber (0.250 L). Air flow passed through an humidifier before being introduced into the aeration chamber in order to prevent volume variations linked to water evaporation. A heating system (Haake DC30) was used to maintain the temperature at $T \pm 0.5^{\circ}\text{C}$ in the whole system. The respiration chamber was equipped with a dissolved oxygen probe (Oxi 340i, WTW) and the pH in the aeration vessel was measured with a Crison pH 28 electrode. When the oxygen level dropped below $2 \text{ mg O}_2 \text{ L}^{-1}$ or the measuring period lasted more than 300 s, the mixed liquor inside the measurement vessel was replaced by pumping aerated mixed liquor from the aeration vessel into the respiration chamber for 75 s, for sufficient time to renew three times its volume. The pH was computer controlled within a narrow pH setpoint $\pm \Delta\text{pH}$ region. When the measured pH value did not lie inside the desired region, acid (HCl, 0.2 N) or base (NaOH, 0.2 N) was added by opening an electromagnetic valve for a very short period of time to adjust the pH.

The 4-20 mA signals of both oxygen and pH probes were collected and logged on a PC equipped with the Advantech Genie software package and combined A/D I/O Modules (Adam 4050/ Adam 4520/ Adam 4018) were selected. Figure 3.6. shows an scheme of the data acquisition system and its electric connections.

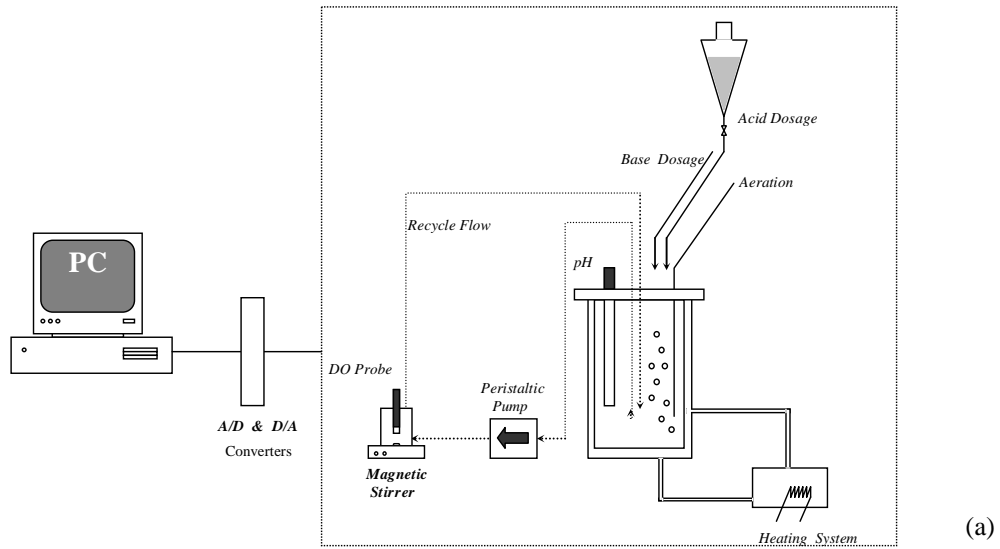


Figure 3.5 – Closed Intermittent-Flow respirometer constructed in this study. Scheme of the respirometer (a) and photograph of the experimental device (b).

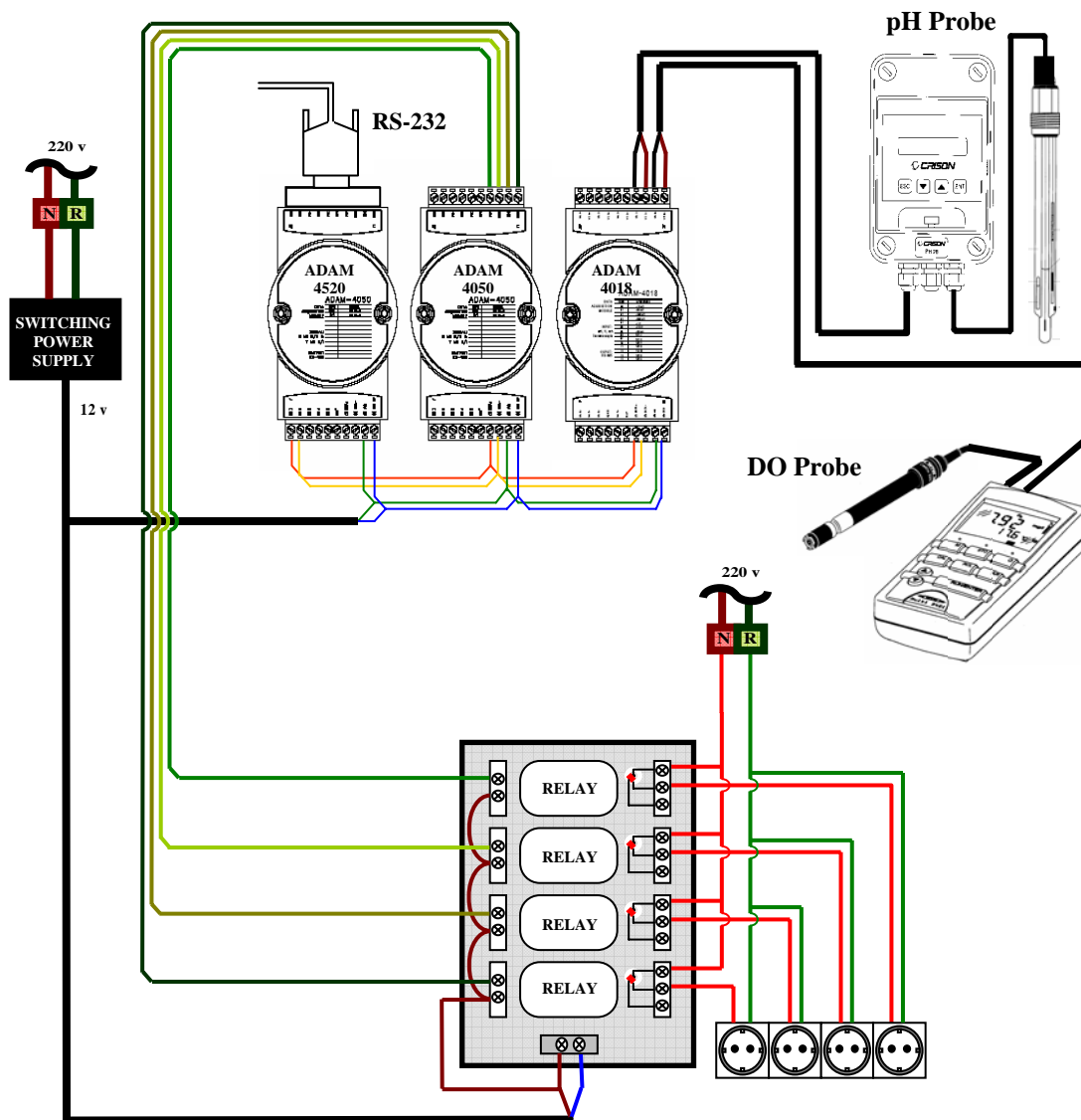


Figure 3.6 – Scheme of the acquisition data system for the closed intermittent-flow respirometer.

The 4-20 mA signals of DO and pH were inserted into the Adam module 4018 which converted these analogical signals to digital signals, which were conducted to the Adam module 4520. The Adam module 4520 acted as the central module and it was connected to the PC by means of a RS-232 connection. This module received the digital input signal emitted by the Adam Module 4018 and transferred it to the computer. The Adam module 4520 also received the digital outputs generated by the computer and transferred them to the Adam module 4050. This module converted the digital output into an analogical output signal, which acted directly on 4 relays (CEBEK). Depending on the signal received by these relays, the peristaltic pump, the acid valve and/or the base valve were opened or closed. Moreover, a switching power supply (MW, Mean well) was used to convert 100-240V to 12V, which was the working voltage of both the Adam modules and the relays (see Figure 3.6).

Figure 3.7 shows two images of the Advantech Genie program written in this study to control the closed intermittent-flow respirometer. As observed in Figure 3.7.(b), the DO profile obtained in batch respirometric tests has the shape of successive waves. The increases of DO in this profile are related to the time periods in which the peristaltic pump was working and renewed the mixed liquor inside the respiration chamber. Subsequently, when the peristaltic pump was stopped and after an idle period where the dissolved oxygen value was stabilized, a linear DO drop was observed. The slope of DO profile versus time is known as the Oxygen Uptake Rate (OUR), which is directly correlated to the aerobic consumption rate of the biodegradable substrate (in this study, COD and/or nitrogen).

The monitored data was then exported to an Excel programme where a previously written MACRO was applied to obtain automatically the so-called respirogram (plot of the OUR versus time). Figure 3.8 shows a DO profile during a respirometric batch test and its corresponding respirogram. As it is stated in Figure 3.4, the respirometric batch experiment is clearly divided in 3 periods. During the first period (period A), the mixed liquor was aerated under endogenous conditions and the endogenous OUR could be assessed. Subsequently, an external substrate (in this case, sodium acetate) was fed into the mixed liquor and a pronounced descent of the DO concentration (related to an increase of the OUR) was registered during a certain period of time (period B). When the substrate was depleted (period C), the total OUR measured in the respirometer returned progressively to the endogenous state.

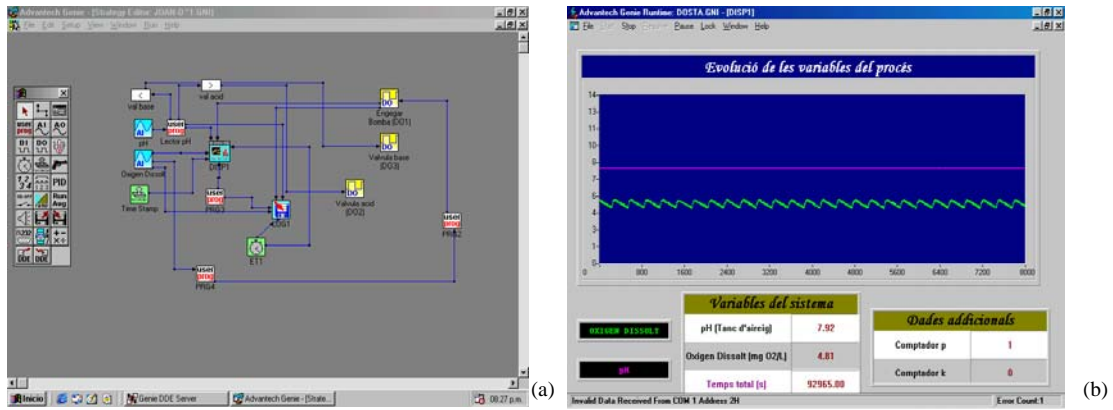


Figure 3.7 – Flow diagram and output graphics of the Advantech Genie programme. (a) Icons of the implemented programme and (b) pH and DO profiles monitored during a respirometric batch test.

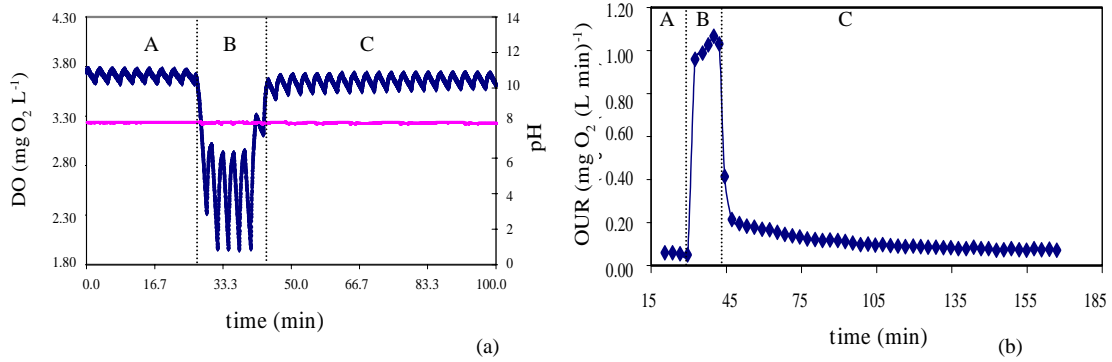


Figure 3.8 – DO profile (a) monitored by the Advantech Genie programme during a respirometric batch test and its corresponding respirogram (b) after applying the macro to the DO profile.

DO (---) pH (---) and OUR (•••)

As it will be further discussed in Chapter 4, respirometry has been proved to be a reliable tool to characterise the most relevant kinetic and stoichiometric parameters involved in both organic carbon and nitrogen removal (Vanrolleghem et al., 1999) under well-defined experimental conditions.

3.3. ANAMMOX ACTIVITY TESTS.

The maximum Specific Anammox Activity (SAA) test employed by Dapena-Mora *et al.* (2007a) in order to analyse the short-term toxicity of several compounds, was applied to assess the influence at short time of the operating temperature on Anammox activity.

It consisted on the measurement of the overpressure generated in closed vials by the produced nitrogen gas along time using a differential pressure transducer (0-5 psi, linearity 0.5% of full-scale, Centerpoint Electronics). In SAA tests, approximately 1.5 g VSS L⁻¹ of sludge (granulated and attached biomass) collected from two lab-scale Anammox SBRs (Dapena-Mora *et al.*, 2004c, Fernández *et al.*, 2006) were washed with phosphate buffer to provide an optimum pH (7.8). Then, 24 mL of the mixed liquor were inserted in 38 mL vials. Mixing at 150 rpm and control of temperature during the tests were provided by an incubator shaker (New Brunswick Scientific, C24 Incubator; Edison, USA). After 30 minutes to acclimate the biomass inside the vials to the operating conditions of the test, 0.5 mL of ammonium sulphate solution and 0.5 mL of sodium nitrite solution were injected into the vials to reach the initial concentrations of 70 mg NH₄⁺-N L⁻¹ and 70 mg NO₂⁻-N L⁻¹.

The reaction was followed by measuring the pressure increase, which is related to nitrogen production according to Equation 3.1, where n is the moles of nitrogen produced per unit of time (moles N day⁻¹), V_G is the volume of the gas phase (L), R is the ideal gas constant (atm L (mol K)⁻¹), T is the temperature (K) and α is the slope of the pressure increase inside the vial versus time (atm day⁻¹).

$$n = \alpha \cdot \frac{V_G}{R \cdot T} \quad (3.1)$$

Then, the maximum SAA expressed in g N (g VSS day)⁻¹ can be assessed according to equation 3.2, where M_{N_2} is the molecular weight of N₂ (g N mole⁻¹), X is the biomass concentration inside the vial (g VSS L⁻¹) and V_L is the volume of the liquid phase (L).

$$SAA = n \cdot \frac{M_{N_2}}{V_L \cdot X} \quad (3.2)$$

3.4. JAR TESTS

The Coagulation/Flocculation tests were performed in a Jar-Test device (Flocculator 2000, KEMIRA Kemwater) with the following steps and temporization: vigorous mixing (30 s), low mixing (15 min) and settle (20 min). Both Coagulant (FeCl_3) and flocculant agents were added to the desired concentration at the beginning of the first step (vigorous mixing). The effectiveness of the Coagulation/Flocculation treatment was evaluated by means of the Chemical Oxygen Demand (COD) and Suspended Solids (SS) reduction yields. Figure 3.9 shows the Jar Test device used in this study.



Figure 3.9 – Jar-test device used in this study.

3.5. SIMULATION OF BIOLOGICAL PROCESSES.

Modelling and parameter estimation were performed by using a Mathematica 4.1 (Wolfram Research, Inc.) programme developed for this study. In this programme, enlarged Activated Sludge Models (ASM; Henze et al., 2000) were implemented to better describe the biological nitrogen removal of highly ammonium loaded wastewaters. As observed in Figure 3.10, the Mathematica 4.1 programme is basically composed by five steps: import of experimental data from an EXCEL document, definition of operating conditions and model parameters, numeric resolution of the differential equations of the Activated Sludge Model, plotting and comparison of both experimental and simulated data and export of simulated data to EXCEL.

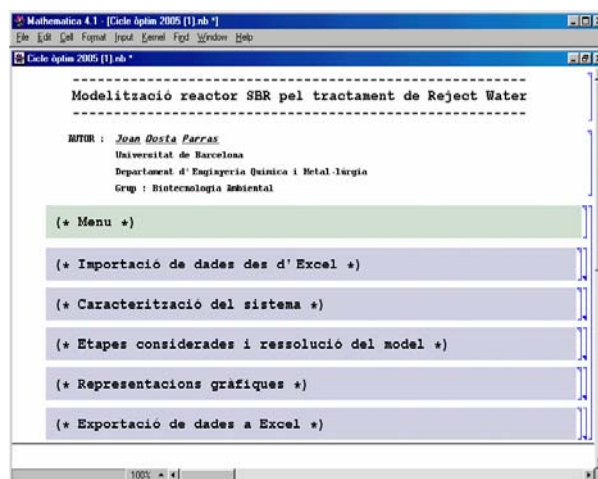


Figure 3.10 – Initial menu of the programme written in Mathematica 4.1 for this study to model the biological nutrient removal

In order to assess the model parameters, several batch respirometric tests were performed under very well defined experimental conditions where the influence of a model constant was highly pronounced (Vanrolleghem et al., 1999). Each parameter was assessed at least three times and, concomitantly with the OUR monitoring, analysis of $\text{NH}_4^+\text{-N}$, $\text{NO}_2^-\text{-N}$ and $\text{NO}_3^-\text{-N}$ were also performed to obtain more reliable experimental values. Parameter estimation was carried out by modelling experimental data from these tests and using the Nelder-Mead Simplex search method, where the weighted sum of squared errors between model outputs and the measured data was minimized.

3.6. SUBSTRATE AND INOCULUM.

Three types of wastewaters were analysed in this study: sludge reject water from a municipal wastewater treatment plant (WWTP), supernatant from anaerobic digestion of the Organic Fraction of Municipal Solid Waste (OFMSW) and supernatant from anaerobically digested piggery wastewater.

Sludge reject water from a municipal WWTP was obtained from a mesophilic anaerobic digester of a WWTP situated in the Barcelona metropolitan area (Spain). This effluent was centrifuged at 2,500 rpm to remove suspended solids before its recirculation to the plant head. Hydrolysed primary sludge was obtained in the same WWTP. All these

streams were collected and kept at 4 °C until its use in the laboratory. In order to inoculate the reactors working with reject water, microorganisms were taken from the sludge withdraws of the WWTP and were adapted to the BNR process in a batch tank where successive increasing nitrogen loads were performed.

The supernatant from wet anaerobic digestion of OFMSW was obtained from the Ecoparc-1 of Barcelona. This stream was collected and kept at 4°C in the laboratory until its treatment. Microorganisms were taken from the sludge withdrawals of the aerobic reactor of the WWTP of the Ecoparc-1.

Liquid fraction of anaerobically digested piggery wastewater was obtained from an anaerobic mesophilic digestion treatment plant through the VALPUREN process (Flotats et al., 2004). To start-up the biological process, the SBR was seeded with nitrifying/denitrifying biomass from another SBR treating sludge reject water from municipal WWTP.

In the Anammox SBR, synthetic wastewater was used as explained in Chapter 9. This biological reactor was inoculated with 7.4 g VSS L⁻¹ of Anammox biomass (attached in a zeolite) coming from a biofilm SBR treating synthetic wastewater (Fernández *et al.*, 2006). Attached biomass from the same biofilm SBR and granular biomass from another SBR were employed in order to perform the SAA tests.

3.7. ANALYTICAL METHODS.

The analytical methods used in this work are detailed here. These analyses were performed according to the '*Standard Methods for the examination of Water and Wastewater*' (APHA, 1998) in the laboratories of the University of Barcelona (UB), the University of Santiago de Compostela (USC) and/or the scientific-technical services of the University of Barcelona. Once the samples were withdrawn from the reactor, they were immediately centrifuged at 1,000 rpm during 10 min in order to stop the biological activity.

3.7.1. Solids content.

Total solids (TS) and Volatile Total Solids (VTS) were determined following the 2540B and 2540E reference methods of the Standard Methods for the Examination of Water and Wastewater (APHA, 1998), respectively. A known volume of wastewater (V) was added in a porcelain capsule previously weighed (W_1) and it was maintained 24 h at 105°C in order to evaporate completely the water. The porcelain capsule was introduced in a desiccator for 10 minutes to balance temperature and was weighed (W_2). By means of Equation 3.3, the TS concentration could be calculated. Subsequently, the porcelain with the TS was maintained during 1h at 550°C. After being 10 minutes in the desiccator, the weigh of the porcelain and the non-volatile TS were determined (W_3). Then, VTS was calculated by means of Equation 3.4.

$$TS (g L^{-1}) = \frac{W_2(g) - W_1(g)}{V (L)} \quad (3.3)$$

$$VTS (g L^{-1}) = \frac{W_2(g) - W_3(g)}{V (L)} \quad (3.4)$$

Total suspended Solids (TSS) and Volatile Suspended Solids (VSS) were determined following the reference methods 2540D and 2540E of the Standard Methods (APHA, 1998), respectively. A known volume of wastewater (V) was filtered through a 0.45µm standard filter, previously weighed (W_4). Then, the filter with the TSS was maintained at 105 °C during 1h, was introduced in a desiccator for 10 minutes and was weighed (W_5). TSS concentration was calculated according to Equation 3.5. Finally, the filter with TSS was maintained at 550 °C for 15 minutes, was introduced in a desiccator for 10 minutes and was weighed (W_6). The VSS were calculated by means of Equation 3.6.

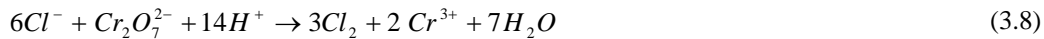
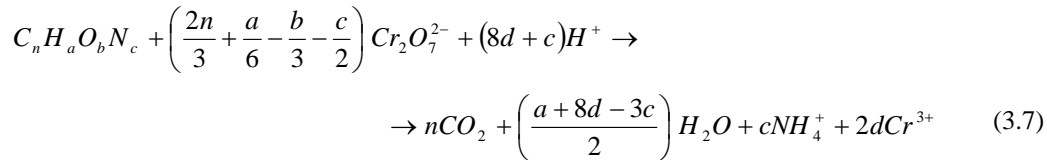
$$TSS (g L^{-1}) = \frac{W_5(g) - W_4(g)}{V (L)} \quad (3.5)$$

$$VSS (g L^{-1}) = \frac{W_5(g) - W_6(g)}{V (L)} \quad (3.6)$$

3.7.2. Chemical Oxygen Demand (COD) and Biological Oxygen Demand (BOD)

The COD and the BOD indicate the quantity of matter present in a wastewater sample that is susceptible to be oxidized. Both the COD and the BOD are expressed in terms of $\text{mg O}_2 \text{ L}^{-1}$.

The COD is defined as the quantity of oxygen used in biological and non-biological oxidation of materials (organic and inorganic) in water. The reference method 5220C (APHA, 1998) was the standard method used to assess the COD. It consisted on the complete oxidation of the matter contained in the liquid sample with a strong oxidizing agent (potassium dichromate) under acidic conditions (achieved by the addition of sulphuric acid). Equation 3.7 shows the reaction of potassium dichromate with organic compounds. Silver sulphate was used as a catalyst of the reaction. Since chloride may interfere in the determination of COD (see Equation 3.8), mercuric sulphate was also added to avoid chloride interference.



To be exact, 2.5 mL of the wastewater sample were mixed with 1.5 mL of sodium dichromate 0.04 mol L^{-1} (with 80 g L^{-1} of mercury (II) sulphate) and 3.5 mL of silver sulphate solution 10 g L^{-1} in sulphuric acid. Concomitantly with the samples, 4 patrons with 0, 250, 500 and 1000 mg COD L^{-1} (potassium biphtalate) were analysed. Subsequently, the samples were maintained at $150 \text{ }^\circ\text{C}$ during 2h in a COD digester (see Figure 3.11) to ensure the complete reaction to take place. After the digestion, the samples were introduced in a refrigerator during 10 hours to allow the solids formed to be decanted. Finally, the absorbance at $\lambda=620 \text{ nm}$ of the COD samples was analysed by means of a spectrophotometer (Shimadzu UV-1203; see Figure 3.11). From the correlation obtained between the COD from the patrons and the absorbance at $\lambda=620 \text{ nm}$, the COD of every sample was calculated by means of Equation 3.9.

$$\text{COD (mg O}_2 \text{ L}^{-1}) = m \cdot \text{ABS} + b \quad (3.9)$$

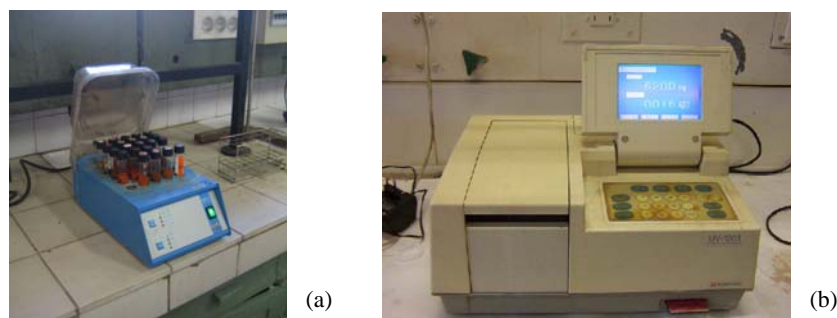


Figura 3.11 - Apparatus used to perform the analysis of COD.

On the other hand, the BOD is defined as the quantity of oxygen used by microorganisms to stabilize decomposable organic matter under aerobic conditions. The standard method with reference 5210B (APHA, 1998) was the one used to assess the BOD. It consisted on the measurement of the rate of oxygen use under incubation in the dark at 20°C for 5 days. The apparatus used to perform this analysis was the WTW OxiTop measuring system (Weilheim, Germany).

3.7.3. Total Ammonium Nitrogen.

Total Ammonium Nitrogen Concentration ($\text{NH}_4^+\text{-N}$) was analysed with an specific ammonia electrode (Crison, Micro pH2002 model) following the standard method with reference 4500-NH₃D (APHA, 1998). A strong base (NaOH) was added to the samples in order to convert completely $\text{NH}_4^+\text{-N}$ to free ammonia nitrogen. Immediately, the electrode was submerged into the sample and provided a potential in mV (ΔV). This potential was correlated to $\text{NH}_4^+\text{-N}$ concentration by means of the semilogarithmic expression of Equation 3.10. Every time the samples were analysed, 4 patrons of 5, 25, 50 and 100 mg $\text{NH}_4^+\text{-N L}^{-1}$ were analysed to calibrate the electrode.

$$\text{Ln}(N - \text{NH}_4^+) = a(\Delta V) + b \quad (3.10)$$

In Chapter 9, $\text{NH}_4^+\text{-N}$ was analysed using the phenol-hypochloride method (Wheatherburn, 1967; Standard Method with reference 4500-NH₃F) carried out in a spectrophotometer (Shimadzu, UV-1603) at $\lambda = 635$ nm. The relation between absorbance

at 635 nm and $\text{NH}_4^+\text{-N}$ was obtained by the analysis of 6 patrons within the range 0–1 mg $\text{NH}_4^+\text{-N L}^{-1}$.

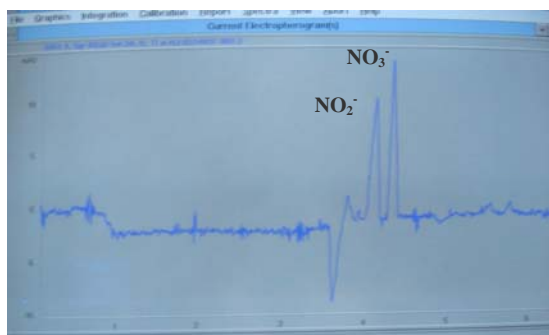
3.7.4. Nitrites, Nitrates and Phosphates.

Nitrite ($\text{NO}_2^-\text{-N}$), nitrate ($\text{NO}_3^-\text{-N}$) and phosphate ($\text{PO}_4^{3-}\text{-P}$) concentrations were analysed by Capillary Electrophoresis (CE). Once the samples were withdrawn from the reactor, they were centrifuged at a Relative Centrifugal Force (g) of 2295 for 10 min and filtered through 0.45 μm cellulose paper filters to remove suspended solids before being fed to the CE device (Hewlett Packard 3D; See Figure 3.12).

The Capillary Electrophoresis is used to separate ionic species by their charge and frictional forces. In this technique, electrically charged analytes (such as Cl^- , NO_2^- , NO_3^- and/or PO_4^{3-}) migrate in a conductive liquid medium under the influence of an electric field. The separation of the analytes is produced, since their migration velocity is related to their size to charge ratio. Therefore, low molecular weighted analytes (such as chlorides) migrates quickly. As they migrate, these analytes are detected near the outlet end of the capillary. The output of the detector is sent and logged in a computer and these data is displayed as an electropherogram (detector response versus time). In this electropherogram, separated anions appear as peaks with different retention times (see Figure 3.12(b)). The identification and evaluation of the concentration of nitrites, nitrates and phosphates is based on several patrons of $\text{NO}_2^-\text{-N}$, $\text{NO}_3^-\text{-N}$ and $\text{PO}_4^{3-}\text{-P}$ in the range of 0 - 80 mg L^{-1} analysed concomitantly with the actual samples.



(a)



(b)

Figure 3.12 - CE device (a) and electropherogram of a patron with nitrites and nitrates (b).

3.7.5. Volatile Fatty Acids (VFA)

In this study, VFA concentration and composition analysis were performed by gas chromatography (Hewlett-Packard-5890A, see figure 3.13) equipped with a Flame Ionisation Detector (FID) and using nitrogen as gas carrier (Llabrès and Mata-Álvarez, 1988). The exact operation conditions are detailed in Benabdallah El-Hadj (2006). A complex mixture is separated into its components by eluting the components from a heated column packed with sorbent by means of a moving-gas phase. Qualitative and quantitative information is obtained from analyzing the peaks appearing on a chromatogram. The identification and evaluation of the concentration of VFA is based on several patrons of VFA supplied by Supelco. Figure 3.13 (b) shows a typical chromatogram of VFAs standard mixture (Supelco, Ref. 46975-U).

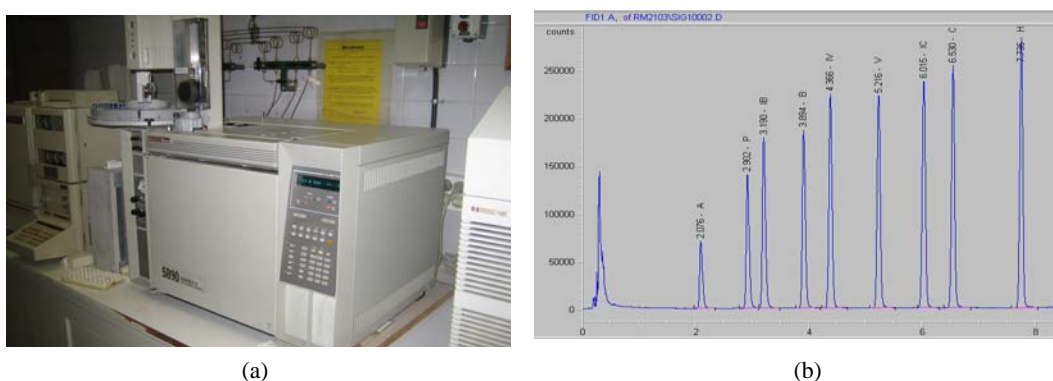


Figure 3.13 - Gas chromatograph (a) and a typical chromatogram of a VFA standard mixture (b)

3.7.6. Alkalinity

Alkalinity is a measure of the buffering capacity of a water or wastewater to neutralize acids. The buffering capacity of a wastewater is mainly related to the bases bicarbonate (HCO_3^-) and carbonate (CO_3^{2-}). However, the possible presence of other buffering species such as hydroxide (OH^-), borates, silicates, phosphates, ammonium, sulfides, and organic ligands can also provide alkalinity to the wastewater.

Alkalinity was measured in a titrator (Schott-TA20 plus) that automatically performed the addition of HCl 0.1 N (in steps of 0.5 mL) to 20 mL of wastewater sample. Figure 3.14 shows the experimental set-up used for alkalinity measurements. By means of the

evaluation of the acid/base titration curve, the equivalency point of the CO₂ was assessed and, therefore, the alkalinity of the sample. Alkalinity is usually expressed in terms of mg CaCO₃ L⁻¹ or mol CO₃²⁻ L⁻¹.



Figure 3.14 – Titrator used to perform alkalinity measurements.

3.7.7. Sludge Volumetric Index (SVI)

The Sludge Volumetric Index (SVI) is the volume of settled sludge after 30 minutes of sedimentation (V₃₀) per unit of VSS. The SVI can be calculated from Equation 3.11 where X is the total VSS present in the mixed liquor used to perform the analysis. For practical needs, rough estimates from Table 3.1 can be applied.

$$SVI (mL g^{-1} VSS) = \frac{V_{30} (mL)}{X (g VSS)} \quad (3.11)$$

Table 3.1 – Relationship between SVI and Activated Sludge settling characteristics (adapted from Grady et al. (1999))

SVI (mL g ⁻¹ VSS)	Sludge settling and compaction characteristics (-)
< 80	Excellent
80 – 150	Moderate
> 150	Poor

4. Operation and model description of a sequencing batch reactor treating reject water for Biological Nitrogen Removal over nitrite.

ABSTRACT

The aim of this study was the start-up, operation and model description of a sequencing batch reactor (SBR) for biological nitrogen removal (BNR) from a reject water (800-900 mg NH₄⁺-N L⁻¹) from a municipal wastewater treatment plant (WWTP). The SBR was operated with 3 cycles per day, temperature 30°C, SRT 11 days and HRT 1 day. During the operational cycle, three alternating aerobic/anoxic periods were performed to avoid alkalinity restrictions. Oxygen supply and working pH range were controlled to achieve the BNR over nitrite, which makes the process more economical. Under steady state conditions, a total nitrogen removal of 0.87 kg N (m³ day)⁻¹ was reached.

A four-step nitrogen removal model was developed to describe the process. This model enlarges the IWA activated sludge models for a more detailed description of the nitrogen elimination processes and their inhibitions. A closed intermittent-flow respirometer was set up for the estimation of the most relevant model parameters. Once calibrated, model predictions reproduced experimental data accurately.

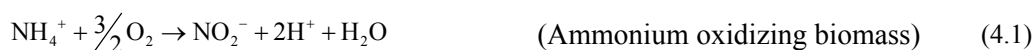
The most relevant parts of this chapter are published in:

Dosta, J., Galí, A., Benabdallah el-Hadj, T., Macé, S., Mata-Álvarez, J. (2007) Operation and model description of a sequencing batch reactor treating reject water for biological nitrogen removal via nitrite. *Bioresource Technology*. Vol 98 (11) pp 2065-2075

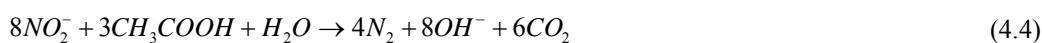
4.1 INTRODUCTION

As explained in chapter 1, in Wastewater Treatment Plants (WWTPs), the supernatant from centrifugation of anaerobically digested sludge (reject water) contains up to 25% of the total nitrogen load in a flow, and it is usually returned to the head of the sewage treatment works (Macé and Mata-Álvarez, 2002). Biological Nitrogen Removal (BNR) from this wastewater (800-900 mg NH₄⁺-N L⁻¹) can be achieved in the existing WWTP. An efficient alternative is the use of a sequencing batch reactor (SBR) for the treatment of this highly loaded water, since nitrogen removal efficiencies of more than 90% have been reported (Arnold *et al.*, 2000; Rostron *et al.*, 2001).

The BNR process is divided into two steps: the oxidation of ammonium to nitrate (nitrification) and the nitrate reduction to nitrogen gas (denitrification). Nitrification is defined as a two-step process, where ammonium is firstly oxidized to nitrite (nitritation, equation 1) and subsequently nitrite is oxidized to nitrate (nitratation, equation 2).



Denitrification is then the reduction of NO₃⁻ to NO₂⁻ (equation 3) and further on to N₂ (equation 4) by the catabolism of heterotrophic bacteria. This process is carried out under anoxic conditions and with a biodegradable carbon source, such as acetate, as electron donor.



Some authors (Abeling and Seyfreid, 1992; Hellinga *et al.*, 1999; Wett and Rauch, 2003) have discussed the beneficial effects of performing the BNR process via nitrite, since it suggests a saving of 25% of the aeration costs and 40% of the external carbon source needed during denitrification, as well as a reduction in the amount of sludge produced. Many ways have been described in literature to achieve the BNR process via nitrite. Anthonisen *et al.* (1976) determined the effect of ammonia (NH₃) and nitrous acid (HNO₂) concentration upon the ammonium oxidation and the nitrite oxidation kinetics.

These authors demonstrated that Nitrite Oxidizing Biomass (NOB) is inhibited at concentrations higher than 0.2-2.8 mg HNO₂ L⁻¹ and/or 0.1-1.0 mg NH₃ L⁻¹, while Ammonium Oxidizing Biomass (AOB) is inhibited by unionised ammonia concentrations higher than 10-150 mg NH₃ L⁻¹. Wett and Rauch (2003) corroborated these experimental results and experienced a partial inhibition of nitrite oxidizers in a SBR treating extremely ammonium loaded landfill leachate and reject water. Grunditz and Dalhammar (2001) also reported that NOB kinetics are more affected by basic values of pH than AOB. Furthermore, many authors (Guisasola *et al.*, 2005; Pollice *et al.*, 2002; Ruiz *et al.*, 2003) have reported that, at reduced dissolved oxygen concentrations, ammonium oxidation is favoured over NOB activity due to a greater oxygen affinity for the first step of nitrification. Another technique to achieve the inhibition of NOB consists of the SHARON process (Hellings *et al.*, 1999). This process is based on the careful selection of a low sludge retention time (SRT) and a high operating temperature (35°C), which enables the proliferation of AOB and the total wash-out of NOB.

Activated sludge models (Henze *et al.*, 2000) represent the most widespread and successful approach to characterise the nutrient removal process for design and control (Copp *et al.*, 2002; Seco *et al.*, 2004). The biological nature of wastewater treatment processes implies that their model parameters must be determined (model calibration) according to the local situation (Vanrolleghem *et al.*, 1999). Respirometry is the most popular tool used for model calibration and it consists of the measurement and analysis of the biological oxygen consumption under well defined experimental conditions (Rozich and Gaudy, Jr., 1992; Spanjers *et al.*, 1998).

On the other hand, the IWA models (Henze *et al.*, 2000) describe nitrification as a single step process, since nitrite does not usually appear as an intermediate product under the typical temperature range and ammonium concentrations of secondary biological reactors from municipal WWTP. However, these models must be modified to describe properly high ammonium loaded wastewater treatments and/or to study the BNR via nitrite.

In this study, a BNR via nitrite strategy in a SBR was implemented for the treatment of a specific reject water (Barcelona Metropolitan Area). Moreover, the SBR working sequence under steady state conditions was characterised by means of a modified version of the IWA ASM models (Henze *et al.*, 2000) previously calibrated using respirometry.

4.2. RESULTS AND DISCUSSION

4.2.1. Reject water characterisation

Table 4.1 shows the average composition of the reject water used in the experiments. This wastewater was mainly characterised by a high ammonium concentration (800-900 mg $\text{NH}_4^+\text{-N L}^{-1}$) and a high temperature, which made its treatment at 30°C feasible. The bicarbonate to ammonium ratio on a molar basis was approximately 1, which means that the alkalinity of the wastewater was not sufficient to buffer the complete nitrification process but only about half the process. Consequently, the reactor performance should include the alternation of different Nitrification/Denitrification (N/DN) stages, since denitrification compensates in part for the alkalinity lost during the nitrification process.

Table 4.1 - Average composition of the centrifuged sludge effluent during 2004.

Component	Units	Value
SS	mg L ⁻¹	675
COD	mg L ⁻¹	1500-2000
NH ₄ ⁺ -N	mg L ⁻¹	800-900
P-total	mg L ⁻¹	19.3
HCO ₃ ⁻	mg L ⁻¹	3000
HCO ₃ ⁻ /N ratio	mol HCO ₃ ⁻ (mol NH ₄ ⁺ -N) ⁻¹	0.98
Temperature	°C	35
pH	-	8.2

Moreover, reject water from anaerobic digestion of sludge from a municipal WWTP is commonly characterised by a low BOD/N ratio (Hellings *et al.*, 1999; Vandaele *et al.*, 2000; Wett and Rauch, 2003). In order to assess the biodegradability of the reject water COD under study, two respirograms were evaluated. The first one was run at 30°C and a pH range of 8.0 ± 0.1 and the second one under the same experimental conditions but with 12 mg L⁻¹ of Allyl-Thiourea (ATU) as a nitrification inhibitor (Vanrolleghem *et al.*, 1999). In these experiments, 150 mL of wastewater were added to 2.85 L of endogenous mixed liquor with 620 mg VSS L⁻¹. The respirograms (Figure 4.1) show the very low biodegradable oxygen demand at short time (BOD_{ST}) fraction of the wastewater, which

demonstrates the requirement for an external biodegradable carbon source for denitrification.

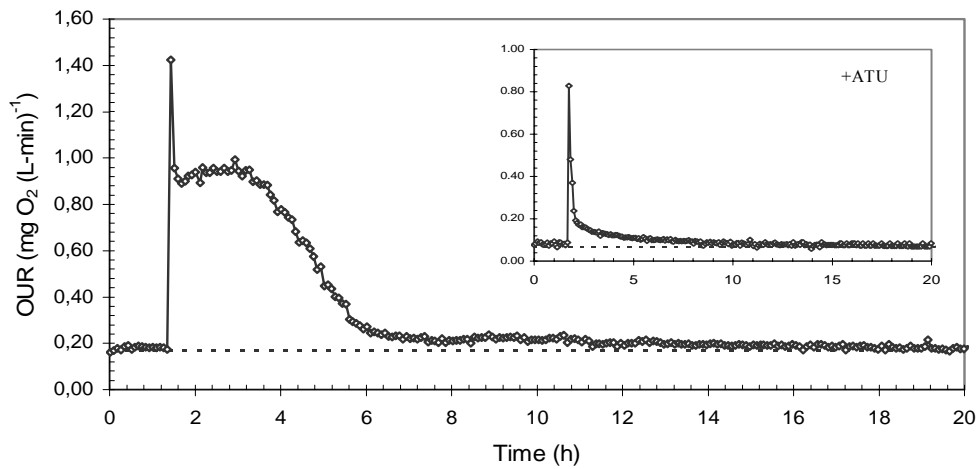


Figure 4.1 – Respirogram obtained for the determination of BOD_{ST} of reject water under study without nitrification inhibition and (insertion) with 12 mg L⁻¹ of ATU. Experimental data (o) and endogenous OUR (---)

4.2.2. Start-up of the SBR

The SBR reactor operated in this study was inoculated with activated sludge from a secondary reactor of a municipal WWTP. In order to treat highly ammonium loaded wastewaters in an SBR, the biomass inside the reactor must be specially enriched in nitrifying biomass (denitrification is carried out by facultative heterotrophic bacteria that can be present in activated sludge and grows faster than autotrophic biomass). Consequently, the secondary sludge was adapted to nitrification by successive additions of ammonium chloride to a batch reactor (3L) continuously aerated under controlled pH conditions (8.0 ± 0.1). Figure 4.3 shows the specific Ammonium Uptake Rate (sAUR) along one month, time enough to achieve good nitrifying activity. The increase of sAUR can be adjusted to an exponential expression, since autotrophic biomass grew under non-limiting substrate conditions. The VSS concentration experienced a pronounced decrease during the first days of acclimation due to the decay of heterotrophic biomass present in secondary sludge.

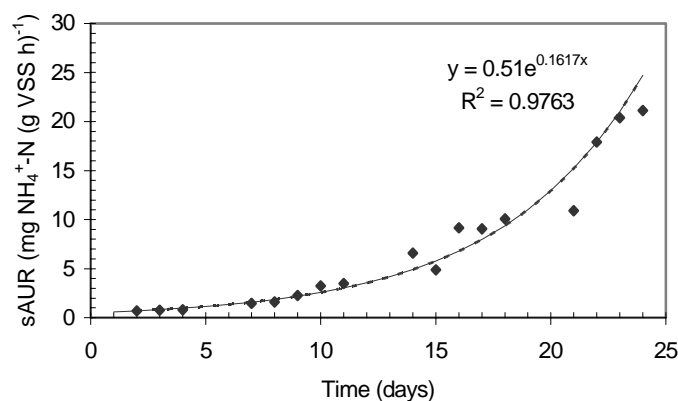


Figure 4.2 – sAUR evolution during the enrichment of secondary activated sludge to the nitrification process.

Experimental sAUR (·) and exponential fit (-)

After one month of acclimation of secondary activated sludge to the nitrification process, this biomass was mixed with secondary sludge from a municipal WWTP and inserted in a SBR to treat reject water in cycles of 8 hours.

4.2.3. Reject water treatment in a SBR

A SBR seeded with the previously developed nitrifying activated sludge was operated with an 8 h cycle at 30°C. Hydraulic retention time (HRT) and SRT were set at 1 and 11 days, respectively. Each cycle consisted of nine stages: aerobic fill (0.25 h), aerobic (1.75h), anoxic (1.00 h), aerobic (1.50h), anoxic (0.50 h), aerobic (1.5h), anoxic (0.75 h), settle (0.5 h) and draw (0.25 h). The aerobic to anoxic time ratio was set around 2 and the air flow was regulated during aerobic periods to maintain a DO level below 1 mg L⁻¹, in order to ensure the nitrite route (Guisasola *et al.*, 2005; Ruiz *et al.*, 2003). Sodium acetate was used as electron donor during anoxic periods since the BOD_{ST} present in the reject water was not suitable for denitrification. The reactor was operated with three internal N/DN subcycles in order to avoid alkalinity limitations and nitrification inhibition due to high HNO₂ concentrations. Figure 4.3 presents the pH and DO profiles during the operation at stationary state, where it is demonstrated that the pH remained within an optimal range (7.5-8.5) without external chemical additions. Biomass content expressed as VSS was 3 g VSS L⁻¹.

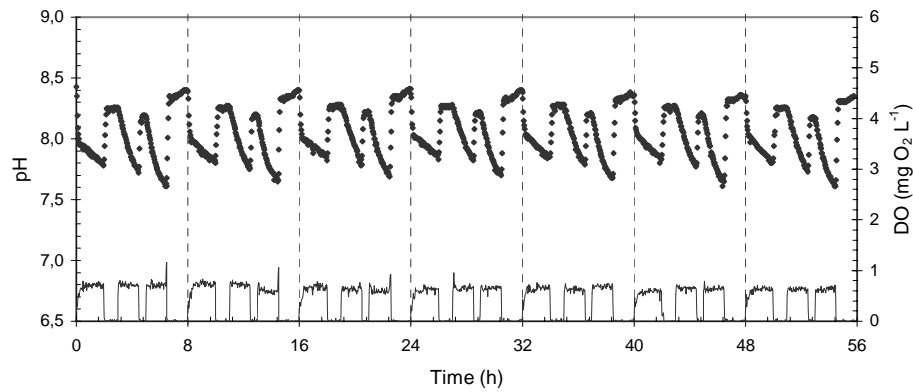


Figure 4.3 – Experimental pH and DO profiles during consecutive cycles inside the SBR under steady state conditions. pH (●), DO (—) and cycle delimitation (---).

Nitrogen was completely removed at the end of cycle operation, as can be appreciated from Figure 4.4, where the relevant state variables of a representative cycle are shown. Nutrient removal rates of $19 \text{ mg N-NH}_4^+ (\text{g VSS h})^{-1}$ during nitrification and $40 \text{ mg N-NO}_2^- (\text{g VSS h})^{-1}$ during denitrification were achieved at stationary state.

4.2.4. Four-step nitrogen removal Model

A modification of the Activated Sludge Models (Henze *et al.*, 2000) was developed in order to describe the BNR process in the activated sludge system under study. Table 4.2 present the processes considered to model the system. Nitrification was described as a two step process, since operational conditions favoured nitritation over nitrataion. Moreover, kinetic expressions for both nitrification reactions included non-competitive inhibition terms for NH_3 and HNO_2 based on the study of Anthonisen *et al.* (1976), as described by Wett and Rauch (2003). Denitrification was also described as a two step process, where nitrate is firstly reduced to nitrite, which is subsequently reduced to nitrogen gas. Two correction factors for heterotrophic growth under anoxic conditions were considered in order to assess the kinetics for both nitrogen reduction reactions. Lineal death was assumed for the decay process of both heterotrophic and autotrophic organisms in order to make the mathematical model as simple as possible. It was assumed that variation in biomass concentration during one cycle of operation was not important and, therefore, both heterotrophic and autotrophic active fractions were considered to be

constant. Hydrolysis of slowly biodegradable COD was not considered, since it did not affect the BNR process significantly.

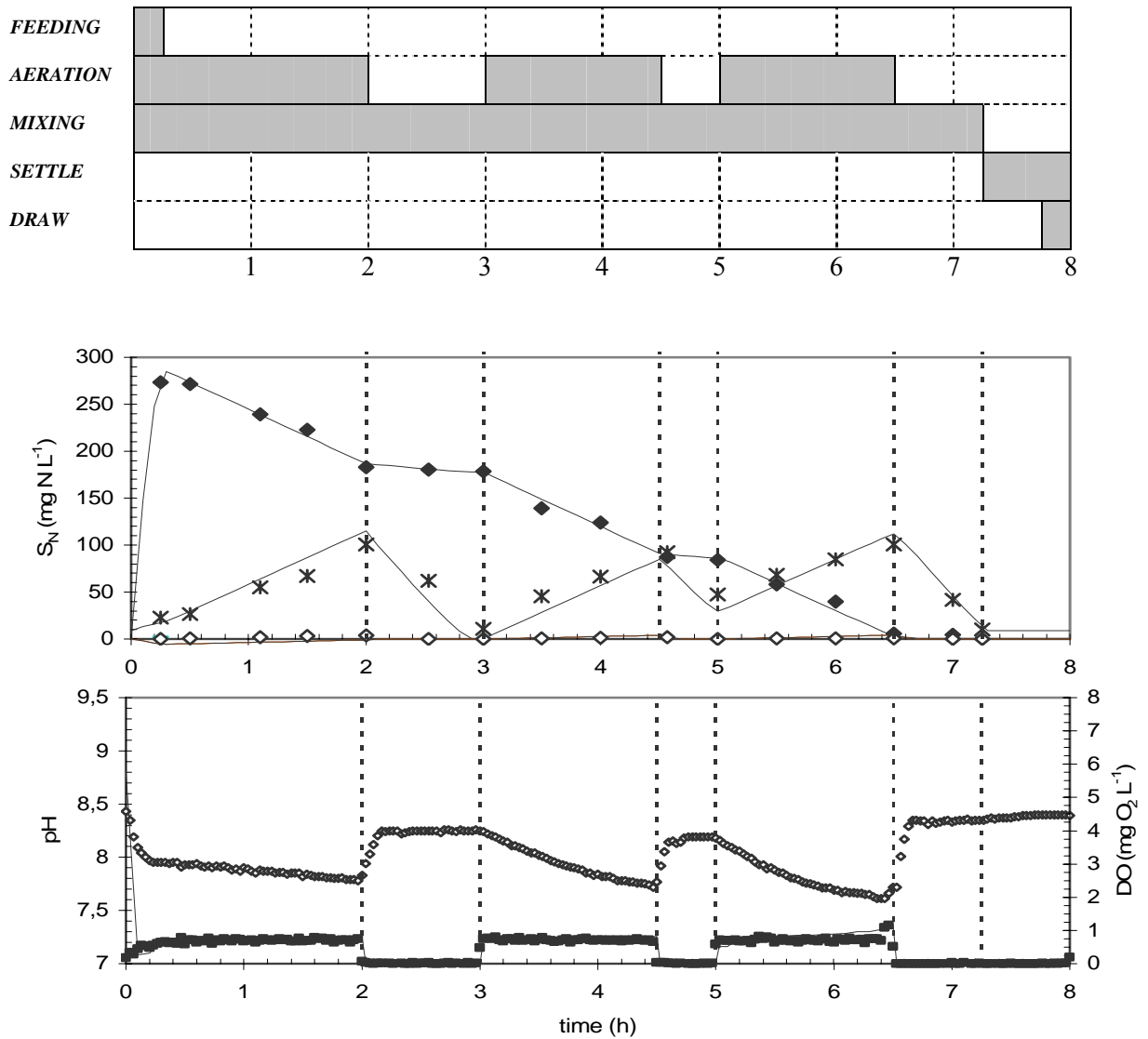


Figure 4.4 – Experimental and modelled profiles of (a) $\text{NH}_4^+\text{-N}$, $\text{NO}_2^-\text{-N}$ and $\text{NO}_3^-\text{-N}$ and (b) pH and dissolved oxygen.

Experimental data: $\text{NH}_4^+\text{-N}$ (\blacklozenge); N-NO_2^- (*); N-NO_3^- (\diamond); pH (\circ); DO (\bullet) and stage delimitations (---). Simulated data (—).

Table 4.2 – Kinetic equations of the considered processes

(j) Processes	Kinetic rate equations ($\rho_i > 0$)
Heterotrophic organisms	
(1) Heterotrophic aerobic growth on S_S Heterotrophic anoxic growth on S_S	$\mu_{mH} \frac{S_S}{K_S + S_S} \frac{S_O}{S_O + K_{OH}} F_{H,pH} X_{BH}$
(2) Nitrate reduction to nitrite	$\eta_{NO_3 \rightarrow NO_2} \mu_{mH} \frac{S_S}{K_S + S_S} \frac{K_{OH}}{S_O + K_{OH}} \frac{S_{NO_3}}{K_{NO_3} + S_{NO_3}} F_{H,pH} X_{BH}$
(3) Nitrite reduction to Nitrogen gas	$\eta_{NO_2 \rightarrow N_2} \mu_{mH} \frac{S_S}{K_S + S_S} \frac{K_{OH}}{S_O + K_{OH}} \frac{S_{NO_2}}{K_{NO_2} + S_{NO_2}} F_{H,pH} X_{BH}$
(4) Heterotrophic decay	$b_H X_{BH}$
Autotrophic organisms	
(5) Aerobic growth of AOB	$\mu_{m,AOB} \frac{S_{NH}}{K_{NH} + S_{NH}} \frac{K_{NH_3}^{AOB}}{K_{NH_3}^{AOB} + S_{NH_3}} \frac{K_{HNO_2}^{AOB}}{K_{HNO_2}^{AOB} + S_{HNO_2}} \frac{S_O}{S_O + K_{O,AOB}} \frac{S_{ALK}}{K_{ALK} + S_{ALK}} X_{AOB}$
(6) Aerobic growth of NOB	$\mu_{m,NOB} \frac{S_{NO_2}}{K_{NO_2} + S_{NO_2}} \frac{K_{NH_3}^{NOB}}{K_{NH_3}^{NOB} + S_{NH_3}} \frac{K_{HNO_2}^{NOB}}{K_{HNO_2}^{NOB} + S_{HNO_2}} \frac{S_O}{S_O + K_{O,NOB}} \frac{S_{ALK}}{K_{ALK} + S_{ALK}} X_{NOB}$
(7) Autotrophic decay	$b_A (X_{AOB} + X_{NOB})$
Operation conditions	
(8) Oxygen supply	$K_L a_{O_2} (S_O - He_{O_2} P_{P,O_2})$

Table 4.3 shows the model applied in this study in Petersen Matrix format. As it is observed, the autotrophic stoichiometric coefficients were distinguished in those related to nitrification and those referred to nitrification.

In the present work, pH was not modelled but its evolution during the cycle was taken into account in order to detect possible restrictions in kinetic rates linked to NH_3 and/or HNO_2 concentrations. However, alkalinity restriction was taken into account by means of a Monod type equation as described in the IWA Activated Sludge Models (Henze *et al.*, 2000). For every component and process studied, a continuity function was applied as described in the IWA models (Henze *et al.*, 2000). Table 4.4 shows the coefficients used to apply the continuity functions in the biological system under study.

Table 4.3 – Petersen Matrix of the proposed Activated Sludge Model

	S_S	S_I	S_O	S_{NH}	S_{NO_2}	S_{NO_3}	S_{M_2}	X_I	X_{BH}	X_{AOB}	X_{NOB}	S_{ALK}
<i>Heterotrophic aerobic growth on S_S</i>	$-\left(\frac{1}{Y_H}\right)$		$-\left(\frac{1-Y_H}{Y_H}\right)$	$-i_{SB}$					1			$\left(\begin{smallmatrix} * \\ \end{smallmatrix}\right)$
<i>Nitrate reduction to nitrite</i>	$-\left(\frac{1}{Y_H}\right)$			$-i_{SB}$	$\left(\frac{1-Y_H}{1.14Y_H}\right)$	$-\left(\frac{1-Y_H}{1.14Y_H}\right)$			1			$\left(\begin{smallmatrix} * \\ \end{smallmatrix}\right)$
<i>Nitrite reduction to Nitrogen gas</i>	$-\left(\frac{1}{Y_H}\right)$			$-i_{SB}$	$-\left(\frac{1-Y_H}{1.71Y_H}\right)$		$\left(\frac{1-Y_H}{1.71Y_H}\right)$		1			$\left(\begin{smallmatrix} * \\ \end{smallmatrix}\right)$
<i>Heterotrophic decay</i>			-1						-1			$\left(\begin{smallmatrix} * \\ \end{smallmatrix}\right)$
<i>Aerobic growth of AOB</i>			$-\left(\frac{3.43-Y_{AOB}}{Y_{AOB}}\right)$	$-i_{SB} - \left(\frac{1}{Y_{AOB}}\right)$	$\left(\frac{1}{Y_{AOB}}\right)$					1		$\left(\begin{smallmatrix} * \\ \end{smallmatrix}\right)$
<i>Aerobic growth of NOB</i>			$-\left(\frac{1.14-Y_{NOB}}{Y_{NOB}}\right)$	$-i_{SB}$	$-\left(\frac{1}{Y_{NOB}}\right)$	$\left(\frac{1}{Y_{NOB}}\right)$					1	$\left(\begin{smallmatrix} * \\ \end{smallmatrix}\right)$
<i>Autotrophic decay</i>			-1						-1			$\left(\begin{smallmatrix} * \\ \end{smallmatrix}\right)$
<i>Oxygen supply</i>			1									$\left(\begin{smallmatrix} * \\ \end{smallmatrix}\right)$

$\left(\begin{smallmatrix} * \\ \end{smallmatrix}\right)$ Stoichiometric parameters calculated from continuity equations

Table 4.4 – Coefficients used in this study for the application of continuity functions

Component	Units	COD	N	Charge
		[$i_{COD,i}$] (g COD)	[$i_{N,i}$] (g N)	[$i_{Charge,i}$] (mole charge +)
S_O	(g O ₂)	-1		
S_S (acetate)	(g COD)	1		-1/64
S_{NH}	(g NH ₄ ⁺ -N)		1	1/14
S_{NO2}	(g NO ₂ ⁻ -N)		1	-1/14
S_{NO3}	(g NO ₃ ⁻ -N)		1	
S_{N2}	(g N ₂ -N)		1	
S_I	(g COD)	1		
X_S	(g COD)	1	$i_{N,XS}$	
X_I	(g COD)	1	$i_{N,SI}$	
X_{BH}	(g COD)	1	0.07	
X_{AOB}	(g COD)	1	0.07	
X_{NOB}	(g COD)	1	0.07	
X_{TSS}	(g TSS)			
S_{ALK}	(mol HCO ₃ ⁻)			-1

4.2.5. Calibration of the model

In order to characterise the biological degradation process in the optimum working cycle, the relevant kinetic and stoichiometric parameters (detailed in Table 4.5) involved in both organic carbon and nitrogen removal were determined. Respirometry was the tool used to calibrate these model parameters. Suggested values from literature were assumed for those parameters which were not determined experimentally.

The respirometric batch tests used to assess the model parameters and their significance are discussed below. Before the application of a respirometric test, biomass from the withdrawals of the SBR was aerated at least during 12 hours at controlled pH (8.0) in absence of nutrients to assure that it was under endogenous conditions (Dircks *et al.*, 1999).

Table 4.5 – Average values of model parameters for the case studied.

Parameter	T (°C)	Value	Units	Reference
Heterotrophic biomass				
Y_H	30	0.62 ± 0.01	mg COD (mg COD) ⁻¹	Present study
$\mu_{mH} X_{BH}$	30	495.5 ± 30.5	mg cell COD (L h) ⁻¹	Present study
b_H	30	0.043 ± 0.01	day ⁻¹	Present study
K_S	30	15 ± 8	mg COD L ⁻¹	Present study
K_{OH}	30	0.19 ± 0.05	mg O ₂ L ⁻¹	Present study
$\eta_{NO_2 \rightarrow N_2}$	30	0.78 ± 0.03	(-)	Present study
$\eta_{NO_3 \rightarrow NO_2}$	30	0.18 ± 0.05	(-)	Present study
K_{NO_2}	30	0.9 ± 0.3	mg N-NO ₂ L ⁻¹	Present study
K_{NO_3}	30	1.4 ± 0.2	mg N-NO ₃ L ⁻¹	Present study
$\dot{i}_{X,B}$	10-20	0.07	mg NH ₄ ⁺ -N (mg COD) ⁻¹	Henze <i>et al.</i> (2000)
Autotrophic biomass				
Y_{AOB}	30	0.22 ± 0.01	mg COD (mg NH ₄ ⁺ -N) ⁻¹	Present study
Y_{NOB}	30	0.08	mg COD (mg NO ₂ ⁻ -N) ⁻¹	Hellinga <i>et al.</i> (1999)
$\mu_{mAOb} X_{AOB}$	30	18.5 ± 0.5	mg cell COD (L h) ⁻¹	Present study
$\mu_{mNOB} X_{NOB}$	30	0.42 ± 0.28	mg cell COD (L h) ⁻¹	Present study
b_A	30	0.20	day ⁻¹	Henze <i>et al.</i> (2000) and Ekama and Marais (1984)
K_{NH}	30	1.27 ± 0.4	mg NH ₄ ⁺ -N L ⁻¹	Present study
K_{NO}	-	0.11	mg NO ₂ ⁻ -N L ⁻¹	Marsili-Libelli and Tabani (2002)
K_{OA}	30	0.15 ± 0.07	mg O ₂ L ⁻¹	Present study
K_{ON}	30	0.55 ± 0.09	mg O ₂ L ⁻¹	Present study
$K_{NH_3}^{AOB}$	-	3000	mg NH ₃ -N L ⁻¹	Wett and Rauch (2003)
$K_{NH_3}^{NOB}$	-	20	mg NH ₃ -N L ⁻¹	Wett and Rauch (2003)
K_{HNO_2}	-	2.8	mg HNO ₂ -N L ⁻¹	Wett and Rauch (2003)
K_{ALK}	10-20	0.5	mmol HCO ₃ ⁻ L ⁻¹	Henze <i>et al.</i> (2000)

4.2.5.1. Stoichiometric parameters assessment.

Heterotrophic yield coefficient. In activated sludge systems, biochemical principles dictate that the removal of substrate is accomplished by generating biomass and consuming dissolved oxygen. The concept of yield is one of the major modelling tools used for the correct assessment of excess biomass generation and oxygen consumption in relation to substrate removal. The heterotrophic yield coefficient defines the amount of biomass formed per unit of organic matter removed for heterotrophic growth. This parameter, which is expressed in $\text{mg cell COD} (\text{mg COD consumed})^{-1}$ is explained in Figure 4.5.

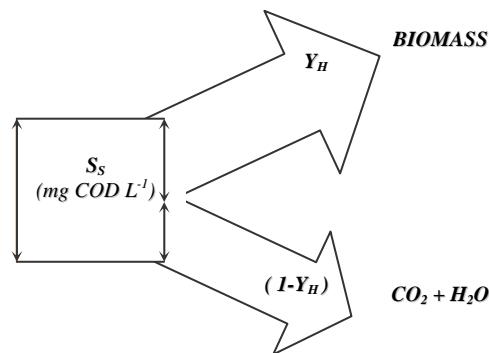


Figure 4.5 – Scheme of the heterotrophic yield coefficient.

An accurate assessment of the heterotrophic yield coefficient, Y_H , is of great importance, not only because this parameter influences sludge production and oxygen utilization but also because it has an impact on the value of other parameters whose determination requires a value of Y_H (Orhon and Artan, 1994; Vanrolleghem *et al.*, 1999).

The actual heterotrophic yield coefficient, Y_H , was evaluated through a respirometric batch experiment in which four different pulses of a completely biodegradable organic substrate were added to an endogenous activated sludge sample (Brands *et al.*, 1994; Dircks *et al.*, 1999; Vanrolleghem *et al.*, 1999). Sodium acetate was used in this experiment since it was the external COD added during the anoxic periods of the studied case.

A typical respirogram obtained in this test is shown in Figure 4.6 (a). As it is observed in this Figure, the OUR response of activated sludge due to the addition of sodium acetate is

clearly divided in two phases for every addition of substrate: At the first one (phase I), the OUR measurement gives a very fast response and then, after a short period of time, the respiration rate experiences a sudden drop followed by a constantly decreasing respiration (phase II). Phase I ('feast phase') represents the primary metabolism where excess substrate is present in the mixed liquor and high (and increasing) OUR values are recorded due to the adaptation of microorganisms to the sudden high concentration of organic substrate and/or a non-limited growth of heterotrophs. The second step ('famine phase') corresponds to the transformation of a secondary substrate (a storage biopolymer like Polyhydroxialcanoates, PHA, and/or glycogen) during the previous stage (Karahan-Gül *et al.*, 2003). Storage of excess substrate is available under feast phase conditions and contributes to a more balanced growth for microorganisms capable to perform the storage of biopolymers (Van Loosdrecht and Heijnen, 1997).

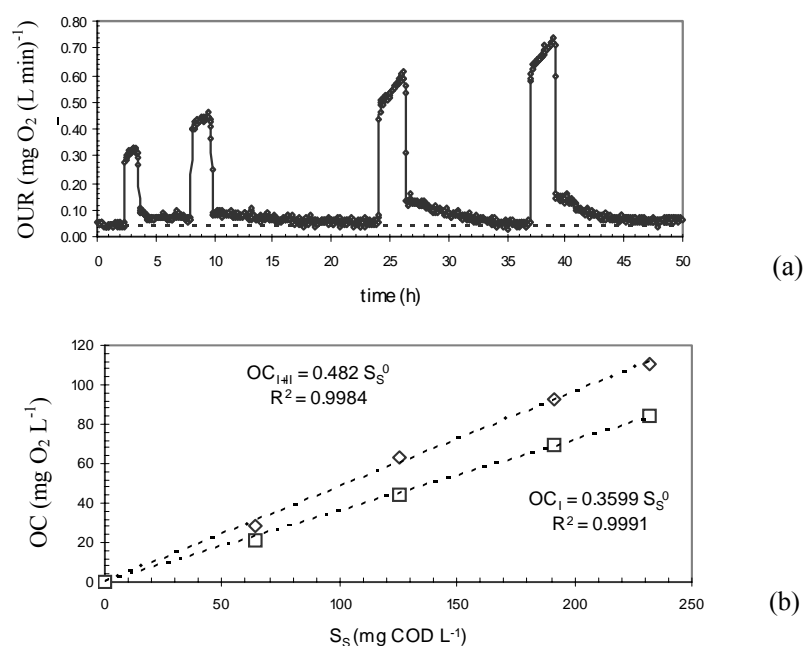


Figure 4.6 – Experimental assessment of Y_H . Respirogram obtained in a representative respirometric batch test (a) and plot of the oxygen consumption related to the addition of completely biodegradable substrate (b).

Plot (a): OUR (\blacklozenge) and endogenous OUR (---) // Plot (b) : OC_{I+II} (\diamond) and OC_I (\square)

If the Petersen matrix commonly used in activated sludge modelling (Henze *et al.*, 2000) is created for the consumption of readily biodegradable COD (Table 4.6), the oxygen

uptake rate and the substrate removal rate can be defined by Equations 4.5 and 4.6, respectively. From the combination of these two equations, it is obtained expression 4.7, which indicates that the area between exogenous OUR and time (oxygen consumption, OC) related to a known COD addition (S_S) could lead to the assessment of Y_H (Vanrolleghem *et al.*, 1999; Gutiérrez, 2003).

Table 4.6 – Petersen matrix notation for the consumption of readily biodegradable COD by heterotrophic biomass

	S_S	S_O	S_{NH}	X_{BH}	
<i>Heterotrophic growth on S_S</i>	$-\left(\frac{1}{Y_H}\right)$	$-\left(\frac{1-Y_H}{Y_H}\right)$	$-i_{XB}$	1	$\mu_{mH} \frac{S_S}{K_S + S_S} \frac{S_O}{K_{OH} + S_O} X_{BH}$

$$OUR_{EX} = -\frac{d S_O}{dt} = \frac{(1-Y_H)}{Y_H} \mu_{m,H} \frac{S_S}{K_S + S_S} \frac{S_O}{S_O + K_{OH}} X_{BH} \quad (4.5)$$

$$\frac{d S_S}{dt} = -\frac{1}{Y_H} \mu_{mH} \frac{S_S}{K_S + S_S} \frac{S_O}{K_{OH} + S_O} X_{BH} \quad (4.6)$$

$$\int OUR_{EX} dt = -(1-Y_H) \int dS_S \quad (4.7)$$

$$OC_{EX} = (1-Y_H) S_S \quad (4.8)$$

Therefore, the plot of the cumulative respiration rate (oxygen consumed, OC) versus the added biodegradable organic substrate concentration enabled the calculation of $(1-Y_H)$ as the slope (see Figure 4.6 b). This experiment was run at 30°C and a pH value of 8.0 ± 0.1 with a low concentration of MLVSS, which provided a suitable low OUR that improved the heterotrophic yield assessment.

Dircks *et al.* (1999) reported two types of heterotrophic yield coefficients: $Y_{H,I+II}$ which considers oxygen consumption in both feast and famine phases and is equivalent to the one described in ASM models (Henze *et al.*, 2000) and $Y_{H,I}$ which considers exclusively the oxygen consumed during the primary metabolism. As stated in figure 4.6 (b) the actual heterotrophic yield coefficients, $Y_{H,I+II}$ i $Y_{H,I}$, were 0.62 and 0.72 mg cell COD formed (mg COD consumed)⁻¹, respectively. Both experimental values are in good

agreement with those reported in literature (Henze *et al.*, 1987; Dircks *et al.*, 1999; Vanrolleghem *et al.*, 1999). However, the considered heterotrophic yield in this study was $Y_{H,I+II}$, since the storage of acetate in the form of biopolymers did not have an important impact on the biological nitrogen removal process over nitrite.

Autotrophic yield coefficients. In ASM models (Henze *et al.*, 2000) where nitrification is modelled as a one-step reaction in which ammonium is directly converted to nitrate, the autotrophic yield coefficient (Y_A) is defined as the quantity of biomass produced per unit of ammonium removed. In the present study, nitrification is modelled as a two-step reaction where ammonium is firstly oxidized to nitrite by AOB and further into nitrate by NOB. Therefore, two autotrophic yield coefficients were defined: Y_{AOB} , which is the quantity of biomass produced per unit of ammonium removed during nitrification and Y_{NOB} , which is the quantity of biomass produced per unit of nitrite removed during nitrification. Figure 4.7 shows a schematic diagram of the definition of Y_{AOB} and Y_{NOB} .

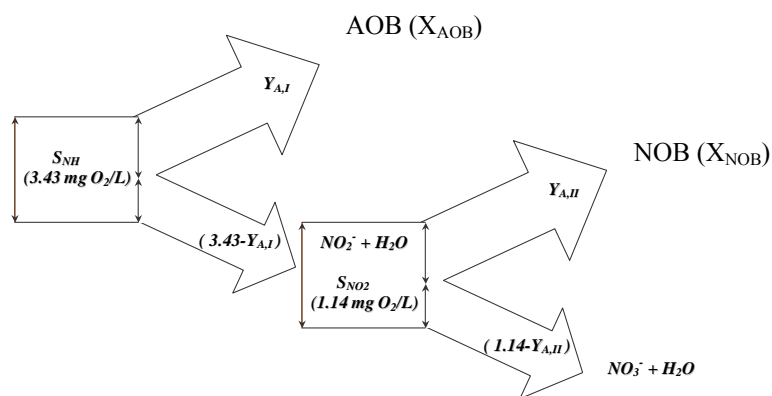


Figure 4.7 – Scheme of the AOB and NOB yield coefficients.

Similarly to the heterotrophic yield coefficient assessment, the actual autotrophic yield coefficient for AOB, Y_{AOB} , was estimated from a respirometric batch experiment (30°C , $\text{pH } 8.0 \pm 0.1$, $200 \text{ mg VSS L}^{-1}$) in which three different pulses of ammonia were added to the endogenous activated sludge sample (see Figure 4.8). Concentrations of ammonium, nitrite and nitrate were determined experimentally during the respirometric test and an insignificant amount of nitrate was detected.

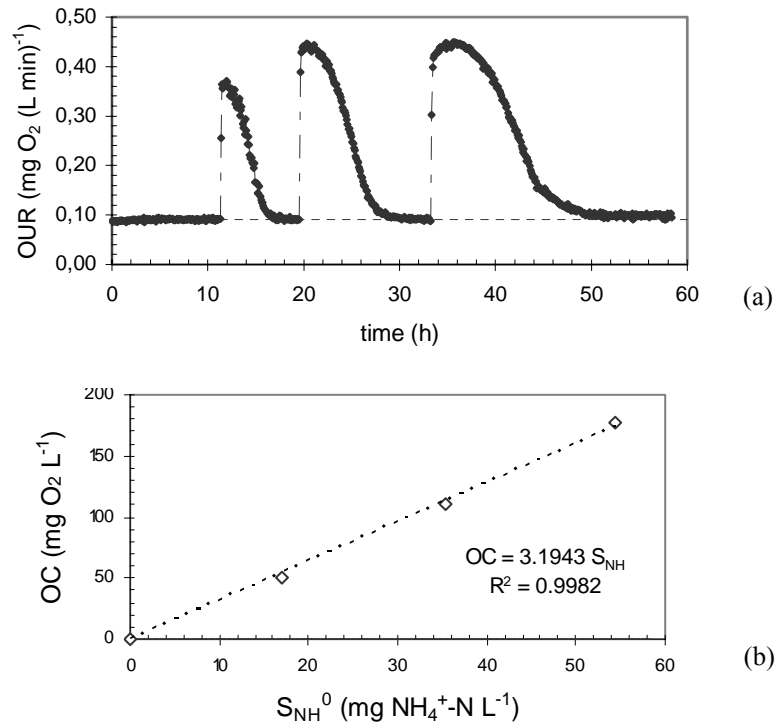


Figure 4.8 – Experimental assessment of Y_{AOB} . Respirogram obtained in a representative respirometric batch test (a) and plot of the oxygen consumption related to the addition of ammonium chloride (b).

OUR (\blacklozenge) and endogenous OUR (---)

The modified Activated Sludge Model used in this study is presented in Table 4.7 for the experimental conditions of this respirometric test. Since nitrite oxidizers activity was nearly zero, the exogenous OUR can be expressed by Equation 4.9 and Ammonium Uptake Rate (AUR) can be described by Equation 4.11. By combining these two expressions, Equation 4.12 and 4.13 are obtained.

Consequently, as described by the ASM model, the plot of the OC due to exogenous activity versus added NH_4^+-N concentration yielded a straight line with $(3.43 - Y_{\text{AOB}})$ as the slope. As shown in Figure 4.8 (b), the actual AOB yield coefficient for the system under study was $0.22 \text{ mg cell COD formed (mg NH}_4^+-\text{N oxidized)}^{-1}$, which is consistent with other reported values (Marsili-Libelli and Tabani, 2002).

Table 4.7 – Petersen matrix notation for the consumption of ammonium and (subsequently) nitrite by autotrophic biomass

	S_O	S_{NH}	S_{NO_2}	S_{NO_3}	X_{AOB}	X_{NOB}	X_{BH}	
Aerobic growth of AOB	$-\left(\frac{3.43 - Y_{AOB}}{Y_{AOB}}\right)$	$-\left(\frac{1}{Y_{AOB}}\right)$	$\left(\frac{1}{Y_{AOB}}\right)$		1			$\mu_{m,AOB} \frac{S_{NH}}{K_{NH} + S_{NH}} \frac{S_O}{S_O + K_{O,AOB}} X_{AOB}$
Aerobic growth of NOB	$-\left(\frac{1.14 - Y_{NOB}}{Y_{NOB}}\right)$		$-\left(\frac{1}{Y_{NOB}}\right)$	$\left(\frac{1}{Y_{NOB}}\right)$		1		$\mu_{m,NOB} \frac{S_{NO_2}}{K_{NO_2} + S_{NO_2}} \frac{S_O}{S_O + K_{O,NOB}} X_{NOB}$
Decay of AOB	-1				-1			$b_A X_{AOB}$
Decay of NOB	-1					-1		$b_A X_{NOB}$
Decay of heterotrophs	-1						-1	$b_H X_{BH}$

$$OUR_{EX} = -\frac{dS_O}{dt} = \frac{(3.43 - Y_{AOB})}{Y_{AOB}} \mu_{m,AOB} \frac{S_{NH}}{K_{NH} + S_{NH}} \frac{S_O}{S_O + K_{O,AOB}} X_{AOB} \quad (4.9)$$

$$AUR = \frac{dS_{NH}}{dt} = \frac{1}{Y_{AOB}} \mu_{m,AOB} \frac{S_{NH}}{K_{NH} + S_{NH}} \frac{S_O}{S_O + K_{O,AOB}} X_{AOB} \quad (4.10)$$

$$\int OUR_{EX} dt = -(3.43 - Y_{AOB}) \int dS_{NH} \quad (4.11)$$

$$OC_{EX} = (3.43 - Y_{AOB}) S_{NH} \quad (4.12)$$

Since nitrite oxidizers were highly inhibited, the autotrophic yield coefficient for NOB, Y_{NOB} , was considered to be 0.08 mg cell COD (mg N-NO₂)⁻¹ as reported by Hellinga *et al.* (1999). A value of 0.07 mg NH₄⁺-N (mg cell COD)⁻¹ was established for the nitrogen content of biomass, i_{XB} , since this parameter does not vary significantly from one biological system to another (Henze *et al.*, 2000).

4.2.5.2. Kinetic parameters assessment.

Decay coefficient assessment. The decay coefficient for heterotrophic biomass with lineal death, b_H , was determined following the protocol established by Marais and Ekama (1976). Sludge withdrawn from the lab-scale reactor was put into an aerated non-fed batch reactor up to a concentration of 4000 mg MLVSS L⁻¹. The endogenous OUR and VSS concentration were measured over a period of several days. Figure 4.9 shows the results obtained in this respirometric test

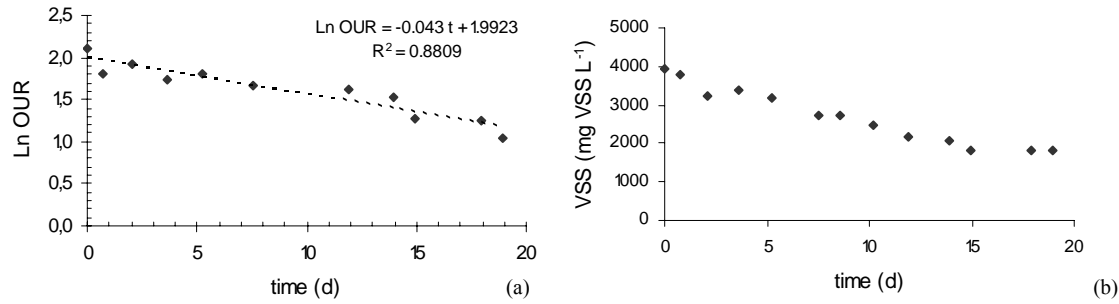


Figure 4.9 – Experimental assessment of lineal decay constant, b_H .

Plot of $\text{Ln OUR}_{\text{END}}$ versus time (a) and evolution of biomass (VSS) during the respirometric test.

The Activated Sludge Model presented in Table 4.8 can describe the respirometric batch test used to assess the heterotrophic lineal decay constant b_H . Equation 4.13 could be used to predict the OUR registered along the experiment and Equation 4.14 represents the theoretical evolution of heterotrophic biomass. If both Equations are combined, the mathematical expression 4.17 is obtained. Therefore, the plot of Ln OUR versus time yielded the actual value of the heterotrophic lineal decay constant as the slope.

Table 4.8 – Petersen matrix notation for the decay process of heterotrophic biomass

	S_O	X_{BH}	
Heterotrophic decay	-1	-1	$b_H X_{BH}$

$$OUR = -\frac{d S_O}{d t} = b_H X_{BH} \quad (4.13)$$

$$\frac{d X_{BH}}{d t} = -b_H X_{BH} \quad (4.14)$$

$$X_{BH} = X_{BH}^0 e^{-b_H t} \quad (4.15)$$

$$OUR = b_H X_{BH}^0 e^{-b_H t} \quad (4.16)$$

$$\text{Ln}(OUR) = \text{Ln}(b_H X_{BH}^0) - b_H t \quad (4.17)$$

As shown in Figure 4.9(a), the logarithm of the endogenous respiration rate versus time representation provides a straight line with the decay coefficient for heterotrophic biomass (lineal death), b_H , as slope (Sollfrank and Gujer, 1991). The value determined was 0.043 day^{-1} , which is similar to the $0.06\text{-}0.15 \text{ days}^{-1}$ stated by Metcalf and Eddy (1991). This decay constant value for lineal decay could be converted to the heterotrophic decay constant for death-regeneration process ($b_H^{\text{Death-Regeneration}}$) by applying Equation 4.18 (Orhon and Artan, 1994), where f_p is the particulated inert fraction of biomass.

$$b_H^{\text{Death-regeneration}} = \frac{b_H^{\text{Lineal death}}}{(1-Y_H(1-f_p))} \quad (4.18)$$

Moreover, Figure 4.9 (b) shows the evolution of VSS observed during the whole experiment. According to Oles and Wilderer (1991), the VSS disappeared at the end of this experiment (in theory, it is considered a very long time) with respect to the initial VSS, $(X_{\text{BH,TOTAL}}-X_{\text{BH,FINAL}})/ X_{\text{BH,TOTAL}}$, yields an estimation of the viable biomass inside an activated sludge sample. For the case studied, this viability factor assumes that approximately the 54.3 % of biomass is active. In fact, this calculation provides a minimum value of active biomass, since several days were necessary to accumulate the biomass necessary for this experiment from the SBR withdrawals.

Finally, a value of 0.20 d^{-1} was established for both AOB and NOB as the autotrophic decay coefficient (b_A). This value results from the application of the b_A temperature dependency equation proposed by Ekama and Marais (1984) to the default b_A value at 20°C proposed in ASM3 (Henze *et al.*, 2000).

Maximum heterotrophic growth rate under aerobic conditions. The maximum heterotrophic growth rate under aerobic conditions $\mu_{m,H}$ is, concomitantly with the half-saturation constant for substrate (K_S), an essential kinetic parameter to characterise the COD removal capacity and the biomass production of the activated sludge under study. This parameter was assessed by means of two respirometric procedures: the one proposed by Kappeler and Gujer (1992) and the one proposed by Spanjers and Vanrolleghem (1995).

The methodology of Kappeler and Gujer (1992) is based on the addition of a high quantity of readily biodegradable substrate to a mixed liquor with activated sludge under endogenous conditions with non-limiting dissolved oxygen concentration. The Food to Microorganisms ratio (F/M or S_{10}/X_{10}) on COD basis described by these authors was around 4/1. Therefore, they proposed a high addition of substrate to a low quantity of active biomass to assure an exponential growth of heterotrophs in presence of excess substrate.

Table 4.9 shows the matrix notation of the activated sludge model describing the respirometric test proposed by Kappeler and Gujer (1992). Equations 4.19 and 4.23 describe the OUR and the heterotrophic biomass evolution during the respirometric experiment, respectively. Due to non-limiting conditions of substrate and dissolved oxygen in the mixed liquor (Equations 4.20 and 4.21), evolution of OUR and X_{BH} can be simplified and modelled by Equations 4.22 and 4.24, respectively. By combining these equations, the expression 4.27 is obtained, which justifies the possibility of assessing $(\mu_{mH}-b_H)$ as the slope of the plot of Ln OUR versus time.

Table 4.9 – Petersen matrix notation for the maximum heterotrophic growth rate assessment.

	S_S	S_O	S_{NH}	X_{BH}	
<i>Heterotrophic aerobic growth on S_S</i>	$-\left(\frac{1}{Y_H}\right)$	$-\left(\frac{1-Y_H}{Y_H}\right)$	$-i_{XB}$	1	$\mu_{mH} \frac{S_S}{K_S + S_S} \frac{S_O}{K_{OH} + S_O} X_{BH}$
<i>Decay of heterotrophs</i>		1		-1	$b_H X_{BH}$

$$OUR = -\frac{d S_O}{d t} = \frac{1-Y_H}{Y_H} \mu_{mH} \frac{S_S}{K_S + S_S} \frac{S_O}{K_{OH} + S_O} X_{BH} + b_H X_{BH} \quad (4.19)$$

$$\text{If } S_S \gg K_S \rightarrow \frac{S_S}{K_S + S_S} = 1 \quad (4.20)$$

$$\text{If } S_O \gg K_{OH} \rightarrow \frac{S_O}{K_{OH} + S_O} = 1 \quad (4.21)$$

$$OUR = \frac{1-Y_H}{Y_H} \mu_{mH} X_{BH} + b_H X_{BH} \quad (4.22)$$

$$\frac{d X_{BH}}{d t} = \mu_{mH} \frac{S_s}{K_s + S_s} \frac{S_o}{K_{OH} + S_o} X_{BH} - b_H X_{BH} \quad (4.23)$$

$$\frac{d X_{BH}}{d t} = (\mu_{mH} - b_H) X_{BH} \quad (4.24)$$

$$X_{BH} = X_{BH}^0 e^{(\mu_{mH} - b_H)t} \quad (4.25)$$

$$OUR = \frac{1 - Y_H}{Y_H} (\mu_{mH} + b_H) X_{BH}^0 e^{(\mu_{mH} - b_H)t} \quad (4.26)$$

$$\ln OUR = \ln \left(\frac{1 - Y_H}{Y_H} (\mu_{mH} + b_H) X_{BH}^0 \right) + (\mu_{mH} - b_H)t \quad (4.27)$$

The respirometric tests carried out in this study consisted on the addition of a high quantity of substrate (namely, sodium acetate 800 mg COD L⁻¹) to a very low quantity of activated sludge (approximately, 200 mg VSS L⁻¹) under controlled pH (8.0 ± 0.1) and temperature (30 °C) conditions. Figure 4.10 (a) shows a representative respirogram obtained when this methodology was applied. The oxygen uptake rate experienced an important increase due to non-limited exponential growth of heterotrophic biomass as considered in the IWA Activated sludge Models (Henze *et al.*, 2000). As observed in Figure 4.10 (b), the plot of Ln OUR versus time enabled the assessment of $\mu_{m,H}$. The $\mu_{m,H}$ value with a major reproductibility was 4.2 days⁻¹. However, a high variability of this parameter was observed (in the range of ± 0.7 days⁻¹) depending on the quantity of active biomass used in the respirometric test. This high variability when applying the methodology of Kappeler and Gujer (1992) was also reported by Vanrolleghem *et al.* (1999). These authors justified this observation, since high substrate/biomass ratio gives rise to significant growth of the biomass during the experiment. This means that the observed kinetic characteristics are no longer representative of the microbial population, but only for the organisms that become dominant during the experiment. Novak *et al.* (1994) gave practical evidence for this hypothesis by evaluating results from experiments with different F/M ratios. A 2.5 higher specific growth rate was obtained at high F/M ratios.

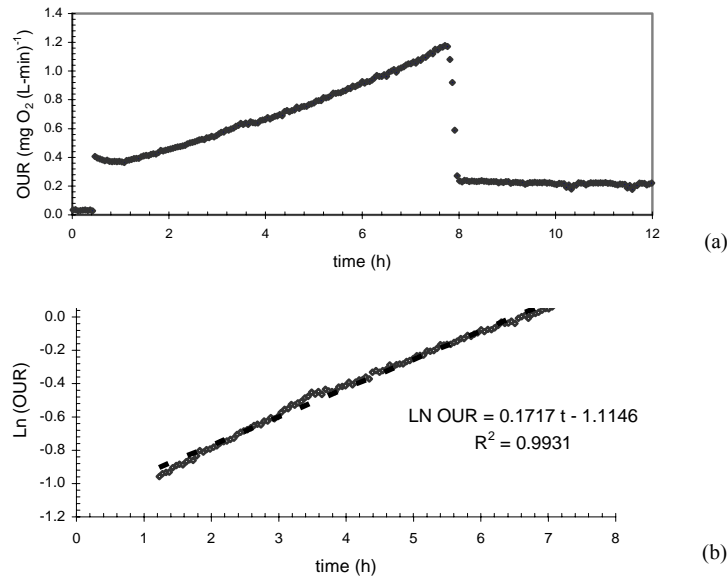


Figure 4.10 – Experimental assessment of μ_{mH} according to the methodology established by Kappeler and Gujer (1992). Representative obtained respirogram (a) and plot of Ln OUR versus time (b). OUR (◆); pH (*) and lineal adjustment (---)

Considering these experimental results, Spanjers and Vanrolleghem (1995) presented the so-called $S_{t_0}/X_{t_0}=1/200$ experiment for heterotrophic biomass experiments with a much lower substrate to biomass ratio. In order to work with non-limiting substrate concentrations, the active biomass concentration in the respirometric procedure was high. Spanjers and Varolleghem concluded that $\mu_{m,H}$ can be assessed in a reliable way if only the values of Y_H i X_{BH} are perfectly known. If not, only combination of parameters could be assessed.

Consequently, it was decided to study the combination of parameters $\mu_{mH} X_{BH}$, due to the high variability of the isolated value of μ_{mH} . The combination of parameters $\mu_{mH} X_{BH}$ for the evaluation of maximum aerobic heterotrophic growth rate was assessed by applying the so-called $S_{t_0}/X_{t_0}=1/200$ experiment for heterotrophic biomass at 30°C (Spanjers and Vanrolleghem, 1995). The biomass concentration used in this study was 985 mg VSS L⁻¹ and the initial readily biodegradable substrate concentration was approximately 425 mg COD L⁻¹. A representative respirogram obtained when this

methodology was applied is shown in Figure 4.11. From the maximum OUR reached in this kind of respirometric experiments, the average value of $\mu_{mH} X_{BH}$ expressed per unit of VSS was $163.9 \text{ mg cell COD (g VSS h)}^{-1}$.

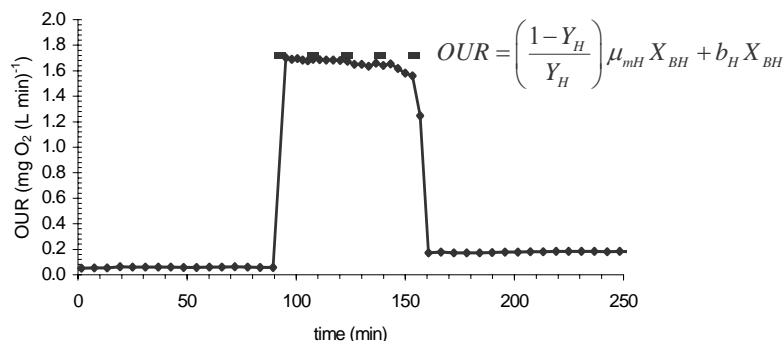


Figure 4.11 – Experimental assessment of the combination $\mu_{mH} X_{BH}$ according to the so-called $S_{t0}/X_{t0}=1/200$ experiment (Spanjers and Vanrolleghem, 1995). OUR (\blacklozenge) and endogenous OUR (\blacksquare)

Correction factors for heterotrophic growth rate under anoxic conditions. Heterotrophic growth rate under anoxic conditions (denitrification) was modelled as a two-step process, considering the same Monod Kinetic expressions used for aerobic conditions multiplied by two correction factors ($\eta_{NO_3 \rightarrow NO_2}$ and $\eta_{NO_2 \rightarrow N_2}$) and two S_{NO} (NO_X-N) switching functions (see Table 4.2). Correction factors were used because heterotrophic biomass shows a reduced substrate oxidation rate during anoxic conditions with respect to aerobic conditions, since only a fraction of the heterotrophic biomass is able to use nitrite or nitrate as electron acceptor (facultative) under anoxic conditions (Orhon and Artan, 1994).

These kinetic parameters were evaluated experimentally with the simultaneous operation of three batch reactors. One reactor was aerated and the other two worked under absence of oxygen but with nitrate and nitrite, respectively, as the final electron acceptors. An excess amount of external carbon source (sodium acetate) was used in order to study affinity constants of nitrite and nitrate under anoxic conditions. OUR profile was determined for the aerated reactor ($985 \text{ mg VSS L}^{-1}$) and nitrite and nitrate concentration profiles were analysed for anoxic tests ($1655 \text{ mg VSS L}^{-1}$ and $1535 \text{ mg VSS L}^{-1}$, respectively) as presented in Figure 4.12. No nitrite accumulation was observed in the

anoxic test using nitrate as final electron acceptor. Therefore, nitrite reduction to nitrogen gas was faster than nitrate reduction to nitrite, which is in concordance with literature (Abeling and Seyfried, 1992). Moreover, the activated sludge studied in this work was accustomed to reduce nitrite during anoxic periods, since nitrate was hardly formed during nitrification.

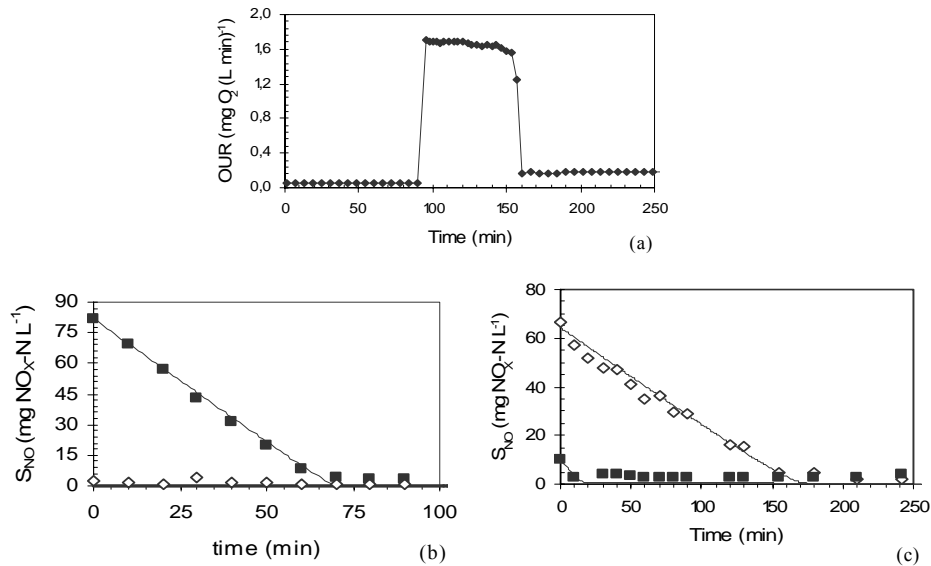


Figure 4.12 – Experimental determination of anoxic correction factors for heterotrophic growth. Respirogram in aerobic reactor (a) and NO_x⁻-N profiles inside anoxic reactors using nitrite (b) and nitrate (c) as final electron acceptor.

OUR (●); N-NO₂ (■); N-NO₃ (◇) and simulated data (—)

Table 4.10 shows the matrix notation of the activated sludge model describing the respirometric test to assess the correction factors for heterotrophic growth under anoxic conditions. Equations 4.28, 4.29 and 4.30 describe the oxygen uptake rate, the nitrate uptake rate and the nitrite uptake rate during the experiment, respectively. Combining these equations, the expressions 4.31 and 4.32 to determine the correction factor for heterotrophic growth under anoxic conditions (over nitrate and nitrite, respectively) can be obtained.

Table 4.10 – Petersen matrix notation for the correction factor of heterotrophic anoxic growth assessment.

	S_S	S_O	S_{NH}	S_{NO_2}	S_{NO_3}	S_{N_2}	X_{BH}	
<i>Aerobic heterotrophic growth on S_S</i>	$-\left(\frac{1}{Y_H}\right)$	$-\left(\frac{1-Y_H}{Y_H}\right)$	$-i_{XB}$				1	$\mu_{mH} \frac{S_S}{K_S + S_S} \frac{S_O}{S_O + K_{OH}} X_{BH}$
<i>Nitrate reduction to nitrite</i>	$-\left(\frac{1}{Y_H}\right)$		$-i_{XB}$	$\left(\frac{1-Y_H}{1.14 Y_H}\right)$	$-\left(\frac{1-Y_H}{1.14 Y_H}\right)$			$\eta_{NO_3 \rightarrow NO_2} \mu_{mH} \frac{S_S}{K_S + S_S} \frac{K_{OH}}{S_O + K_{OH}} \frac{S_{NO_3}}{K_{NO_3} + S_{NO_3}} X_{BH}$
<i>Nitrite reduction to nitrogen gas</i>	$-\left(\frac{1}{Y_H}\right)$		$-i_{XB}$	$-\left(\frac{1-Y_H}{1.71 Y_H}\right)$		$\left(\frac{1-Y_H}{1.71 Y_H}\right)$		$\eta_{NO_2 \rightarrow N_2} \mu_{mH} \frac{S_S}{K_S + S_S} \frac{K_{OH}}{S_O + K_{OH}} \frac{S_{NO_2}}{K_{NO_2} + S_{NO_2}} X_{BH}$
<i>Heterotrophic decay</i>		1					-1	$b_H X_{BH}$

$$OUR_{EX} = -\frac{dS_O}{dt} = \frac{1-Y_H}{Y_H} \mu_{mH} \frac{S_S}{K_S + S_S} \frac{S_O}{K_{OH} + S_O} X_{BH} \quad (4.28)$$

$$NUR_{NO_3 \rightarrow NO_2} = -\frac{dS_{NO_3}}{dt} = \frac{1-Y_H}{1.14 Y_H} \eta_{NO_3 \rightarrow NO_2} \mu_{mH} \frac{S_S}{K_S + S_S} \frac{K_{OH}}{S_O + K_{OH}} \frac{S_{NO_3}}{K_{NO_3} + S_{NO_3}} X_{BH} \quad (4.29)$$

$$NUR_{NO_2 \rightarrow N_2} = -\frac{dS_{NO_2}}{dt} = \frac{1-Y_H}{1.71 Y_H} \eta_{NO_2 \rightarrow N_2} \mu_{mH} \frac{S_S}{K_S + S_S} \frac{K_{OH}}{S_O + K_{OH}} \frac{S_{NO_2}}{K_{NO_2} + S_{NO_2}} X_{BH} \quad (4.30)$$

$$\eta_{NO_3 \rightarrow NO_2} = \frac{1.14 NUR_{NO_3 \rightarrow NO_2}}{OUR_{EX}} \quad (4.31)$$

$$\eta_{NO_2 \rightarrow N_2} = \frac{1.71 NUR_{NO_2 \rightarrow N_2}}{OUR_{EX}} \quad (4.32)$$

In this study, both correction factors were evaluated by comparison of the OUR and NUR values obtained. Half saturation constants for nitrite and nitrate under anoxic conditions were also estimated from these experiments. Average values of anoxic correction factors and nitrite and nitrate half saturation constants are presented in Table 4.5.

Maximum autotrophic growth rate under aerobic conditions. The experimental assessment of the actual $\mu_{m,A}$ is essential to characterise autotrophic biomass, since it determines the maximum autotrophic growth rate for autotrophic microorganisms and, consequently, the minimum sludge age necessary to develop a nitrifying cultivation. For the system under study, nitrification process is modelled as a two step process (nitritation

and nitrataion), considering different maximum autotrophic growth rate constants for each nitrification step. In the same way as for the evaluation of $\mu_{m,H}$, $\mu_{m,AOB}$ was evaluated by means of two respirometric procedures: the one proposed by Kappeler and Gujer (1992) and the one reported by Spanjers and Vanrolleghem (1995).

In Table 4.11, the Petersen matrix for the aerobic growth of AOB is detailed. From this notation, equations 4.33 and 4.37 can be formulated to model oxygen consumption and autotrophic biomass growth, respectively. If dissolved oxygen and substrate are present in non-limiting concentrations (equations 4.34 and 4.35), oxygen and biomass evolution can be simulated by Equations 4.36 and 4.39, respectively. Combining these equations, the Expression 4.41 is arised and it is justified that $(\mu_{m,AOB}-b_A)$ can be assessed as the slope of Ln OUR versus time.

Table 4.11 – Petersen matrix notation for $\mu_{m,AOB}$ assessment.

	S_O	S_{NH}	S_{NO_2}	X_{BH}	X_{AOB}	
<i>Aerobic growth of AOB</i>	$-\left(\frac{3.43-Y_{AOB}}{Y_{AOB}}\right)$	$-i_{XB} - \left(\frac{1}{Y_{AOB}}\right)$	$\left(\frac{1}{Y_{AOB}}\right)$		1	$\mu_{m,AOB} \frac{S_{NH}}{K_{NH} + S_{NH}} \frac{S_O}{S_O + K_{O,AOB}} X_{AOB}$
<i>Decay of AOB</i>	1			-1		$b_A X_{AOB}$

$$OUR = -\frac{dS_O}{dt} = \frac{3.43-Y_{AOB}}{Y_{AOB}} \mu_{m,AOB} \frac{S_{NH}}{K_{NH} + S_{NH}} \frac{S_O}{S_O + K_{O,AOB}} X_{AOB} + b_A X_{AOB} \quad (4.33)$$

$$\text{If } S_{NH} \gg K_{NH} \rightarrow \frac{S_{NH}}{K_{NH} + S_{NH}} \approx 1 \quad (4.34)$$

$$\text{If } S_O \gg K_{O,AOB} \rightarrow \frac{S_O}{K_{O,AOB} + S_O} \approx 1 \quad (4.35)$$

$$OUR = \frac{3.43-Y_{AOB}}{Y_{AOB}} \mu_{m,AOB} X_{AOB} + b_A X_{AOB} \quad (4.36)$$

$$\frac{dX_{AOB}}{dt} = \mu_{m,AOB} \frac{S_{NH}}{K_{NH} + S_{NH}} \frac{S_O}{S_O + K_{O,AOB}} X_{AOB} - b_A X_{AOB} \quad (4.37)$$

$$\frac{dX_{AOB}}{dt} = (\mu_{m,AOB} - b_A) X_{AOB} \quad (4.38)$$

$$X_{AOB} = X_{AOB}^0 e^{(\mu_{m,AOB}-b_A)t} \quad (4.39)$$

$$OUR = \frac{3.43 - Y_{AOB}}{Y_{AOB}} (\mu_{m,AOB} + b_A) X_{AOB}^0 e^{(\mu_{m,AOB} + b_A)t} \quad (4.40)$$

$$\ln OUR = \ln \left(\frac{3.43 - Y_{AOB}}{Y_{AOB}} (\mu_{m,AOB} + b_A) X_{AOB}^0 \right) + (\mu_{m,AOB} + b_A)t \quad (4.41)$$

Therefore, the respirometric test consisted in the addition of an elevated quantity of $\text{NH}_4^+\text{-N}$ (Ammonium chloride; approximately $75 \text{ mg NH}_4^+\text{-N L}^{-1}$) to a low quantity of endogenous biomass (approximately, 50 mg VSS L^{-1}), as recommended by the authors of the methodology. The OUR experienced a high increase due to the non-limited exponential increase reported in the IWA ASM models (Henze *et al.*, 2000). This respirometric test was carried out at 30°C and under controlled pH conditions (8.0 ± 0.1). Figure 4.13 shows a representative respirogram obtained when using this procedure and the plot of $\ln OUR$ versus time to assess $\mu_{m,AOB}$. The $\mu_{m,AOB}$ value with major reproduction for the studied biomass was 1.15 days^{-1} . However, a strong variability of this parameter was observed ($\pm 0.15 \text{ days}^{-1}$) depending on the working biomass concentration.

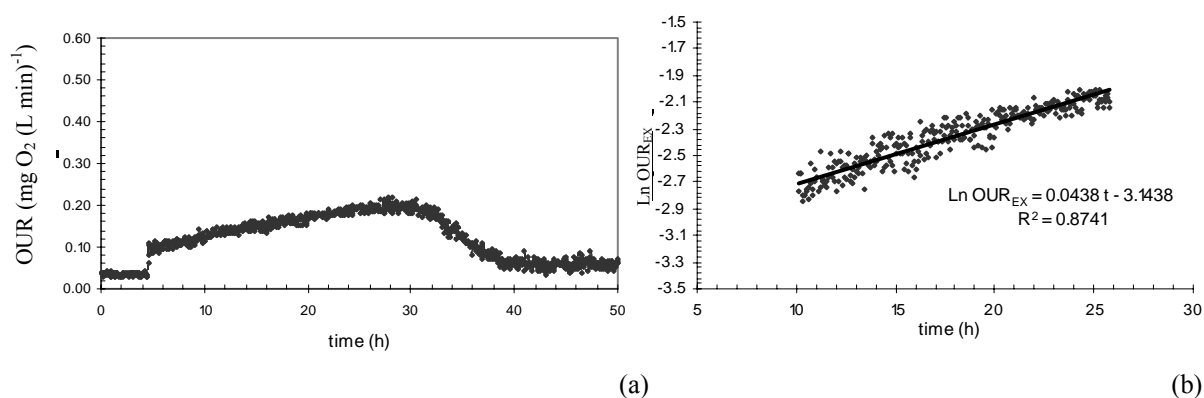


Figure 4.13 – Experimental assessment of the maximum autotrophic growth rate ($\mu_{m,AOB}$)

According to the methodology established by Kappeler and Gujer (1992).

Respirogram obtained (a) and plot of $\ln OUR_{EX}$ versus time (b).

OUR (\blacklozenge); pH ($*$) and regression line (—)

Therefore, it was decided to assess the combined parameters $\mu_{m,AOB} X_{AOB}$ and $\mu_{m,NOB} X_{NOB}$ for the evaluation of maximum autotrophic growth rate for AOB and NOB using a $S_{t0}/X_{t0}=1/200$ respirometric experiment (30°C , $\text{pH } 8.0 \pm 0.1$) for autotrophic biomass (Spanjers and Vanrolleghem, 1995), in which OUR, $\text{NH}_4^+\text{-N}$, $\text{NO}_2^-\text{-N}$ and $\text{NO}_3^-\text{-N}$ profiles were analysed.

To assess the combined parameters $\mu_{m,AOB} X_{AOB}$, approximately 0.7 g VSS L⁻¹ of endogenous biomass were inserted in the closed intermittent-flow respirometer and an addition of NH₄⁺-N (ammonium chloride, 50 mg NH₄⁺-N L⁻¹) was performed. A representative respirogram obtained is presented in Figure 4.14. Both DO and initial NH₄⁺-N concentrations were not limiting for biomass activity. Therefore, the maximum exogenous OUR obtained in this set of experiments is directly related to $\mu_{m,AOB} X_{AOB}$ as shown in Figure 4.14. Nitrite oxidation to nitrate was hardly detected during this experiment due to the characteristics of the activated sludge. The value of $\mu_{m,AOB} X_{AOB}$ per unit of biomass was on average basis $(\mu_{m,AOB} X_{AOB})/X_{VSS} = 6.06$ mg cellular COD (g VSS h)⁻¹ and did not present a strong variability.

Furthermore, $\mu_{m,NOB} X_{NOB}$ for the evaluation of maximum autotrophic growth rate for NOB was evaluated from a set of batch tests (30°C, pH 8.0 ± 0.1) in which a pulse of nitrite (90 mg NO₂⁻-N L⁻¹) was added to an endogenous activated sludge sample. NO₂⁻-N and NO₃⁻-N were analysed over a period of several hours. Figure 4.14 (b) shows the evolution of NO₃⁻-N in a representative batch test. The average value of $\mu_{m,NOB} X_{NOB}$ expressed per unit of VSS was 0.144 mg cell COD (g VSS h)⁻¹.

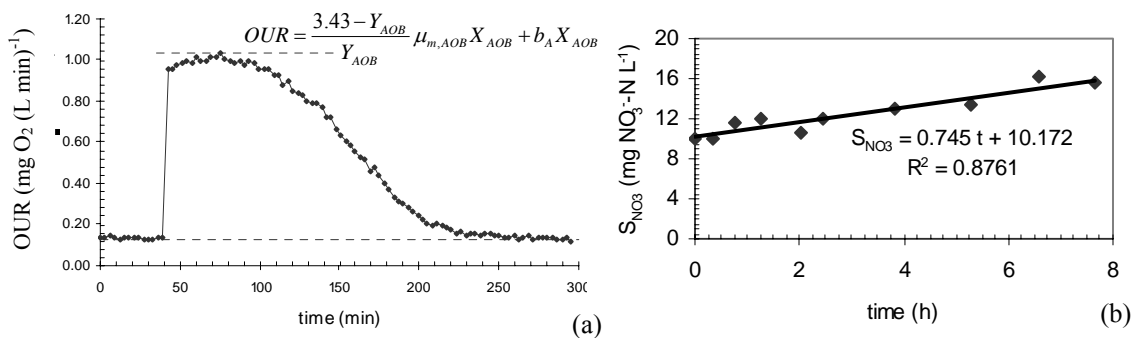


Figure 4.14 – Experimental assessment of the combined parameters $\mu_{m,AOB} X_{AOB}$ (a) and $\mu_{m,NOB} X_{NOB}$ (b). OUR (◆); OUR_{END} (----) and NO₃⁻-N (●)

Half-saturation constants for substrate. As explained in Chapter 1, in IWA Activated Sludge Models (Henze *et al.*, 2000), the kinetics of biological growth are described by Monod type equations characterised by a maximum growth rate constant and a half-saturation constant for substrate (as shown in Equations 4.42, 4.43 and 4.44, for readily

biodegradable COD, $\text{NH}_4^+\text{-N}$ and $\text{NO}_2^-\text{-N}$, respectively). Therefore, the experimental assessment of these parameters are essential for modelling purposes.

$$\frac{dX_{BH}}{dt} = \mu_{m,H} \frac{S_S}{K_S + S_S} X_{BH} \quad (4.42)$$

$$\frac{dX_{AOB}}{dt} = \mu_{m,AOB} \frac{S_{NH}}{K_{NH} + S_{NH}} X_{AOB} \quad (4.43)$$

$$\frac{dX_{NOB}}{dt} = \mu_{m,NOB} \frac{S_{NO_2}}{K_{NO_2} + S_{NO_2}} X_{NOB} \quad (4.44)$$

Half-saturation constants for organic substrate (K_S) and ammonium (K_{NH}) were determined by applying the method described by Cech *et al.* (1984). This methodology consisted on the analysis of the oxygen consumption rate at different substrate concentrations. It was carried out in a watertight respiration chamber where several injections of organic substrate or $\text{NH}_4^+\text{-N}$ were performed to endogenous biomass from the SBR. Exogenous OUR was measured as the difference between endogenous OUR and the total OUR registered in every test. Figure 4.15 shows the experimental set-up used and its operation.

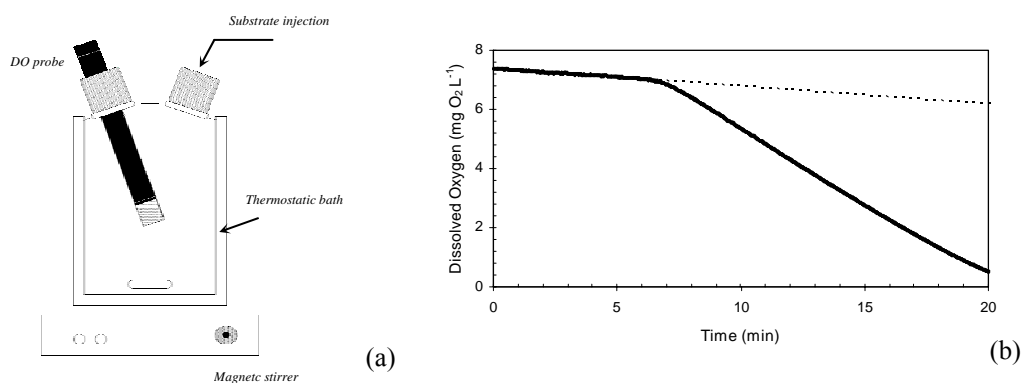


Figure 4.15 – Experimental device used to assess substrate half-affinity constants. (a) Respiration Chamber and (b) experimental DO profile. Experimental data (·) and endogenous respiration (--).

The exogenous OUR was divided by the maximum value of exogenous OUR registered in the whole experiment to calculate the relative activity (μ/μ_{\max}) depending on substrate concentration. In Figure 4.16, representative experiments for the assessment of K_S and

K_{NH} are shown, concomitantly with their simulation. Average values obtained at 30°C were $K_S = 15 \text{ mg COD L}^{-1}$ and $K_{NH} = 1.1 \text{ mg NH}_4^+ \text{-N L}^{-1}$, which are very similar to those proposed in the IWA Activated Sludge Models (Henze *et al.*, 2000).

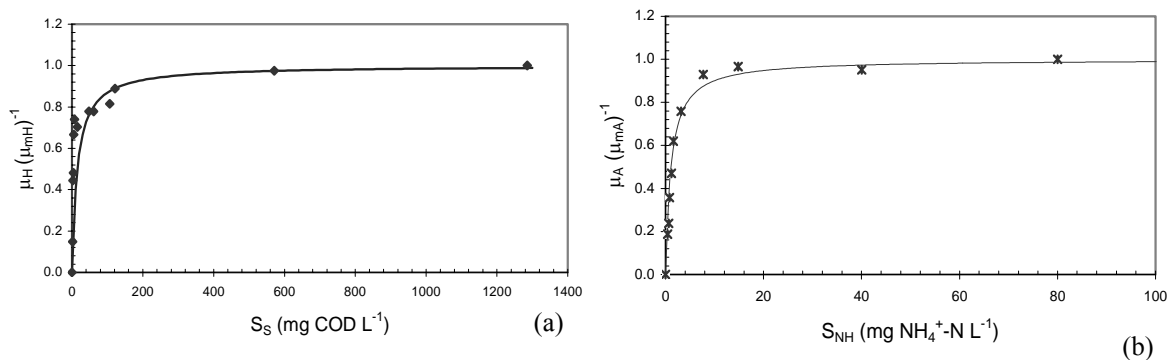


Figure 4.16 – Assessment of K_S (a) and K_{NH} (b).

$\mu_H (\mu_{mH})^{-1}$ (\blacklozenge); $\mu_A (\mu_{mA})^{-1}$ ($*$) and simulated data (—)

Oxygen affinity constants. Usually, oxygen affinity constants were assumed from literature instead of being measured. However, in the last years these model parameters have gained more concern for modelling purposes. Particularly, half-saturation constants for oxygen in nitrification ($K_{O,AOB}$) and denitrification ($K_{O,NOB}$) are two key parameters to model partial nitrification or nitrification over nitrite processes.

Oxygen affinity constants for heterotrophic biomass (K_{OH}), ammonium oxidizers (K_{OA}) and nitrite oxidizers (K_{ON}) were determined through a respirometric test in which the DO drop in a watertight respiration chamber was monitored after the injection of substrate (the respirometric device is presented in Figure 4.15). In this experiment, the system worked with neither external aeration nor substrate limitations. Biomass concentration ranged from 0.6 to 1.2 g VSS L^{-1} , temperature was maintained at 30 °C and pH was maintained between 7.5 and 8.5. Oxygen affinity constants were estimated by fitting the experimental DO profiles to an oxygen Monod expression for several respirometric tests with different F/M ratios. $K_{O,NOB}$ was estimated for a biomass particularly enriched in NOB. Monod expressions used to describe the DO influence on heterotrophs, AOB and NOB activity are detailed in equations 4.45, 4.46 and 4.47, respectively. Figure 4.17 shows representative experimental and theoretical DO profiles of this kind of experiment.

In these respirometric tests, K_{OH} and $K_{O,AOB}$ were determined from biomass of the SBR withdrawals. However, $K_{O,NOB}$ was estimated for a biomass particularly enriched in NOB.

$$OUR_{EX} = -\left(\frac{1-Y_H}{Y_H}\right) \mu_{m,H} \frac{S_O}{K_{OH} + S_O} X_{BH} \quad (4.45)$$

$$OUR_{EX} = -\left(\frac{3.43 - Y_{AOB}}{Y_{AOB}}\right) \mu_{m,AOB} \frac{S_O}{K_{O,AOB} + S_O} X_{AOB} \quad (4.46)$$

$$OUR_{EX} = -\left(\frac{1.14 - Y_{NOB}}{Y_{NOB}}\right) \mu_{m,NOB} \frac{S_O}{K_{O,NOB} + S_O} X_{NOB} \quad (4.47)$$

Oxygen affinity constant for heterotrophic biomass, K_{OH} , was $0.19 \text{ mg O}_2 \text{ L}^{-1}$, which is in good agreement with the values observed by Henze *et al.* (2000). As expected, AOB presented a higher oxygen affinity than NOB. Besides, these parameters were quite low when compared with other reported values from literature, probably due to the reduced oxygen supply inside the reactor.

Table 4.12 – Comparison of the K_{OA} and K_{ON} values obtained with other values from literature.
(after Guisasola *et al.*, 2004)

$K_{O,AOB}$ (mg O ₂ L ⁻¹)	$K_{O,NOB}$ (mg O ₂ L ⁻¹)	Temperature (°C)	Reference
0.15	0.55	30	Present study
0.5	1	30	Sperandio <i>et al.</i> , 2007
0.25	0.5	35	Dold <i>et al.</i> , 2007
0.94 ± 0.091	-	25 - 35	Van Hulle <i>et al.</i> , 2004
0.72 ± 0.02	1.75 ± 0.01	25	Guisasola <i>et al.</i> , 2004
	0.5-2	25	Henze <i>et al.</i> , 2000
1.45	1.1	35	Hellinga <i>et al.</i> , 1998
0.6	1.3	20	Wiesmann, 1994
0.16	0.54	30	Hunik <i>et al.</i> , 1994
0.3	0.6	28	Nowak <i>et al.</i> , 1995
	0.4	25	EPA, 1993

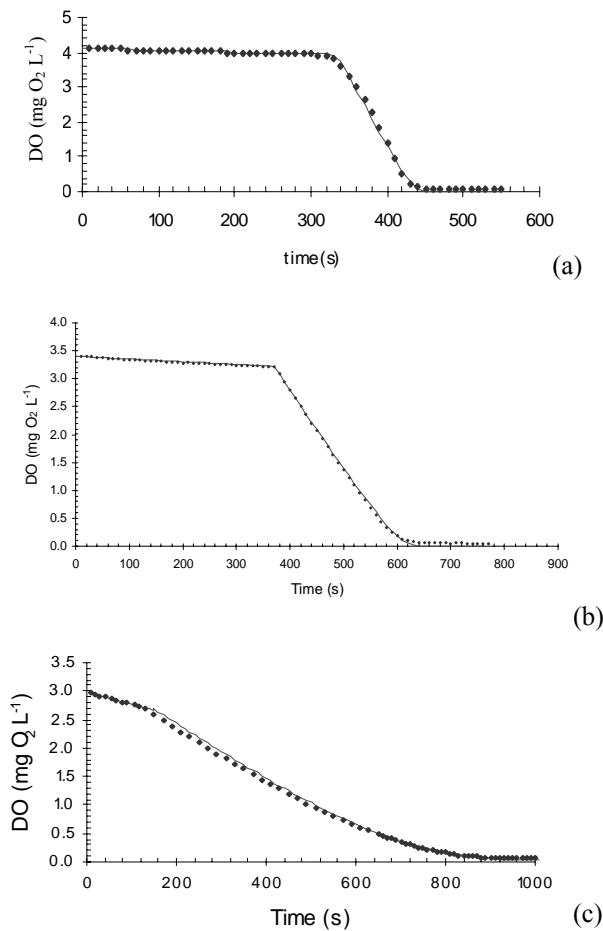


Figure 4.17 – $K_{O,H}$ (a), $K_{O,AOB}$ (b) and $K_{O,NOB}$ (c) assessment. Experimental (●) and simulated (—) data.

4.2.5.3. Influence of pH and Temperature.

pH influence. As it is stated in Chapter 1, both heterotrophic and autotrophic biomass are highly affected by the operating pH range. In order to evaluate the pH influence on nitrifying/denitrifying activated sludge, a reliable and rapid procedure was developed: Aliquots (250 mL) of endogenous nitrifying-denitrifying biomass were adjusted at the desired pH setpoint ± 0.05 and the working temperature. Subsequently, the mixed liquor was inserted into a watertight and stirred respiration chamber equipped with a dissolved oxygen electrode and an injection port. The DO concentration slowly decreased giving the endogenous Oxygen Uptake Rate (OUR_{END}) as the slope (see Figure 4.15). After

several minutes, 5 mL of a previously pH and temperature controlled substrate solution (ammonium chloride for nitrifying biomass or sodium acetate for heterotrophic biomass) were injected to the mixed liquor and a subsequent sudden drop in the DO profile was observed due to microbial substrate consumption. Thus, exogenous OUR (OUR_{EX}) could be determined. Since OUR_{EX} is proportional to the maximum growth rate, relative biomass activity can be calculated as the ratio between OUR_{EX} for every studied condition and the maximum OUR_{EX} of the experiment. Therefore, for the optimum pH condition, the relative biomass activity is 1.

These experiments were run with approximately $0.45 \text{ g VSS L}^{-1}$, which provided a suitable low OUR that improved the OUR_{EX} profile assessment, since the DO drop was not extremely pronounced and the pH did not change significantly due to relatively low substrate consumption. Substrate concentration inside the respiration chamber was sufficiently high ($75 \text{ mg NH}_4^+\text{-N L}^{-1}$ or $200 \text{ mg COD L}^{-1}$) to avoid substrate limiting growth rates.

Two representative relative microbial activity profiles for heterotrophic and autotrophic biomass versus pH are presented in Figure 4.18, which are in concordance with other reported values (Orton and Arhan, 1994; Grunditz and Dalhammar, 2001). The experimental profile clearly shows that nitrifying biomass activity is more affected by pH than heterotrophic biomass and both maximum growth rates are reached at a pH region near 8.0.

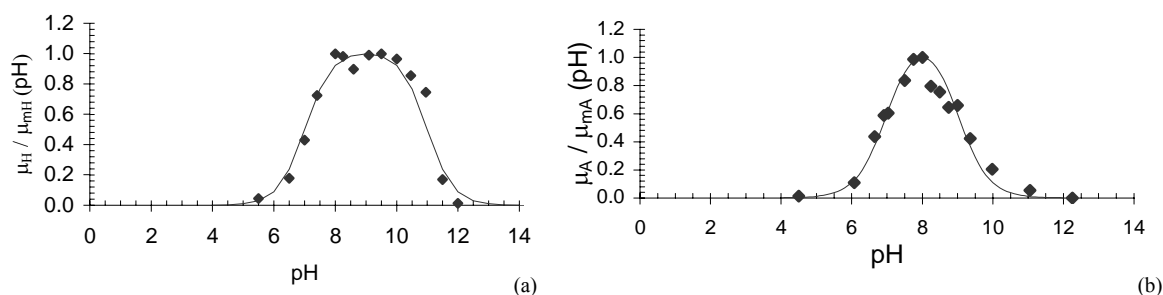


Figure 4.18 - Biomass relative activity versus pH and temperature. Relative activity ($32 \text{ }^\circ\text{C}$) versus pH for (a) heterotrophic and (b) autotrophic biomass.

Moreover, the experimentally assessed pH dependency function can be modeled combining Monod kinetics and non-competitive inhibition for proton concentration (H^+) as described by Siegrist *et al.* (1993) and Serralta *et al.* (2004). Equation 4.48 represents the process rate at the actual pH, $r(pH)$, as the process rate at the optimum pH, $r(pH_{opt})$, multiplied by a pH dependency function (F_{pH}). This pH dependency function is calculated by means of Equation 4.49 (Serralta *et al.*, 2004) where pH is the actual pH value, pH_{OPT} is the optimum pH value, K_{pH} and $K_{I,pH}$ are the model affinity and inhibition constants for proton concentration. Due to the simetric characteristics of the pH dependency equation selected in this work, K_{pH} and K_H are correlated according to Equation 4.50.

$$r(pH) = F_{pH} r(pH_{opt}) \quad (4.48)$$

$$F_{pH} = \left(\frac{10^{-pH}}{K_{pH} + 10^{-pH}} \frac{K_{I,pH}}{K_{I,pH} + 10^{-pH}} \right) \left/ \left(\frac{10^{-pH_{opt}}}{K_{pH} + 10^{-pH_{opt}}} \frac{K_{I,pH}}{K_{I,pH} + 10^{-pH_{opt}}} \right) \right. \quad (4.49)$$

$$S_{H,opt} = \sqrt{K_{pH} K_{I,pH}} \quad (4.50)$$

Experimental and simulated data can be compared in Figure 4.18 and the values for the calibrated model parameters that minimize the sum of squared errors are presented in Table 4.13. These values demonstrate that autotrophic biomass is more sensitive to pH fluctuations than heterotrophic biomass and confirm that the optimum pH value for both autotrophic and heterotrophic biomass is located in a pH near neutrality but slightly basic.

Table 4.13 – Parameters obtained for pH dependency modelling.

	Heterotrophic biomass	Autotrophic biomass
-Log [K_H]	6.95	6.91
-Log [$S_{H,opt}$]	9.00	7.97
R^2	0.974	0.980

Temperature influence. When the optimum pH value was evaluated, the same procedure was carried out at this pH condition but changing the temperature set point. Temperature influence profiles for heterotrophic and autotrophic biomass are presented in Figure 4.19. These graphics are similar to other reported temperature effect studies (Hellinga *et al.*, 1999, Grunditz and Dalhammar, 2001).

A simplification of the half-Arrhenius equation (Equation 4.51 and 4.52) has been reported to be reliable within a limited temperature range of approximately 10-40°C (Orhon and Artan, 1994). In these Equations, $r(T)$ is the process rate at the actual temperature (T), $r(T_{Ref})$ is the process rate at a reference temperature (T_{Ref}), F_T is the temperature dependency function and θ is the temperature coefficient.

$$r(T) = F_T r(T_{Ref}) \quad (4.51)$$

$$F_T = \theta^{(T-T_{Ref})} \quad (4.52)$$

For the studied case, it gives good correlation between experimental and predicted data (Figure 4.19) in the range of 10-33°C. Above this temperature range, the model equation provides non-realistic high biomass activity. Table 4.14 presents the average temperature coefficient value (θ) assessed for heterotrophic and autotrophic microorganisms, which are in good agreement with literature (Orhon and Artan, 1994; Henze *et al.*, 2000; Ferrer and Seco, 2003). Therefore, the Activated Sludge Model can be extended for the studied case to take into account variations in biomass activity depending on the reactor's temperature.

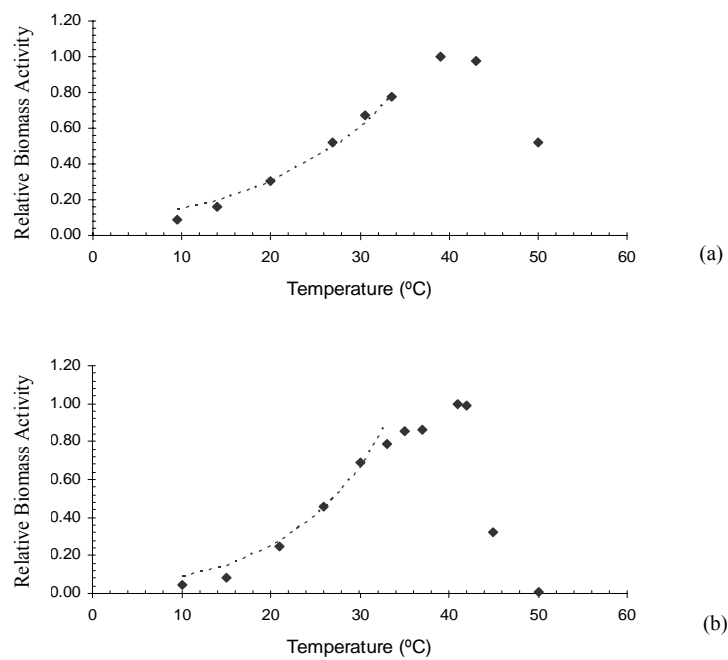


Figure 4.19 – Relative activity of heterotrophic (a) and autotrophic (b) biomass versus temperature. Experimental (♦) and simulated (—) data.

Table 4.14 – Obtained parameter values to model the temperature dependency of AOB and heterotrophic biomass.

	Heterotrophic biomass	AOB
θ	1.073	1.106
R^2	0.995	0.987

4.2.6. Simulation of experimental results

The determination of the main kinetic and stoichiometric parameters of the Activated Sludge Model allowed the simulation of the N/DN process during a representative SBR working sequence. As stated above, a modified version of the classic activated sludge models was used to describe properly the reactions that took place in the case studied.

In order to evaluate the aeration level inside the SBR, the global oxygen mass transfer coefficient, $K_L a_{O_2}$, was assessed experimentally. During one cycle of operation, the amount of wastewater added at the beginning of the cycle was reduced to 85%, which implied that ammonium concentration was depleted 30 minutes before the end of the third nitrification stage. During these 30 minutes, an experiment was carried out to determine $K_L a_{O_2}$, as depicted in Figure 4.20. Once the ammonium concentration was exhausted in the mixed liquor, aeration was stopped and the decline in dissolved oxygen was monitored. Endogenous OUR (OUR_{END}) was evaluated as the slope of oxygen drop and subsequently the SBR was reaerated until the DO concentration reached a constant level. This constant DO concentration resulted from the equilibrium between oxygen supply until dissolved oxygen saturation level (S_O^*) was reached and the OUR_{END} as described by equation 4.53. The actual $K_L a_{O_2}$ coefficient was determined as 0.5 min^{-1} by fitting the experimental DO profile to the aforementioned theoretical equation.

$$\frac{d S_O}{dt} = K_L a_{O_2} (S_O^* - S_O) - OUR_{END} \quad (4.53)$$

Figure 4.4 shows the analysed DO, pH, NH_4^+ -N, NO_2^- -N and NO_3^- -N profiles and their corresponding simulation during a representative 8 h cycle under steady state conditions. The theoretical results from the differential equations system provided good correlation between measured and simulated data.

Reject water was added at the beginning of the cycle and a concentration of $290 \text{ mg NH}_4^+\text{-N L}^{-1}$ was reached. During aerobic phases, $\text{NH}_4^+\text{-N}$ concentration decreased, producing $\text{NO}_2^-\text{-N}$ and reducing the pH value. After the nitrification stage, denitrification took place by mixing the reactor's contents anoxically together with the addition of a stoichiometric amount of an appropriate external organic substrate as electron donor (sodium acetate). During the denitrification stages, variation of $\text{NH}_4^+\text{-N}$ was so small that the experimental results showed practically no ammonia concentration change. The use of three internal N/DN stages during the react period of the working sequence implied that pH remained within a narrow pH region (7.5-8.5) around the optimum pH value for AOB (Grunditz and Dalhammar, 2001). Besides, this strategy prevented the accumulation of $\text{NO}_2^-\text{-N}$ inside the SBR, avoiding HNO_2 toxicity problems associated with both nitrifying and denitrifying biomass (Abeling and Seyfried, 1992). Likewise, free ammonia concentration during the whole cycle did not affect the first step of the nitrification process as predicted by the simulation model.

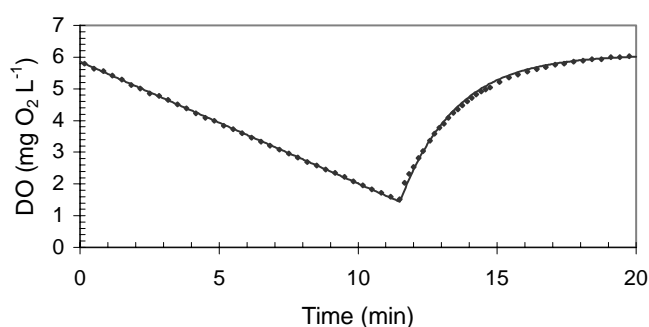


Figure 4.20 – Experimental assessment of K_{LaO_2} . Experimental data (●) and Simulated data (—)

During the first few minutes of the first nitrification stage, there was a reduced rate of nitrification since competition for oxygen between AOB and heterotrophic biomass took place until the low BOD_{ST} inside the SBR was exhausted. Once BOD_{ST} was depleted, the DO level rose up to $0.8 \text{ mg O}_2 \text{ L}^{-1}$, which favoured nitrification over nitrataion, due to their different oxygen affinities. This reduced DO level (well predicted by the model) implied that the actual Ammonium Uptake Rate (AUR) was reduced to 85% of the maximum elimination rate. Moreover, NOB was partially inhibited by the free ammonia concentration inside the reactor. The combined effect of reduced oxygen supply and high ammonium concentration during the operational cycle resulted in a high inhibition of NOB and led to the BNR via nitrite process, with its corresponding beneficial effects.

pH evolution during the three nitrification stages was considerably different. During the first aerobic stage, pH decrease was slower than in the following ones, despite the fact that nutrient removal rate was approximately the same. This phenomenon was caused by alkalinity consumption during ammonium oxidation and, consequently, buffer capacity inside the reactor went down. Subsequent denitrification periods recovered partially the alkalinity previously consumed.

4.3. CONCLUSIONS

- ✓ In this study, a SBR was used to carry out BNR via nitrite for the treatment of a real reject water from a municipal WWTP. This highly ammonium concentrated wastewater had a reduced buffer capacity and a very low BOD_{ST} concentration. Consequently, an external carbon source for denitrification was required for its treatment.
- ✓ Nitrogen was completely removed when operating with 3 cycles per day, temperature 30°C, SRT 11 days and HRT 1 day. During the operational cycle, three alternating oxic/anoxic periods were performed to avoid alkalinity restrictions. Furthermore, oxygen supply and working pH range were controlled in order to achieve BNR via nitrite, making the process considerably more economic. Under steady state conditions, an sAUR and sNUR of 19 mg NH_4^+ -N g^{-1} VSS h^{-1} and 40 mg NO_2^- -N g^{-1} VSS h^{-1} , respectively, were reached.
- ✓ IWA activated sludge models were modified to describe BNR via nitrite. Both nitrification and denitrification were described as two-step reactions inhibited by ammonia and nitrous acid concentrations.
- ✓ A closed intermittent-flow respirometer was set up for the most relevant model parameters assessment. The main kinetic and stoichiometric parameters for carbon oxidation and nitrogen removal lay inside the range described in literature. As expected, oxygen affinity constant for ammonium oxidizers was very low due to the reduced oxygen supply inside the SBR.

- ✓ The proposed model showed very good agreement between ammonium, nitrite, nitrate and dissolved oxygen experimental and simulated values under steady state conditions.

5. Modelling of a sequencing batch reactor to treat the supernatant from anaerobic digestion of the organic fraction of municipal solid waste.

ABSTRACT

Similarly to Chapter 4, a lab-scale Sequencing Batch Reactor (SBR) was tested to remove COD and $\text{NH}_4^+\text{-N}$ from the supernatant of Anaerobic Digestion of the Organic Fraction of Municipal Solid Waste. This supernatant was characterised by a high ammonium concentration ($1.1 \text{ g NH}_4^+\text{-N L}^{-1}$) and an important content of slowly biodegradable and/or recalcitrant COD ($4.8 \text{ g total COD L}^{-1}$). Optimum SBR operating sequence was reached when working with 3 cycles per day, 30°C , SRT 12 days and HRT 3 days. During the time sequence, two aerobic/anoxic steps were performed to avoid alkalinity restrictions. Oxygen supply and working pH range were controlled to promote the nitrification over nitrite. Under steady state conditions, COD and nitrogen removal efficiencies of more than 65% and 98%, respectively, were achieved. The closed intermittent-flow respirometer constructed in this Thesis was used to characterise and model the SBR performance. The IWA Activated Sludge Models were modified to describe the biological nitrogen removal over nitrite, including the inhibition of nitrification by unionised ammonia and nitrous acid concentrations, the pH dependency of both autotrophic and heterotrophic biomass, pH calculation and the oxygen supply and stripping of CO_2 and NH_3 . Once calibrated by respirometry, the proposed model showed very good agreement between experimental and simulated data.

The most relevant parts of this chapter are published in:

Dosta, J., Galí, A., Macé, S., Mata-Álvarez, J. (2007) Modelling of a sequencing batch reactor to treat the supernatant from anaerobic digestion of municipal solid waste. *J. Chem. Tech. Biotech.* 82(2) 158-164.

5.1 INTRODUCTION

The Ecoparc-1 of Barcelona is a very large plant for anaerobic digestion and composting of the Organic Fraction of Municipal Solid Waste (OFMSW). Its main objective is to pre-select recyclable fractions still present in the Municipal Solid Waste (MSW) (such as plastics, paper, metals, ...) and to treat the OFMSW in order to produce biogas and compost of quality (Mata-Álvarez, 2002). Within this framework, the waste conducted to incineration and/or landfilling is minimized and the MSW management results in a very environmentally sustainable solution.

There are basically two types of MSW that enters to the Ecoparc-1: source sorted OFMSW and mixed MSW. The source sorted OFMSW (high quality) is pre-treated in a mechanical separation system and is planned to introduce into anaerobic digesters. On the other hand, the mixed MSW is pre-selected in a more complex mechanical separation system to obtain the OFMSW (low quality) without inappropriate materials, which is treated by means of a wet mesophilic anaerobic digestion Linde-KCA technology (De Baere, 2005), as depicted in Figure 5.1.

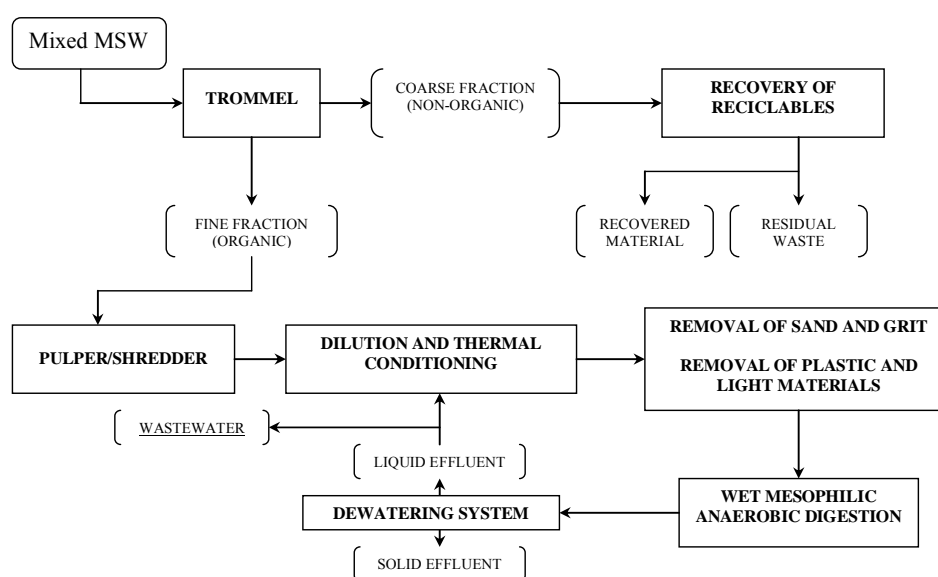


Figure 5.1- Schematic flow-diagram of the treatment of mixed MSW in the Ecoparc-1.

The digested effluent is conducted to a dewatering system where it is divided into two fractions: solid and liquid effluent. The dewatered solid material is treated by means of tunnel composting (Haug, 1993). The liquid effluent (supernatant of anaerobic digestion of the OFMSW) is, in part, used as process water to dilute the OFMSW before being fed to the anaerobic digester and the excess water is treated in a wastewater treatment plant. Since the supernatant of anaerobic digestion of the OFMSW is characterised by a high ammonium concentration and an important content of slowly biodegradable and/or recalcitrant COD, its treatment in a Sequencing Batch Reactor (SBR) for simultaneous COD and Nitrogen removal is feasible (Macé and Mata-Álvarez, 2002).

Macé *et al.* (2006) optimised a SBR strategy to treat this effluent by means of a nitrification/denitrification via nitrite process, obtaining an HRT of 3 days, a COD removal efficiency of more than 65% and a total nitrogen removal efficiency of more than 98%. In this treatment, the oxygen supply and the external COD requirements to denitrify were minimized. Moreover, no chemicals were needed to control the pH. A Zahn-Wellens test and a dilution test were carried out to examine the origin of the reduced COD biodegradation. These tests showed that the low COD biodegradation observed in the optimum SBR cycle was not due to a lack of nutrients nor to the presence of toxic compounds. Therefore, low biodegradation was related to the presence of refractory compounds (Macé *et al.*, 2005).

The Activated Sludge Models (ASM) of the IWA (Henze *et al.*, 2000) are a very useful tool to obtain a deep explanation of the biological nutrient removal processes that take place in a digester. However, these models have some limitations, since they cannot predict the nitrification/denitrification process via nitrite and the pH influence and evolution during a biological treatment.

This Chapter focuses on the modelling of the SBR strategy proposed by Macé *et al.* (2006) to treat the supernatant from the anaerobic digestion of the OFMSW of the Ecoparc-1. Moreover, the results obtained lead to a better understanding of the inhibitions and biological processes developed inside the digester.

5.2 RESULTS AND DISCUSSION

5.2.1 Wastewater Characterisation

Table 5.1 shows the main characteristics of the supernatant tested during the years 2003-2004 compared with other similar supernatants of AD of OFMSW from the literature. As observed, this type of wastewater is characterised by a high content in COD and $\text{NH}_4^+\text{-N}$.

Although its concrete composition was strongly dependant on the season of the year, it always presented a low BOD_5 to COD ratio in the range of 0.06-0.28. In order to assess the Biological Oxygen Demand at Short Time (BOD_{ST}) of this wastewater, two respirograms were performed (with and without nitrification inhibition) that showed the low quantity of BOD_{ST} with respect to the ammonia concentration. These respirograms are presented in Figure 5.2. The low $\text{BOD}_{\text{ST}}/\text{N}$ ratio, typical for process waters from biowaste fermentation, implies that full nitrogen removal is hardly reachable without addition of an exogenous source of carbon (Graja and Wilderer, 2001). Consequently, acetic acid was used as the external carbon source to denitrify, since it could be present in internal streams of the plant that were planned to test in future work. Moreover, its alkalinity to nitrogen ratio on molar basis (1.4-1.6) was not sufficient to buffer the complete nitrification process in a single step.

Table 5.1- Average composition of the supernatant tested and other similar supernatants from AD of OFMSW (after Graja and Wilderer, 2001)

Reference	COD_{TOT} (g L^{-1})	BOD_5 (g L^{-1})	$\text{BOD}_5/\text{COD}_{\text{TOT}}$ (-)	$\text{NH}_4^+\text{-N}$ (mg L^{-1})	NTK (mg L^{-1})	$\text{PO}_4^{3-}\text{-P}$ (mg L^{-1})	pH (-)	TSS (g L^{-1})
This study (Average)	4.8	0.58	0.12	1118	-	11	8.3	1.9
(Interval range)	3.5-5.2	0.2-1.5	0.06-0.29	690-1326	-	7-14	8.2-8.4	1.6-2.57
Kautz & Nelles (1995)	3-23.8	0.7-10	0.05-0.45	229-963	305-1,558	-	7.6-8.4	4.8-15.7
Kübler (1996)	7.3-28.3	1.65-7.1	0.23-0.25	510-2600	-	-	7.8	9.6-20.6
Loll (1998)	2.3-36.2	0.66-13.7	0.29-0.38	565-1,490	-	4.8-20	7.3-8.3	-
Bidlingmaier (2000)	3-24	0.7-3.5	0.05-0.4	200-1,800	-	30-150	7.6-8.5	-
Müller (1999)	3-15	1-15	0.3-1.0	500-2,500	-	-	-	-

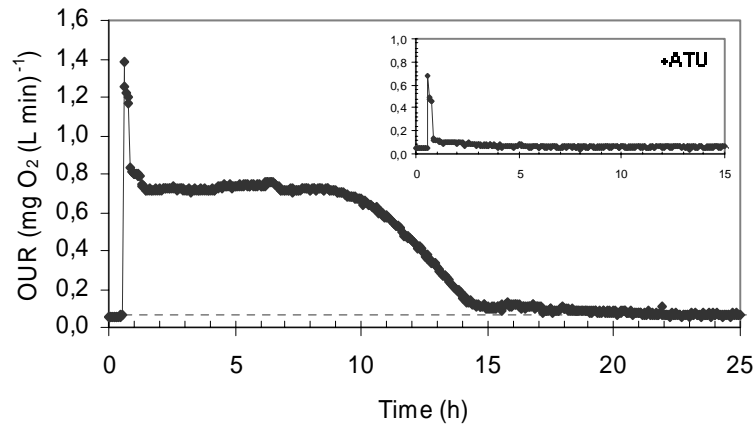


Figure 5.2 – Respirogram obtained for the determination of BOD_{ST} of supernatant from AD of the OFMSW under study without nitrification inhibition and (insertion) with 12 mg L^{-1} of ATU. Experimental data (\blacklozenge) and endogenous OUR (---)

5.2.2. Optimum SBR operation

In previous work (Macé *et al.*, 2006) the SBR strategy for the treatment of the OFMSW was optimized, reaching a total nitrogen removal of $0.36 \text{ kg N (m}^3 \text{ day)}^{-1}$. The main characteristics of the operating cycle are presented in Table 5.2.

Table 5.2- Main characteristics of the optimum SBR operating strategy for the treatment of OFMSW.

Parameter	Units	Value
Cycle Length	h	8
Time distribution		
Aerobic Feeding	h	0.25
Aerobic	h	2.00
Anoxic	h	0.67
Aerobic	h	2.75
Anoxic	h	0.83
Settle and draw	h	1.50
HRT	days	3
Total Nitrogen Removal	$\text{kg N (m}^3 \text{ day)}^{-1}$	0.36
SRT	days	12
VSS	g VSS L^{-1}	3.5
Temperature	$^{\circ}\text{C}$	30
Dissolved Oxygen	$\text{mg O}_2 \text{ L}^{-1}$	< 1.50
pH range	-	7.6 – 8.4

The biological nitrogen removal was divided into two nitrification/denitrification periods to maintain the pH between the range 7.6-8.4 and improve the process efficiency. Wastewater was added at the beginning of the cycle in order to reach a high initial concentration (namely, 120 mg NH₄⁺-N L⁻¹) and, therefore, a maximum Ammonium Uptake Rate (AUR). Acetic acid was used in the subsequent denitrification to recover part of the alkalinity consumed in the previous stage. Since the dosage of acetic acid lead to a pH decrease, the stoichiometric quantity needed to denitrify the total NO₂⁻-N produced was divided in two equal additions injected at the beginning of each anoxic period. Considering the nitrifying biomass inhibition by NH₃ and HNO₂ reported by Anthonisen *et al.* (1976) and the working pH range of the studied system, the maximum free ammonia concentration was only capable to inhibit Nitrite Oxidizing Biomass (NOB) but not Ammonium Oxidizing Biomass (AOB). Nitrite concentrations were always below 80 mg NO₂⁻-N L⁻¹ and, therefore, neither AOB nor NOB were inhibited by nitrous acid concentration. Moreover, DO concentration was maintained below 1.5 mg O₂ L⁻¹ to assure the nitrite route to take place.

5.2.3. Activated sludge Model extended for nitrite route description

The IWA Activated Sludge Models (Henze *et al.*, 2000) were modified to describe BNR over nitrite for highly ammonium loaded wastewaters. As previously explained in Chapter 4, nitrification was described as a two-step reaction where ammonium is firstly oxidized to nitrite by AOB and, subsequently, nitrite is oxidized to nitrate by NOB. Both reactions are potentially inhibited by unionised ammonia and nitrous acid concentrations (Anthonisen *et al.*, 1976), expressed in the model equations by means of non-competitive inhibition kinetics as described by Wett and Rauch (2003). Equation 5.1 presents this expression, where F_{INH} is the inhibition function for free NH₃ and HNO₂, $K_{NH_3}^a$ represents the NH₃ inhibition constant for the autotrophic biomass a , $K_{HNO_2}^a$ the HNO₂ inhibition constant for the autotrophic biomass a , and S_{NH_3} and S_{HNO_2} are the concentrations of NH₃ and HNO₂ obtained through the acid/base equilibrium inside the reactor. Values of inhibition constants were assumed from the literature (Wett and Rauch, 2003).

$$F_{INH} = \frac{S_{NH_3}}{K_{NH_3}^a + S_{NH_3}} \frac{S_{HNO_2}}{K_{HNO_2}^a + S_{HNO_2}} \quad (5.1)$$

Denitrification was also considered as a two-step process where nitrate was initially reduced to nitrite and then to nitrogen gas by heterotrophic biomass. For heterotrophic

growth under anoxic conditions, two correction factors ($\eta_{NO_3 \rightarrow NO_2}$ and $\eta_{NO_2 \rightarrow N_2}$) were considered in order to assess the kinetics for both reactions of nitrogen reduction.

Different heterotrophic cell yield coefficients were considered under aerobic and anoxic conditions, since the heterotrophic yield under anoxic conditions (Y_H^{DN}) is reduced relative to its aerobic value (Y_H) (Muller *et al.*, 2004).

Lineal death was established for the decay process of both heterotrophic and autotrophic organisms in order to make the mathematical model as simple as possible.

Oxygen supply and stripping of CO₂ and NH₃ were considered using the two-film theory as stated in Equations 5.2, 5.3 and 5.4. In these Equations, He_{O_2} , He_{CO_2} and He_{NH_3} are the Henry's law constants of O₂, CO₂ and NH₃, respectively, and P_{P,O_2} , P_{P,CO_2} and P_{P,NH_3} are the partial pressures of O₂, CO₂ and NH₃ in the air supplied to the mixed liquor, respectively. For CO₂ and NH₃, the partial pressures considered were 3.0 10⁻⁴ and 0.0 atm, respectively (Magr  *et al.*, 2007)

$$\frac{d S_{O_2}}{dt} = K_L a_{O_2} (S_{O_2} - He_{O_2} P_{P,O_2}) \quad (5.2)$$

$$\frac{d S_{CO_2}}{dt} = K_L a_{CO_2} (S_{CO_2} - He_{CO_2} P_{P,CO_2}) \quad (5.3)$$

$$\frac{d S_{NH_3}}{dt} = K_L a_{NH_3} (S_{NH_3} - He_{NH_3} P_{P,NH_3}) \quad (5.4)$$

$K_L a_{CO_2}$ was based on $K_L a_{O_2}$ by correcting it for different diffusion coefficients as stated in Equation 5.5 (Hellin  *et al.*, 1999; Serralta, 2004), where D_{O_2} and D_{CO_2} are the diffusivities of O₂ and CO₂, respectively. Stripping of NH₃ and Henry's law constants at 30°C were determined by using the correlations proposed by Musvoto *et al.* (2000a; 2000b).

$$\frac{K_L a_{O_2}}{K_L a_{CO_2}} = \sqrt{\frac{D_{O_2}}{D_{CO_2}}} \quad (5.5)$$

Two new components, inorganic carbon (S_C) and proton (S_H) concentration, were defined in order to evaluate restrictions linked to alkalinity and pH limitations as described by Serralta *et al.* (2004). The stoichiometric parameters related to S_C and S_H were calculated by applying the continuity functions of C and H as detailed in section 1.4.2. The composition matrix of the proposed model and the conversion factors used for C and N are presented in Table 5.3 and 5.4, respectively.

Table 5.3 – Composition matrix of the proposed model (after Serralta *et al.*, 2004)

Component	Units	COD	N	C	H
		$[i_{COD,i}]$	$[i_{N,i}]$	$[i_{C,i}]$	$[i_{H,i}]$
		(g COD)	(g N)	(mole C)	(mole H)
S_O	(g O ₂)	-1			
S_S (CH ₃ COOH)	(g DQO)	1		2/64	1/64
S_{NH}	(g NH ₄ ⁺ -N)		1		-1/14
S_{NO2}	(g NO ₂ ⁻ -N)		1		1/14
S_{NO3}	(g NO ₃ ⁻ -N)		1		1/14
S_{N2}	(g N ₂ -N)		1		
S_I	(g COD)	1		$i_{C,SI}$	
X_I	(g COD)	1	$i_{N,SI}$	$i_{C,XI}$	
X_{BH}	(g COD)	1	$i_{N,XBH}$	$i_{C,XBH}$	
X_{AOB}	(g COD)	1	$i_{N,XAOB}$	$i_{C,XAOB}$	
X_{NOB}	(g COD)	1	$i_{N,XNOB}$	$i_{C,XNOB}$	
S_{IC}	(mole C)			1	2
S_H	(mole H)				-1

Table 5.4 – Conversion factors for C and N content in biomass and inert matter. (after Serralta *et al.*, 2004)

	C			N		
	$i_{C,i} [\text{mole C (g COD)}^{-1}]$			$i_{N,i} [\text{g N (g COD)}^{-1}]$		
	Coefficient	Value	Reference	Coefficient	Value	Reference
S_I	$i_{C,SI}$	0.03	Siegrist <i>et al.</i> , 1993	$i_{N,SI}$	0.01	Henze <i>et al.</i> , 2000
X_I	$i_{C,XI}$	0.03	Siegrist <i>et al.</i> , 1993	$i_{N,XI}$	0.03	Henze <i>et al.</i> , 2000
X_{BH}	$i_{C,XBH}$	5/160	Henze <i>et al.</i> , 2000	$i_{N,XBH}$	0.07	Henze <i>et al.</i> , 2000
X_{AOB}	$i_{C,XAOB}$	5/160	Henze <i>et al.</i> , 2000	$i_{N,XAOB}$	0.07	Henze <i>et al.</i> , 2000
X_{NOB}	$i_{C,XNOB}$	5/160	Henze <i>et al.</i> , 2000	$i_{N,XNOB}$	0.07	Henze <i>et al.</i> , 2000

The pH dependency function (F_{pH}) for both autotrophic and heterotrophic biomass was included in the model combining Monod kinetics and non-competitive inhibition for H^+ concentration as proposed by Siegrist *et al.* (1993) and Seco *et al.* (2004). This mathematical expression is presented in Equation 4.49 (see Chapter 4).

Acid-base equilibrium of inorganic carbon, acetic acid, phosphoric acid and water were considered in order to predict the distribution of species in the liquid media. Acid-Base dissociation constants were determined for the operating temperature (30°C) by using Equation 5.6 (Lide, 1993; Campos and Flotats, 2003). The coefficients used in this study are detailed in Table 5.5.

$$pKa_i = pKa_i(0^\circ C) + a_i T + b_i T^2 + c_i T^3 \quad (5.6)$$

Table 5.5- Dissociation constants and temperature dependency coefficients considered in this study (Lide, 1993)

	Equilibrium	$pKa_i(0^\circ C)$	a	b	c
ACETIC ACID	$CH_3COOH \Leftrightarrow CH_3COO^- + H^+$	4.7803	-0.0023	$6/10^5$	$-2/10^7$
CARBONATE (1)	$H_2CO_3 \Leftrightarrow HCO_3^- + H^+$	6.5787	-0.0133	0.0002	$-8/10^7$
CARBONATE (2)	$HCO_3^- \Leftrightarrow CO_3^{2-} + H^+$	9.2839	-0.0133	$9/10^5$	$-2/10^7$
PHOSPHATE (1)	$H_3PO_4 \Leftrightarrow H_2PO_4^- + H^+$	2.0473	0.0019	$5/10^5$	0
PHOSPHATE (2)	$H_2PO_4^- \Leftrightarrow HPO_4^{2-} + H^+$	7.3144	-0.0073	0.0001	$-6/10^7$
PHOSPHATE (3)	$HPO_4^{2-} \Leftrightarrow PO_4^{3-} + H^+$	12.6576	0	0	0
WATER	$H_2O \Leftrightarrow H^+ + OH^-$	14.934	-0.0425	0.0002	$-6/10^7$

For the assessment of the Acid-base dissociation constants for ammonium and nitrous acid, expressions 5.7 and 5.8 were used (Anthonisen *et al.*, 1976).

$$(Ka)_{NH_3} = e^{\left(\frac{-6344}{T+273}\right)} \quad (5.7)$$

$$(Ka)_{HNO_2} = e^{\left(\frac{-2300}{T+273}\right)} \quad (5.8)$$

Furthermore, the influences of ionic strength and activity coefficients on the acid-base dissociation constants for all the species contemplated in the model were also taken into account. Ionic strength was calculated according to Equation 5.9, where I is the ionic

strength, m is the total number of charged species present in solution, Z_i is the charge of specie 'i', and C_i is the concentration of specie 'i'.

$$I = \frac{1}{2} \sum_{i=1}^m Z_i^2 c_i \quad (5.9)$$

Equation 5.10 shows the Debye-Hückel equation used to calculate the activity coefficients of each charged specie considered in the proposed model. These activity coefficients were calculated for each time step as a function of the ionic strength of the mixed liquor. In Equation 5.10, both A_d and B_d are constants dependant of the temperature and the dielectric constant (ϵ) of the reaction medium, and a_i is a parameter dependant of the ion's size.

$$\text{Log } \gamma_i = -\frac{A_d Z_i^2 I^{1/2}}{(1 + B_d a_i I^{1/2})} \quad (5.10)$$

For neutral species (except water), the activity coefficients were calculated by means of the Helgenson (1969) Equation as expressed by Expression 5.11, where $\alpha_i = 0.1$.

$$\text{Log } \gamma_i = \alpha_i I \quad (5.11)$$

These activity coefficients were used to correct Equilibrium constants. Equation 5.12 shows an example of the modification of the Equilibrium constant of acetic acid by the activity coefficients of the species involved in this acetic acid/acetate acid-base equilibrium. In this Equation, γ_{CH_3COOH} , γ_{H^+} and $\gamma_{CH_3COO^-}$ are the activity coefficients of acetic acid, protons and acetate, respectively; S_{CH_3COOH} , S_{H^+} and $S_{CH_3COO^-}$ are the concentrations of acetic acid, protons and acetate, respectively; and $(pKa)_{CH_3COOH}$ is the pKa of the acetic acid/acetate acid base equilibrium.

$$10^{(pKa)_{CH_3COOH}} = \frac{(\gamma_{CH_3COOH} S_{CH_3COOH})}{(\gamma_{H^+} S_{H^+})(\gamma_{CH_3COO^-} S_{CH_3COO^-})} \quad (5.12)$$

Table 5.6 shows the complete model in matrix format used to describe the SBR operation and in Table 5.7 the biological processes considered in the model and their rate equations are listed.

Table 5.6 – Petersen Matrix of the proposed Activated Sludge Model

	S_S	S_I	S_O	S_{NH}	S_{NO_2}	S_{NO_3}	S_{N_2}	X_I	X_{BH}	X_{AOB}	X_{NOB}	S_C	S_H
Aerobic growth of heterotrophs on S_S	$-\left(\frac{1}{Y_H}\right)$		$-\left(\frac{1-Y_H}{Y_H}\right)$	$-i_{NH}$				1				(*)	(1)
Reduction of nitrate to nitrite	$-\left(\frac{1}{Y_{H,NO_3}}\right)$			$-i_{NH}$	$\left(\frac{1-Y_{H,NO_3}}{1.14Y_{H,NO_3}}\right)$	$-\left(\frac{1-Y_{H,NO_3}}{1.14Y_{H,NO_3}}\right)$		1				(*)	(2)
Reduction of nitrite to nitrogen gas	$-\left(\frac{1}{Y_{H,NO_2}}\right)$			$-i_{NH}$	$-\left(\frac{1-Y_{H,NO_2}}{1.71Y_{H,NO_2}}\right)$	$-\left(\frac{1-Y_{H,NO_2}}{1.71Y_{H,NO_2}}\right)$	$\left(\frac{1-Y_{H,NO_2}}{1.71Y_{H,NO_2}}\right)$	1				(*)	(3)
Decay of heterotrophs			$-(1-f_d)$	(*)				f_d	-1			(*)	(4)
Aerobic growth of AOB			$-\left(\frac{343-Y_{AOB}}{Y_{AOB}}\right)$	$-i_{NH}-\left(\frac{1}{Y_{AOB}}\right)$		$\left(\frac{1}{Y_{AOB}}\right)$				1		(*)	(5)
Aerobic growth of NOB			$-\left(\frac{114-Y_{NOB}}{Y_{NOB}}\right)$	$-i_{NH}$	$-\left(\frac{1}{Y_{NOB}}\right)$	$-\left(\frac{1}{Y_{NOB}}\right)$	$\left(\frac{1}{Y_{NOB}}\right)$				1	(*)	(6)
Decay of autotrophs			$-(1-f_d)$	(*)				f_d	-1			(*)	(7)
O_2 supply			1									(*)	(8)
Stripping of CO_2												-1	(9)
Stripping of NH_3				-1								(*)	(10)

(*) Stoichiometric parameters calculated from continuity equations

Table 5.7 – Kinetic equations of the considered processes

(j)	Processes	Kinetic rate equations ($\rho_1 > 0$)
Heterotrophic organisms		
(1)	Heterotrophic aerobic growth on S_S Heterotrophic anoxic growth on S_S	$\mu_{mH} \frac{S_S}{K_S + S_S} \frac{S_O}{S_O + K_{OH}} F_{H,pH} X_{BH}$
(2)	Nitrate reduction to nitrite	$\eta_{NO_3 \rightarrow NO_2} \mu_{mH} \frac{S_S}{K_S + S_S} \frac{K_{OH}}{S_O + K_{OH}} \frac{S_{NO_3}}{K_{NO_3} + S_{NO_3}} F_{H,pH} X_{BH}$
(3)	Nitrite reduction to Nitrogen gas	$\eta_{NO_2 \rightarrow N_2} \mu_{mH} \frac{S_S}{K_S + S_S} \frac{K_{OH}}{S_O + K_{OH}} \frac{S_{NO_2}}{K_{NO_2} + S_{NO_2}} F_{H,pH} X_{BH}$
(4)	Heterotrophic decay	$b_H X_{BH}$
Autotrophic organisms		
(5)	Aerobic growth of AOB	$\mu_{m,AOB} \frac{S_{NH}}{K_{NH} + S_{NH}} \frac{K_{NH_3}^{AOB}}{K_{NH_3}^{AOB} + S_{NH_3}} \frac{K_{HNO_2}^{AOB}}{K_{HNO_2}^{AOB} + S_{HNO_2}} \frac{S_O}{S_O + K_{O,AOB}} F_{AOB,pH} X_{AOB}$
(6)	Aerobic growth of NOB	$\mu_{m,NOB} \frac{S_{NO_2}}{K_{NO_2} + S_{NO_2}} \frac{K_{NH_3}^{NOB}}{K_{NH_3}^{NOB} + S_{NH_3}} \frac{K_{HNO_2}^{NOB}}{K_{HNO_2}^{NOB} + S_{HNO_2}} \frac{S_O}{S_O + K_{O,NOB}} F_{NOB,pH} X_{NOB}$
(7)	Autotrophic decay	$b_A (X_{AOB} + X_{NOB})$
Operation conditions		
(8)	Oxygen supply	$K_L a_{O_2} (S_O - He_{O_2} P_{P,O_2})$
(9)	Stripping of CO_2	$K_L a_{CO_2} (S_{CO_2} - He_{CO_2} P_{P,CO_2})$
(10)	Stripping of NH_3	$K_L a_{NH_3} (S_{NH_3} - He_{NH_3} P_{P,NH_3})$

Similarly to Serralta *et al.* (2004), pH was calculated by means of a mass balance equation for proton concentration (see Equation 5.13)

$$S_H = [H^+] + [HPO_4^{2-}] + 2[H_2PO_4^-] + 3[H_3PO_4] + [HCO_3^-] + 2[H_2CO_3] + [CH_3COOH] + [HNO_2] - [OH^-] - [NH_3] \quad (5.13)$$

The set of equations described above were implemented in a software program (Mathematica 4.1) to simulate the studied biological process. The scheme of the model structure (depicted in Figure 5.3) was the one described by Wett and Rauch (2003). For

the time interval considered ($\Delta t = 0.10\text{h}$), a calculation of the evolution of the compounds concentration was carried out. Then, pH variation was calculated and biological process kinetics and dissociation equilibrium were corrected by this pH value as an input for the next time step (Δt).

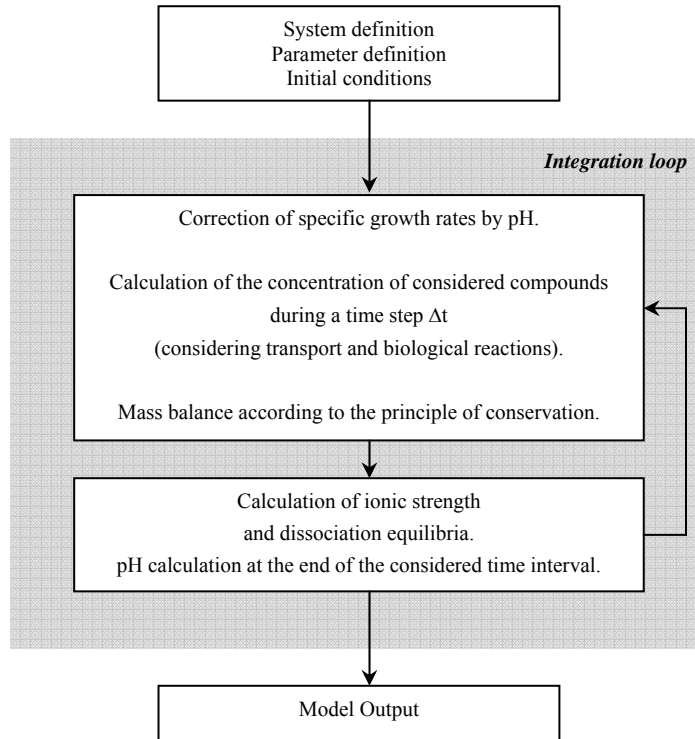


Figure 5.3 – Scheme of the model structure (after Wett and Rauch, 2003).

5.2.4. Model Calibration

Before the application of the Activated Sludge Model extended for nitrite accumulation prediction and pH calculation, the main kinetic constants and stoichiometric coefficients were assessed by respirometry. Average values of the most relevant parameters assessed in this work are presented in Table 5.8. Figure 5.4 shows the determination of some of the most relevant model parameters.

Y_H and Y_{AOB} were determined according to the respirometric procedures of section 4.2.5.1. pH influence on these parameters were also tested, but a negligible effect of pH on both heterotrophic and autotrophic yields were observed.

On the other hand, K_S was determined as explained in section 4.2.5.2 (*Half-saturation constants for substrate*) for different pH values, obtaining a similar value as the one reported in Chapter 4 for SBR treatment of reject water. K_{NH} was determined with a set of 4 experiments with different NH_4^+ -N loads. For all these tests, oxygen concentration was above 2 mg L^{-1} in order to avoid limiting conditions linked to this substrate and pH was controlled above 7.5. The ammonium consumption for every experiment is presented in Figure 5.4 (d). From the initial substrate uptake rate of every test, a plot of the relative nitrifying activity versus initial NH_4^+ -N concentration was represented to obtain the ammonium half-saturation constant (see insertion of Figure 5.4d). The whole set of experiments was modelled obtaining the best fit using a value of $K_{NH} = 4.12 \text{ mg } NH_4^+\text{-N L}^{-1}$.

Oxygen affinity constants for both autotrophic and heterotrophic biomass were assessed according to the batch respirometric test detailed in section 4.2.5.2 (*Oxygen affinity constants*). As observed in Table 5.8, $K_{O, AOB}$ was very reduced which is related to the fact that low DO concentrations were present in the growing medium during the aerobic periods of the SBR. Finally, $\mu_{mH} X_{BH}$, $\eta_{NO_2 \rightarrow N_2} \mu_{mH} X_{BH}$ and $\mu_{mAOB} X_{AOB}$ were assessed according to the procedures described in section 4.2.5.2.

Table 5.8 - Average values of the kinetic and stoichiometric parameters obtained by respirometry

Parameter	Units	Value
Heterotrophic Biomass		
Y_H	mg cellular COD (mg consumed COD) ⁻¹	0.74 ± 0.02
$\mu_{m,H} X_{BH}$	mg cellular COD (L h) ⁻¹	642.1 ± 45.8
$\left[\frac{Y_H (1 - Y_H^{DN})}{Y_H^{DN} (1 - Y_H)} \right] \eta_{NO_2 \rightarrow N_2}$	-	0.75 ± 0.02
$\left[\frac{Y_H (1 - Y_H^{DN})}{Y_H^{DN} (1 - Y_H)} \right] \eta_{NO_3 \rightarrow NO_2}$	-	0.21 ± 0.06
K_S	mg COD L ⁻¹	16.3 ± 2.3
K_{OH}	mg O ₂ L ⁻¹	0.17 ± 0.03
Autotrophic Biomass		
Y_{AOB}	mg cellular COD (mg consumed NH_4^+ -N) ⁻¹	0.24 ± 0.03
$\mu_{m,AOB} X_{AOB}$	mg cellular COD (L h) ⁻¹	10.0 ± 0.8
$\mu_{m,NOB} X_{NOB}$	mg cellular COD (L h) ⁻¹	1.3 ± 0.4
K_{NH}	mg NH_4^+ -N L ⁻¹	4.1 ± 1.3
K_{OA}	mg O ₂ L ⁻¹	0.23 ± 0.03

Heterotrophic and autotrophic decay ratios (b_H and b_A , respectively) at 30°C were assumed from literature using their default values at 20°C proposed in the ASM3 (Henze *et al.*, 2000) combined with the b_H temperature dependency proposed by Ferrer and Seco (2003) and the b_A temperature dependency reported by Ekama and Marais (1984). A value of 0.54 mg cellular COD (mg consumed COD)⁻¹ for Y_H^{DN} was assumed from literature (Muller *et al.*, 2004).

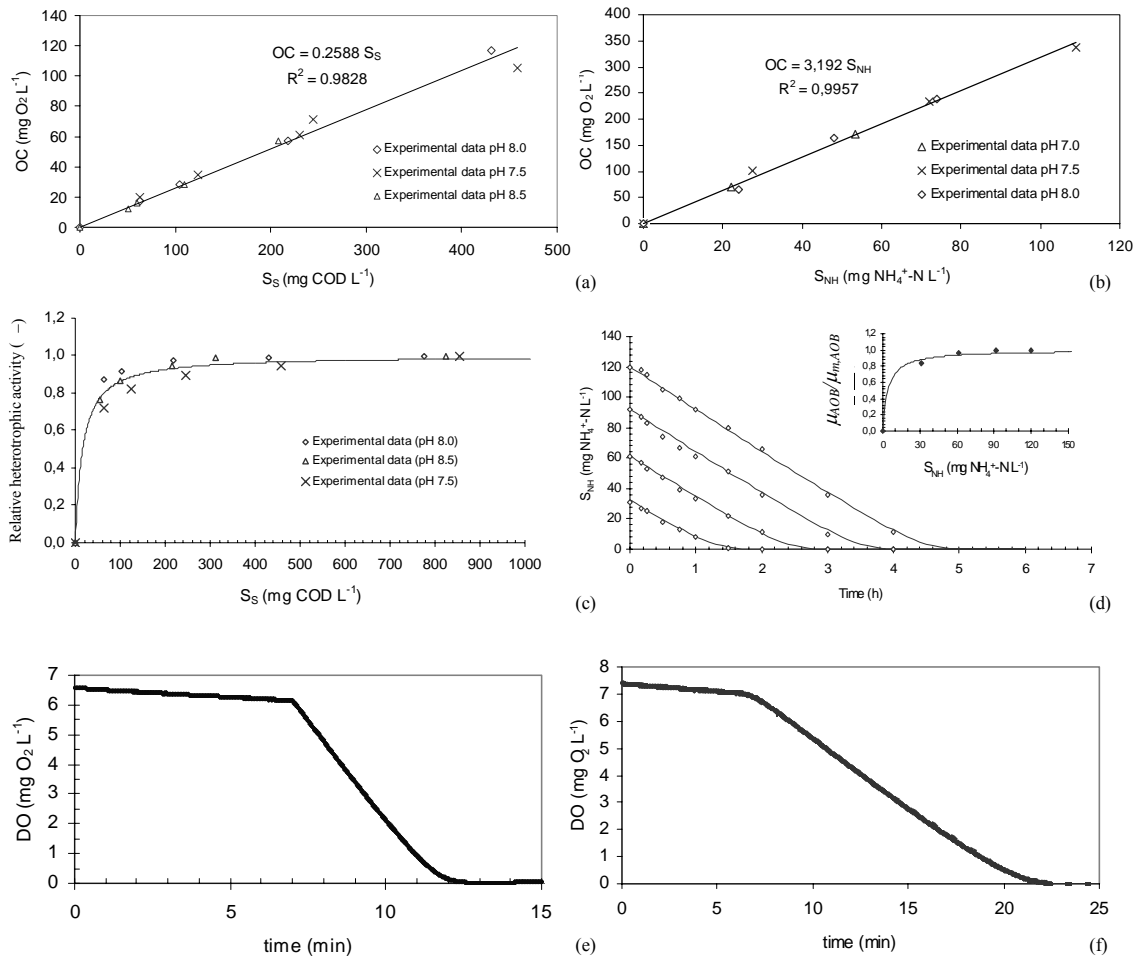


Figure 5.4 – Experimental assessment (♦) and simulation (–) of Y_H , Y_{AOB} , K_S , K_{NH} , K_{OH} and $K_{O, AOB}$ for the biomass to treat supernatant from AD of the OFMSW.

Since both heterotrophic and autotrophic growth rates have been reported to be very dependant on the pH (Orhon and Artan, 1994), its influence was taken into account. For heterotrophic biomass, the influence of pH obtained for a similar nitrifying-denitrifying biomass was considered (see Chapter 4). On the other hand, the autotrophic biomass inhibition for pH was determined as follows: 225 mg $\text{NH}_4^+\text{-N L}^{-1}$ with alkalinity in a molar ratio of approximately 1:1 were added to the aeration chamber of the respirometer with endogenous biomass coming from the withdrawals of the lab-scale SBR under study. In this experiment temperature was maintained at 30°C but pH was not controlled. Due to the nitrification process, pH decreased during the test and, therefore, nitrifying activity was reduced. Since $\text{NH}_4^+\text{-N}$ oscillated between non-limiting concentrations during the whole experiment, the exogenous OUR is proportional to the maximum specific autotrophic growth rate at the actual pH. The maximum OUR (OUR_{MAX}) encountered was related to the optimum pH value. Therefore, pH dependency (F_{pH}) can be calculated by plotting $\text{OUR}/\text{OUR}_{\text{MAX}}$ versus pH. Figure 5.5 shows the results obtained for several tests and the modelling of this dependency.

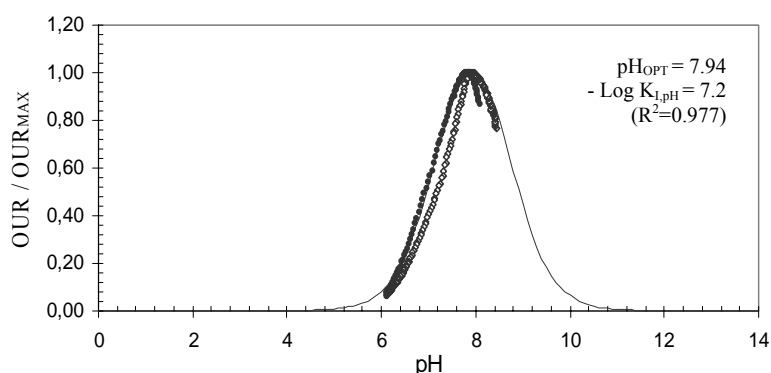


Figure 5.5 - pH influence on nitrifying activity. (Experimental data 1 ●; Experimental data 2 ◊; Modelled data —)

5.2.5. Modelling of the SBR performance

Figure 5.6 shows the experimental profiles of $\text{NH}_4^+\text{-N}$, $\text{NO}_2^-\text{-N}$ and pH in a representative SBR cycle compared with the model predictions. Oxygen level was maintained inside the SBR below $1.5 \text{ mg O}_2 \text{ L}^{-1}$, thus after calculations the oxygen mass transfer coefficient was approximately 0.3 min^{-1} . When considering the values of the aforementioned parameters, the modelling of nitrogen compounds evolution was very accurate. As

observed in Figure 5.5, the supernatant of AD of OFMSW was fed at the beginning of the cycle until a concentration of approximately $120 \text{ mg NH}_4^+\text{-N L}^{-1}$ was reached. During aerobic phases, $\text{NH}_4^+\text{-N}$ concentration decreased producing $\text{NO}_2^-\text{-N}$. Predicted $\text{NH}_4^+\text{-N}$ losses due to stripping of NH_3 were below 5%. The $\text{NH}_4^+\text{-N}$ was consumed nearly 45 min before the ending of the second aerobic period. This time interval was used as a security margin to prevent possible destabilizations associated to fluctuations in the ammonium loading. After the nitrification stage, denitrification took place by mixing anoxically the reactor's content together with the addition of the stoichiometric amount of acetic acid. During anoxic periods, $\text{NH}_4^+\text{-N}$ variation was so small that the experimental results hardly provided any ammonia concentration change.

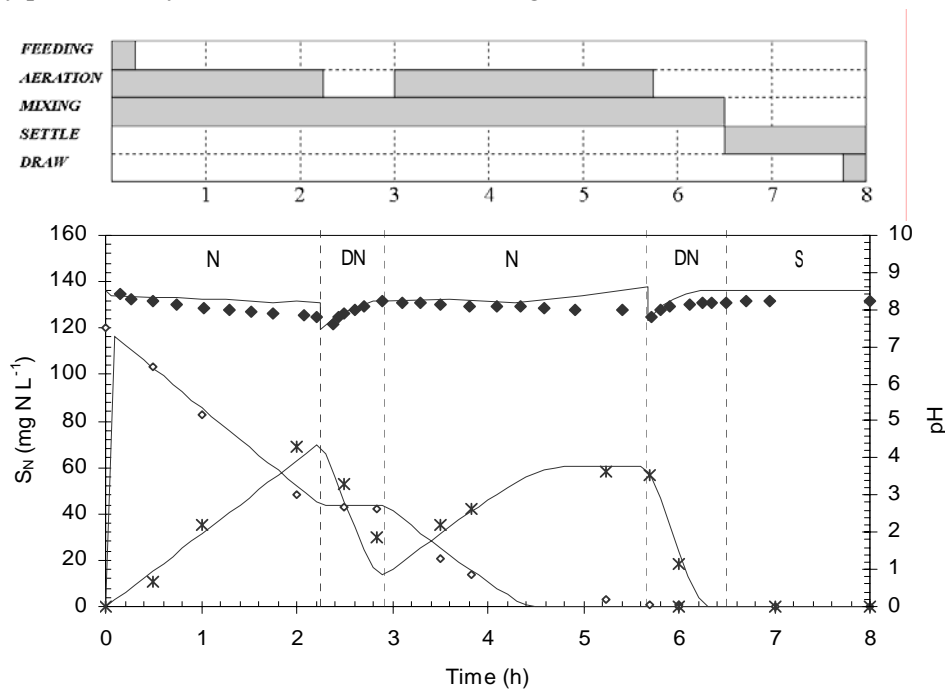


Figure 5.6 - Main parameters in a working cycle under steady state conditions.
 ($\text{NH}_4^+\text{-N}$ \diamond ; $\text{NO}_2^-\text{-N}$ *; pH \blacklozenge ; simulated data —; stage delimitation ---)

pH evolution was also well-predicted by the proposed model, although the simulated pH was slightly higher than the experimental pH profile, which is related to the simplifications used to describe the system. However, the shape of the modelled pH profile is very similar to the one obtained in the laboratory and it provides an interesting explanation of the processes that take place inside the reactor. Due to the appropriated alkalinity to nitrogen ratio of the wastewater tested and the intermediate denitrification

step, pH oscillated in a narrow range (7.6-8.4) very close to the optimum value (8.0). During nitrification, pH decreased since the biological oxidation of ammonium to nitrite consumes alkalinity. When ammonium was depleted in the second nitrification period, a rising of the pH level was observed which is also predicted by the model, because the stripping of an acid gas (H_2CO_3) led to a basification of the liquid medium. At the beginning of every anoxic period, pH decreased due to the addition of acetic acid but it was rapidly recovered because of the subsequent alkalinity production in the denitrification process. Finally, during the sedimentation period, pH did not vary, since neither nitrites nor nitrates were present in the media and the denitrifying biomass activity was stopped.

5.3. CONCLUSIONS

- ✓ The IWA Activated Sludge Model is enlarged to describe the nitrification/denitrification process over nitrite for the treatment of the supernatant from Anaerobic Digestion (AD) of the Organic Fraction of Municipal Solid Wastes (OFMSW). The main extensions of this model are to consider both nitrification and denitrification as two step reactions, to include the tools to calculate pH, to model the stripping of CO_2 and NH_3 , and to take into account the influence of pH, NH_3 and HNO_2 on the kinetics of biological processes.
- ✓ The respirometric procedure established in Chapter 4 is used to assess the main stoichiometric and kinetic parameters for model calibration. Moreover, a respirometric batch test to analyse the influence of pH on ammonium oxidizers is proposed.
- ✓ An optimum Sequencing Batch Reactor (SBR) operating cycle to treat the supernatant is modelled by means of the proposed model giving good agreement between experimental and simulated data. Free ammonia and low dissolved oxygen concentrations were identified as the operational factors responsible for the inhibition of Nitrite Oxidizing Biomass (NOB).

6. COD and Nitrogen removal of supernatant of anaerobically digested piggery wastewater in a biological SBR with a Coagulation/Flocculation step.

ABSTRACT

The supernatant from mesophilic anaerobic digestion of piggery wastewater is characterised by a high amount of COD (4.1 g COD L^{-1}), ammonium ($2.3 \text{ g NH}_4^+\text{-N L}^{-1}$) and suspended solids (2.5 g SS L^{-1}). This effluent can be efficiently treated by means of a Sequencing Batch Reactor (SBR) strategy for biological COD, SS and nitrogen removal including a Coagulation/Flocculation step. Total COD and SS reduction yields higher than 66 % and 74 %, respectively, and a total nitrogen removal (over nitrite) of more than 98% were reached when working with HRT 2.7 days, SRT 12 days, temperature 32°C , three aerobic/anoxic periods, without external control of pH and under limited aeration flow. The inhibition of nitrite oxidizing biomass was achieved by the working free ammonia concentration and the restricted air supply (dissolved oxygen concentration below $1 \text{ mg O}_2 \text{ L}^{-1}$). Since a part of the total COD was colloidal and/or refractory, a Coagulation/Flocculation step was implemented inside the SBR operating strategy to meet a suitable effluent quality to be discharged. Several Jar-tests demonstrated that the optimal concentration of FeCl_3 was 800 mg L^{-1} . A respirometric assay showed that this coagulant dosage did not affect the biological activity of nitrifying/denitrifying biomass.

The most relevant parts of this chapter are published in:

Dosta, J., Rovira, J., Galí, A., Macé, S., Mata-Álvarez, J. (2007) Integration of a coagulation/flocculation step in a Biological Sequencing Batch Reactor for COD and nitrogen removal of supernatant of anaerobically digested piggery wastewater. *Bioresource Technology*. (Accepted paper)

6.1 INTRODUCTION

Spain is the European Union's second-largest pig meat producer behind Germany with 3% of the world output and 16% of the EU production (Lence, 2005). According to the Catalanian government, the 28% of Spanish pig production takes place in Catalonia, where more than 10,000,000 m³ year⁻¹ of animal slurry (mainly pig slurry) are produced. Figure 6.1 shows the distribution of pig slurry produced in Europe and in Spain.

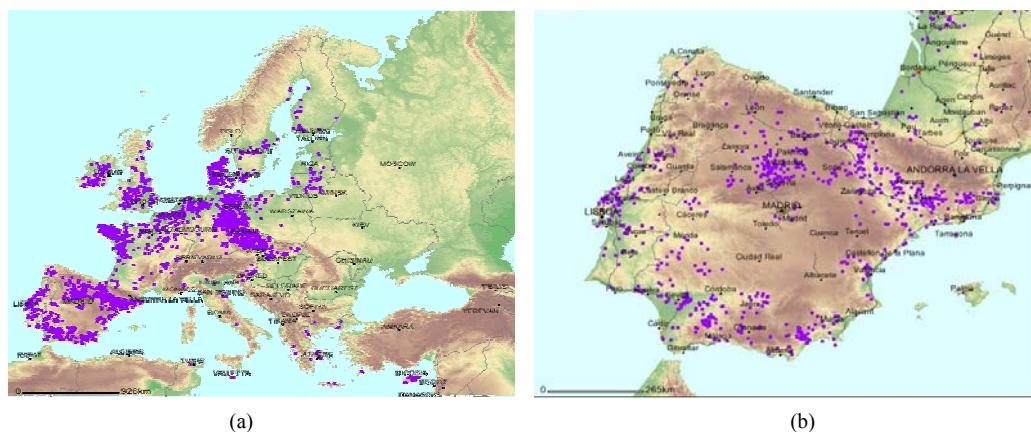


Figure 6.1 – Distribution of pig slurry production in the European Union (a) and Spain (b). (areas of pig slurry production ■).

Pork producers in the areas with the heaviest concentration of production facilities in Catalonia are forming cooperatives to take advantage of EU subsidies for alternative sources of energy, by building waste-disposal plants that transform slurry into electricity and fertilizer (Lence, 2005). Anaerobic digestion has been applied in a variety of forms and scales to stabilize the organic matter in piggery wastes. This process achieves an effective organic matter and pathogen reduction and generates biogas which is a useful fuel (Llabrés-Luengo and Mata-Álvarez, 1987; Chynoweth *et al.*, 1999; Flotats *et al.*, 2004). However, the effluent of anaerobic digestion of piggery waste is characterised by a high ammonia load that must be treated. As discussed in chapter 1, this effluent can be treated by physico-chemical (air stripping, steam stripping, MAP process), physical-biological (biofilm air-lift reactor, membrane bioreactor) and/or biological (SBR, SHARON chemostat) processes (Siegrist, 1996; Hans and Helle, 1997; Macé and Mata-Álvarez, 2002; van Loosdrecht and Salem, 2005). From an economical point of view, biological nitrogen removal over nitrite is preferred since its relative cost is highly reduced when compared with other alternatives (STOWA, 1996).

As stated in previous chapters, the biological nitrogen removal over nitrite provides two important benefits with respect to the conventional biological nitrogen removal (over nitrate): a saving of 25 % of oxygen consumption and 40% of organic carbon source in denitrification (Hellinga *et al.*, 1999). Several ways to achieve the nitrite route have been reported in literature. At temperatures over 20°C, the minimum Sludge Retention Time (SRT) of Ammonium Oxidizing Biomass (AOB) is lower than that for Nitrite Oxidizing Biomass (NOB). Therefore, the proliferation of AOB and the total wash-out of NOB can be achieved working in a narrow range of SRT between the minimum SRT for AOB and the minimum SRT for NOB at the working temperature, which is the basis of the continuous chemostat SHARON process (Hellinga *et al.*, 1999; Van Dongen *et al.*, 2001). Recently, the SHARON process has been successfully carried out to treat raw piggery wastewater (Hwang *et al.*, 2005). Another way to promote the nitrite route is working with free ammonia concentrations and/or free nitrous acid concentrations in the mixed liquor that are capable to inhibit NOB but do not affect the activity of AOB (Anthonisen *et al.*, 1976; Wett and Rauch, 2003). Moreover, if there is a low Dissolved Oxygen (DO) concentration inside the reactor (less than 1.5 mg L⁻¹), nitrate formation is restricted, since ammonia oxidation rate is favoured in front of nitrite oxidation kinetics. However, this last strategy alone is not enough to completely avoid the nitrate formation (Piciorneau *et al.*, 1997; Garrido *et al.*, 1997; Pollice *et al.*, 2002; Van Loosdrecht and Salem, 2006).

Supernatant from anaerobic digestion of piggery wastewater contains an important amount of colloidal organic matter which is difficult to oxidize biologically (Laridi *et al.*, 2005). With biological processes, high removal levels of the biodegradable fraction are achieved, but for refractory and/or very slowly biodegradable COD, other treatment strategies should be applied. Coagulation is known as a process that allows the aggregation of suspension particles present in the wastewater, in order to optimize the sedimentation or flotation step in which these particles have to be separated from water (Company, 2000). The coagulant agents more widely used are aluminium and iron salts. The addition of polyelectrolites or flocculant agents can enhance floc formation and, therefore, the separation process. The resulting pH decrease depends on the alkalinity of the wastewater tested and the coagulant dosage. pH has been identified as the most restrictive parameter in the coagulation step since it affects the hydrolysis equilibrium produced as a consequence of the coagulant agent addition (Poon and Chu, 1999).

The aim of this study is to evaluate the biological treatment of the supernatant of anaerobically digested piggery wastewater in an SBR to remove COD and nitrogen. Considering that an important fraction of the COD coming from an anaerobic digestion process is refractory, the insertion of a Coagulation/Flocculation step within the SBR operating strategy is also studied.

6.2 RESULTS AND DISCUSSION

6.2.1. Wastewater Characterisation

Liquid fraction of anaerobically digested piggery was obtained from an anaerobic mesophilic digestion treatment plant through the VALPUREN process (Flotats *et al.*, 2004) as described in section 1.5.3 . The main wastewater characteristics are shown in Table 6.1, where two periods are distinguished although the wastewater characteristics did not change extremely.

Table 6.1 – Composition of the piggery reject water tested in this study

Component	PERIOD 1		PERIOD 2		Units
	Average	Range	Average	Range	
Total COD	3.2	2.8– 3.7	4.1	3.9 – 4.7	g COD L ⁻¹
Centrifuged COD	-	-	3.4	3.2 – 3.8	g COD L ⁻¹
Soluble COD	-	-	2.9	2.7 – 3.2	g COD L ⁻¹
NH ₄ ⁺ -N	2200	2100 - 2290	2265	2110 – 2340	mg NH ₄ ⁺ -N L ⁻¹
NO ₂ ⁻ -N	7	5 - 9	< 3	0 - 6	mg NO ₂ ⁻ -N L ⁻¹
NO ₃ ⁻ -N	n.d.	-	n.d.	-	mg NO ₃ ⁻ -N L ⁻¹
pH	8.7	-	8.6	8.5 – 8.8	-
TS	14.6	14.3 – 14.9	8.3	8.0 – 8.7	g TS L ⁻¹
VTS	7.4	7.2– 7.6	4.0	3.9 – 4.1	g VTS L ⁻¹
SS	3.8	3.5 – 4.1	2.5	1.9 – 3.0	g SS L ⁻¹
VSS	2.9	2.9 – 3.0	1.8	1.4 – 2.2	g VSS L ⁻¹
Ratio Alkalinity/NH ₄ ⁺	2.2	2.0 -2.4	1.78	1.46 – 1.98	mol HCO ₃ ⁻ (mol N-NH ₄ ⁺) ⁻¹
BOD ₅ /N	0.27	-	0.21	0.19 - 0.27	mg BOD ₅ (mg N) ⁻¹
Temperature	37	-	37	-	°C

n.d. not detected

It is important to highlight the high ammonium load ($2.1\text{-}2.3 \text{ mg NH}_4^+\text{-N L}^{-1}$) and its large content of solids of the wastewater under study. The alkalinity to ammonium ratio on molar basis was in the range 1.46-2.20 (in Period 1, this ratio was slightly higher than in Period 2). Since a ratio of 2 is needed to buffer the complete nitrification reaction in a single step and considering that denitrification leads to a recovery of the half alkalinity consumed during the nitrification process, no restrictions linked to alkalinity requirements were expected.

In order to assess the biodegradability of the total COD present in the wastewater tested, a respirogram was performed (see Figure 1) as follows: 200 mL of wastewater were added to 2.80 L of endogenous biomass from the SBR withdrawals under controlled temperature (30°C) and pH conditions (8.0 ± 0.1). Centrifuged COD and $\text{NH}_4^+\text{-N}$ were analysed along the respirometric test. As observed in Figure 6.2, the BOD at short time (corresponding to the first initial peak of the respirogram) was not enough to be used in denitrification. Similarly to other supernatants of anaerobic digestion (Hellinga *et al.*, 1999; Graja and Wilderer, 2001), this wastewater had a very low $\text{BOD}_5/\text{NH}_4^+\text{-N}$ ratio, which implies the use of methanol as an external carbon source to denitrify.

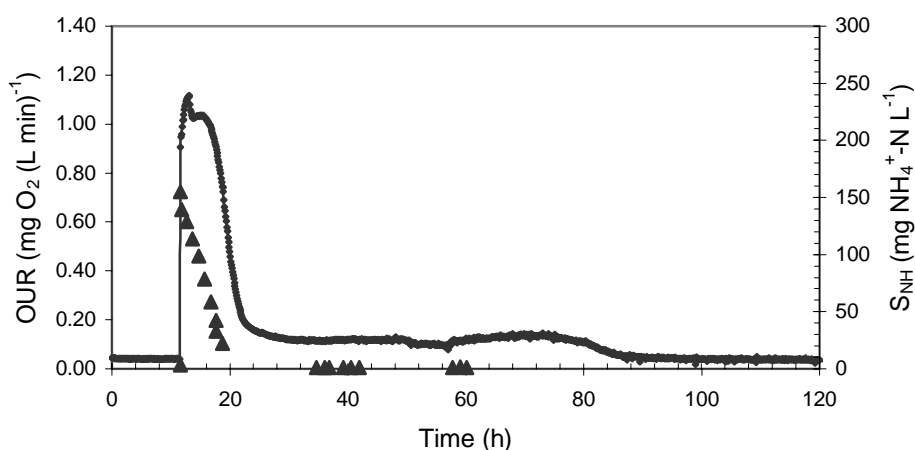


Figure 6.2. Representative respirogram obtained for the determination of BOD_{ST} of supernatant of anaerobically digested piggyery wastewater of Period 2. (OUR (\bullet) and $\text{NH}_4^+\text{-N}$ (\blacktriangle)).

6.2.2. Sequencing Batch Reactor operation

Considering the results obtained in Chapters 4 and 5, several parameters were set at a certain value: temperature was fixed at 32 °C, according to the temperature at which mesophilic anaerobic digestion of pig manure takes places (37 °C); the sludge retention time was set at 12 days (Bortone, 1992); the length of the cycle was established at 8 hours and the organic carbon source used to denitrify was methanol. To start-up the biological process, the SBR was seeded with nitrifying/denitrifying biomass from another SBR treating highly ammonium loaded wastewater (see Chapter 4).

Different cycles were carried out with the aim of achieving the maximum nitrogen removal over nitrite. In each cycle, 3 internal aerobic/anoxic periods were performed in order to maintain the pH within the optimum range. Each time one of the parameters of the cycle was changed, the reactor was operated during 1.5-2 months under steady-state conditions. In Table 6.2 it is summarized the main operating characteristics of the cycles performed (C-1 to C-5).

Table 6.2 - Summary of the main parameters obtained in the studied cycles

	C-1	C-2	C-3	C-4	C-5	Units
<i>Cycle Characteristics</i>						
Aerobic/Anoxic periods	3	3	3	3	3	-
1 filling at the beginning of the cycle	Yes	Yes	-	-	-	-
Filling at the beginning of each nitrification step	-	-	Yes	Yes	Yes	-
Aerobic/anoxic time ratio	1.8	1.8	1.8	1.8	1.8	-
External control of pH	No	No	No	No	No	-
<i>Operational data</i>						
HRT	6.6	3.2	3.7	2.7	2.7	days
Nitrogen removal efficiency	0.35	0.77	0.66	0.84	0.87	mg NH ₄ ⁺ -N (L day) ⁻¹
SRT	12	12	12	12	12	days
VSS	5.0	5.5	6.9	7.3	7.4	g VSS L ⁻¹
Minimum pH	8.0	8.2	8.0	8.0	7.4	-
Maximum pH	9.3	9.4	9.4	9.4	9.3	-
<i>Nitrogen removal</i>						
% NH ₄ ⁺ -N removal	>99	>99	97	99	>99	-
% NO _x -N removal	>99	>99	99	99	>98	-

The first four cycles were performed with the wastewater of Period 1. The last cycle strategy (C-5) was the same as strategy C-4, but using wastewater from Period 2. As observed, the main difference between the results obtained in C-4 and C-5 is located in the operating range of pH. Since the alkalinity to ammonium ratio in wastewater of Period 2 was lower than in Period 1, a minimum pH of 7.4 was obtained in C-5. However, the operating pH range oscillated between non-limiting values for nitrifying/denitrifying biomass without external addition of chemicals to control the pH.

According to the fill stage, it was seen that better results were obtained when the digested piggery wastewater was introduced at the beginning of each nitrification stage instead of those cases in which the same amount of wastewater was introduced only at the very beginning of the cycle. Since the wastewater tested had a relatively high pH (8.5-8.8) and at the end of denitrification high pH values were reached (9.3-9.4), it was preferred to split the quantity of wastewater fed to the SBR into 3 additions to avoid high $\text{NH}_4^+\text{-N}$ concentrations at basic pH that could inhibit AOB and would lead to a loss by stripping of NH_3 . Air supply was regulated to reach a DO concentration below $1.0 \text{ mg O}_2 \text{ L}^{-1}$ during aerobic periods to promote the nitrite route and to minimize the foaming effect and the stripping of NH_3 . The best SBR performance was obtained when working at HRT 2.7 days (C-5). pH remained within an optimal range of 7.4 - 9.3, without chemicals addition.

In Table 6.3, the distribution of the SBR sequence is detailed. Figure 6.3 shows the pH and DO profiles of 8 consecutive cycles working under steady state conditions.

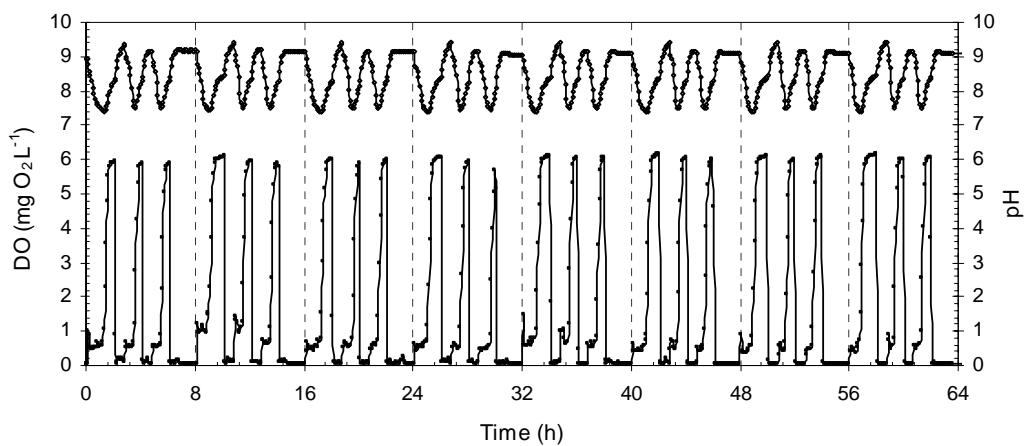


Figure 6.3 - pH and DO profiles during 12 consecutive optimized SBR operating cycles under stationary state conditions. (pH (—), DO (—)) and cycle delimitation (- - -).

Table 6.3- Main characteristics of the SBR operating strategy for the treatment of supernatant from Anaerobic digestion of piggery wastewater.

Parameter	Units	Value (Without Coagulation/Flocculation step)	Value (With Coagulation/Flocculation step)
Cycle Length	h	8	8
Time distribution			
Aerobic Feeding	min	3	3
Aerobic	min	117	117
Anoxic	min	45	45
Aerobic feeding	min	2	2
Aerobic	min	73	73
Anoxic	min	45	45
Aerobic feeding	min	2	2
Aerobic	min	73	73
Anoxic	min	65	45
Coagulation/Flocculation	min	-	20
Settle and draw	min	55	55
HRT	days	2.7	2.7
Total COD Removal	kg COD (m ³ day) ⁻¹	0.88	1.17
Total Nitrogen Removal	kg N (m ³ day) ⁻¹	0.87	0.87
SRT	days	12	12
SS	g SS L ⁻¹	8.5 – 9.6	9.7– 10.1
VSS	g VSS L ⁻¹	7.1 – 7.8	7.5 – 8.0
VSS/SS	-	0.8 - 0.84	0.78 – 0.79
Temperature	°C	32	32
Dissolved Oxygen	mg O ₂ L ⁻¹	< 1.0 mg O ₂ L ⁻¹	< 1.0 mg O ₂ L ⁻¹
pH range	-	7.4 – 9.3	7.1 – 9.3

Experimental profiles of NH₄⁺-N, NO₂⁻-N, NO₃⁻-N, Alkalinity, pH and DO during a representative SBR cycle are presented in Figure 6.4, where it is observed that three additions of wastewater were performed at the beginning of every aerobic period. Oxygen concentration was maintained between 0.8-1.0 mg O₂ L⁻¹ and pH was reduced during the oxidation of NH₄⁺ to NO₂⁻. When NH₄⁺ was depleted, a rising of DO was observed due to the diminution in oxygen uptake rate and an increase of pH was detected due to stripping of CO₂. In the subsequent anoxic periods, 2.5 mg COD-methanol (mg NO₂⁻-N formed)⁻¹ were added as electron acceptor to denitrify based on Galí *et al.* (2005) results. A rising of pH and, therefore, a recovering of alkalinity was observed during the anoxic periods.

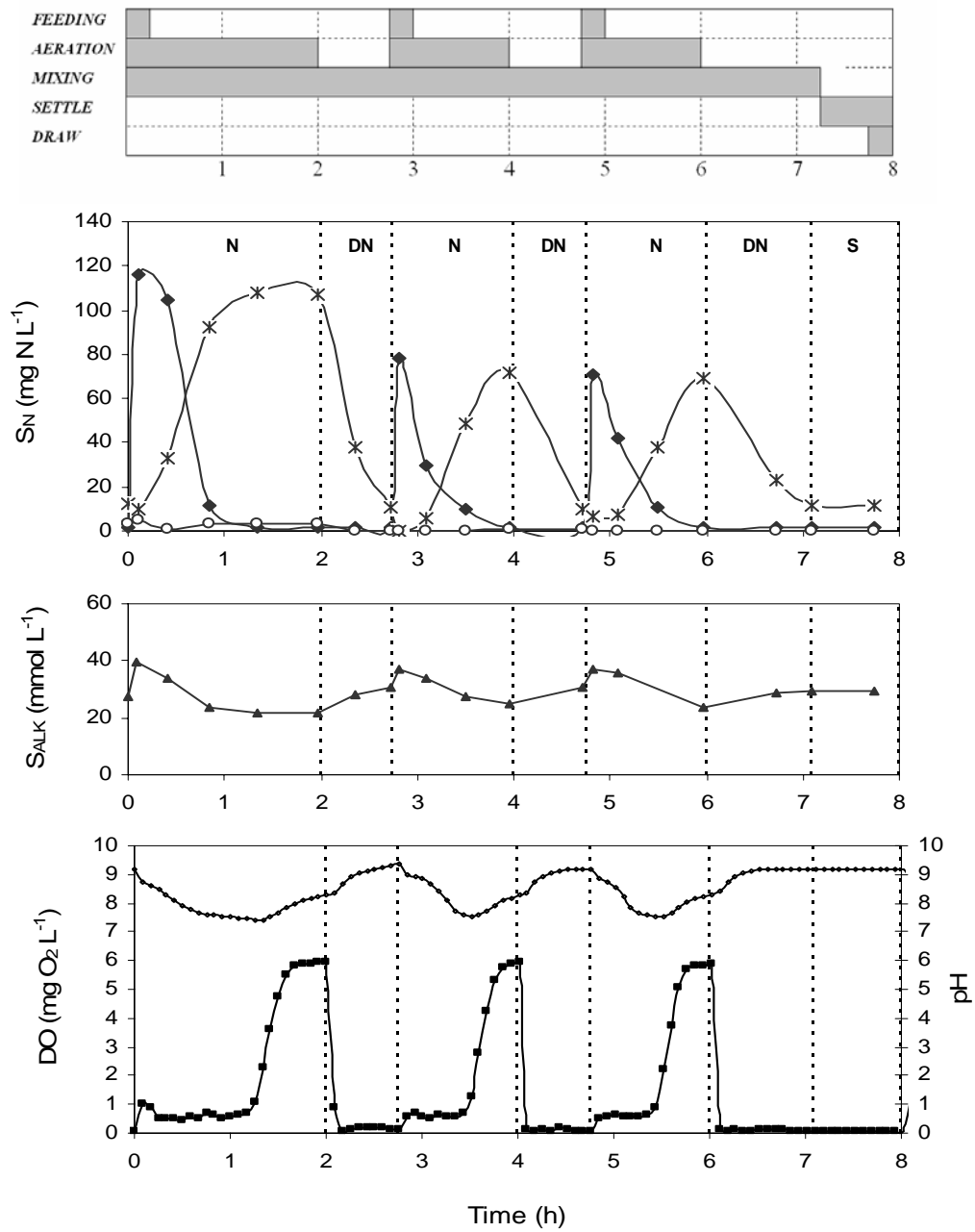


Figure 6.4 - Experimental concentrations inside the SBR. $\text{NH}_4^+\text{-N}$ (\blacklozenge), $\text{NO}_2^-\text{-N}$ (\times), $\text{NO}_3^-\text{-N}$ (\circ), Alkalinity (\blacktriangle), pH ($\circ\text{-}\circ\text{-}\circ$) and DO (\blacksquare).

6.2.3. Optimisation study of the Coagulation/Flocculation step

In the SBR treatment of supernatant of anaerobic digestion of piggery wastewater the biological reduction of COD was restricted (55-60%) since piggery wastewaters contain varied and high amounts of organic matter (proteins, antibiotic compounds, organic acids) which are difficult to oxidize biologically or chemically (Laridi *et al.*, 2005). A Coagulation/Flocculation step was studied in order to produce an effluent suitable for stream discharge.

The coagulation agent selected was FeCl_3 based on Macé *et al.* (2005c) results. Several Jar-Tests were carried out in which different FeCl_3 dosages (from 0 to 2500 mg L^{-1}) were added to the effluent of the SBR. Figure 6.5a shows the average COD reduction yields obtained in the experiments. When FeCl_3 was dosed, SS reduction yields were in the range of 8-15%, without a clearly marked dependency with the coagulant dosage. Due to the acidity of FeCl_3 , an important reduction in the effluent pH was observed (also shown in Figure 6.5a). A maximum COD reduction yield was detected when $1800 \text{ mg FeCl}_3 \text{ L}^{-1}$ were added. Figure 6.6 shows the coloration of the samples treated in the Jar tests. Here it is observed that when more than $1800 \text{ mg FeCl}_3 \text{ L}^{-1}$ are used, an excess of coagulant is introduced and the treated effluent acquires the characteristic coloration of FeCl_3 .

Considering that $1,500 \text{ mg COD L}^{-1}$ was the legal limit for discharge into the public sewer (Generalitat de Catalunya, 1992), $800 \text{ mg FeCl}_3 \text{ L}^{-1}$ was selected as the optimal coagulant dosage, since it provided an effluent with less than $1200 \text{ mg COD L}^{-1}$ and an effluent pH of approximately 6.5. For FeCl_3 concentrations above $1250 \text{ mg FeCl}_3 \text{ L}^{-1}$, harmful effluent pH values for biomass activity (<6.0) and a flotation of the flocculated solid material were observed. Therefore, the possibility of the Coagulation/Flocculation step using FeCl_3 doses higher than $1250 \text{ mg FeCl}_3 \text{ L}^{-1}$ inside the operational SBR cycle would be rejected, since it could lead to a wash-out of biomass.

Moreover, the use of a cationic flocculant was also tested to evaluate its effect in the increasing of volume, weight and cohesion of the floccules formed. A set of Jar-tests were carried out in which several doses of flocculant (from 0 to 60 mg L^{-1} , as recommended by the supplier) were added, but for this specific case a quantifiable improvement in the COD and SS reduction yields was not observed.

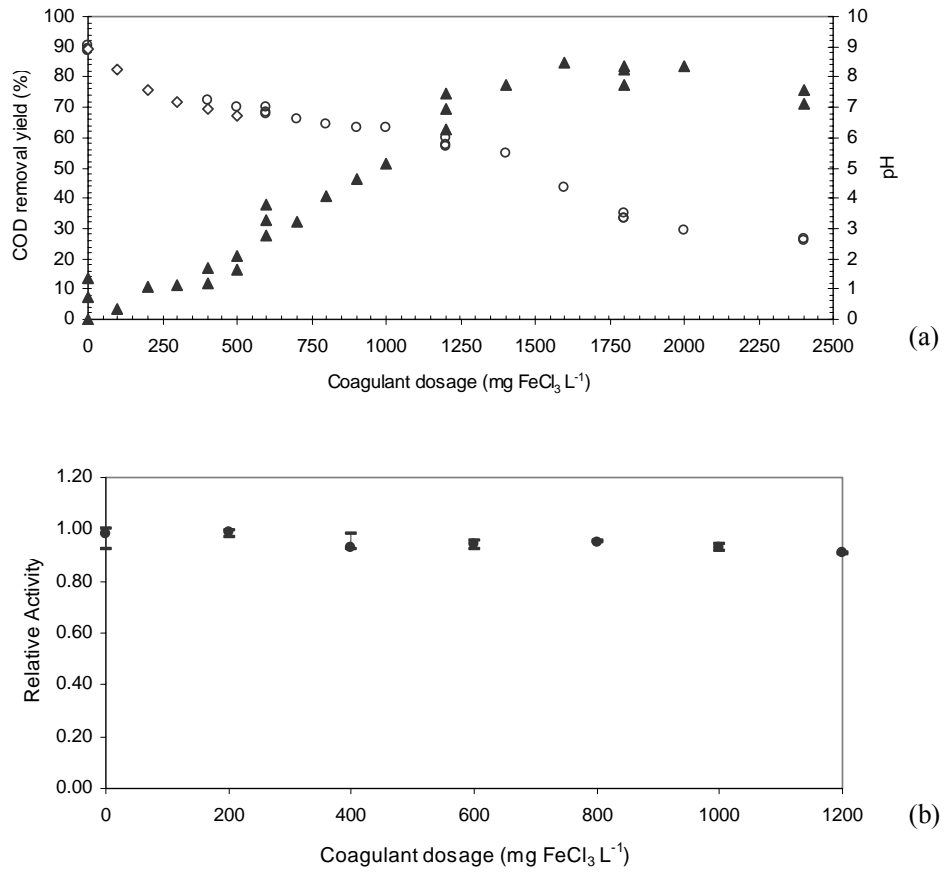


Figure 6.5 – COD removal yields (▲) and effluent pH (○) during the Jar-Test using several FeCl₃ doses (a) and relative activity of nitrifying biomass (◆) with several FeCl₃ doses (b).

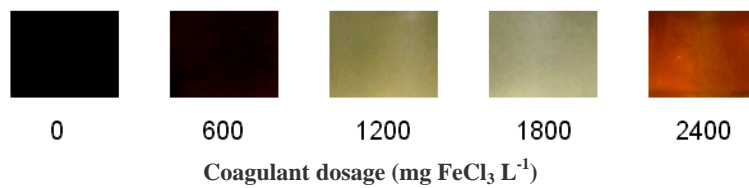


Figure 6.6 – Coloration of the treated effluents after coagulation/flocculation depending on the coagulant dosage used.

Before the insertion of the Coagulation/Flocculation step inside the operational SBR cycle, several respirometric tests were carried out to assess the effect of the selected FeCl_3 concentration on biomass activity at constant pH (8.0 ± 0.1). Biomass from the withdrawals of the SBR (approximately, $730 \text{ mg VSS L}^{-1}$) were introduced in the respirometer under non-limiting substrate ($\sim 140 \text{ mg NH}_4^+\text{-N L}^{-1}$) and DO ($>3 \text{ mg O}_2 \text{ L}^{-1}$) conditions. When the external Oxygen Uptake Rate (OUR_{EX}) was determined, consecutive dosages of FeCl_3 up to 1200 mg L^{-1} were injected without a quantifiable decrease in biomass activity (see Figure 6.5b). The Relative Activity of nitrifying biomass was obtained as the ratio between the OUR_{EX} in every case and the maximum OUR_{EX} of the whole respirometric test.

Considering all the aforementioned results, the use of $800 \text{ mg FeCl}_3 \text{ L}^{-1}$ was selected as the best dosage to obtain an effluent with suitable quality to be discharged.

6.2.4. Introduction of the Coagulation/Flocculation step in the SBR cycle

The insertion of a Coagulation/Flocculation step inside the operational SBR cycle was implemented in the last anoxic period just before the settle and draw operation. A dosage of $800 \text{ mg FeCl}_3 \text{ L}^{-1}$ related to the added volume of wastewater per cycle was performed in this step. In Table 6.3, the most relevant operational parameters of this strategy are presented. As observed, the nitrogen removal efficiency was maintained, but the COD and the total SS removal efficiencies were increased. Moreover, the SS concentration in the mixed liquor was slightly increased by 10-14 % and the VSS/SS ratio was reduced due to the Coagulation/Flocculation of colloidal material.

Figure 6.7 shows the pH and DO profiles in 8 consecutive SBR operational cycles working under steady-state conditions. Figure 6.8 shows a detailed $\text{NH}_4^+\text{-N}$, $\text{NO}_2^-\text{-N}$, $\text{NO}_3^-\text{-N}$, Alkalinity, pH and DO profiles during one representative SBR cycle under these experimental conditions. The evolution of these parameters was similar to the obtained profiles without the addition of FeCl_3 . However, during the last 15 minutes of the third anoxic period pH decreased significantly due to the dosage of FeCl_3 . Therefore, the alkalinity values were reduced when compared with the previous strategy. The composition (on average basis) of the treated wastewater is presented in Table 6.4. As observed, the achieved effluent quality related to SS, COD and $\text{NH}_4^+\text{-N}$ was suitable for stream discharge into the public sewer.

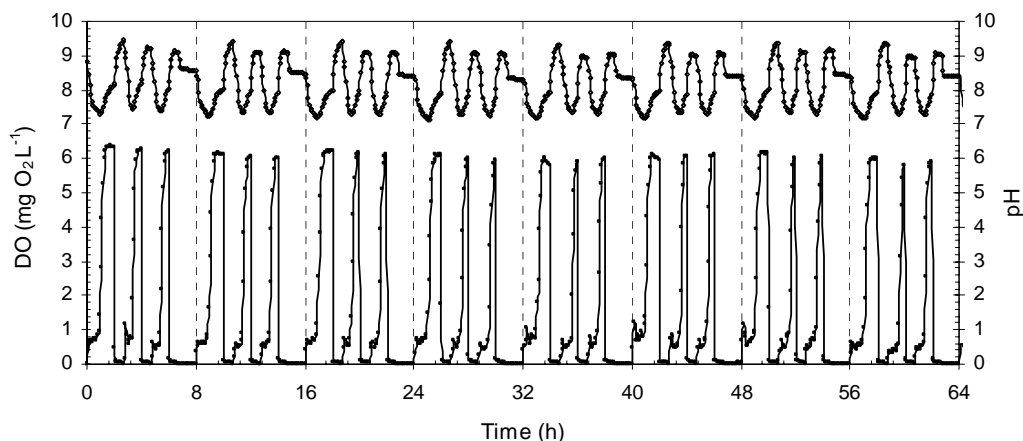


Figure 6.7 - pH and DO profiles during 8 consecutive optimized SBR operating cycles with a Coagulation/Flocculation step under stationary state conditions. (pH (●), DO (■) and cycle delimitation (- - -)).

Table 6.4 – Comparison of the effluent quality obtained with and without the Coagulation/Flocculation step inside the SBR operational cycle.

Component	Effluent SBR without Coagulation/Flocculation step	Effluent SBR with Coagulation/Flocculation step	Units
COD _{TOTAL}	1.92 – 2.05	1.27 – 1.48	g COD L ⁻¹
COD _{CENTRIFUGED}	1.68 – 1.82	0.94 – 1.10	g COD L ⁻¹
NH ₄ ⁺ -N	< 2	< 2	mg NH ₄ ⁺ -N L ⁻¹
NO ₂ ⁻ -N	< 15	< 15	mg NO ₂ ⁻ -N L ⁻¹
NO ₃ ⁻ -N	n.d.	n.d.	mg NO ₃ ⁻ -N L ⁻¹
pH	8.9 – 9.1	8.2 – 8.5	-
Alkalinity	26.8 – 29.3	18.0 – 20.4	mmol L ⁻¹
TS	5.3 – 5.6	5.7 – 6.4	g TS L ⁻¹
VTS	2.3 – 3.0	2.1 – 2.9	g VTS L ⁻¹
SS	0.45 – 0.65	0.41 – 0.60	g SS L ⁻¹
VSS	0.31 – 0.42	0.25 – 0.37	g VSS L ⁻¹

n.d. not detected

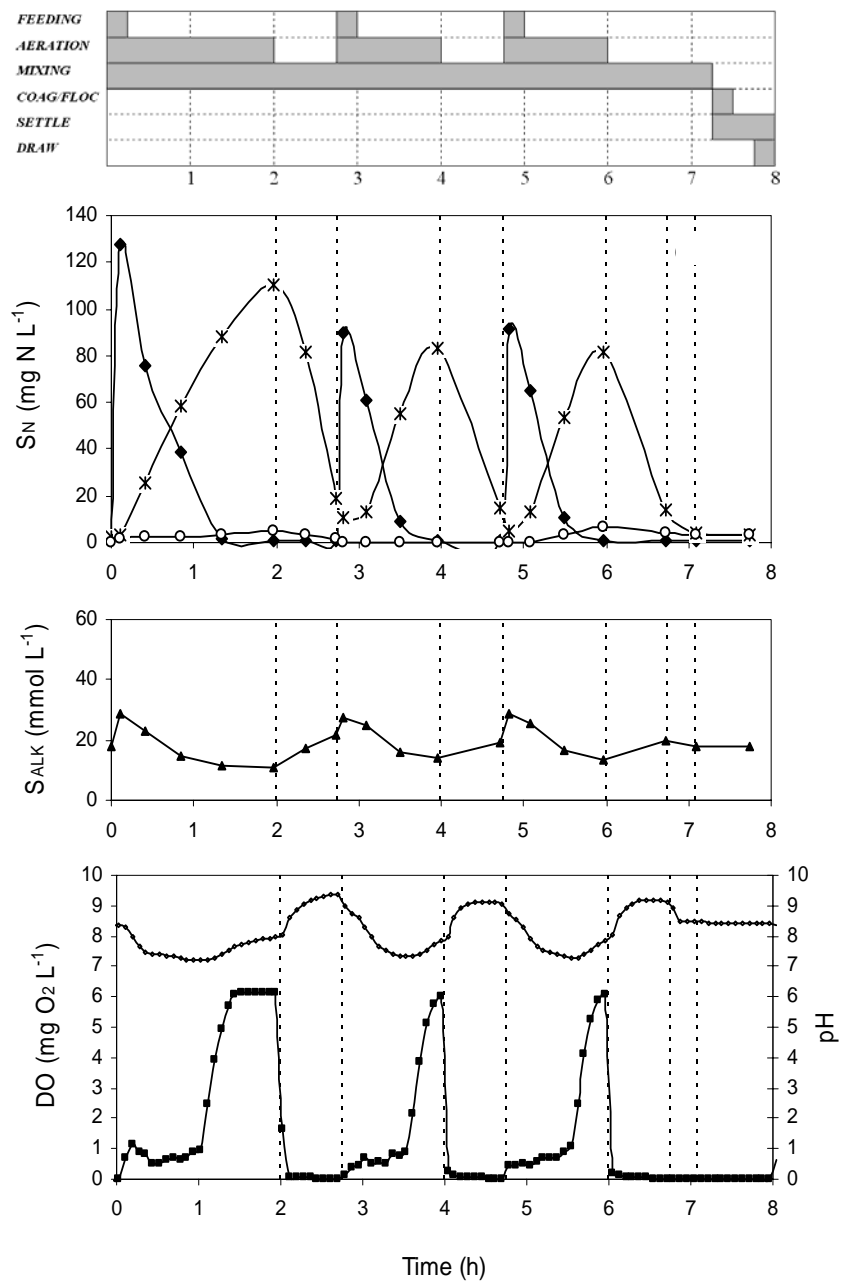


Figure 6.8 - Experimental concentrations inside the SBR with a Coagulation/Flocculation step. $\text{NH}_4^+\text{-N}$ (\blacklozenge), $\text{NO}_2^-\text{-N}$ (\times), $\text{NO}_3^-\text{-N}$ (\circ), Alkalinity (\blacktriangle), pH ($\circ\text{-}\circ\text{-}\circ$) and DO (\blacksquare).

6.2.5. Influence of experimental conditions of the SBR on Nitrogen removal

In order to provide a mathematical explanation of the inhibitions that could occur inside the SBR operating strategy, the influence of several parameters in the biological nitrogen removal process was studied.

Methanol and ammonia concentration as substrate. Figure 6.9 shows the plot of Oxygen consumed related to the substrate concentration (methanol or ammonia) removed. These stoichiometric coefficients were determined as explained in section 4.2.5.1. As observed, the actual yield coefficients ($Y_H = 0.61 \text{ mg cell COD (mg COD consumed)}^{-1}$; $Y_{AOB} = 0.20 \text{ mg cell COD (mg NH}_4^+\text{-N consumed)}^{-1}$) were similar to those obtained in Chapter 4 and 5 for nitrifying/denitrifying biomass for the treatment of sludge reject water of a municipal WWTP and supernatant from AD of the OFMSW.

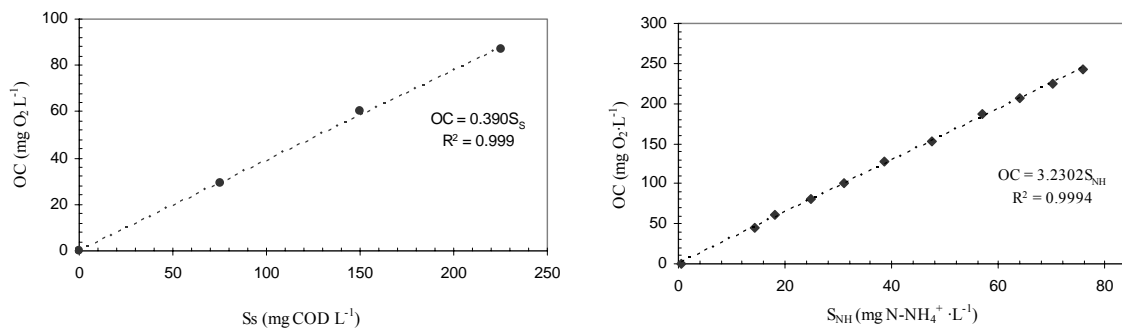


Figure 6.9 - Experimental assessment of Y_H and Y_{AOB} for nitrifying/denitrifying biomass from an SBR treating anaerobically digested piggery wastewater.

Half-saturation constant for methanol (K_S) was determined by applying the method described by Cech *et al.* (1984). Results of this experiment are shown in Figure 6.10. The K_S value of $10.2 \text{ mg COD L}^{-1}$ obtained in this work is similar to the one proposed in the IWA models (Henze *et al.*, 2000). Since NH_3 instead of NH_4^+ is the actual substrate for nitrifying biomass, two respirometric tests were run at two different controlled pH values (7.5 and 8.0) and without oxygen limitations, in which $125 \text{ mg NH}_4^+\text{-N L}^{-1}$ were added to an endogenous biomass coming from the withdrawals of the SBR. During the experiments, an intensive analysis of $\text{NH}_4^+\text{-N}$ and OUR was performed. By adjusting a curve to the $\text{NH}_4^+\text{-N}$ profile and considering the ammonia acid-base equilibrium proposed in Chapter 5 (Anthonisen *et al.*, 1976), the dependency of the biomass relative activity

with free ammonia concentration was evaluated (see Figure 6.10). The obtained value for K_{NH_3} was $0.45 \text{ mg NH}_3\text{-N L}^{-1}$, which is in accordance with the $0.47 \text{ mg NH}_3\text{-N L}^{-1}$ reported by Hellinga *et al.* (1999), the $0.75 \text{ mg NH}_3\text{-N L}^{-1}$ obtained by Van Hulle *et al.* (2004) for SHARON nitrifying biomass and the 0.32 found by Hunik *et al.* (1992) for a pure culture of *Nitrosomonas europaea*.

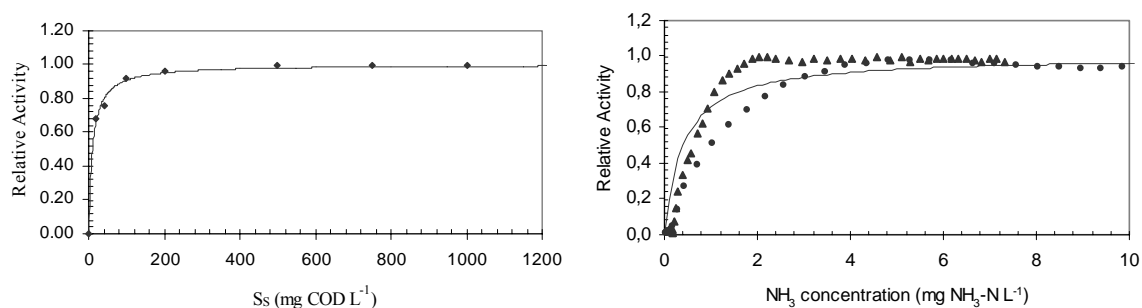


Figure 6.10 - Experimental assessment of K_S (0.998) and K_{NH_3} ($R^2 = 0.949$) for nitrifying/denitrifying biomass from an SBR treating anaerobically digested piggery wastewater with a coagulation/flocculation step.

Dissolved Oxygen concentration. Oxygen affinity constants (K_{OH} and $K_{\text{O,AOB}}$) were assessed by triplicate through a batch test in which the DO drop was monitored in a respiration cell without aeration after the injection of substrate. The plot of the time derivative of the DO concentration versus the concentration itself yields a Monod curve expressing oxygen limitation of the biomass activity (Van Hulle *et al.*, 2004). Both oxygen affinity constants (see Figure 6.11) were very reduced (namely, $K_{\text{OH}} = 0.24 \text{ mg O}_2 \text{ L}^{-1}$ and $K_{\text{O,AOB}} = 0.15 \text{ mg O}_2 \text{ L}^{-1}$), probably due to the restricted air supply inside the SBR.

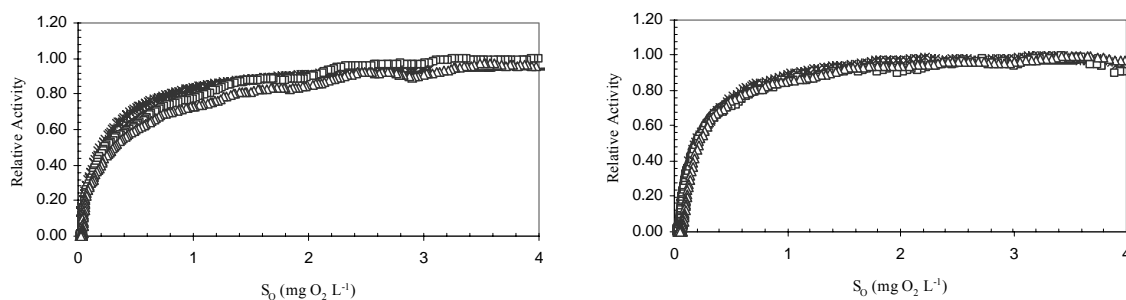


Figure 6.11 - Experimental assessment of K_{OH} ($R^2 = 0.9905$) and $K_{\text{O,AOB}}$ ($R^2 = 0.9811$) for nitrifying/denitrifying biomass from an SBR treating anaerobically digested piggery wastewater with a coagulation/flocculation step.

Inhibition by high free ammonia concentrations. Three respirometric batch tests under controlled temperature (32°C) but at different working pH (two at pH 8.0 and one at pH 8.5) were carried out to determine the inhibition at short term of nitrifying biomass related to free ammonia concentrations. The strategy reported by Van Hulle *et al.* (2004) was applied, obtaining the results presented in Figure 6.12. In this experiment it is clear that the actual inhibitor of AOB is NH_3 , since in Figure 6.12(a) it is represented the relative Activity in front of total ammonium nitrogen ($\text{NH}_4^+ + \text{NH}_3$) concentration and in Figure 6.12(b) in front of free ammonia (NH_3) concentration. As observed, a decrease in biomass activity was detected for NH_3 concentrations above 50 $\text{mg NH}_3\text{-N L}^{-1}$.

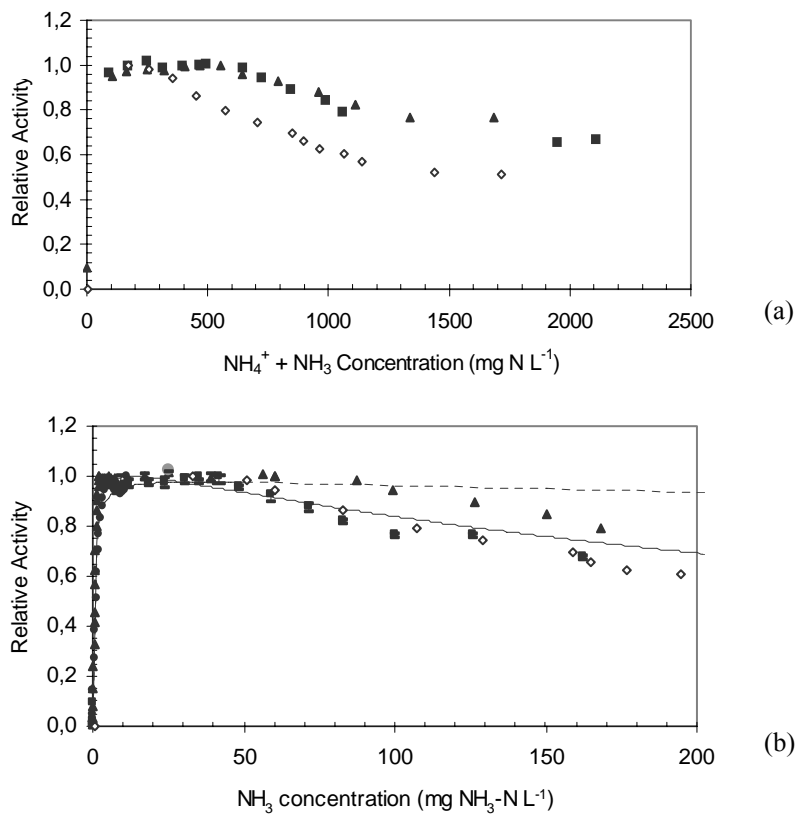


Figure 6.12 - Respirometric analysis for the assessment of the inhibition by total ammonium nitrogen ($\text{NH}_4\text{-N}+\text{NH}_3\text{-N}$) and NH_3 on AOB. Experimental data at pH 8.0 (\blacktriangle , \blacksquare); Experimental data at pH 8.5 (\diamond) and simulated data using the calibrated model of this study (—) and using the model of Chapters 4 and 5 from literature (---).

The results obtained are consistent with the observations of Chung *et al.* (2005) who reported that the activity of ammonium oxidizers was not negatively influenced for free ammonia concentrations up to 50 mg NH₃-N L⁻¹. However, the observed value in this work is higher than the 10 mg NH₃-N L⁻¹ reported by Groeneweg *et al.* (1994) for nitrosomonas but is lower than the 93 and 300 mg NH₃-N L⁻¹ reported by Hellinga *et al.* (1999) and van Hulle *et al.* (2004), respectively, for suspended biomass of a SHARON process. Kim *et al.* (2005) recorded a total inhibition of AOB activity for free ammonia concentrations above 78 mg NH₃-N L⁻¹, but the suspended biomass analysed in this work was more resistant to free ammonia concentrations. The NH₃ dependency on AOB was modelled by non-competitive inhibition kinetics as reported by Wett and Rauch (2003). As observed in Equation 6.1, the NH₃ dependency equation was divided for the maximum value of this equation which corresponds to the optimum NH₃ concentration (S_{NH₃,OPT}). The value of K_{NH₃}^{AOB} that minimized the sum of squared errors was 369 mg NH₃-N L⁻¹ (R² = 0.852). The simulation of free ammonia inhibition using the assumed value in the simulations of Chapters 4 and 5 is compared in Figure 6.12 with the simulation of the experimental data of this study. As observed, both simulations were similar in the operating range of NH₃-N of this work.

$$\frac{\mu_{AOB}}{\mu_{m,AOB}} = \frac{\frac{S_{NH_3}}{K_{NH_3} + S_{NH_3}} \frac{K_{NH_3}^{AOB}}{K_{NH_3}^{AOB} + S_{NH_3}}}{\frac{S_{NH_3,OPT}}{K_{NH_3} + S_{NH_3,OPT}} \frac{K_{NH_3}^{AOB}}{K_{NH_3}^{AOB} + S_{NH_3,OPT}}} \quad (6.1)$$

Inhibition by high free nitrous acid concentrations. Similarly to the NH₃ inhibition test, four respirometric batch tests (at pH 7.0 and 7.5, temperature 32°C) were carried out to evaluate the inhibition of AOB related to nitrous acid concentrations. Figure 6.13 shows the results obtained. As observed, when total nitrite concentrations (Figure 6.13a) are converted to nitrous acid concentrations (Figure 6.13b), it is clear that the inhibition of AOB is related to HNO₂ and independent of the working pH value.

The shape of the inhibition is very similar to the proposed dependencies of Van Hulle *et al.* (2004). However, the biomass analysed in this work is more sensitive to HNO₂ concentrations than the SHARON biomass investigated by Van Hulle *et al.* (2004). This fact can be probably caused by the operational conditions of the different

microorganisms: the SHARON biomass analysed by Van Hulle *et al.* (2004) worked with total nitrite concentrations in the range of 750 mg NO₂⁻-N L⁻¹ at a pH below 7.0 (35 °C) while the biomass analysed in this work worked with a maximum total nitrite concentration of 110 mg NO₂⁻-N L⁻¹ at pH between 7.1-9.3 (32 °C). The inhibition by HNO₂ was modelled by non-competitive Monod kinetics (see Figure 6.13) as described by Wett and Rauch (2003). A value of K_{HNO₂}^{AOB} of 0.17 mg HNO₂-N L⁻¹ yielded the minimum sum of squared errors (R² = 0.948). This value confirms that in the system under study, autotrophic biomass was hardly inhibited by HNO₂ concentrations (in the most unfavourable case, autotrophic biomass had the 91% of the maximum activity due to HNO₂ concentrations).

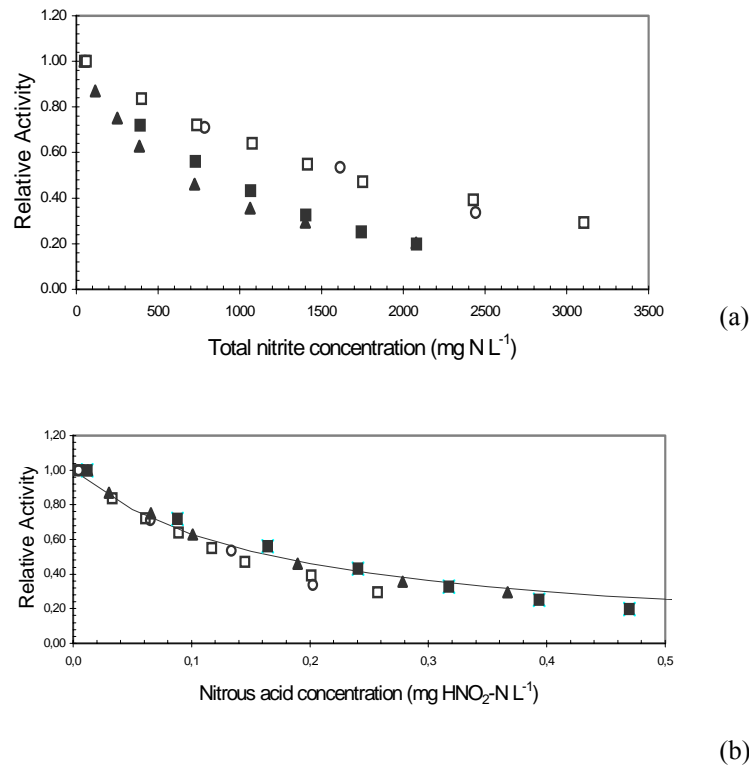


Figure 6.13. Respirometric analysis for the assessment of the inhibition by total nitrite concentration and HNO₂ on AOB. Experimental data at pH 7.0 (▲, ■); Experimental data at pH 7.5 (○, □) and simulated data (—)

Operational pH range. Heterotrophic and autotrophic growth rates have been reported to be very dependant on the pH (Orhon and Artan, 1994). In chapter 4 (section 4.2.5.3), it is

demonstrated that pH influence on nitrifying organisms is more important than for heterotrophic biomass.

In this Chapter, the autotrophic biomass inhibition for pH was determined at 32 °C as follows: 200 mg $\text{NH}_4^+\text{-N L}^{-1}$ were added to the aeration chamber of the respirometer with endogenous biomass. pH was regulated at 9.2 since it was the maximum pH value obtained in the whole SBR operating cycle. Subsequently, pH control was suppressed and pH decreased due to the nitrification process with the consequent reduction of nitrifying activity. Since $\text{NH}_4^+\text{-N}$ oscillated between non-limiting concentrations during the whole experiment, the exogenous OUR was proportional to the maximum specific autotrophic growth rate at the actual pH. The maximum OUR (OUR_{MAX}) encountered was related to the optimum pH value. Therefore, pH dependency (F_{pH}) can be calculated by plotting $\text{OUR}/\text{OUR}_{\text{MAX}}$ versus pH. Figure 6.14 shows the results obtained for three tests and the modelling of this dependency by means of a combination of Monod kinetics and non-competitive inhibition for H^+ concentration (Equation 4.49), minimizing the sum of squared errors ($\text{pH}_{\text{OPT}} = 8.15$; $-\text{Log}(K_{\text{H}}) = 7.44$; $R^2 = 0.987$).

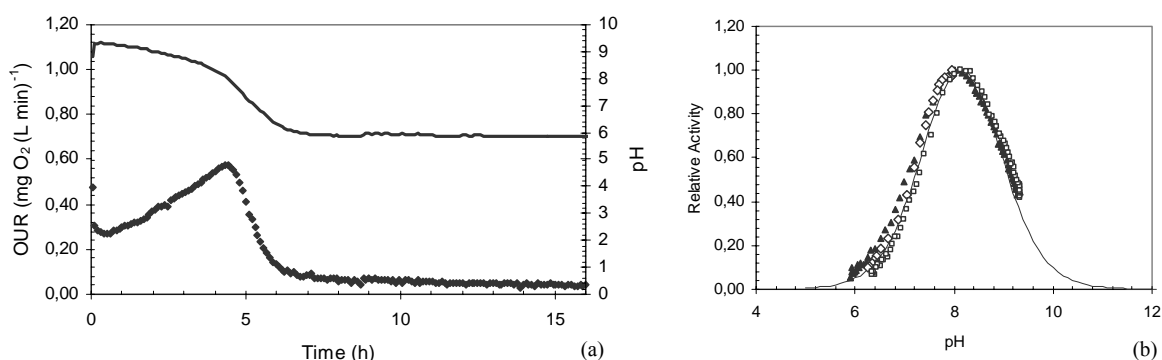


Figure 6.14 - Respirogram obtained for the evaluation of pH influence in nitrification kinetics (a) and experimental relative activity of AOB versus pH. (Figure a: OUR (♦) and pH(—) ; Figure b: Experiment 1 (▲), Experiment 2 (◇), Experiment 3 (□) and simulated data (—)

Effect of operating parameters during the SBR cycle. Since the effect of NH_3 as substrate and inhibitor, HNO_2 , DO and pH has been analysed in respirometric batch tests, the analysis of the operating SBR cycle can be performed in a more detailed way.

As observed in Figure 6.8, during the operating SBR cycle to treat supernatant from AD of piggery wastewater, the highest free ammonia concentration is reached at the beginning of the first aerobic period, where a total ammonium concentration of 125 mg $\text{NH}_4^+\text{-N L}^{-1}$ at pH=8.7 is achieved. These conditions lead to a free ammonia concentration of 27.2 mg $\text{NH}_3\text{-N L}^{-1}$, which reduces NOB activity (according to Wett and Rauch (2003), these conditions lead to 34.4% of NOB maximum activity) but it do not highly affect AOB activity (92% of AOB maximum activity, based on the results obtained in this chapter).

On the other hand, the maximum $\text{HNO}_2\text{-N}$ concentration is reached at the end of the first aerobic period (110 mg $\text{NO}_2^-\text{-N L}^{-1}$ at pH=7.1). These unfavourable conditions correspond to a concentration of 0.016 mg $\text{HNO}_2\text{-N L}^{-1}$. Although nitrifying biomass is very sensible to HNO_2 concentrations (see Figure 6.13), the highest HNO_2 concentration reached during the whole cycle does not generate an important inhibition to AOB (only 9% of inhibition). According to Wett and Rauch, NOB biomass is also not affected by this HNO_2 concentration. However, it is important to perform intermediate denitrification periods, not only to recover par of the alkalinity consumed during nitrification but also to prevent $\text{NO}_2^-\text{-N}$ accumulation that could lead to the inhibition of nitrifying biomass.

The operating pH range (7.1-9.3) does not affect in a very considerable way the activity of both AOB and NOB, since it is the optimum range for the development of nitrifying biomass (see Figures 1.8 and 6.14).

The operating SRT (12 days) does not represent a limitation for the development of NOB biomass as stated in Figure 1.4. However, at the working temperature (32 °C) the maximum specific growth rate of AOB is slightly higher than the one of NOB, which could also contribute to the low activity of NOB. The difficulties related to the experimental assessment of the specific maximum growth rates ($\mu_{m,\text{AOB}}$ and $\mu_{m,\text{NOB}}$) instead of the combined parameters $\mu_{m,\text{AOB}}X_{\text{AOB}}$ and $\mu_{m,\text{NOB}}X_{\text{NOB}}$, represents a limitation in order to quantify the contribution of temperature to the inhibition of nitrite oxidation.

Finally, considering the DO concentration inside the digester (0.75 mg $\text{O}_2 \text{L}^{-1}$), the effect of oxygen was a key parameter in the inhibition of nitrite oxidation kinetics. AOB activity at the lowest DO concentration was the 83.3% of the maximum AOB activity. On the

other hand, NOB activity was reduced to the 57% of its maximum activity. Therefore, the implemented air supply contributes to the restriction of nitrite oxidation.

Attending at the aforementioned considerations, NH_3 and dissolved oxygen concentrations are clearly identified as the main factors that lead to the biological nitrogen removal over nitrite.

6.3 CONCLUSIONS

- ✓ The biological treatment of the supernatant of anaerobically digested piggery wastewater in a sequencing batch reactor with a Coagulation/Flocculation step inside the operational cycle has been proved to be an efficient alternative to remove COD, SS and NH_4^+ -N.
- ✓ The SBR sequence consisted on three alternating aerobic/anoxic periods under controlled air supply to promote the biological nitrogen removal over nitrite. Several Jar-Tests showed that a dosage of 800 mg FeCl_3 was necessary to meet the effluent standards established by the legislation. Moreover, respirometric tests demonstrated that nitrifying biomass activity was not negatively affected by this coagulant dosage. The Coagulation/Flocculation step was inserted into the operational SBR cycle during the last 15 minutes of the third anoxic period.
- ✓ The implementation of this treatment led to a COD reduction yield of more than 66%, a SS decrease above 74% and a biological NH_4^+ -N removal of more than 98%, obtaining a suitable effluent for stream discharge into the public sewer. The total suspended solids drained from the reactor were increased only by a 10-14 %.
- ✓ The effect on biomass activity of several substrates and inhibitors, such as NH_3 , HNO_2 , pH and DO, was analysed by respirometric batch tests. These experiments showed that the nitrifying biomass developed in the digester was very resistant to free ammonia concentrations up to 50 mg $\text{NH}_3\text{-N L}^{-1}$. However, free nitrous acid concentrations promoted an important decrease of ammonium oxidizers activity. An optimum pH value of 8.15 was encountered for this biomass, which had a very low oxygen affinity constant.

- ✓ Considering the observed effect of the operational parameters in respirometric batch tests, it was clear that the operating NH_3 concentration was the most important inhibitor to nitrite oxidation. Moreover, the DO concentration also played a considerable role in the inhibition of NOB

7. Operation of the SHARON-Denitrification process to treat sludge reject water using hydrolysed primary sludge to denitrify.

ABSTRACT

Another efficient biological treatment to treat reject water from anaerobic digestion of sewage sludge is the SHARON-Denitrification process, which takes place in a chemostat reactor where aerobic/anoxic periods are alternated under specific HRT and temperature conditions that favours ammonium oxidizers growth and assures the total wash-out of nitrite oxidizers, achieving the biological nitrogen removal over nitrite.

An optimized performance of this process to treat Spanish reject water was obtained using methanol and working at HRT 2 days, 33°C and cycle length 2 hours. Supernatant of hydrolysed primary sludge was tested to denitrify. Since BOD was not extremely high in the primary sludge, the fluid dynamics of the system were changed with respect to the strategy with methanol but maintaining the reject water influent flow-rate. The use of hydrolysed primary sludge improved the process efficiency since the alkalinity present in the primary sludge buffered the process until an optimum pH range.

The most relevant parts of this chapter are published in:

Dosta, J., Galí, A., Benabdallah El-Hadj, T., Mata-Álvarez, J. (2007) Operation of the SHARON-Denitrification process to treat sludge reject water using hydrolysed primary sludge to denitrify. *Water Environment Research*. (Accepted paper).

7.1 INTRODUCTION

As explained in Chapter 1, an efficient biological process to treat reject water is the patented SHARON (Single reactor High activity Ammonia Removal Over Nitrite) process combined with denitrification (Hellinga *et al.*, 1999; Van Loosdrecht and Salem, 2005), which is a continuous process where BNR is performed over nitrite. The SHARON process is based on the fact that, at temperatures above 20°C, nitrite oxidizers have a distinctly lower growth rate than ammonium oxidizers (Brouwer *et al.*, 1996; Hellinga *et al.*, 1999). Therefore, if a short residence time and a high working temperature (usually 35°C) are carefully selected, the total wash-out of Nitrite Oxidizing Biomass (NOB) is feasible. In the SHARON-Denitrification process, intermittent aeration is imposed, and both denitrification and concomitant pH control are possible (Mulder and van Kempen, 1997; Verstraete and Philips, 1998; Mulder *et al.*, 2001). However, since the reject water of AD of sewage sludge is characterised by an unfavourable BOD/NH₄⁺-N ratio, an organic carbon source must be added during the anoxic periods to denitrify.

Many organic compounds, including carbohydrates, alcohols, organic acids and amino acids can serve as effective carbon sources for heterotrophic denitrifying organisms. Methanol, ethanol, acetate and/or glucose are often employed for denitrification, since these chemicals are available at a relatively low cost (Orhon and Artan, 1994; Constantin and Fick, 1997). For an environmental point of view, the use of alternative carbon sources coming from internal flows from the same WWTP is recommended. Several studies focused in the use of organic carbon sources from residual wastes or wastewaters have been developed: Aesoy and Odegaard (1994) reported that biologically hydrolysed sludge (Volatile Fatty Acids (VFA) constituted 66% of the soluble COD) could be used as carbon source to denitrify in a rotating biofilm contactor. Canziani *et al.* (1995) studied the feasibility of using hydrolysed primary sludge under mesophilic conditions (SRT 1 day) from a WWTP for biological nitrogen (and/or phosphorous) removal, concluding that the addition of this stream could lead to an increase of the denitrification efficiency by 4-10% with respect to the influent total nitrogen. Barlindhaug and Odegaard (1996) investigated the quality of thermally treated hydrolysed sludge as carbon source for denitrification. Subsequently Aesoy *et al.* (1998) tested thermally treated hydrolysed sludge (180 °C, 30 min) as organic carbon source to denitrify synthetic wastewater in a packed bed reactor, obtaining a denitrification efficiency similar to the one registered

when using ethanol. Aravinthan *et al.* (2001) tested several pre-treatments (namely, alkaline, acid, autoclaved, alkaline autoclaved and acid autoclaved solubilization methods) to hydrolyze excess sludge from a sequencing fluidized bed bioreactor treating synthetic wastewater, in order to increase its biodegradability and use it in denitrification processes. These authors encountered that autoclaved alkaline sludge hydrolysate gave the fastest denitrification rate. Elefsiniotis *et al.* (2004) reported good denitrification efficiencies when using the VFAs naturally generated in a lab-scale acid-phase anaerobic digester (treating a 1:1 mixture of start-rich industrial and municipal wastewater) as an organic carbon source to denitrify. Finally, Galí *et al.* (2006a) reported good denitrification efficiencies when hydrolysed primary sludge was used as the carbon source to denitrify in a sequencing batch reactor (SBR) treating sludge reject water for biological nitrogen removal over nitrite.

Some studies of the SHARON-Denitrification process at lab-scale conditions have been carried out in the last years. Among many others, Hellinga *et al.* (1998) reported that an average ammonium conversion in the range of 80-85% were obtained in a SHARON-Denitrification process with the following operational conditions: temperature 35 °C, HRT 1.5 days, cycles of 2 hours (80 min aerobic and 40 min anoxic) and 60% of the total denitrification (1 g methanol g⁻¹ converted NH₄⁺-N). Fux *et al.* (2003) reported removal rates of nitrification and denitrification of 0.3 kg NH₄⁺-N m⁻³ day⁻¹ and 0.55 kg NO₂⁻-N m⁻³ day⁻¹, respectively, for the treatment of reject water when working at 28.9 °C, total HRT about 4 days, 2.7 mg O₂ L⁻¹, 0.885 mg MLSS L⁻¹, cycle length 2 hours (50% aerobic and 50% anoxic) and using methanol to denitrify. Galí *et al.* (2006b) reported a total nitrogen removal above 95% in the treatment of 0.4 kg N (m³ day)⁻¹ when working with a SHARON-Denitrification process at 33°C, HRT 2 days (50% aerobic and 50% anoxic), using methanol to denitrify and without external control of pH.

This process have also been scaled up to full-scale conditions in the Utrecht WWTP (900 kg TKN day⁻¹) and the Rotterdam Dokhaven WWTP (850 kg TKN day⁻¹) where nitrogen removal efficiencies of more than 90% were achieved when working with a total retention time of 1.5 days, aerobic/anoxic periods of 2 hours (1.33h for partial nitrification and 0.67h for denitrification), temperature 35°C and using methanol to denitrify (Grontmij, 2004). The success of operations at Utrecht and Rotterdam led to the construction of other similar facilities like the Zwolle (410 kg TKN day⁻¹), the Beverwijk (1200 kg TKN day⁻¹) and the Groningen WWTPs. Moreover, a full-scale demonstration

facility of the SHARON process will be implemented in the Wards Island plant of New York City by 2007 (Grontmij, 2004).

The aim of this study is to test the possible use of an internal flow of the WWTP rich in readily biodegradable COD to denitrify in anoxic periods of the SHARON-Denitrification at lab-scale conditions. Moreover, the effluent quality obtained with a lab-scale SHARON-Denitrification process using methanol and using this internal flow to perform the denitrification steps is compared.

7.2 RESULTS AND DISCUSSION

7.2.1. Reject water composition

Table 7.1 shows the average composition of the real reject water used in the experiments. During the experimentation, the exact composition of the wastewater changed and, consequently, two periods are distinguished.

Table 7.1 – Average composition of the reject water tested in this study.

Component	Units	PERIOD 1		PERIOD 2	
		Average Value	Interval range	Average Value	Interval range
TS	g TS L ⁻¹	-	-	1.73	1.62 – 1.84
VTS	g VTS L ⁻¹	-	-	0.94	0.90 - 0.98
SS	g SS L ⁻¹	0.70	0.45-0.95	0.76	0.68 – 0.82
VSS	g VSS L ⁻¹	0.60	0.35-0.85	0.65	0.61 – 0.69
Total COD	mg COD L ⁻¹	1,700	1,400-2,000	1,296	1,215 – 1,436
Soluble COD	mg COD L ⁻¹	-	-	554	441 – 657
NH ₄ ⁺ -N	mg NH ₄ ⁺ -N L ⁻¹	800	700-900	699	656 – 747
NO _x ⁻ -N	mg NO _x ⁻ -N L ⁻¹	n.d.	-	n.d.	-
Alkalinity/ NH ₄ ⁺ -N ratio	mol (mol) ⁻¹	1.04	1.00 - 1.12	0.97	0.95 – 1.01
pH	-	8.0	7.96 – 8.22	7.91	7.86 – 7.93
Temperature	°C	35	-	35	-

n.d. not detected

However, this wastewater was always characterised by a high ammonium concentration (600-900 mg NH₄⁺-N L⁻¹), a high temperature (35°C) and a bicarbonate to ammonium ratio in molar basis near 1.0, which means that the alkalinity of the wastewater is not capable to buffer the complete nitrification process but only about the half process.

Moreover, reject water from anaerobic digestion of sewage sludge from a municipal WWTP is commonly characterised by a low BOD/N ratio (Arnold *et al.*, 2000; Hellinga *et al.*, 1999; Vandaele *et al.*, 2000; Wett and Rauch, 2003) that implies the use of an external carbon source to denitrify. As discussed above, this external carbon source could be synthetic or (if possible) the VFA present in another wastewater stream of the same municipal WWTP.

7.2.2. SHARON-Denitrification using methanol to denitrify

The SHARON-Denitrification process using methanol as the external carbon source to denitrify was carried out at lab-scale conditions. The strategy proposed by Galí *et al.* (2006b) after an optimization study of the SHARON-Denitrification process for sludge reject water was implemented in this work. Temperature was maintained at 33 ± 0.1 °C. Retention time was set at 2 days and the duration of the nitrification/denitrification cycles was 2 hours (1h aerobic and 1h anoxic). The stoichiometric amount of methanol per gram of NO₂⁻-N formed were added during the first 30 minutes of every anoxic period to prevent its accumulation for the subsequent aerobic stage, which would reduce the nitrifying activity due to oxygen competition with heterotrophic biomass. To start-up the process, concentrated VSS from the withdrawals of an SBR for biological nitrogen removal over nitrite of reject water were introduced inside the lab-scale digester and the aforementioned conditions were established. The behaviour of the SHARON-Denitrification process without external pH control was analysed during three months. During the first two months (Period 1, P-1) the ammonium load and the alkalinity to nitrogen ratio of the wastewater tested was slightly higher than the analyzed in the subsequent 1 month period (Period 2, P-2). The most relevant operational parameters under steady-state operation obtained in this study are presented in Table 7.2, where it is observed that the nitrogen removal efficiency was above 96% during P-1 and slightly lower, around 87%, during P-2. This reduction in nitrogen removal efficiency also led to an increase of the DO level and a descent of the pH range related to a reduction in the alkalinity of the biological system.

Table 7.2 – Main characteristics of the operating strategy of the SHARON-Denitrification process when using methanol and supernatant from hydrolysed primary sludge.

Parameter	Units	SHARON-DN using methanol		SHARON-DN using primary sludge
		(PERIOD 1)	(PERIOD 2)	
Cycle length	h	2	2	2
Time distribution				
Aerobic react	h	1	1	1
Anoxic react	h	1	1	1
Influent Flow-rate (reject water)	mL min ⁻¹	1.4	1.3	1.3
Influent Flow-rate (C source)	mL min ⁻¹	< 0.5	< 0.5	2.9
HRT	days	2.0	2.1	1.4
SRT	days	2.0	2.1	1.4
VSS	g VSS L ⁻¹	1.20	1.09	0.68 - 1.35
Temperature	°C	33	33	33
Dissolved oxygen range (aerobic)	mg O ₂ L ⁻¹	> 3.0	3.2 - 4.9	2.4 - 4.3
pH range	-	6.8 – 8.0	6.6 - 7.7	7.4 – 8.6
Average AUR				
during aerobic periods	mg NH ₄ ⁺ -N (L h) ⁻¹	33.0	24.9	30.8
Average NUR				
during anoxic periods	mg NO ₂ ⁻ -N (L h) ⁻¹	31.7	23.3	29.0
Nitrogen removal efficiency	%	96.7	87.3	98.5

Figure 7.1 shows representative pH and DO profiles during two days of operation under steady-state conditions of Period 2. As observed, pH range oscillated within 6.6-7.7, due to the restricted alkalinity of the wastewater tested. The DO concentration inside the reactor was increased along the aerobic step due to the reduction of nitrifying activity associated to the pH descent. Moreover, in Figure 7.2 the effluent concentrations of NH₄⁺-N and NO₂⁻-N during the three months of operation are presented. As observed, the average effluent concentration (obtained from daily integrated samples) of ammonium was 8.4 (P-1) and 60.2 mg NH₄⁺-N L⁻¹ (P-2) and the average effluent concentration of nitrite was 11.5 (P-1) and 28.5 mg NO₂⁻-N L⁻¹ (P-2). Nitrate formation was not detected.

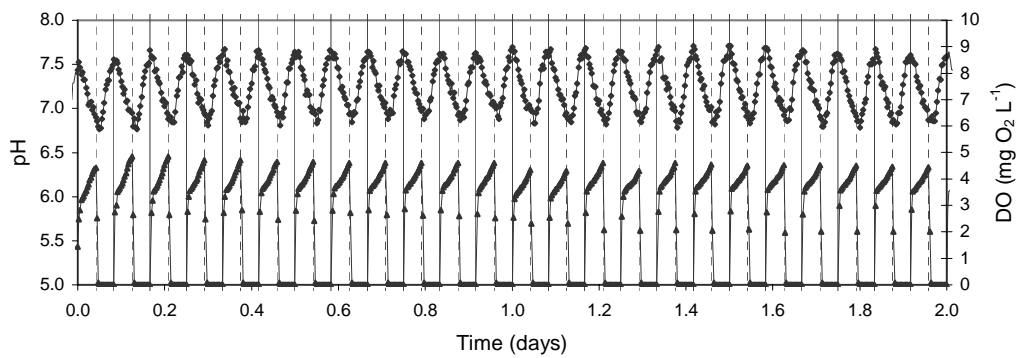


Figure 7.1 – Experimental DO (▲) and pH (●) profiles of 24 consecutive SHARON-Denitrification cycles (using methanol to denitrify) under steady-state operation of Period 2.

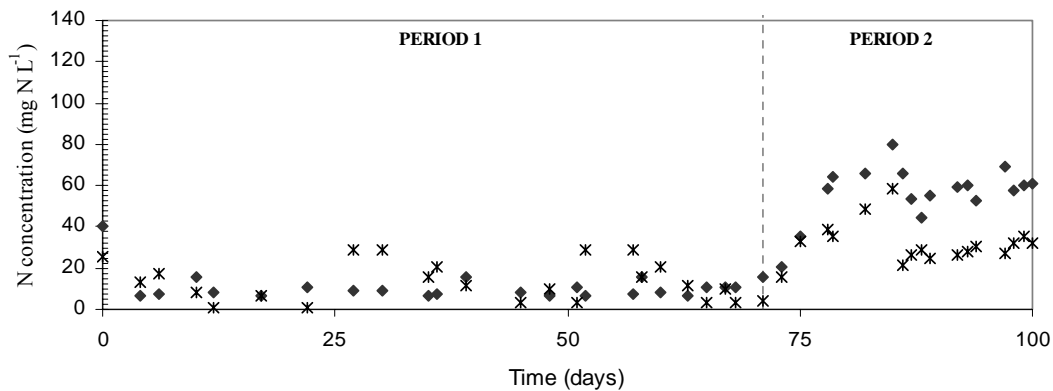


Figure 7.2 – Experimental profiles of effluent $\text{NH}_4^+\text{-N}$ (◆) and $\text{NO}_2^-\text{-N}$ (⋈) during 3 months of steady-state operation in the SHARON-Denitrification process using methanol to denitrify.

Table 7.3 shows the composition of the effluent of the SHARON-Denitrification reactor in Period 2. Considering that this effluent is recirculated to the main stream of the WWTP, the obtained effluent quality is acceptable. The Percentages of soluble COD and nitrogen removal from the reject water were, respectively, 37.3 and 87.3%. In Table 7.2, the average Ammonium Uptake Rate (AUR) and Nitrite Uptake Rate (NUR) are shown. AUR and NUR were calculated according to Equations 7.1 and 7.2, respectively, where Q_1 is the daily influent flow-rate of the reject water, $S_{\text{NH,REJECT WATER}}$ and $S_{\text{NO,REJECT WATER}}$ are the $\text{NH}_4^+\text{-N}$ and $\text{NO}_2^-\text{-N}$ concentration in reject water, respectively; $S_{\text{NH,EFFLUENT}}$ and

$S_{NO,EFFLUENT}$ are the $\text{NH}_4^+\text{-N}$ and $\text{NO}_2^-\text{-N}$ concentration in the effluent, respectively; $S_{NO,PRODUCED}$ is the $\text{NO}_2^-\text{-N}$ produced due to the oxidation of $\text{NH}_4^+\text{-N}$ calculated as reported in the ASM models (Henze *et al.*, 2000) considering $Y_{AOB}=0.20$ mg cell COD (mg $\text{NH}_4^+\text{-N}$ consumed) $^{-1}$ (Galí *et al.*, 2006b) and $i_{XB}=0.07$ mg $\text{NH}_4^+\text{-N}$ (mg COD) $^{-1}$; and t_N and t_{DN} are the time destined daily to nitrification and denitrification, respectively.

$$AUR = \frac{Q_1(S_{NH_4,REJECT\ WATER} - S_{NH_4,EFFLUENT})}{t_N} \quad (7.1)$$

$$NUR = \frac{Q_1(S_{NO_2,PRODUCED} + S_{NO_2,REJECT\ WATER} - S_{NO_2,EFFLUENT})}{t_{DN}} \quad (7.2)$$

Table 7.3 – Quality of the effluent wastewater of the SHARON-Denitrification process when using methanol and supernatant from hydrolysed primary sludge as electron donor to denitrify.

	SS (g SS L $^{-1}$)	VSS (g VSS L $^{-1}$)	COD _{CENTRIFUGED} (g COD L $^{-1}$)	$\text{NH}_4^+\text{-N}$ (mg N L $^{-1}$)	$\text{NO}_2\text{-N}$ (mg N L $^{-1}$)	$\text{NO}_3\text{-N}$ (g N L $^{-1}$)
<i>SHARON-DN</i> <i>using methanol</i>	1.19 ± 0.07	1.09 ± 0.22	0.53 ± 0.11	60.2 ± 17.6	28.5 ± 14.4	n.d.
<i>SHARON-DN</i> <i>using primary sludge</i>	1.83 ± 0.12	1.35 ± 0.21	0.59 ± 0.19	9.6 ± 3.8	20.2 ± 10.2	n.d.

n.d.: not detected

As stated in Figure 7.2, during Period 2, $\text{NO}_2^-\text{-N}$ concentration was always lower than the $\text{NH}_4^+\text{-N}$ effluent concentration, which is in concordance with the experimental results obtained by Fux *et al.* (2003). Considering that the alkalinity to nitrogen ratio of this wastewater was very close to 1.0 (see Table 7.1) and that denitrification is only capable to recover the half alkalinity consumed during nitrification, this fact could be explained, since the required alkalinity to nitrogen ratio (2.0) to oxidize all the $\text{NH}_4^+\text{-N}$ concentration could not be reached.

7.2.3. Selection of an internal flow of the WWTP to denitrify.

Since the wastewater tested had a very reduced BOD/ $\text{NH}_4^+\text{-N}$ ratio and the use of methanol represents an additional cost to reduce the content of nitrogen in the effluent stream (0.2-0.3 Euros kg $^{-1}$ N removed according to STOWA, 1996), the possible use of an internal flow of the WWTP to denitrify was evaluated.

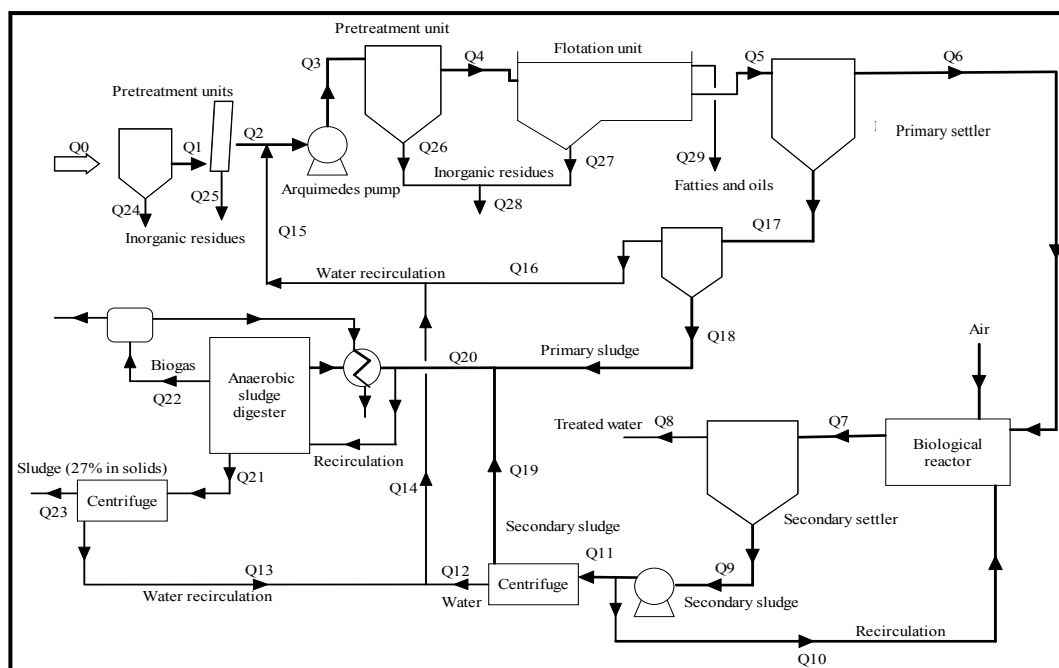
Figure 7.3 shows a schematic diagram of the municipal WWTP under study and includes the average flow rates of the main streams. As it is observed, the influent wastewater ($49,000 \text{ m}^3 \text{ day}^{-1}$) is initially conducted to a primary treatment. The solid fraction of this stream (primary sludge, Q18) is separated from wastewater and inserted in a primary settler before being fed to the mesophilic anaerobic digester. After this primary treatment, the wastewater is introduced in a conventional activated sludge system. The concentrated sludge from the secondary settler is, in part, inserted in the secondary settler (Q11). Afterwards, primary and secondary sludge are mixed and introduced in the anaerobic digester to produce electricity and thermal energy. The effluent from anaerobic digestion is centrifuged: the solid fraction is treated by composting and the liquid fraction (sludge reject water, $275 \text{ m}^3 \text{ day}^{-1}$) requires treatment.

Analyzing the flow scheme of the WWTP in Figure 7.3, there are some streams that could be suitable to denitrify: the influent municipal wastewater (Q1), influent wastewater of the secondary reactor (after the primary treatment, Q6), the hydrolysed secondary sludge from the secondary settler (Q11) and the hydrolysed primary sludge from the primary settler (Q18). Table 7.4 shows the characterization of these internal flows.

Influent municipal wastewater (Q1) and influent of the secondary reactor (Q6).

Although the carbon present in the influent stream of the WWTP and the influent wastewater of the secondary biological reactor would be useful to denitrify (BOD_5 values are presented in Table 7.4), its use was rejected since a great amount of these wastewaters would be necessary and, consequently, the reactor's volume would be extremely large.

Hydrolysed secondary sludge (Q11). The hydrolysed secondary sludge obtained from the bottom of the secondary clarifier could also be utilized to denitrify but its use was discarded since the kinetics of denitrification using endogenous carbon at 30°C were too slow when compared with the use of methanol or acetic acid (Galí *et al.*, 2006b) which is in concordance with Henze *et al.* (2002).



Line	(m ³ day ⁻¹)	Line	(m ³ day ⁻¹)
Q0	46,300	Q14	1,107
Q1	46,300	Q15	2,672
Q2	46,300	Q16	1,565
Q3	49,000	Q17	1,800
Q4	49,000	Q18	235
Q5	49,000	Q19	60
Q6	47,200	Q20	295
Q7	64,800	Q21	300
Q8	46,300	Q22	-
Q9	17,600	Q23	-
Q10	16,700	Q24	-
Q11	900	Q25	-
Q12	840	Q26	-
Q13	275	Q27	-

Figure 7.3 – WWTP flow diagram and flow-rates (average values of 2004)

Table 7.4 – Average composition of several internal flows of the WWTP.

Parameter	Units	Influent stream of the WWTP	Influent stream of the secondary reactor	Hydrolysed primary sludge	Hydrolysed secondary sludge
TS	(g TS L ⁻¹)	2.35	1.80	43.6	3.50
VTS	(g VTS L ⁻¹)	0.75	0.33	34.1	2.2
SS	(g SS L ⁻¹)	0.58	0.12	36.0	2.2
VSS	(g VSS L ⁻¹)	0.55	0.12	29.7	2.0
COD _{TOTAL}	(g COD L ⁻¹)	1.0	0.4	55.9	1.9
COD _{SOL}	(g COD L ⁻¹)	0.25	0.08	5.3	0.06
BOD ₅	(g BOD L ⁻¹)	0.4	0.2	-	-
VFA	(g COD L ⁻¹)	-	-	4.7	-
NH ₄ ⁺ -N	(g N L ⁻¹)	0.05	0.03	0.19	0.04
NO _x -N	(g N L ⁻¹)	< 0.01	< 0.01	< 0.06	< 0.015
pH	(-)	7.5	7.6	6.6	7.3

Hydrolysed primary sludge (Q18). The hydrolysed primary sludge (from the bottom of the primary thickener, approximately after HRT 0.5 days) contains an important BOD at short time (characterisation shown in Table 7.4) which can be used to denitrify.

However, due to its high content in total solids, this primary sludge should be centrifuged before being inserted in the SHARON-Denitrification process. To test the biological process performance when using supernatant of hydrolysed primary sludge to denitrify at lab-scale, the following pre-treatment was applied: it was sieved and then conserved at 4°C during 3 days to favour solids precipitation. In order to minimize changes in the supernatant of hydrolysed primary sludge, two litres bottle of supernatant was prepared every day and kept at 4°C. The main characteristics of the supernatant of primary sludge used in this work are presented in Table 7.5. In Figure 7.4, it is presented a respirogram of the supernatant of hydrolysed primary sludge where 175 mL of primary sludge were added to 3.0 L of a mixed liquor with biomass from the withdrawals of an SBR reactor (see Chapter 4) and 12 mg ATU L⁻¹ to inhibit nitrifying activity. In this plot, it can be noticed that the biodegradable COD of the hydrolysed primary sludge can be divided into two fractions: a readily biodegradable COD related to short-chain VFAs and slowly biodegradable COD. As observed in Table 7.5, approximately 80% of the soluble COD was mainly composed by VFA, and more than the 90% of the total COD was biodegradable. Moreover, the use of the supernatant of primary sludge to denitrify

implies the introduction of an additional $\text{NH}_4^+\text{-N}$ load to the biological system ($190 \text{ mg NH}_4^+\text{-N L}^{-1}$) and a considerable volume of this internal wastewater stream to denitrify.

Table 7.5 – Composition of the supernatant of the pre-treated hydrolysed primary sludge

Component	Units	Average Value	Interval range
TS	g TS L^{-1}	4.13	4.07 – 4.17
VTS	g VTS L^{-1}	3.56	3.30 – 3.70
SS	g SS L^{-1}	0.34	0.32 – 0.35
VSS	g VSS L^{-1}	0.32	0.31 – 0.34
$\text{COD}_{\text{CENTRIFUGED}}$	g COD L^{-1}	5.98	5.72 – 6.04
$\text{COD}_{\text{SOLUBLE}}$	g COD L^{-1}	5.01	4.87 – 5.26
VFA	g COD L^{-1}	4.02	3.78 – 4.27
$\text{NH}_4^+\text{-N}$	$\text{mg NH}_4^+\text{-N L}^{-1}$	190	175 - 196
$\text{NO}_x^-\text{-N}$	$\text{mg NO}_x^-\text{-N L}^{-1}$	< 20	-
pH	-	6.44	6.41 – 6.47

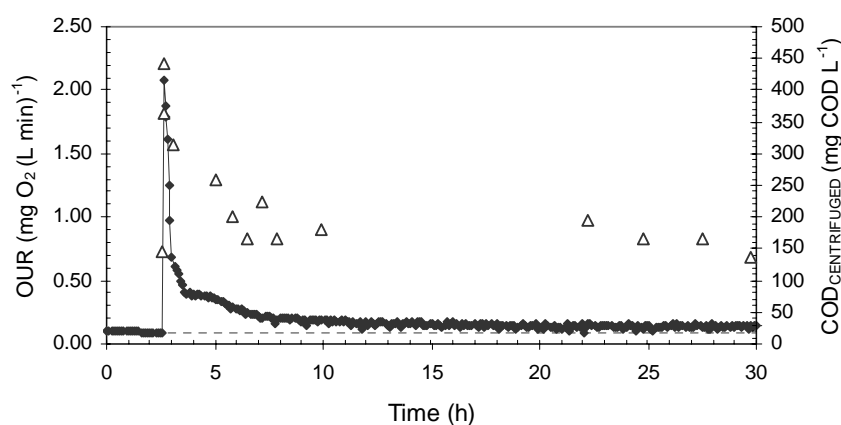


Figure 7.4 – Repirogram of the hydrolysed primary sludge.
OUR(\blacklozenge), endogenous OUR (- - -) and centrifuged COD (Δ).

Although the carbon present in the influent stream of the WWTP and the influent wastewater of the secondary biological reactor would be useful to denitrify, its use was rejected since a great amount of these wastewaters would be necessary and, consequently, the reactor's volume would be extremely large. The hydrolysed secondary sludge

obtained from the bottom of the secondary clarifier could also be utilized to denitrify but its use was discarded since the kinetics of denitrification using endogenous carbon at 30°C were too slow when compared with the use of methanol or acetic acid (which is in concordance with Henze *et al.*, 2002).

7.2.4. SHARON-Denitrification using supernatant of hydrolysed primary sludge to denitrify

Once the steady-state operation of the SHARON-Denitrification process using methanol as the external carbon source was well-defined, the methanol was substituted by supernatant of hydrolysed primary sludge. Since the biodegradable COD of this internal flow was not extremely concentrated, the fluid dynamics of the system were changed with respect to the strategy with methanol but maintaining the influent flow-rate of the reject water. Considering that the supernatant of hydrolysed primary sludge had nearly 4 g COD L⁻¹ related to VFA concentrations, after calculations it was decided to add 1 L day⁻¹ of this carbon source. This would lead to a total retention time of 1.4 days, but the reject water treated per day was the same as the SHARON-Denitrification with methanol.

The substitution of methanol by supernatant of primary sludge was drastic, since it was considered that the VFAs contained in the primary sludge were as easily biodegradable as methanol by the facultative heterotrophs developed under the previous experimental conditions. However, since the supernatant of primary sludge had a low pH value, during the first day of operation, alkalinity was controlled by dosing NaHCO₃ when pH dropped below 6.7. Then, the control of pH was totally suppressed and the reactor performance evolved to a stationary state. In Table 7.2, the most relevant operational parameters are presented during the two weeks of operation.

In Figure 7.5, a representative pH and DO profile of two days of operation of the SHARON-Denitrification process using hydrolysed primary sludge to denitrify are presented. In this plot, it is proved that the use of supernatant of hydrolysed primary sludge improved the kinetics with respect to the use of methanol since the alkalinity present in the primary sludge buffered the process until an optimum pH range (namely, 7.4-8.6).

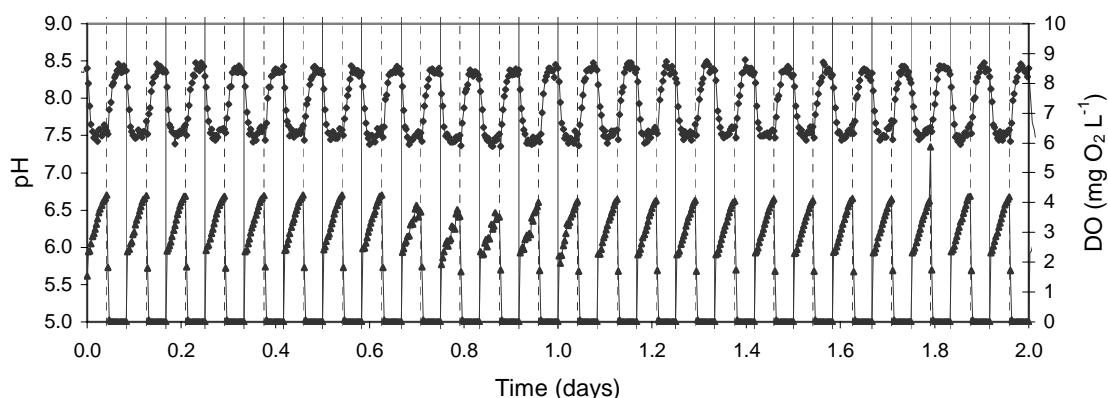


Figure 7.5 – Experimental DO (▲) and pH (●) profiles of 24 consecutive SHARON-Denitrification cycles (using supernatant of hydrolysed primary sludge to denitrify) under steady-state operation.

Moreover, the shape of the DO profile of this SHARON-Denitrification process is sensibly different from the one obtained when using methanol. The DO level inside the reactor (from 2.4 to 4.3 mg O₂ L⁻¹) was inversely proportional to the oxygen uptake rate. It is observed that when pH decreased, the DO level was increased which means that the nitrifying activity was reduced. Since the oxygen supply was the same in both SHARON-Denitrification processes, it is noticed that biomass activity when using hydrolysed primary sludge was higher than when using methanol. Moreover, the DO rise during aerobic periods of the SHARON-Denitrification process using primary sludge to denitrify was more pronounced than when using methanol. This fact can be explained as follows: since the pH dependency of nitrifying activity follows a Gaussian expression with optimum pH near 8.0 (Grunditz and Dalhammar, 2001; Dosta *et al.*, 2005) for lower pH values, lower increase in nitrifying activity is detected.

Figure 7.6 shows the results obtained for NH₄⁺-N and NO₂⁻-N concentrations in the effluent of the SHARON-Denitrification process using hydrolysed primary sludge to denitrify. The first day corresponds to the changing of methanol to primary sludge as a carbon source. Therefore, it is stated that the process was rapidly adapted to the new COD substrate.

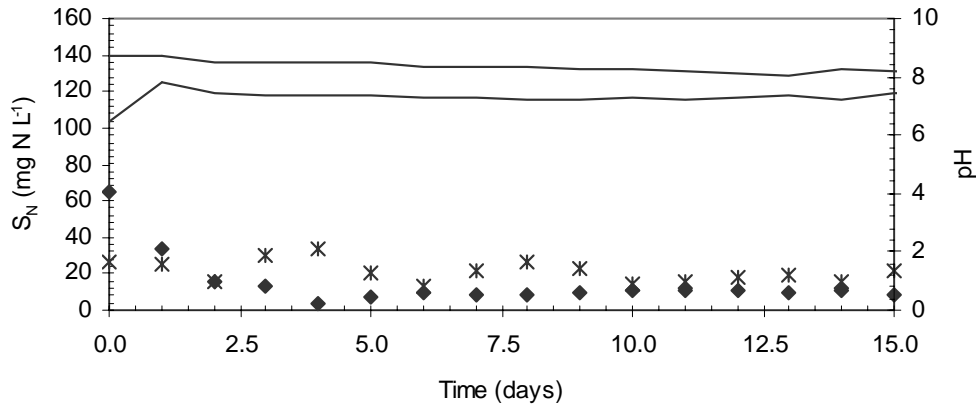


Figure 7.6 – Experimental profiles of effluent NH₄⁺-N (◆), NO₂⁻-N (Ж) and pH range (— ; minimum and maximum) during 15 days of steady-state operation in the SHARON-Denitrification process using supernatant of hydrolysed primary sludge to denitrify.

The effluent quality obtained in this process was better than the one obtained when methanol was utilised and the average nitrogen removal efficiency (calculated by means of Equation 3) was 96.7%. In Equation 7.3, Q_1 and Q_2 are the daily influent flow-rates of reject water and hydrolysed primary sludge, respectively, t_N and t_{DN} are referred to the daily Nitrification and Denitrification times, respectively, and $N_{REJECT\ WATER}$, $N_{PRIMARY\ SLUDGE}$ and $N_{EFFLUENT}$ are the total nitrogen (NH₄⁺-N + NO₂⁻-N) of the reject water, the primary sludge and the effluent, respectively.

$$\% N_{REMOVAL} = \frac{\left[(Q_1 N_{REJECT\ WATER} t_{N+DN} + Q_2 N_{PRIMARY\ SLUDGE} 0.5 t_{DN}) - ((Q_1 + Q_2) N_{EFFLUENT} t_{N+DN}) \right]}{(Q_1 N_{REJECT\ WATER} t_{N+DN} + Q_2 N_{PRIMARY\ SLUDGE} 0.5 t_{DN})} \times 100 \quad (7.3)$$

Values of the average AUR and NUR are also provided in Table 7.2. These parameters were calculated according to Equations 7.4 and 7.5, where $S_{NH_4^+ PRIMARY\ SLUDGE}$ and $S_{NO_2^- PRIMARY\ SLUDGE}$ are the NH₄⁺-N and NO₂⁻-N concentration in hydrolysed primary sludge, respectively. As observed, average AUR and NUR values were improved when hydrolysed primary sludge were used to denitrify.

$$AUR = \frac{Q_1 S_{NH_4, REJECT WATER} + Q_2 S_{NH_4, PRIMARY SLUDGE} - (Q_1 + Q_2)(S_{NH_4, REJECT WATER} - S_{NH_4, EFFLUENT})}{t_N} \quad (7.4)$$

$$NUR = \frac{Q_1 (S_{NO_2, PRODUCED} + S_{NO_2, REJECT WATER} + S_{NO_2, PRIMARY SLUDGE} - S_{NO_2, EFFLUENT})}{t_{DN}} \quad (7.5)$$

On the other hand, considering the quantity of solids in the pre-treated hydrolysed primary sludge (see Table 7.5), the increase of VSS was higher when supernatant of hydrolysed primary sludge was used to denitrify since more biomass was formed, due to the consumption of more biodegradable COD by heterotrophic biomass.

Another important aspect to consider is the low temperature of supernatant of the hydrolysed primary sludge in real conditions, since the saving in costs related to methanol (approximately, 0.2-0.3 Euros kg^{-1} N removed) could not compensate the possible need of external thermal control. On the other hand, Hellinga *et al.* (1998) reported that at their process conditions (reject water concentration of 1000 mg $\text{NH}_4^+\text{-N L}^{-1}$, 60% of denitrification), the exothermic reactions led to a net temperature increase of 9 °C. This heat production could maintain the desired temperature range (33°C) in the studied biological system.

7.3 CONCLUSIONS

- ✓ The application of the SHARON-Denitrification process to treat supernatant from anaerobic digestion of sewage sludge can reduce its ammonium load to more than 85%.
- ✓ The customary use of methanol to denitrify can be avoided by the utilization of supernatant of hydrolysed primary sludge, since it contains a proper amount of readily biodegradable COD.

- ✓ When supernatant of hydrolysed primary sludge is used to denitrify, the biological efficiency is improved considerably since it buffers the system within an optimal pH range (7.5-8.5).

- ✓ Since BOD was not highly concentrated in the supernatant of hydrolysed primary sludge, the fluid dynamics of the biological system were changed significantly with respect to the strategy with methanol but maintaining the reject water influent flow-rate. Therefore, the HRT was 2.0-2.1 days when using methanol and 1.4 days when using hydrolysed primary sludge. However, the SHARON/Denitrification process achieved good nitrogen removal efficiencies when working with hydrolysed primary sludge due to a higher biomass activity.

8. Modelling of partial nitrification in a SHARON chemostat and in a sequencing batch reactor to achieve a suited influent to the Anammox process.

ABSTRACT

In this study, two biological nitrogen removal treatments of sludge reject water were tested at lab scale conditions to achieve an appropriate influent to the Anammox process. These two processes were the SHARON process and the partial nitrification in a Sequencing Batch Reactor (SBR). Both processes showed a good performance in the generation of an effluent with a $\text{NH}_4^+\text{-N}$ to $\text{NO}_2^-\text{-N}$ on molar basis of approximately 1.

In order to provide an explanation of the processes and inhibitions that take place inside the digesters, both biological systems were modelled by means of the Activated Sludge Model presented in Chapter 5. Activated sludge from the withdrawals of both reactors was analysed in respirometric batch tests to calibrate the model. The calibrated model provided a good match between experimental and simulated data and showed the key factors that lead to the obtention of an effluent ready to be fed to an Anammox reactor.

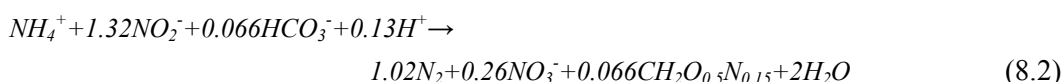
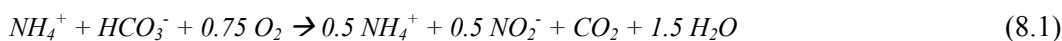
Part of this chapter is published in:

Galí, A., Dosta, J., Van Loosdrecht, M.C.M., Mata-Álvarez, J. (2007) Two ways to achieve an Anammox influent from reject water treatment: partial SBR nitrification and SHARON process. *Process Biochemistry*, 42(4), 715-720.

8.1 INTRODUCTION

In municipal wastewater treatment plants (WWTP), the supernatant from centrifugation of anaerobically digested sludge (reject water) contains 15-25% of the total nitrogen load in a flow, and it is usually returned to the main stream (van Dongen *et al.*, 2001; Fux *et al.*, 2002). As stated in Chapter 1, this effluent can be treated by stable partial nitrification in a first aerobic reactor combined with anaerobic ammonium oxidation (Anammox) in a second tank to ensure total nitrogen removal throughout an autotrophic process (Jetten *et al.*, 1997; van Loosdrecht and Salem, 2006).

In view of coupling a partial nitrification unit with an Anammox unit, nitrite oxidising biomass (NOB) activity should be suppressed and total $\text{NH}_4^+\text{-N}$ should be oxidised for about 50% to $\text{NO}_2^-\text{-N}$ by ammonium oxidizing biomass (AOB) as presented in Equation 8.1 (Hellinga *et al.*, 1999; Van Hulle, 2005). Subsequently, the Anammox process would convert ammonium directly to N_2 gas with nitrite as electron acceptor in the absence of oxygen and biodegradable COD. Equation 8.2 shows the stoichiometry of the Anammox reaction (Strous, 2000; van Dongen *et al.*, 2001; Dapena-Mora *et al.*, 2004 Mosquera-Corral *et al.*, 2005;). When compared with conventional nitrification/denitrification (over nitrate), this autotrophic process avoids the requirement of an organic carbon source to denitrify, allows to save over 60 % of the oxygen supply and produces little sludge (Fux *et al.*, 2002).



The partial nitrification to obtain an appropriate influent for the Anammox process can be carried out by means of a continuously aerated SHARON process (Hellinga *et al.*, 1999). This process is based on the carefully selection of a high operating temperature (35°C) and a low HRT without sludge retention, that enables the proliferation of AOB and the total wash-out of NOB. Since sludge rejection water is characterised by an alkalinity to ammonium ratio on a molar basis around 1.0-1.2 (see Chapter 4), about the 50-60% of the ammonium will be oxidised to nitrite, resulting in an appropriate influent for the Anammox process (Hellinga *et al.*, 1999; Fux *et al.*, 2002). The SHARON/Anammox

technology has recently been implemented in the Rotterdam, Dokhaven WWTP in the Netherlands (van Kempen *et al.*, 2001; van Loosdrecht and Salem, 2006).

Another technique to achieve an influent of approximately 50% NH_4^+ -N and 50% NO_2^- -N, is the use of a Sequencing Batch Reactor (SBR) strategy based on the NOB inhibition by unionised ammonia concentrations (Galí *et al.*, 2007). Anthonisen *et al.* (1976) reported that NOB is inhibited for concentrations larger than 0.2-2.8 mg $\text{HNO}_2 \text{ L}^{-1}$ and/or 0.1-1.0 mg $\text{NH}_3 \text{ L}^{-1}$, while AOB is inhibited by unionised ammonia concentrations larger than 10-150 mg $\text{NH}_3 \text{ L}^{-1}$.

The aim of this study is to model a lab-scale SHARON chemostat process and a partial nitrification in a lab-scale SBR for the treatment of sludge reject water of a Spanish municipal WWTP to achieve an appropriate influent to the Anammox process. In order to provide a theoretical explanation of the processes and inhibitions that take place inside the digesters, both biological systems were modelled by means of the IWA Activated Sludge Models (Henze *et al.*, 2000) extended for nitrite route description and pH calculation.

8.2 RESULTS AND DISCUSSION

8.2.1. Extended Activated Sludge Model

As stated in Chapter 5, some modifications of IWA Activated Sludge Models are necessary to describe biological nitrogen removal over nitrite. Nitrification was described as a two-step reaction (nitritation and nitrataion), which are potentially inhibited by unionised ammonia and nitrous acid concentrations (Anthonisen *et al.*, 1976). These inhibitions were inserted in the model by means of non-competitive inhibition kinetics as described by Wett and Rauch (2003). Oxygen supply and stripping of CO_2 and NH_3 were considered using the two-film theory. Inorganic carbon and proton concentration were defined as two new components in order to evaluate restrictions linked to alkalinity and pH limitations (Serralta *et al.* 2004). A pH dependency function for autotrophic biomass was included in the model as reported by Seco *et al.* (2004). Acid-base equilibrium of carbonic acid, nitrous acid, ammonium, phosphoric acid and water were considered in order to predict the distribution of species in the liquid media. The influence of ionic strength and activity coefficients on the acid-base dissociation constants for all the

species included in the model were also taken into account. pH was calculated by means of a mass balance equation for proton concentration. This model was implemented in a software program (Mathematica 4.1) to simulate the studied biological processes. The model structure was the one described by Wett and Rauch (2003). A more detailed explanation of the proposed model can be found in Chapter 5. However, only the processes detailed in Table 8.1 were considered to model the autotrophic partial nitrification (the aerobic degradation of slowly biodegradable organic carbon present in reject water was considered negligible for the purposes of this study).

Table 8.1– Processes and Kinetic equations used to model the partial nitrification process in a SBR and a SHARON chemostat.

(j)	Processes	Kinetic rate equations ($\rho_1 > 0$)
Autotrophic organisms		
(1)	<i>Aerobic growth of AOB</i>	$\mu_{m,AOB} \frac{S_{NH_3}}{K_{NH_3} + S_{NH_3}} \frac{K_{NH_3}^{AOB}}{K_{NH_3}^{AOB} + S_{NH_3}} \frac{K_{HNO_2}^{NOB}}{K_{HNO_2}^{NOB} + S_{HNO_2}} \frac{S_O}{S_O + K_{O,AOB}} F_{AOB,pH} X_{AOB}$
(2)	<i>Aerobic growth of NOB</i>	$\mu_{m,NOB} \frac{S_{NO_2}}{K_{NO_2} + S_{NO_2}} \frac{K_{HNO_2}^{NOB}}{K_{HNO_2}^{NOB} + S_{HNO_2}} \frac{K_{NH_3}^{NOB}}{K_{NH_3}^{NOB} + S_{NH_3}} \frac{S_O}{S_O + K_{O,NOB}} F_{NOB,pH} X_{NOB}$
(3)	<i>Autotrophic decay</i>	$b_A (X_{AOB} + X_{NOB})$
Heterotrophic organisms		
(4)	<i>Heterotrophic decay</i>	$b_H X_{BH}$
Operation conditions		
(5)	<i>Oxygen supply</i>	$K_L a_{O_2} (S_O - He_{O_2} P_{P,O_2})$
(6)	<i>Stripping of CO₂</i>	$K_L a_{CO_2} (S_{CO_2} - He_{CO_2} P_{P,CO_2})$
(7)	<i>Stripping of NH₃</i>	$K_L a_{NH_3} (S_{NH_3} - He_{NH_3} P_{P,NH_3})$

8.2.2. Reject water composition

Table 8.2 shows the average composition of the reject water used in the experiments, which is very similar to the wastewaters tested in Chapter 4 and Chapter 7. This wastewater was mainly characterised by a high ammonium concentration and a low

BOD₅/N ratio (< 0.20 mg BOD (mg NH₄⁺-N)⁻¹). The alkalinity to ammonium ratio in molar basis was approximately 1, which means that the alkalinity of the wastewater was only capable to buffer about the half nitrification process.

Table 8.2- Average composition of the reject water tested in this study

Component	SHARON	SBR
SS (g SS L ⁻¹)	0.71	0.68
VSS (g VSS L ⁻¹)	0.61	0.6
COD _{TOT} (g COD L ⁻¹)	1.43	1.75
NH ₄ ⁺ -N (g N L ⁻¹)	0.71	0.82
NO _x -N (g N L ⁻¹)	n.d.	n.d.
Alkalinity/ NH ₄ ⁺ -N (mole mole ⁻¹)	1.09	0.98
pH	8.3	8.0

n.d.: not detected

Izzet *et al.* (1991) detected a variation of influent alkalinity to ammonium ratio from 1.02 to 1.44 for sludge reject water, which differs considerably from the ratio 1.0, usually assumed in literature. In this study little variation of the ammonium to alkalinity ratio was detected, although fluctuations in the influent ammonium concentration were observed. However, assuming that the nitrite to ammonium ratio on molar basis for the Anammox stoichiometry is approximately 1.32, it was considered that these fluctuations could be assumed in the Anammox process without nitrite accumulation episodes.

8.2.3. Partial nitrification in a SBR

The partial nitrification of reject water in an SBR was performed in cycles of 4h, with HRT 0.35 days, SRT 5 days, temperature 30°C and an average biomass concentration of 1.2 g VSS L⁻¹. Air flow was regulated during aerobic periods, maintaining a dissolved oxygen (DO) level above 3 mg O₂ L⁻¹. The operating cycle was divided in 3 steps: aerobic fill (0.3 h), aerobic react (3.3 h) and settle and draw (0.4 h). The exchanged volume per cycle was the 50% of the reactor. Wastewater was added at the beginning of the cycle achieving a concentration of nearly 600 mg NH₄⁺-N L⁻¹. Due to the restricted alkalinity of this wastewater, only 200 mg NH₄⁺-N L⁻¹ were oxidised to NO₂⁻-N obtaining an Anammox suited effluent with approximately 400 mg NH₄⁺-N L⁻¹ and 400 mg NO₂⁻-N L⁻¹. Nitrate formation was not detected due to the inhibition of nitrite oxidizing biomass

activity by free ammonia. Figure 8.1 shows the experimental profiles of pH and DO in 6 consecutive SBR cycles working under steady-state conditions. Experimental profiles of $\text{NH}_4^+\text{-N}$, $\text{NO}_2^-\text{-N}$, Alkalinity, DO and pH during one representative SBR cycle are presented in Figure 8.2.

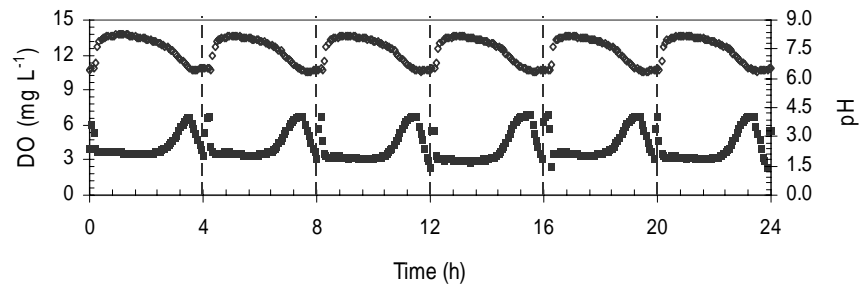


Figure 8.1- Experimental profiles of DO and pH during 6 consecutive SBR cycles working under steady-state conditions. (Dissolved oxygen ■; pH ○; cycle delimitation - - -)

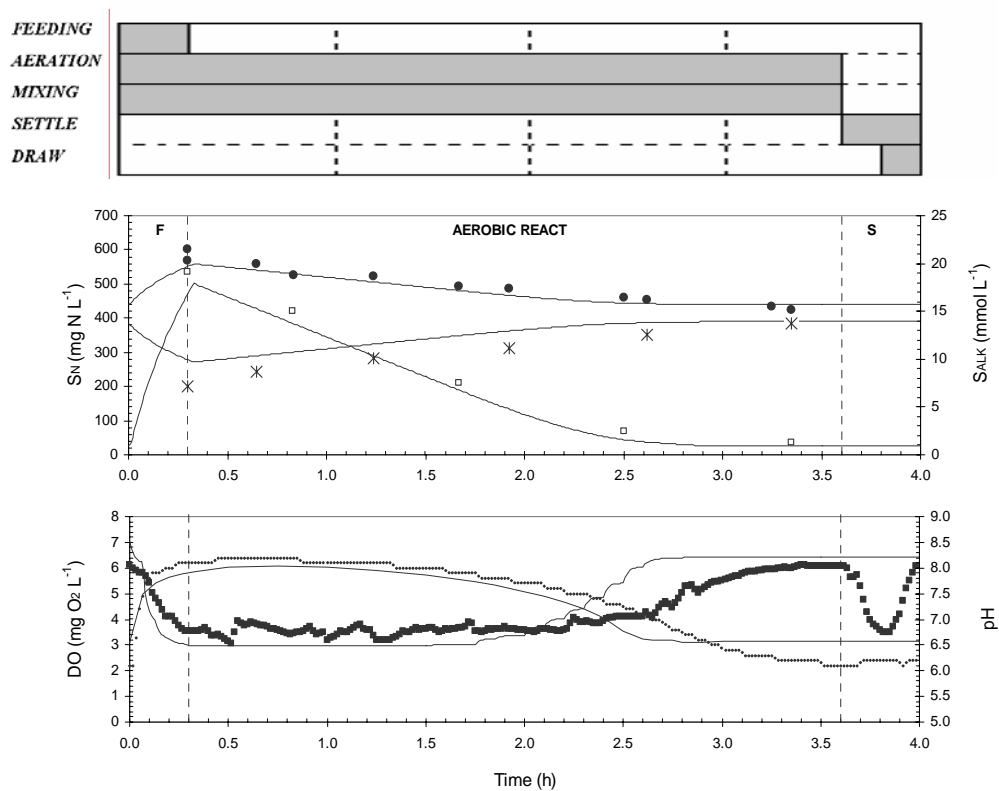


Figure 8.2 - Experimental and modelled profiles during the SBR cycle. ($\text{NH}_4^+\text{-N}$ ●; $\text{NO}_2^-\text{-N}$ ✕; Alkalinity □; Dissolved oxygen ■; pH ○; simulated data —; stage delimitation - - -)

Since Calibration and validation of activated sludge models is an inherent part of any type of model application (Vanrolleghem *et al.*, 1999), biomass from the withdrawals of the SBR was analysed in respirometric batch tests.

The combined parameters $\mu_{mAOB} X_{AOB}$ at controlled pH (8.0±0.1) and temperature (30°C) for the evaluation of maximum autotrophic growth rate for AOB were determined through a $S_{t0}/X_{t0}=1/200$ respirometric experiment for autotrophic biomass (Spanjers and Vanrolleghem, 1995). The actual autotrophic yield coefficient (Y_{AOB}) was estimated according to Kappeler and Gujer (1992). Half-saturation constant for free ammonia (K_{NH_3}) was determined as described in Chapter 6 (section 6.2.5). Oxygen affinity constant for ammonium oxidizers ($K_{O, AOB}$) was assessed as described by Guisasola *et al.* (2005). The inhibition constants for NH_3 and HNO_2 were assumed from literature (Wett and Rauch, 2003).

In Table 8.3 the values obtained for these parameters are presented and Figure 8.3 shows representative plots of the parameters assessed for this biomass.

Table 8.3 – Model parameters (average values) for Partial Nitrification in a SBR and SHARON.

Parameter	Value	Units
<u>Partial nitrification in a SBR</u>		
Y_{AOB}	0.20 ± 0.01	mg cell COD (mg NH_4^+ -N consumed) ⁻¹
$\mu_{m, AOB} X_{AOB}$ (pH 8.0)	13.1 ± 0.3	mg cell COD (L h) ⁻¹
$K_{O, AOB}$	0.34 ± 0.07	mg O ₂ L ⁻¹
K_{NH_3}	0.38 ± 0.03	mg NH ₃ -N L ⁻¹
<u>SHARON reactor</u>		
Y_{AOB}	0.20 ± 0.01	mg cell COD (mg NH_4^+ -N consumed) ⁻¹
$F_{pH} \mu_{m, AOB} X_{AOB}$	8.78	mg cell COD (L h) ⁻¹
$K_{O, AOB}$	0.56 ± 0.06	mg O ₂ L ⁻¹
K_{NH_3}	0.55 ± 0.04	mg NH ₃ -N L ⁻¹

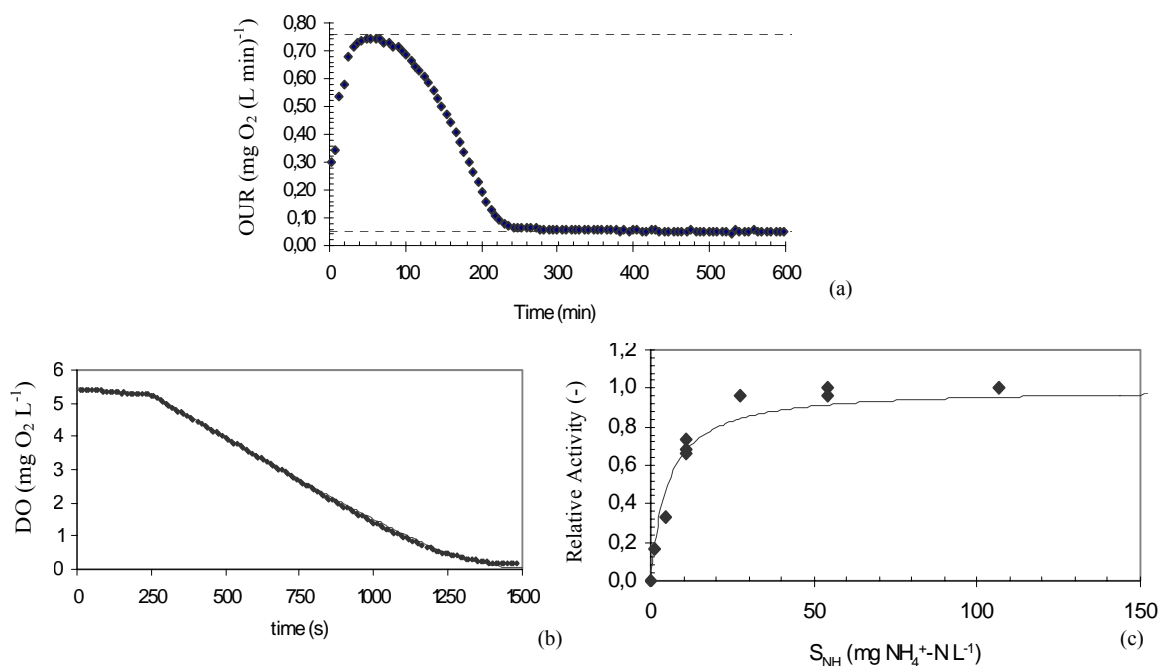


Figure 8.3- Assessment of Y_{AOB} and $\mu_{mAOB}X_{AOB}$ (a), $K_{O, AOB}$ (b), and K_{NH_3} (c) for the biomass developed in a SBR for partial nitrification of sludge reject water.

Moreover, pH influence in AOB activity was assessed through the oxygen profile of a representative SBR operating cycle. The area between the DO profile and the endogenous DO level is proportional to the oxygen consumed during the cycle. From an oxygen mass balance, the oxygen mass transfer coefficient, K_{LaO_2} , can be calculated (0.75 min^{-1}). This value allows the measurement of the exogenous oxygen uptake rate (OUR) from the DO profile. Since the DO concentration and the ammonium concentration were almost non-limiting, the exogenous OUR was proportional to the maximum autotrophic growth rate at the corresponding pH. Therefore, the relation between the exogenous OUR at every pH provides the relative activity of autotrophic biomass in front of pH (see Figure 8.4). This dependency (F_{pH}) was adjusted to Equation 4.49 (Seco *et al.*, 2004). The minimum sum of squared errors between experimental and modelled data was obtained for $pH_{OPT} = 7.98$, $\text{Log } K_{I,pH} = -8.26$ and $\text{Log } K_{pH} = -7.70$.

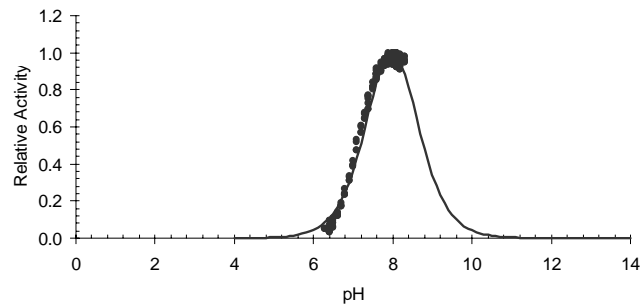


Figure 8.4 - pH dependency of AOB in the SBR treatment of reject water to obtain a suited influent to the Anammox process (Experimental (●) and modelled (—) data)

When considering all the aforementioned parameters values, the simulation of the SBR process was very accurate (see Figure 8.2). During the settle and draw period, when aeration was stopped, DO concentration decreased due to the endogenous OUR. This phenomenon was not taken into account in the model. Possible disagreements between theoretical and experimental data are related to the assumptions used in the model.

From the analysis of the different operating parameters, the reasons that lead to the obtention of a suited Anammox influent can be clarified: Free ammonia concentration was the responsible of the high inhibition observed for NOB. Considering the AOB and NOB inhibition constants reported by Wett and Rauch (2003), at the beginning of the cycle ($560 \text{ mg NH}_4^+\text{-N L}^{-1}$, $\text{pH}=8.2$) the free ammonia concentration do not affect AOB, while NOB activity remains at the 24 % of the maximum activity. On the other hand, the restricted alkalinity content of the wastewater makes that, when approximately the 50% of $\text{NH}_4^+\text{-N}$ was consumed, pH remained at a value of 6.2 that leads to an AOB activity below the 8 % of its maximum activity (see Figure 8.4). Moreover, under the experimental conditions obtained at the end of the cycle ($400 \text{ mg NH}_4^+\text{-N L}^{-1}$; $\text{pH } 6.2$), free ammonia concentration as a substrate was limiting, and the Monod term for NH_3 as a substrate was 0.61. Both pH and NH_3 effects were the responsible that at the end of the cycle, AOB activity was almost stopped. Dissolved oxygen was always above $3 \text{ mg O}_2 \text{ L}^{-1}$. Considering the oxygen affinity constant assessed for this biomass ($0.34 \text{ mg O}_2 \text{ L}^{-1}$), the Monod term for oxygen was always above 0.90. Nitrous acid concentration also played a considerable role: at the end of the feeding step ($280 \text{ mg NO}_2^-\text{-N L}^{-1}$; $\text{pH } 8.2$) the HNO_2 inhibition term was very close to 1, but as pH decreased, the influence of HNO_2 on both AOB and NOB activity was slightly increased. At the end of the cycle ($400 \text{ mg NO}_2^-\text{-N L}^{-1}$; $\text{pH } 6.2$) the inhibition term for HNO_2 concentrations on AOB and NOB was 0.85.

Therefore, as expected, in this SBR process the main factors that contribute to the inhibition of NOB and the oxidation of only the half of ammonium present in the wastewater are the working free ammonia concentration and the alkalinity (and, therefore, the pH) present inside the digester.

8.2.4. Partial nitrification in a SHARON chemostat.

Galí *et al.* (2007) studied the performance of the SHARON reactor for sludge reject water, reaching an optimal performance when working at HRT 1 day, temperature 35°C, $\text{DO} > 2 \text{ mg O}_2 \text{ L}^{-1}$ and biomass concentration around 0.4 g VSS L^{-1} . pH was stabilized at 6.2 - 6.7 as observed in Figure 8.5 where the DO and pH profiles of 1 day of steady-state operation of the SHARON process is presented. The effluent obtained had an average $\text{NH}_4^+\text{-N}$ to $\text{NO}_2^-\text{-N}$ ratio on molar basis of approximately 1, ready to be treated in an Anammox process.

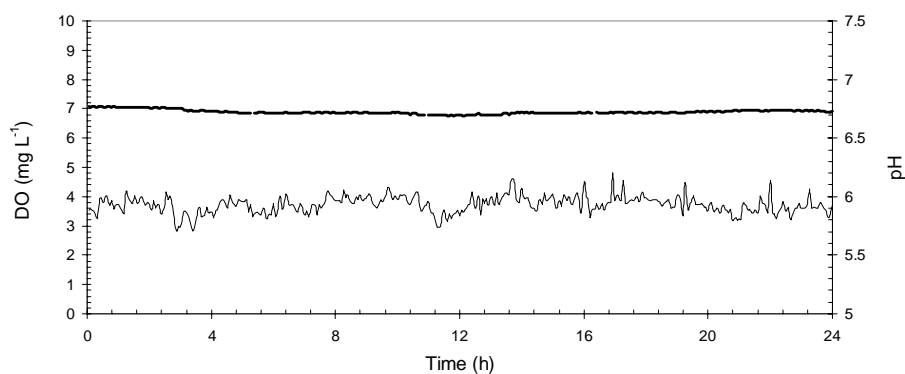


Figure 8.5 - Experimental profiles of DO and pH during 1 day of steady state operation of the SHARON process. (pH — and DO —)

To model the process performance, Y_{AOB} , K_{NH_3} and $K_{\text{O}_2, \text{AOB}}$ were determined at 35°C following the procedures explained in section 8.2.3. The experimental values obtained for these parameters are presented in Table 8.3, and Figure 8.6 presents representative plots for the experimental assessment of these parameters. The experimental $K_{\text{O}_2, \text{AOB}}$ obtained in this study was sensibly lower than the $0.94 \text{ mg O}_2 \text{ L}^{-1}$ reported by Van Hulle *et al.* (2004), probably due to the higher DO concentration inside the digester ($> 5 \text{ mg O}_2 \text{ L}^{-1}$) used by

these authors. On the other hand, the half-saturation constant for ammonia obtained in this work was similar to the one reported by Hellings *et al.* (1999).

The combined parameters $F_{pH} \mu_{mAOB} X_{AOB}$ were determined by the application of an ammonium mass balance (see Equation 8.3). Since the process was carried out at constant pH, this procedure to determine $F_{pH} \mu_{mAOB} X_{AOB}$ (which includes the inhibition of pH) was used to simplify the calibration effort. A good pH dependency function of AOB in the SHARON reactor can be found in Van Hulle *et al.* (2004).

$$0 = \frac{Q_{FEED}}{V_{REACTOR}} (S_{NH,WW} - S_{NH}) - \left(\frac{1}{Y_{AOB}} + i_{XB} \right) \left(\frac{S_{NH_3}}{K_{NH_3} + S_{NH_3}} \right) \left(\frac{K_{NH_3}^{AOB}}{K_{NH_3}^{AOB} + S_{NH_3}} \right) \left(\frac{S_O}{K_{O,AOB} + S_O} \right) \left(\frac{K_{HNO_2}^{AOB}}{K_{HNO_2}^{AOB} + S_{HNO_2}} \right) F_{pH} \mu_{m,AOB} X_{AOB} \quad (8.3)$$

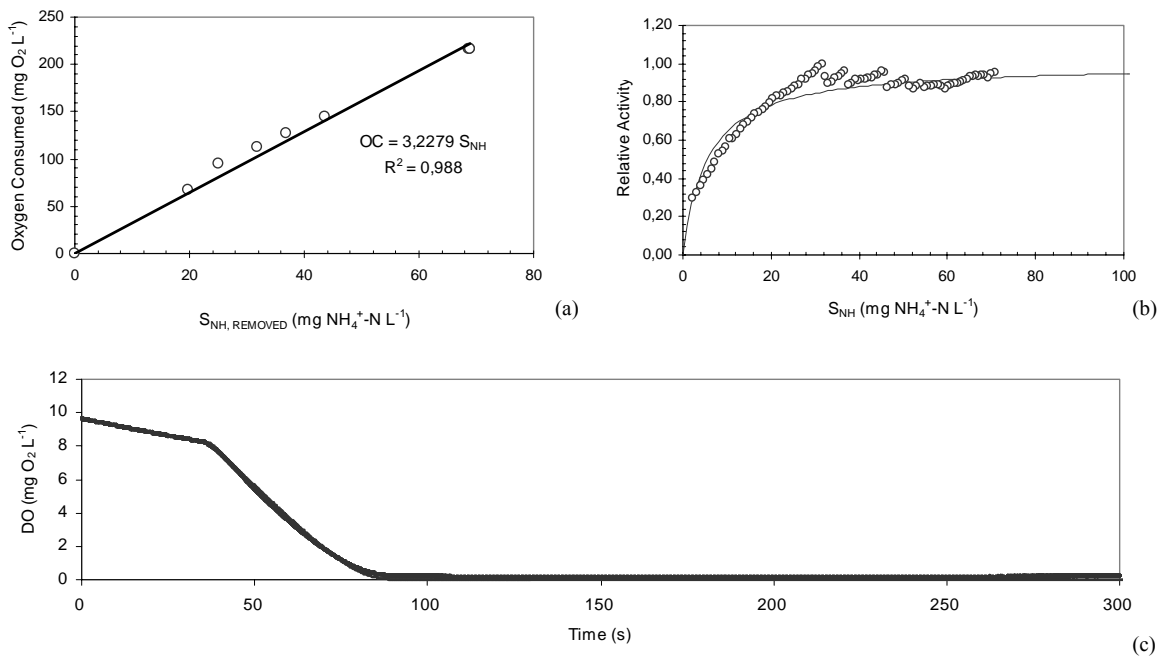


Figure 8.6 - Assessment of Y_{AOB} (a), $\mu_{mAOB} X_{AOB}$ (b), $K_{O,AOB}$ (c), and K_{NH_3} (d) for the biomass developed in a SHARON chemostat for partial nitrification of sludge reject water. Modelled results (—)

K_{La} for oxygen was obtained by trial and error until the experimental DO profile was adjusted to the modelled one. The set of equations were solved yielding the results shown in Figure 8.7, where they can be compared with the experimental results obtained during

50 days of steady state operation (Galí *et al.*, 2007). As observed, a good match between experimental and theoretical data was achieved. The calculated pH was slightly lower than the actual experimental value which is related to the simplifications assumed in the model (only the most relevant acid/base species of the biological system were considered).

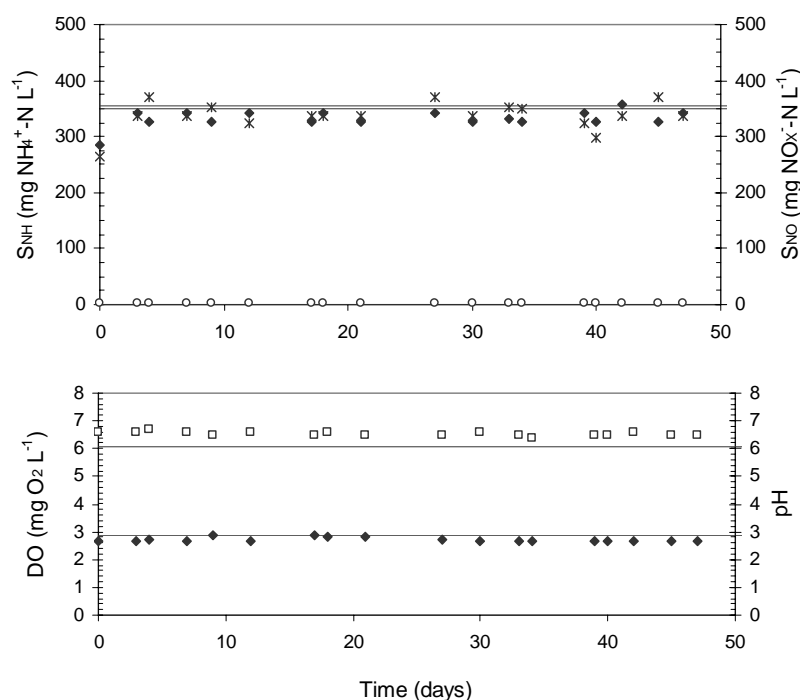


Figure 8.7 - Experimental and modelled profiles during the SHARON operation under steady-state conditions. ($\text{NH}_4^+\text{-N}$ ●; $\text{NO}_2^-\text{-N}$ ✕; $\text{NO}_3^-\text{-N}$ ○; Dissolved oxygen ■; pH □; modelled results —)

As stated in Chapter 1, in the SHARON process, the key factor that yields the total wash out of nitrite oxidizers is the selected SRT at the relatively high operating temperature. However, the effect of the operating DO, NH_3 and HNO_2 concentrations on AOB activity can be quantified in order to better understand the studied SHARON process.

Dissolved oxygen was regulated at a value of $3 \text{ mg O}_2 \text{ L}^{-1}$. Considering that the oxygen affinity constant of this biomass was $0.56 \text{ mg O}_2 \text{ L}^{-1}$, the aeration conditions lead to an actual AOB activity around the 85% of the maximum AOB activity. On the other hand, considering the NH_3 concentration present in the liquid media, $\approx 0.63 \text{ mg NH}_3\text{-N L}^{-1}$, and the half-saturation constant of NH_3 for AOB previously assessed in batch respirometric

tests ($0.55 \text{ mg NH}_3\text{-N L}^{-1}$), it is observed that the activity of AOB was reduced a 47% with respect to its maximum value due to the low availability of NH_3 . Therefore, ammonium oxidizing biomass activity is restricted due to the pH value and the NH_3 concentration, which makes that not all the $\text{NH}_4^+\text{-N}$ is converted to nitrite but only about the half. Moreover, it is important to highlight here that the low NH_3 concentration in the mixed liquor would not represent an important inhibition to NOB biomass if it could be present in the medium.

Finally, the nitrous acid concentration inside the SHARON reactor, $\approx 0.39 \text{ mg HNO}_2\text{-N L}^{-1}$, does not represent a high inhibition to ammonium oxidizers. Considering the inhibition constant for AOB proposed by Wett and Rauch ($K_{\text{HNO}_2}^{\text{AOB}} = 2.8 \text{ mg HNO}_2\text{-N L}^{-1}$), the AOB activity would have approximately the 87% of its maximum activity.

Therefore, it is observed that the selected SRT at high temperature is the responsible of the total wash-out of nitrite oxidizers (as reported by Hellinga *et al.*, 1999). Furthermore, the limited AOB growth rate is related to the value of pH and the low NH_3 concentration in the liquid medium.

8.2.5. Comparison of the partial nitrification in a SBR and in a SHARON chemostat.

In Table 8.4, the main operational characteristics of the tested SBR and SHARON chemostat processes are presented. As observed, both processes were capable to provide a constant and suited influent to the Anammox process, but the SBR could assume a higher ammonium load than the SHARON reactor. This fact is due to the higher biomass concentration (related to the sludge retention (SRT) and VSS) and the working pH range inside the SBR reactor. This is also demonstrated in Table 8.3, where it is stated that the maximum autotrophic activity ($\mu_{m,\text{AOB}} X_{\text{AOB}}$) value for the SBR process is higher than for the SHARON process.

However, the maximum specific growth rate of ammonium oxidizers ($\mu_{m,\text{AOB}}$) for the SHARON process is higher than the one obtained for partial nitrification in the SBR at the same pH value, because the SHARON process favours high microbial specific growth rates (Hellinga *et al.*, 1999).

Table 8.4 – Main operational characteristics in the SBR and in the SHARON chemostat.

Parameters	Units	SBR	SHARON
Ammonium loading rate	kg NH ₄ ⁺ -N (m ³ day) ⁻¹	2.2	0.7
HRT	days	0.35	1
SRT	days	5	1
VSS	g VSS L ⁻¹	1.2	0.4
Temperature	°C	30	35
DO concentration	mg O ₂ L ⁻¹	>2	>2
pH interval range	-	6.0 – 8.3	6.2 – 6.7

On the other hand, the values of oxygen affinity constants ($K_{O, AOB}$) for both processes did not present substantial differences between the two processes since both of them worked under similar DO concentrations. The half saturation constants of NH₃ for both biological systems were sensibly higher than those proposed in the literature for conventional nitrification/denitrification processes (Henze *et al.*, 2000), because the processes studied here worked under higher ammonium concentrations.

In the SBR the main factor that inhibited NOB was the operating NH₃ concentration, but in the SHARON reactor the key factor was the applied HRT at 35°C that assured the total wash-out of nitrite oxidizers.

Considering the characteristics of the wastewater tested in this study, both processes managed well and produced the desired effluent (NOB was completely inhibited). Furthermore, both processes were capable to assume substantial variations in flow rate and composition (Galí *et al.*, 2007). However, for wastewaters with a very lower ammonium load, the inhibition of NOB by free ammonia and nitrous acid concentrations obtained in the SBR could not be guaranteed, while the SHARON process would also wash out NOB, avoiding nitrate formation. On the other hand, for wastewaters with a very higher ammonium load, the SBR treatment proposed in this work could lead to a high free ammonia concentration at the beginning of the cycle that could be lost by stripping and/or could inhibit ammonium oxidizers. In this case, the inhibition of AOB could be avoided by performing the feeding of reject water during the first 3 hours of the

SBR cycle. Besides, the inhibition of AOB by high free nitrous acid could also represent a limitation for both the SBR and the SHARON process. The model developed in this work provides a useful tool to plan the most appropriate treatment strategy for the partial nitrification of different types of highly ammonium loaded wastewaters to obtain a suited influent to the Anammox process.

8.3 CONCLUSIONS

- ✓ Two efficient alternatives for the partial nitrification of a spanish sludge reject water in view of coupling it with an Anammox unit are the use of an SBR process (with total inhibition of NOB by NH_3 and HNO_2 concentrations) and a SHARON chemostat (where the wash out of NOB is due to the operating temperature and SRT).
- ✓ The SBR treatment was capable to assume a higher nitrogen loading rate (namely, $2.2 \text{ kg NH}_4^+\text{-N (m}^3 \text{ day)}^{-1}$) than the one obtained by the SHARON process ($0.7 \text{ kg NH}_4^+\text{-N (m}^3 \text{ day)}^{-1}$). This fact is related to the high sludge retention obtained in the SBR process.
- ✓ Both processes were modelled by means of an IWA Activated Sludge Model extended for nitrite route description and pH calculation. This model was calibrated with simple batch respirometric assays that minimized the calibration effort. Simulated results showed very good agreement with experimental values and provided a theoretical explanation of the inhibitions and processes that took place inside the digesters.
- ✓ The proposed model provides a useful tool to plan the most appropriate treatment strategy for the partial nitrification of different types of highly ammonium loaded wastewaters to obtain a suited influent to the Anammox process.

9. Operation of an Anammox reactor to treat highly ammonium loaded wastewaters at low temperatures.

ABSTRACT

As stated in previous chapters, the fully autotrophic nitrogen removal process (partial nitrification in combination with Anammox) is a promising alternative to conventional biological nitrogen removal processes, since it leads to a substantial reduction of aeration costs, avoids the need of external COD to denitrify and produces little sludge. However, the Anammox process has been usually presented as a biological process that requires heating (usually at 35 °C) to achieve proper removal efficiencies. In this study, the feasibility of the Anammox process at different temperature conditions (namely, 30, 25, 23, 20, 18 and 15 °C) to treat a highly nitrogen loaded synthetic wastewater (with a $\text{NH}_4^+\text{-N}$ to $\text{NO}_2^-\text{-N}$ ratio of 1) has been tested. Previously, as an initial approach to assess the temperature influence at short time on Anammox biomass, several batch activity tests were run for two kinds of Anammox biomass (namely, suspended and zeolite-attached) at controlled temperature conditions. These results were adjusted to the Arrhenius model and were taken as the basis to decide the biomass concentration needed to manage a previously defined nitrogen loading rate in a lab-scale Anammox Sequencing Batch Reactor (SBR) when the operating temperature range was reduced. At 18 °C, a steady state operation was achieved treating $0.30 \text{ kg NH}_4^+\text{-N (L day)}^{-1}$, with a stoichiometry slightly different from that obtained under 30°C. At 18 °C the $\text{NH}_4^+\text{-N}$ to $\text{NO}_2^-\text{-N}$ ratio was 1.04 and the $\text{NO}_3^-\text{-N}$ produced to $\text{NO}_2^-\text{-N}$ consumed ratio was 0.18. As predicted by the model, the system accumulated nitrite when the operating temperature was reduced to 15 °C, so a very slow adaptation of Anammox biomass to low temperatures was observed.

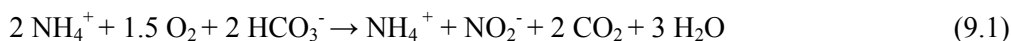
The most relevant parts of this chapter are published in:

Dosta, J., Fernández, I., Vázquez-Padín, J.R., Mosquera-Corral, A., Campos, J.L., Mata-Álvarez, J., Méndez, R. (2007) Short and long-term effects of temperature on the Anammox process. *Journal of Hazardous Materials*. (Accepted paper)

9.1. INTRODUCTION

As explained in the Chapter 1, several kinds of wastewaters are characterized by low carbon to nitrogen ratios and very high ammonia concentrations. For example, during anaerobic digestion of protein-rich sludge, a protein breakdown occurs and about 50% of the sludge bound nitrogen is released to the liquid medium in the form of ammonium (Siegrist, 1996). The supernatant from centrifugation of this stream contains a highly ammonium loaded wastewater (up to 2 g L^{-1} , according to Strous *et al.*, 1997) and a very low content in biodegradable COD. A feasible treatment of these kind of effluents is the combination of a stable partial nitrification in a first aerobic reactor, with anaerobic ammonium oxidation (Anammox) in a second tank to ensure the total nitrogen removal throughout a fully autotrophic nitrogen removal process (STOWA, 1996; Jetten *et al.*, 1997; Dapena-Mora *et al.*, 2004a; van Loosdrecht and Salem, 2006). When compared with conventional nitrification/denitrification, this autotrophic process avoids the requirement of organic carbon source to denitrify, allows saving over 65% of the oxygen supply and produces little sludge (Fux *et al.*, 2002).

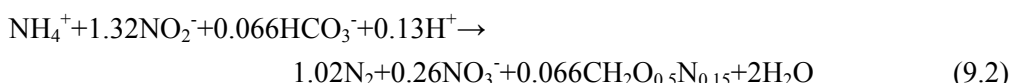
In a first partial nitrification unit, total $\text{NH}_4^+\text{-N}$ should be oxidised for about 50% to $\text{NO}_2^-\text{-N}$ by Ammonium Oxidizing Biomass (AOB) as presented in Equation 9.1.



Several ways to achieve this partial nitrification can be found in literature. In some cases, the nitrite accumulation in aerobic reactors has been achieved due to free ammonia inhibition of Nitrite Oxidizing Biomass (NOB) by high ammonia loads and high pH values at a certain temperature (Anthonisen *et al.*, 1976). Moreover, if there is a low Dissolved Oxygen (DO) concentration inside the reactor (below 1.5 mg L^{-1}), nitrate formation is restricted, since ammonia oxidation rate is favoured in front of nitrite oxidation kinetics (Garrido *et al.*, 1997; Bernet *et al.*, 2001; Pollice *et al.*, 2002; Fux and Siegrist, 2004). However, this last strategy alone is not enough to avoid completely the nitrate formation (Picioreanu *et al.*, 1997; Van Loosdrecht and Salem, 2006). Another technique to avoid nitrate formation is the so-called SHARON process (Hellings *et al.*, 1999; Mosquera-Corral *et al.*, 2005; Fux *et al.*, 2003) which is based on the difference in the growth rate of NOB and AOB at temperatures above 20°C . Recently, Vazquez-Padín

et al. (2006) obtained stable partial nitrification in a nitrifying granular sludge reactor for more than 300 days of operation.

Subsequently, the Anammox process converts ammonium together with nitrite (electron acceptor) directly to dinitrogen gas under anoxic conditions in the absence of any organic carbon source, following the reaction in equation 9.2 (Jetten, 1999). In this process a small amount of nitrate is also produced. Considering the biomass yield, the stoichiometric nitrite to ammonium ratio on molar basis is 1.32 (Jetten, 1999; van Dongen *et al.*, 2001; Mosquera-Corral *et al.*, 2005).



The Anammox process has been developed in several reactor configurations, such as fixed and fluidized bed reactors (Strous *et al.*, 1997; Fux *et al.*, 2004), Sequencing Batch Reactors (SBR) (Strous *et al.*, 1998; Van Dongen *et al.*, 2001; Fux *et al.*, 2002; Dapena-Mora *et al.*, 2004a), gas lift reactors (Sliemers *et al.*, 2003, Dapena-Mora *et al.*, 2004a) or up flow bed reactors (Ahn *et al.*, 2004; Imajo *et al.*, 2004). All these treatment strategies have provided good nitrogen removal efficiencies when implemented at temperatures above 30°C, with the consequent disadvantage of energy consumption.

Several works have been carried out in order to find the optimum range of temperature for the operation of lab-scale Anammox reactors and all of them concluded that the mentioned range was 30-40 °C. Strous *et al.* (1999) determined the effect at short time of pH and temperature on Anammox biomass from a SBR treating synthetic wastewater. These authors found the optimum pH range around 8.0 and the maximum Anammox activity at 40 ± 3 °C. This last finding is consistent with the results obtained by Egli *et al.* (2001) that situated the optimum Anammox activity at 37 °C for an enriched Anammox culture from a rotating disk contactor. Yang *et al.* (2006) situated the optimum temperature for Anammox biomass between 30-35 °C. Moreover, Toh *et al.* (2002) tried to select and enrich an autotrophic anaerobic ammonium oxidation consortium from sludge of a municipal treatment plant in Sydney. They employed two different temperatures, 37 and 55 °C. While mesophilic Anammox activities were successfully obtained in batch and continuous cultures, thermophilic Anammox organisms could not be selected at 55°C.

Despite of all this findings, several works with marine Anammox samples reported measurable activities at temperatures very below 30 °C. Rysgaard *et al.* (2004) analyzed the Anammox activity based on N₂ production in permanently cold (from -1.7 to 4 °C) sediments of the east and west coasts of Greenland and reported an optimum temperature of 12 °C. These authors observed measurable Anammox activity between -2 and 30 °C. Dalsgaard and Thamdrup (2002) also studied the effect of temperature on Anammox activity in marine sediments from the Skagerrak in the Baltic-North Sea transition, and reported an optimal ammonium removal rate at 15 °C and a sharply decrease above 25°C. At 32°C the Anammox activity observed by these authors was almost zero.

Since anaerobic ammonium oxidation with nitrite has now been found in a range of environments including marine sediments, sea ice and anoxic water columns, and it may be responsible for up to 50% of the global removal of fixed nitrogen from the oceans (Dalsgaard *et al.*, 2005), the Anammox treatment of highly ammonium loaded wastewater (previously treated in a partial nitrification treatment unit) at low temperatures seems feasible. The aim of this study is to assess the temperature dependency of Anammox biomass from a lab-scale SBR and to prepare this biomass for the treatment of a real wastewater at relatively low temperatures (15-20 °C).

9.2. RESULTS AND DISCUSSION

9.2.1. Temperature influence on Anammox activity

Suspended and zeolite-attached Anammox biomass from lab-scale reactors (Dapena-Mora *et al.*, 2004c; Fernández *et al.*, 2006), were used to assess the temperature influence on Anammox activity.

The SAA was measured in batch tests by triplicate at temperatures between 10 and 45 °C. The temperature dependency profiles obtained for these two Anammox populations (presented in Figure 9.1.) were consistent with results obtained by other authors (Strous, 2000; Egli *et al.*, 2001). The standard deviation registered for zeolite-attached biomass was higher than that obtained for suspended biomass. This fact is explained by the inaccuracies related to the assessment of VSS in attached biomass systems.

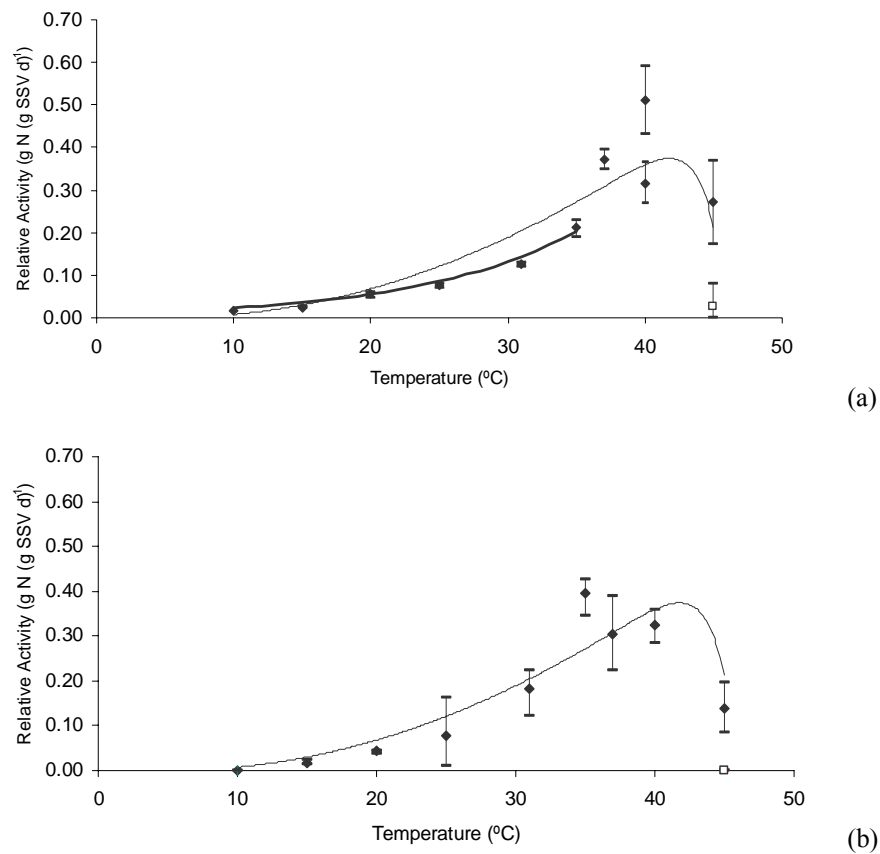


Figure 9.1 – Temperature dependency profiles on suspended (a) and zeolite attached (b) Anammox biomass. (Experimental SAA during the first injection of substrate ●; Experimental SAA during the second injection of substrate ○; Modified Arrhenius model —; Modified Ratkowsky model - -).

The temperature dependency function (F_T) is defined in Equation 9.3 as the mathematical expression (dependant on the actual temperature) that multiplied by a process rate at a reference temperature, $r(T_{REF})$, yields the process rate at the operating temperature, $r(T)$. The reference temperature is usually 293 K. In Figure 9.1, an exponential growth in SAA is observed for values between 10 and 30 °C. At this limited temperature range, a modified Arrhenius equation as reported by Hao et al. (2002) can be adjusted to experimental data as described in Equation 9.4, where F_T is the temperature dependency

function, E_{ACT} is the activation energy (J mol^{-1}), R is the gas constant ($8.32 \text{ J (mol K)}^{-1}$) and T is the actual temperature.

$$r(T) = F_T \cdot r(T_{REF}) \quad (9.3)$$

$$F_T = \exp\left(-\frac{E_{ACT}(T_{REF} - T)}{R \cdot T \cdot T_{REF}}\right) \quad (9.4)$$

When the difference between T and T_{REF} is small, the product $T \cdot T_{REF}$ does not change so much, and Equation 9.4 can be simplified to the expression shown in Equation 9.5, where θ is the temperature coefficient (K^{-1}). θ and E_{ACT} are correlated by Equation 9.6.

$$F_T = \exp(-\theta(T_{REF} - T)) \quad (9.5)$$

$$\theta = \frac{E_{ACT}}{R \cdot T \cdot T_{REF}} \quad (9.6)$$

Figure 9.1 (a) (thick line) shows the modelling of temperature influence on Anammox Activity by the modified Arrhenius model for temperatures between 10 and 30 °C. From this equation, the activation energy of the suspended Anammox population can be determined as 63.1 KJ mol^{-1} . This value is similar to the 70 KJ mol^{-1} reported by Strous *et al.* (1999) and Hao *et al.* (2002), and the 61 KJ mol^{-1} and 51.0 KJ mol^{-1} reported by Dalsgaard and Thamdrup (2002) and Rysgaard *et al.* (2004), respectively, for Anammox biomass from marine sediments. However, above the temperature range of 10-30 °C, the model equation provides non-realistic high biomass activity.

To take into account the inhibition of Anammox biomass at high operating temperatures, the modified Ratkowsky model presented in Equation 9.7 could be used in simulation studies. Although this model has no biological basis, it was the most suitable to describe the temperature dependency profiles obtained by Zwietering *et al.* (1991) and by Van Hulle *et al.* (2004) for SHARON biomass.

$$r(T) = [b \cdot (T - T_{\min})]^2 (1 - \exp(-c(T - T_{\max}))) \quad (9.7)$$

In Equation 9.7, T_{\min} and T_{\max} are the minimum and maximum temperatures at which growth is observed. The model constants (b and c) were obtained by minimizing the sum of squared errors between model outputs and experimental data for the two sets of experimental data obtained in this study. The values for these constants were $b=0.0174$ and $c=0.58$ when T_{\min} and T_{\max} were set at 5 and 46 °C respectively,

The results of the Ratkowsky model (Figure 9.1, thin line) can be compared with experimental data in Figure 9.1. It is important to highlight that these results were obtained analyzing the response of Anammox biomass at short time, considering the nitrogen gas production for the first injection of substrate. The SAA was also analyzed for temperatures above 30°C when a second injection of substrate was added. For temperatures below 41°C, a second injection of substrate represented an improvement of the denitrification rate by approximately a 20-30%, which was in accordance to the findings of Dapena-Mora *et al.* (2007). However, the SAA at 45°C decreased by a 90 % when a second injection of substrate was added. Moreover, the liquid media of this test acquired a slightly orange coloration when the first injection was consumed. The intensity of this coloration increased after the consumption of the second injection. Consequently, an operating temperature of 45 °C led to a segregation of cytochrome c from Anammox biomass to the liquid media (see Figure 9.2).

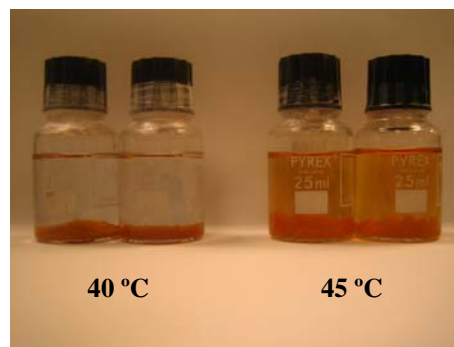


Figure 9.2 – Aspect of the Anammox biomass and the supernatant after the second injection of the Specific Anammox Activity (SAA) test at 40 °C and 45 °C.

In order to justify this observation, the absorbance of UV/Vis spectrum between 300 and 700 nm of the non pre-treated supernatant from the SAA batch tests at 35, 40 and 45°C after the second injection of substrate was analysed. Three representative absorbance profiles for Anammox suspended biomass at these temperatures are presented in Figure 9.3. Here it is observed a maximum peak at 534 nm when working at 45°C. Several studies (van De Graaf et al., 1996; Jetten et al., 1999) demonstrated that visible spectra of cells and cell extracts of Anammox cultures showed an increased signal at 468-470 nm. Recently, Cirpus et al. (2005) analyzed the UV/Vis spectrum of a 10kDa cytochrome c from cell extracts from the Anammox bacterium *Candidatus "Kuenenia stuttgartiensis"* and observed a maximum absorption at 419, 522 and 552 nm. These results are in accordance with the results obtained in this study, where a maximum absorption was detected at 534 nm. Therefore, the Anammox bacteria tested in this work had a maximum SAA at 40 °C and were not capable to work above 45 °C, which is consistent with the findings of Strous et al. (1999).

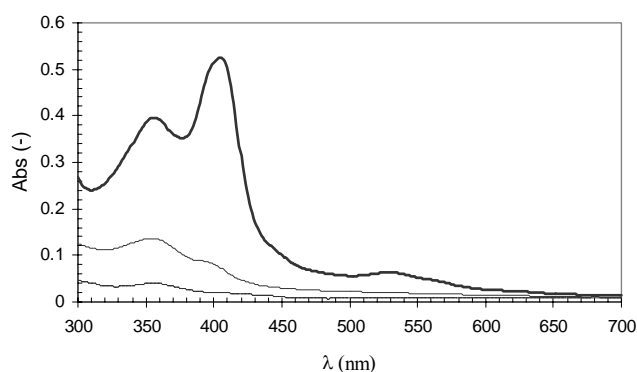


Figure 9.3 – Absorbance profiles of the supernatant of the Anammox Activity Tests at 35 (---), 40 (—) and 45 °C (—).

9.2.2. Reactor performance at reduced temperatures

The aforementioned temperature dependency of Anammox biomass at short time was taken as a first approach to establish the operating conditions of an Anammox SBR to treat highly ammonium-loaded synthetic wastewater at low temperatures. Table 9.1 shows the composition of the synthetic wastewater used in the experimental periods of this study (adapted from van de Graaf *et al.*, 1996). The nitrite to ammonium ratio on

molar basis of this wastewater was 1. NH_4^+ -N and NO_2^- -N concentrations were maintained at 150 mg N L^{-1} along the experimental period of this study. However, when the Anammox activity was reduced due to low temperatures, the total NH_4^+ -N and NO_2^- -N concentrations were modified as explained below.

Table 9.1. - Feeding and trace solution composition.

Feeding composition		Trace solution composition	
Compound	Conc. (mg L^{-1})	Compound	Conc. (g L^{-1})
NH_4^+ -N	150	EDTA	15
NO_2^- -N	150	$\text{ZnSO}_4 \cdot 7 \text{ H}_2\text{O}$	0.43
KHCO_3	1.25	$\text{CoCl}_2 \cdot 6 \text{ H}_2\text{O}$	0.24
CaCl_2	1.41	$\text{MnCl}_2 \cdot 4 \text{ H}_2\text{O}$	0.99
KH_2PO_4	50	$\text{CuSO}_4 \cdot 5 \text{ H}_2\text{O}$	0.25
MgSO_4	58.6	$(\text{NH}_4)_6\text{Mo}_7\text{O}_{24} \cdot 4 \text{ H}_2\text{O}$	0.22
$\text{FeSO}_4 \cdot 7\text{H}_2\text{O}$	9.08	$\text{NiCl}_2 \cdot 6\text{H}_2\text{O}$	0.20
EDTA	6.25	$\text{NaSeO}_4 \cdot 10\text{H}_2\text{O}$	0.20
		H_3BO_3	0.014
Trace solution	1.25 mL L^{-1}	$\text{NaWO}_4 \cdot 2\text{H}_2\text{O}$	0.05

As stated in Chapter 3, the Anammox process was carried out in a lab-scale Sequencing Batch Reactor (SBR) of 1 L, since it has been reported that good mixing and high nitrogen elimination rates can be easily achieved in sequencing batch reactors with suspended (Fux et al., 2002) or granulated biomass (Strous *et al.*, 1998). The biomass was attached in a zeolite (clinoptilolite) supplied by ZeoCat (94-96% of purity) previously sieved to select particles with 0.5-1.0 mm (Fernández *et al.*, 2006). The sludge retention was enhanced by two factors: the biomass characteristics and the time distribution of the SBR operating cycle. On the one hand, Anammox biomass was attached to a zeolite (clinoptilolite) in order to increase the density of the aggregates and, therefore, the Sludge Volumetric Index (SVI). On the other hand, the time distribution of the operating cycle shown in Figure 9.4 was implemented to prevent sludge flotation. This strategy was based on Dapena-Mora *et al.* (2004b) results. As observed, the feeding of the wastewater was performed during the first 5 hours to avoid the inhibition of Anammox biomass due to high NO_2^- -N concentrations. Subsequently, 30 min of stirring without substrate supply were used to deplete completely the nitrite inside the Anammox reactor and to favour the desorption of nitrogen gas bubbles. Table 9.2. shows the main operational characteristics of the Anammox SBR. Since an SAA of $0.04 \text{ g N (g VSS day)}^{-1}$ at $15 \text{ }^\circ\text{C}$ was determined

for the Anammox biomass (attached in a zeolite) and it was decided to treat a nitrogen loading rate of $0.30 \text{ kg N (m}^3 \text{ day)}^{-1}$, the reactor was inoculated with $7.6 \pm 0.2 \text{ g VSS L}^{-1}$ of zeolite-attached Anammox biomass. pH ranged around the optimum pH value reported by Strous (1999).

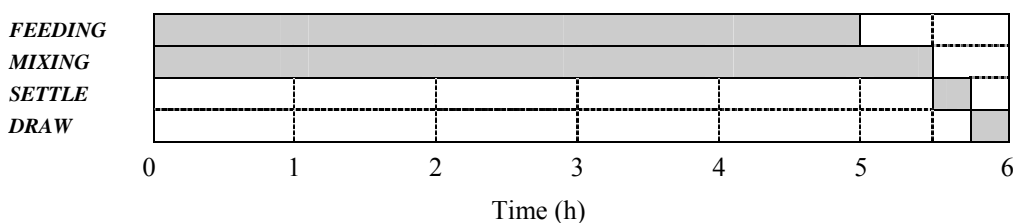


Figure 9.4 – Time distribution in the Anammox SBR cycle.

Table 9.2 – Main operational characteristics of the Anammox SBR.

Parameters	Units	Value
Nitrogen load	$\text{Kg N (m}^3 \text{ day)}^{-1}$	0.3
Cycle length	h	6
Volume	L	1.0
Volume exchange ratio	%	25
HRT	days	1

The reactor was adapted progressively to low temperature operation, since a drastic change in the operational conditions could lead to a destabilization of the biological system. Six experimental periods were carried out to transfer the operation from the mesophilic to the psychrophilic range of temperatures. Table 9.3 specifies the experimental periods, concomitantly with the temperatures and the actual SAA registered.

The $\text{NH}_4^+\text{-N}$ and $\text{NO}_2^-\text{-N}$ profiles during the operation of the Anammox SBR can be observed in Figure 9.5. The nitrogen loading rate and the actual SAA at the operating temperature of each period are also detailed in this Figure.

In a first experimental period, the reactor was inoculated with zeolite-Attached Anammox biomass and was operated at 30 °C with a nitrogen loading rate of 0.30 g N (L day)⁻¹ during 15 days. As observed in Figure 9.5, nitrite (the limiting substrate) was totally depleted in this period and, consequently, the inhibition of Anammox biomass by nitrite concentrations (Dapena-Mora *et al.*, 2007) was completely avoided. The effluent pH was always higher than the influent pH, due to the production of alkalinity related to the Anammox denitrification (see Equation 9.2). In period I, the ratio NO₂⁻-N to NH₄⁺-N was 1.38 ± 0.10, which agrees with the ratio 1.32, commonly assumed in literature (Jetten *et al.*, 1999; van Dongen *et al.*, 2001; Mosquera-Corral *et al.*, 2005). However, the NO₃⁻-N produced per unit of NH₄⁺-N consumed was 0.67 ± 0.05, which was notably higher than the value of 0.26 commonly assumed from the Anammox stoichiometry. Fernández *et al.* (2006) also reported a produced nitrate to removed ammonium ratio higher than the one usually assumed in literature.

Table 9.3 – Experimental periods in the Anammox SBR.

Period	Temperature (°C)	Actual Anammox Activity (g N (L day) ⁻¹)	Duration (days)
I	30	0.59	1-15
II	27	0.37	15-29
III	23	0.37	29-48
IV	20	0.35	48-63
V	18	0.32	63-101
VI	15	0.30 * 0.18 **	101-150

* Value of Anammox Activity measured before the first inhibition by nitrite concentrations

** Value of Anammox Activity measured after the first inhibition by nitrite concentrations

Then, the operating temperature was reduced to 23 °C during 1 SBR cycle. Since a slight accumulation of nitrite was observed at the end of this cycle, it was decided to perform the reduction of the operating temperature progressively. A drastic change in the temperature conditions may lead to a destabilization of the biological system. Therefore, the system was operated at 27°C during 2 weeks (period II) until the temperature was reduced to 23 °C (period III). As observed in Figure 9.5, the nitrite was completely

depleted in period II and the $\text{NH}_4^+\text{-N}$ concentration in the effluent experienced a slightly reduction with respect to the previous experimental period.

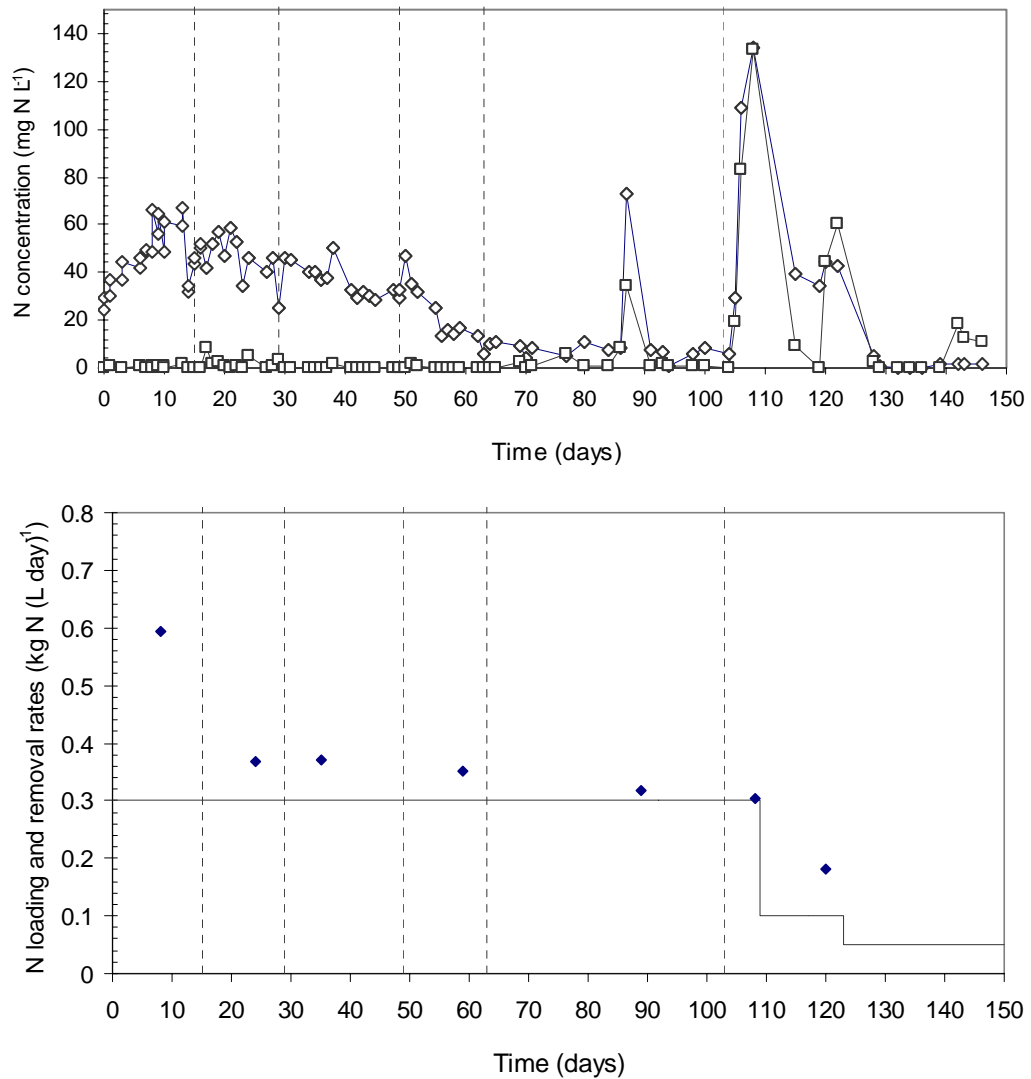


Figure 9.5 – Experimental profiles of $\text{NH}_4^+\text{-N}$ and $\text{NO}_2^-\text{-N}$ in the effluent, nitrogen loading rate and nitrogen removal rate during the operation of the Anammox SBR. ($\text{NH}_4^+\text{-N}$ (\diamond), $\text{NO}_2^-\text{-N}$ (\square), Actual nitrogen removal rate (\blacklozenge), Nitrogen loading rate (—))

In period III, the CaCl_2 concentration in the synthetic wastewater was reduced from the Van der Graaf *et al.* (1996) medium previously used (1.41) to $0.07 \text{ mg CaCl}_2 \text{ L}^{-1}$. This change was performed due to the turbidity and chestnut colour of the mixed liquor of the SBR during the first days of operation at $23 \text{ }^\circ\text{C}$, that could be related to the precipitation of calcium salts (in the supernatant it was not detected an increase of SS). During the start-up of an Anammox Membrane Sequencing Batch Reactor (MSBR), Trigo *et al.* (2006) observed a high inhibition of Anammox biomass due to calcium salts (mainly calcium phosphate) precipitation when using synthetic wastewater with a Ca/P relation of 5.45 g g^{-1} (operating pH, 7.8-8.7) and 2.71 g g^{-1} (operating pH, 8.0-8.7). In a MSBR system, the membrane acts as a barrier that may retain inorganic precipitation in a more efficient way than conventional SBR systems. However, the drastic decrease of the solubility product constant (K_{SP}) of calcium phosphate at low temperatures (Lide, 1993) could lead to an accumulation of salts in the SBR system and the consequent inhibition of Anammox bacteria. When the CaCl_2 concentration in the influent synthetic wastewater was reduced by 95%, precipitation of salts was avoided and the mixed liquor acquired a clear aspect. Subsequently, the operating temperature was reduced to $20 \text{ }^\circ\text{C}$ for two more weeks (period IV). During period III and IV, nitrite was completely consumed and the stoichiometry of the Anammox process changed with temperature, since a decrease of the NH_4^+ -N concentration in the effluent was observed.

In period V, the Anammox SBR was operated during more than 5 weeks at $18 \text{ }^\circ\text{C}$. In this experimental period, a nitrogen loading rate of $0.30 \text{ kg N (m}^3 \text{ day)}^{-1}$ was applied and nitrite (limitant substrate) was completely depleted during the whole experimental period. Table 9.4 shows the stoichiometry observed at $18 \text{ }^\circ\text{C}$ in comparison with the one registered at $30 \text{ }^\circ\text{C}$. The NO_2^- -N to NH_4^+ -N ratio of period V was 1.05 ± 0.01 which differs considerably from the one registered at $30 \text{ }^\circ\text{C}$ (1.38 ± 0.02) and the ratio 1.32 commonly reported in literature (see Equation 2). However, Dalsgaard and Thamdrup (2002) also reported a 1:1 stoichiometry for the reaction between nitrite and ammonium in anoxic incubations of the Anammox process (coming from marine sediments) using synthetic wastewater at a working temperature of $15 \text{ }^\circ\text{C}$.

Therefore, a temperature dependency of the Anammox stoichiometry is observed. Moreover, the NO_3^- -N produced per unit of NH_4^+ -N consumed observed at $18 \text{ }^\circ\text{C}$ was 0.31 ± 0.02 . As observed in Figure 9.5 (b), the SAA was very close to the nitrogen loading rate implemented in the SBR strategy.

Table 9.4 – Ratio of substrate consumption and nitrate production during the operation at 30 and 18 °C.

Temperature (°C)	NO ₂ ⁻ -N / NH ₄ ⁺ -N	NO ₃ ⁻ -N / NH ₄ ⁺ -N
30	1.38 ± 0.02	0.67 ± 0.05
18	1.05 ± 0.01	0.31 ± 0.02

Finally, in period VI the operating temperature was reduced to 15 °C. Since the actual Anammox activity was extremely close to the nitrogen loading rate, after 2 days of operation the reactor became unstable and accumulated nitrite. Then, in day 108, the nitrogen loading rate was reduced to 0.10 kg N (m³ day)⁻¹, but the reactor did not manage properly this nitrogen load. Therefore, 0.05 kg N (m³ day)⁻¹ were implemented on day 123 in order to recover progressively the Anammox biomass activity.

9.2.3. Biomass properties

The physical characteristics of Anammox biomass during the whole experiment did not experienced relevant changes. Fluorescent In-Situ Hybridation (FISH) experiments demonstrated that the Anammox biomass studied in this work belongs to the “*Candidatus Kuenenia stuttgartiensis*” specie (Dapena-Mora *et al.*, 2004c).

The ratio VSS/SS of the biomass was relatively low (0.4-0.43) since it was attached to an inorganic solid (zeolite), which provides to the biomass aggregate a high density. Consequently, the SVI was relatively low (namely, 56.6-60.0 mL g⁻¹ VSS).

Table 9.5 shows some physical properties of samples of the Anammox aggregates taken in periods II and V. As observed, no significant changes took place, being the mean diameter around 1.35 mm. The shape ratio of the Anammox aggregates, defined as the ratio of its longer dimension to its shorter dimension, was 1.5 along the experiment, which demonstrates that the aggregates had an ovoid shape (see Figure 9.6). Moreover, the SBR strategy led to a high sludge retention time in the range of 126-180 days during this study.

Table 9.5 – Physical properties of the Anammox biomass tested in this study.

Parameters	Units	Day 21	Day 70
Shape Ratio	-	1.56	1.53
Average diameter	mm	1.34	1.36
Minimum diameter	mm	0.19	0.12
Maximum diameter	mm	2.90	2.65
Particle mean volume	mL	1.25	1.31

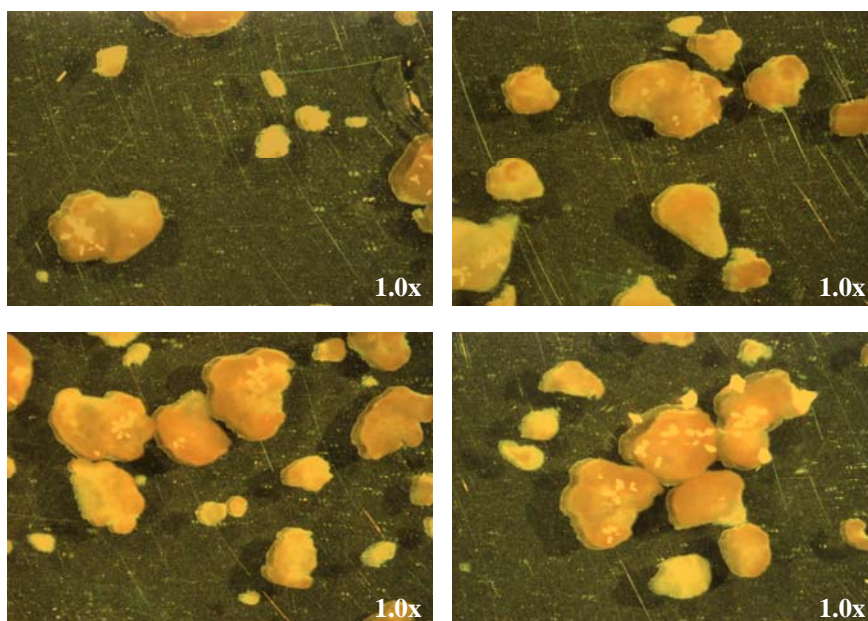


Figure 9.6 – Photographs of the biomass aggregates from the Anammox SBR working at 18°C.

9.3. CONCLUSIONS

- ✓ In this study, an Anammox SBR was operated at low temperatures (18 °C) to treat a highly nitrogen loaded synthetic wastewater (with a $\text{NH}_4^+\text{-N}$ to $\text{NO}_2^-\text{-N}$ ratio of 1.0).

- ✓ The temperature dependency of Anammox biomass was assessed by Specific Anammox Activity (SAA) tests. The maximum SAA was detected at 40°C. For temperatures of 45 °C a decrease in Anammox activity and a cytochrome transfer to the liquid medium was observed.
- ✓ The temperature dependency on Anammox activity was adjusted to the Arrhenius and to a modified Ratkowsky model. The Arrhenius model was adjusted for temperatures between 10 and 30 °C; above this temperature range, the model equation provided non-realistic high biomass activity. The modified Ratkowsky model was capable to reproduce the temperature dependency of Anammox biomass between 10 and 45 °C.
- ✓ The Anammox operating strategy in a SBR must provide high sludge retention, especially when working at low temperatures. In this work, high SRT was obtained by working with zeolite-attached Anammox biomass and by performing 30 minutes of stirring without substrate supply before the sedimentation period to deplete completely the nitrite inside the Anammox reactor and to favour the desorption of nitrogen gas bubbles.
- ✓ The stoichiometry of the Anammox process highly depends on the operating temperature. For 30°C, a NO_2^- -N to NH_4^+ -N ratio of 1.38 was registered, while a value of 1.04 at 17.5 °C was detected. Therefore, this stoichiometry must be taken into account when the Anammox process is operated at low temperatures, since an excess of NO_2^- -N highly inhibits Anammox biomass.

10. General Conclusions and recommendations.

10.1 GENERAL CONCLUSIONS

In this study, three advanced biological nitrogen removal treatments have been tested to treat highly ammonium loaded wastewaters, such as supernatants from anaerobic digestion of protein rich organic substrates. The processes tested were the biological nitrogen removal over nitrite in a SBR, the SHARON/Denitrification process and a combined partial nitrification/Anammox process.

The main conclusions extracted from this work are compiled and discussed in this section.

Referring to Chapter 4 - Operation and model description of a sequencing batch reactor treating reject water for Biological Nitrogen Removal over nitrite.

In this Chapter, an SBR was operated to treat $0.87 \text{ kg (m}^3 \text{ day)}^{-1}$ of sludge reject water from a municipal wastewater treatment plant. The biological nitrogen removal was carried out over nitrite to save 25% of aeration costs and 40% of the biodegradable COD to denitrify. When the biological treatment worked under steady state conditions, the most relevant kinetic and stoichiometric parameters were assessed in a closed intermittent flow respirometer constructed in this study. Then, an extended activated sludge model was proposed to model the SBR performance giving good results. From this chapter, the most relevant conclusions are:

- ✓ An SBR can be efficiently used to carry out the Biological Nitrogen Removal (BNR) over nitrite for the treatment of a real reject water from a municipal WWTP. This highly ammonium concentrated wastewater has a reduced buffer capacity and a very low BOD_{ST} and, consequently, an external carbon source for denitrification is required for its treatment.
- ✓ Nitrogen can be completely removed when operating with 3 cycles per day, temperature 30°C , SRT 11 days and HRT 1 day. During the operational cycle,

three alternating aerobic/anoxic periods should be performed to avoid alkalinity restrictions. Furthermore, oxygen supply and working pH range must be controlled in order to achieve BNR via nitrite, making the process considerably more economic. For the particular studied case, under steady state conditions, an sAUR and sNUR of $19 \text{ mg NH}_4^+\text{-N g}^{-1} \text{ VSS h}^{-1}$ and $40 \text{ mg NO}_2^-\text{-N g}^{-1} \text{ VSS h}^{-1}$, respectively, were reached.

- ✓ It is necessary to modify IWA activated sludge models to describe BNR via nitrite. Both nitrification and denitrification must be described as two-step reactions inhibited by ammonia and nitrous acid concentrations.
- ✓ A closed intermittent-flow respirometer is a very good tool to assess model parameters. The main kinetic and stoichiometric parameters for carbon oxidation and nitrogen removal lay inside the range described in literature for similar biological systems. As expected, oxygen affinity constant for ammonium oxidizers was very low due to the reduced oxygen supply inside the SBR.
- ✓ The proposed model showed very good agreement between ammonium, nitrite, nitrate and dissolved oxygen experimental and simulated values under steady state conditions. Model predictions represent a useful tool to comprehend the processes that take place inside the digester. For this particular case, NOB inhibition was clearly related to the working free ammonia concentration and to dissolved oxygen concentrations inside the digester.

Referring to Chapter 5 - Modelling of a sequencing batch reactor to treat the supernatant from anaerobic digestion of the organic fraction of municipal solid waste.

Similarly to Chapter 4, the SBR technology can be used to treat supernatant from anaerobic digestion of the organic fraction of municipal solid waste (OFMSW). In this study, an SBR strategy to treat this wastewater by means of a BNR over nitrite process was modelled. To this purpose, some extensions were introduced in the model proposed in Chapter 4 in order to include pH calculation. The main conclusions extracted from this chapter are listed below:

- ✓ A model to describe the nitrification/denitrification process via nitrite for the treatment of the supernatant from Anaerobic Digestion (AD) of the Organic

Fraction of Municipal Solid Wastes (OFMSW) is proposed in this paper. The model is based on the one described in Chapter 4, but also includes the tools to calculate pH and consider its influence on the kinetics of biological processes.

- ✓ The respirometric procedure established in Chapter 4 is used to assess the main stoichiometric and kinetic parameters for model calibration. Moreover, a respirometric batch test to analyse the influence of pH on ammonium oxidizers is proposed.
- ✓ An optimum Sequencing Batch Reactor (SBR) operating cycle to treat the supernatant from AD of the OFMSW is modelled by means of the proposed model giving a good match between experimental and simulated data. Similarly to the SBR strategy proposed for the treatment of sludge reject water, in the process studied in this section, free ammonia and low dissolved oxygen concentrations were identified as the operational factors responsible for the inhibition of Nitrite Oxidizing Biomass (NOB).

Referring to Chapter 6 - COD and Nitrogen removal of supernatant of anaerobically digested piggery wastewater in a biological SBR with a Coagulation/Flocculation step.

An SBR strategy to treat supernatant from anaerobic digestion of piggery wastewater was tested in this chapter. Biological nitrogen removal over nitrite was achieved using a SBR strategy similar to those explained in chapters 4 and 5. However, if biological treatment is exclusively utilised, the effluent COD from the treated wastewater do not satisfy legal limits. Therefore, it was studied the inclusion of a coagulation/flocculation step inside the SBR operating cycle. Moreover, the effect of the main operating parameters was analysed. The conclusions extracted from this study are:

- ✓ The biological treatment of the supernatant of anaerobically digested piggery wastewater in a sequencing batch reactor with a Coagulation/Flocculation step inside the operational cycle has been proved to be an efficient alternative to remove COD, SS and $\text{NH}_4^+\text{-N}$.
- ✓ The SBR sequence consisted on three alternating aerobic/anoxic periods under controlled air supply to promote the biological nitrogen removal over nitrite.

Several Jar-Tests showed that a dosage of 800 mg FeCl₃ was necessary to meet the effluent standards established by legislation. Moreover, respirometric tests demonstrated that nitrifying biomass activity was not negatively affected by this coagulant dosage. The Coagulation/Flocculation step was inserted into the operational SBR cycle during the last 15 minutes of the third anoxic period.

- ✓ The implementation of this treatment led to a COD reduction yield of more than 66%, a SS decrease above 74% and a biological NH₄⁺-N removal of more than 98%, obtaining a suitable effluent for stream discharge into the public sewer. The total suspended solids drained from the reactor were increased only by a 10-14 %.
- ✓ The effect on biomass activity of several substrates and inhibitors, such as NH₃, HNO₂, pH and DO, was analysed by respirometric batch tests. These experiments showed that the nitrifying AOB biomass developed in the digester was very resistant to free ammonia concentrations up to 50 mg NH₃-N L⁻¹. However, free nitrous acid concentrations promoted an important decrease of ammonium oxidizers activity. An optimum pH value of 8.15 was encountered for this biomass, which had a very low oxygen affinity constant for AOB kinetics.

Referring to Chapter 7 - Operation of the SHARON-Denitrification process to treat sludge reject water using hydrolysed primary sludge to denitrify.

In Chapter 7, the SHARON/Denitrification process was applied to treat sludge reject water from a municipal WWTP. In this treatment aerobic and anoxic periods were alternated in a continuously fed chemostat reactor. At the beginning of this study, methanol was supplied during anoxic periods as the organic carbon source needed to denitrify. Subsequently, methanol was substituted by an internal stream of the same WWTP (namely, hydrolysed primary sludge). The most relevant conclusions extracted from this investigation are highlighted here:

- ✓ The application of the SHARON-Denitrification process to treat supernatant from anaerobic digestion of sewage sludge can reduce its ammonium load to more than 85%.

- ✓ The customary use of methanol to denitrify can be avoided by the utilization of supernatant of hydrolysed primary sludge, since it contains a proper amount of readily biodegradable COD. For the case under study, the use of other internal streams of the municipal WWTP was rejected due to the low quality of the biodegradable COD (hydrolysed secondary sludge) or the low BOD concentration (influent of the secondary reactor).
- ✓ When supernatant of hydrolysed primary sludge is used to denitrify, the biological efficiency is improved considerably since it buffers the system within an optimal pH range (7.5-8.5).
- ✓ Since BOD was not highly concentrated in the supernatant of hydrolysed primary sludge, the fluid dynamics of the biological system were changed significantly with respect to the strategy with methanol but maintaining the reject water influent flow-rate. Therefore, the HRT was 2.0-2.1 days when using methanol and 1.4 days when using hydrolysed primary sludge. However, the SHARON/Denitrification process achieved good nitrogen removal efficiencies when working with hydrolysed primary sludge due to a higher biomass activity.

Referring to Chapter 8 - Modelling of partial nitrification in a SHARON chemostat and in a sequencing batch reactor to achieve a suited influent to the Anammox process.

In this Chapter, two biological processes for partial nitrification of sludge reject water were investigated, modelled and compared. These processes were the partial nitrification in an SBR and the SHARON process, and represent good alternatives to obtain a suited influent to the Anammox process. In the SBR process, the inhibition of NOB activity was achieved by high free ammonia concentrations. On the other hand, the SHARON process avoided the oxidation of nitrite to nitrate due to the selected operating temperature and HRT. Both processes were modelled using the activated sludge model proposed in Chapter 5, previously calibrated by respirometry. The main conclusions extracted from this study are:

- ✓ Two efficient alternatives for the partial nitrification of sludge reject water in view of coupling it with an Anammox unit are the use of an SBR process (with total

inhibition of NOB by NH_3 concentrations) and a SHARON chemostat (where the wash out of NOB is due to the operating temperature and SRT).

- ✓ The SBR treatment is capable to assume a higher nitrogen loading rate (in this work, $2.2 \text{ kg NH}_4^+\text{-N (m}^3 \text{ day)}^{-1}$) than the one obtained by the SHARON process (for the case under study, $0.7 \text{ kg NH}_4^+\text{-N (m}^3 \text{ day)}^{-1}$). This fact is related to the high sludge retention obtained in the SBR process.
- ✓ Both processes were modelled by means of the Activated Sludge Model extended for nitrite route description and pH calculation presented in Chapter 5. This model was calibrated with simple batch respirometric tests, that minimized the calibration effort. Simulated results showed very good agreement with experimental values and provided a theoretical explanation of the inhibitions and processes that took place inside the digesters.
- ✓ Moreover, the proposed model provides a useful tool to plan the most appropriate treatment strategy for the partial nitrification of different types of highly ammonium loaded wastewaters to obtain a suited influent to the Anammox process.

Referring to Chapter 9 - Operation of an Anammox reactor to treat highly ammonium loaded wastewaters at low temperatures.

In this Chapter, the Anammox process was tested for the treatment of a highly ammonium loaded synthetic wastewater that could represent the effluent wastewater obtained in Chapter 8. Since the Anammox process has been typically described as a process that needs heating at 33-35°C, the effect of low temperatures on Anammox biomass activity was investigated. The main conclusions extracted from this chapter are:

- ✓ An Anammox SBR can be operated at low temperatures (18 °C) to treat a highly nitrogen loaded (synthetic) wastewater (with a $\text{NH}_4^+\text{-N to NO}_2^-\text{-N}$ ratio of 1.0).
- ✓ The temperature dependency of Anammox biomass can be easily assessed by the Specific Anammox Activity (SAA) tests proposed by Dapena-Mora *et al.* (2007a). In this study, the maximum SAA was detected at 40°C. For temperatures

of 45 °C a decrease in Anammox activity and a cytochrome transfer to the liquid medium was observed.

- ✓ The temperature dependency on Anammox activity can be adjusted to the Arrhenius and to a modified Ratkowsky model. The Arrhenius model gives good correlation between experimental and modelled data for temperatures between 10 and 30 °C; above this temperature range, the model equation provided non-realistic high biomass activity. The modified Ratkowsky model is capable to reproduce the temperature dependency of Anammox biomass between 10 and 45 °C.
- ✓ The Anammox operating strategy in a SBR must provide high sludge retention, especially when working at low temperatures. In this work, high SRT was obtained by working with zeolite-attached Anammox biomass and by performing 30 minutes of stirring without substrate supply before the sedimentation period to deplete completely the nitrite inside the Anammox reactor and to favour the desorption of nitrogen gas bubbles.
- ✓ The stoichiometry of the Anammox process highly depends on the operating temperature. For 30°C, a NO_2^- -N to NH_4^+ -N ratio of 1.38 was registered, while a value of 1.04 at 17.5 °C was detected. Therefore, this stoichiometry must be taken into account when the Anammox process is operated at low temperatures, since an excess of NO_2^- -N highly inhibits Anammox biomass.

10.2 RECOMMENDATIONS

For further investigation, the following recommendations are proposed:

Experimental devices.

- In biological reactors, other state variables could be registered and modelled, such as the ORP and the conductivity.
- The addition of acid and/or base to control the pH in the intermittent-flow respirometer should be performed with peristaltic pumps. Moreover, the time

spent to perform the acid and/or base additions could be registered to model alkalinity consumption in batch respirometric tests.

Laboratory experiments.

- In order to evaluate the NH_4^+ -N and NO_2^- -N profiles during the SHARON/Desnitrification process, this process should be performed in a reactor of bigger volume. In that case, as the effluent flow-rate would be higher, more samples could be analysed (not only the integrated sample studied in this work) and the evolution of a SHARON-Denitrification cycle could be analysed and modelled in a more detailed way.
- The biological nitrogen removal over nitrite process could be performed using a granular reactor as described by Arrojo *et al.* (2004) or Vázquez-Padín *et al.* (2006). This type of treatment is very efficient, produces little sludge and spends very few time to perform the settle of biomass.
- The behaviour of the Anammox process to treat anaerobically digested piggery wastewater and/or supernatant from anaerobic digestion of the Organic Fraction of Municipal Solid Waste (previously treated in a partial nitrification unit) could be evaluated.
- The use of alternative biological nitrogen removal processes, such as the autotrophic denitrification with sulphide, the CANON and/or the BABE process could be evaluated at lab-scale conditions.

Modelling of experimental results.

- In this thesis, the maximum activity of heterotrophs and autotrophs is assessed by the combined parameters μ_X . However, it would be interesting to develop and/or use a methodology to assess the maximum specific growth rate (μ) in a reliable way. The assessment of this parameter would lead to a better characterisation of the studied biological processes.

- In this study, the pH has been modelled considering small time intervals and calculating the pH value at the end of each considered interval. This pH value becomes an initial condition for the next time step. In the last years, other extensions of activated sludge and/or anaerobic digestion models have been published considering pH as an state variable (De Gracia *et al.*, 2006; Magrí *et al.*, 2007). Although the utilisation of these kind of models implies more analysis effort for calibrating them, the time necessary to program these models is very reduced when compared with the proposed model.
- Denitrification was modelled in this work considering the conversion of nitrate to nitrite and further to nitrogen gas. However, as stated in the introduction, there are other intermediates that could be formed (NO, N₂O). The conditions that lead to the accumulation of NO and N₂O could be analysed in future work.

11. References.

- Abeling, U., Seyfried, C.F. (1992). Anaerobic-aerobic treatment of high-strength ammonium wastewater - nitrogen removal via nitrite. *Wat. Sci. Tech.*, 26, 1007– 1015.
- Abeling, U., Seyfried, C.F. (1993). Anaerobic-aerobic treatment of potato-starch wastewater. *Wat. Sci. Tech.*, 28(2), 165-176.
- Abma, W., Schultz, C., Mulder, J.M., van Loosdrecht, M.C.M., van der Star, W., Strous, M., Tokutomi, T. (2007) The advance of Anammox. *Water* 21, 36-37.
- Ahn, Y.H., Hwang, I.S., Min, K.S. (2004). Anammox and partial denitrification in anaerobic nitrogen removal from piggery waste. *Wat. Sci. Tech.*, 49 (5–6), 145-153.
- Andrews, J. F. (1993) Modelling and simulation of wastewater treatment processes. *Wat. Sci. Tech.* 28 (11-12) 141-150.
- Anthonisen, A.C., Loehr, R.C., Prakasam, T.B.S., Srinath, E.G. (1976). Inhibition of nitrification by ammonia and nitrous acid. *Journal WPCF*, 48, 835-852.
- APHA (1998). Standard methods for the examination of water and wastewater, 20th edn, *American Public Health Association*, Washington DC, USA.
- Arnold, E., Böhm, B., Wilderer, P.A. (2000). Application of activated sludge and sequencing batch technology to treat reject water from sludge dewatering systems: a comparison. *Wat. Sci. Tech.*, 41, 115-122.
- Arrojo, B., Mosquera-Corral, A., Garrido, J.M., Méndez, R. (2004). Aerobic granulation with industrial wastewater in sequencing batch reactors. *Wat. Res.*, 38, 3389-3399.
- Artan, N., Wilderer, P., Orhon, D., Morgenroth, E., Ozgur, N. (2001) The mechanism and design of sequencing batch reactor systems for nutrient removal – the state of the art. *Wat. Sci. Tech.*, 43, (3), 53-60.
- Austermann-Haun, U., Meyer, H., Seyfried, C., Rosenwinkel, K.H. (1999). Full scale experiences with anaerobic/aerobic treatment plants in the food and beverage industry. *Wat. Sci. Tech.*, 40(1), 305-312.
- Bae, W., Rittman, B.E. (1996) A structured model of dual limitation kinetics. *Biotechnology and bioengineering*, 49, 683-689.
- Barnard, J.L. (1975) Biological nutrient removal without the addition of chemicals. *Wat. Res.* 9 (485-490).
- Bernardes, R.S. (1996) Modelling nutrient removal in a sequencing batch reactor with respirometry. PhD Thesis, *Wageningen Agricultural University*, Wageningen, The Netherlands.
- Bernardes, R.S., Klapwijk, A. (1996) Biological nutrient removal in a sequencing batch reactor treating domestic wastewater. *Wat. Sci. Tech.* 33 (3) 29-38.

- Bernardes, R.S., Spanjers, H., Klapwijk, A. (1996) Modelling respiration rates in a nitrifying SBR treating domestic wastewater. *Env. Tech.* 17 (4), 337-348.
- Béline, F., Boursier, H., Guiziou, F., Paul, E. (2005) Development of a model for biological nitrogen removal reactors treating piggery wastewater. In: *Proceedings of the 3rd IWA Leading-Edge Conference & Exhibition on Water & Wastewater*. 6-8 June 2005. Sapporo, Japan.
- Bernet N., Dangcong P., Delgenès P., Moletta, R. (2001). Nitrification at Low Oxygen Concentration in Biofilm Reactor. *Journal of Environmental Engineering*, 127(3) 266-271
- Bidlingmaier W. (2000) Biologische Abfallverwertung, *Ed. Bidlingmaier*, Ulmer.
- Bock, E., Stüven, R., Schmidt, I., Zart, D. (1995) Nitrogen loss caused by denitrifying *Nitrosomonas* cells using ammonium or hydroxylamine as electron donors and nitrite as electron acceptor. *Arch. Microbiol.* 163. 16-20.
- Bortone, G., Gemeli, S., Rambaldi, A., Tilche, A. (1992) Nitrification, denitrification and biological phosphate removal in sequencing batch reactors treating piggery wastewater. *Wat. Sci. Tech.*, 26, (5-6), 977-985.
- Bortone, G., Malaspina, F., Stante, L., Tilche, A. (1994) Biological nitrogen and phosphorus removal in an anaerobic/anoxic sequencing batch reactor with separated biofilm nitrification. *Wat. Sci. Tech.*, 30, (6), 303-313.
- Brands, E., Liebeskind, M., Dohmann, M. (1994). Parameters for dynamic simulation of wastewater treatment plants with high rate and low rate activated sludge tanks. *Wat. Sci. Tech.*, 30, 211-214.
- Brock, T.D., Madigan, M.T., Martinko, J.M., Parker, J. (1997). *Biology of microorganisms*. 8th ed., *Upper Saddle River NJ*, USA, Prentice Hall.
- Brouwer, M., van Loosdrecht, M.C.M., Heijnen, J.J. (1996). *Behandeling van sticstofrijke retorstromen op rioolwaterzuiveringsinstallaties enkelvoudig reactorsysteem voor de verwijdering via nitriet*. *STOWA rapport 96-01*, STOWA Utrecht, the Netherlands.
- Brouwer, H., Klapwijk, A., Keesman K. J. (1998) Identification of activated sludge and wastewater characteristics using respirometric batch-experiments. *Wat. Res.*, 32, 1240-1254.
- Caffaz, S., Canziani, R., Lubello, C., Santianni, D. (2005) Upgrading of Florence wastewater treatment plant: co-digestion and nitrogen autotrophic removal. *Wat Sci. Tech.* 52(4) 9-17.
- Campos, A.E. (2001). Optimización de la digestión anaerobia de purines de cerdo mediante codigestión con residuos orgánicos de la industria agroalimentaria. PhD thesis. *Universitat de Lleida*. (in Spanish)
- Canigué, R., López, H., Rusalleda, M., Balaguer, M.D., Colprim, J. (2007) Operation of a Partial Nitrification-SBR (PN-SBR) treating urban landfill leachate, to achieve a suitable influent for an anammox reactor. In: *Proceedings of the CLONIC Final Workshop'07. Closing the nitrogen cycle from urban landfill leachate by biological nitrogen removal over nitrite and thermal treatment*. pp. 32-41

- Carucci, A., Chiavola, A., Majone, M., Rolle, E. (1999). Treatment of tannery wastewater in a sequencing batch reactor. *Wat. Sci. Tech.*, 40(1), 253-259.
- Cech, J.S., Chudoba, J., Grau, P. (1984). Determination of kinetic constants of activated sludge microorganisms. *Wat. Sci. Tech.*, 17, 259-272.
- Chen, M., Kim, J.H., Kishida, N., Nishimura, O., Sudo, R. (2004). Enhanced nitrogen removal using C/N load adjustment and real-time control strategy in sequencing batch reactors for swine wastewater treatment. *Wat. Sci. Tech.*, 49(5-6), 309-314.
- Christensen, M.H., Harremoes, P. (1977) Biological Denitrification of sewage: A literature review. *Prog. Wat. Tech.* 8(4/5) p.509
- Chudoba, J., Albokova, J., Cech, J. (1989) Determination of kinetic constants of activated sludge microorganisms responsible for degradation of xenobiotics. *Wat. Res.* 23. 1431-1438.
- Chung, J., Bae, W., Lee, Y., Ko, G., Lee, S., Park, S. (2003). Investigation of the effect of free ammonia concentration upon leachate treatment by shortcut biological nitrogen removal process. In: *IWA Speciality Symposium on Strong Nitrogenous and Agro-Wastewater*, Vol. 1. Seoul, Korea, June 11-13, 2003, 93-104.
- Chung, J., Shim, H., Lee, Y.W., Bae, W. (2005) Comparison of the influence of free ammonia and dissolved oxygen on nitrite accumulation between suspended and attached cells. *Environmental Technology*, 26. 21-33
- Chynoweth, D. P., Wilkie, A.C., Owens, J.M. (1999) Anaerobic Treatment of Piggery Slurry. *Asian-Aus. J. Anim Sci.* 12(4), 1999, 607-628.
- Cirpus, I.E.Y., de Been, M., Op den Camp, H.J.M., Strous, M., Le Paslier, D., Kuenen, G.J., Jetten, M.S.M. (2005). A new soluble 10 kDa monoheme cytochrome c-552 from the anammox bacterium *Candidatus "kuenenia stuttgartiensis"*. *FEMS Microbiology Letters*, 252, 273-278.
- Company (2000). Coagulantes y floculantes aplicados en el tratamiento de aguas. *Gestió i promoció editorial, S.L.* (In spanish).
- Copp, J.B., Vanrolleghem, P., Spanjers, H. (2002). Respirometry in Control of the Activated Sludge Process: Benchmarking Control Strategies. *Scientific and Technical Report No. 12*. IWA Publishing, London, UK.
- Dalsgaard, T., Thamdrup, B. (2002). Factors Controlling Anaerobic Ammonium Oxidation with Nitrite in Marine Sediments. *Applied and Environmental Microbiology*, 68 (8), 3802-3808
- Dalsgaard, T., Thamdrup, B., Canfield, D.E.C. (2005). Anaerobic ammonium oxidation (anammox) in the marine environment. *Research in Microbiology*, 156(4) 457-464.
- Dapena-Mora, A., Campos, J.L., Mosquera-Corral, A., Jetten, M.S.M., Méndez, R. (2004a). Stability of the ANAMMOX process in a gas-lift reactor and a SBR. *Journal of Biotechnology*, 110. 159-170

- Dapena-Mora, A., Arrojo, B., Campos, J.L., Mosquera-Corral, A., Méndez, R. (2004b). Improvement of the settling properties of Anammox sludge in an SBR. *Journal of Chemical Technology and Biotechnology*, 79 (12), 1412-1420.
- Dapena-Mora, A., Van Hulle, SWH, Campos, JL, Mendez, R, Vanrolleghem, PA, Jetten, M (2004c) Enrichment of Anammox biomass from municipal activated sludge: experimental and modelling results. *Journal of Chemical Technology and Biotechnology*. 79 (12): 1421-1428.
- Dapena-Mora, A., (2007). Wastewater treatment by anammox process: A short-circuit in the natural nitrogen cycle. PhD. *University of Santiago de Compostela (USC)*, Spain.
- Dapena-Mora, A., Fernández, I., Campos, J.L., Mosquera-Corral, A., Méndez, R., Jetten, M.S.M. (2007a). Evaluation of activity and inhibition effects on Anammox process by batch tests based on the nitrogen gas production. *Enzyme and Microbial Technology*, 40 (4), 859-865.
- Dapena-Mora, A., Fernández, I., Figueroa, M., Vázquez-Padín, J.R., Mosquera-Corral, A., Campos, J.L., Méndez, R. (2007b). Proceso Anammox: Un cortocircuito en el Ciclo de Nitrógeno para la depuración de aguas residuales. *Retema*. 116: 64-46
- De Baere L. (2004) The role of anaerobic digestion in the treatment of MSW: state of the art. In: *Proceedings of IWA Conference Anaerobic Digestion 2004*, AD 10th, Montreal, Canada, August 29- September 2, 2004, pp 395-400.
- De Gracia, M., Sancho, L., García-Heras, J.L., Vanrolleghem, P., Ayesa, E. (2006) Mass and charge conservation check in dynamic models: Application to the new ADM1 model. *Wat. Sci. Tech.*, 53(1) 225-334.
- Deng Petersen, P., Jensen, K., Lyngsie, P., Hendrik Johansen, N. (2003). Nitrogen removal in industrial wastewater by nitrification and denitrification — 3 years of experience. *Wat. Sci. Tech.* 47(11), 181-188.
- Dircks, K., Pind, P.F., Mosbaek, H., Henze, M. (1999). Yield determination by respirometry – the possible influence of storage under aerobic conditions in activated sludge. *Water SA*, 25, 1. 69-74.
- Dold, P.L., Marais, G.v.R. (1986) Evaluation of the general Activated Sludge Model proposed by the IAWPRC Task Group. *Wat. Sci. Tech.* 18(6). 63-89
- Dold, P.L., Fairlamb, P.M., Jones, R., Takács, I., Murthy, S. (2007) Sidestream modelling incorporated into whole plant simulation. In: *Proceedings of the CLONIC Final Workshop'07. Closing the nitrogen cycle from urban landfill leachate by biological nitrogen removal over nitrite and thermal treatment*. pp. 114-122.
- Egli K., Fanger U., Alvarez P.J.J. (2001) Enrichment and characterization of an anammox bacterium from a rotating biological contactor treating ammonium-rich leachate. *Archives of Microbiology*, 175, 198-207.
- Ekama, G.A., Marais, G.v.R. (1984). Nitrification in theory. Design and operation of nutrient removal Activated Sludge processes. Chapter 5, Pretoria, South Africa, *Water Research Commission*.

- EPA (1975) Process Design Manual for Nitrogen Control, Office of the Technology Transfer, U.S. Environmental Protection Agency, Washington, DC.
- EPA (1993) Manual of nitrogen control. EPA/625/R-93/010 US environmental Protection Agency. Washington DC, USA.
- Fernández I. (2006). Estudio para el desarrollo de reactores Anammox. DEA. *University of Santiago de Compostela (USC)*, Spain. (In Spanish)
- Fernández, I., Vázquez-Padín, J.R., Mosquera-Corral, A., Campos, J.L., Méndez, R. (2006). Biofilm and granular systems to improve Anammox biomass retention, 7th IWA Specialty Conference on Small Water and Wastewater Systems, Mexico City, Mexico.
- Ferrer, J., Seco, A. (2003) Tratamientos biológicos de aguas residuales. Universidad Politécnica de Valencia. Ed. UPV. (in Spanish)
- Flotats, X. (2000) La digestió anaeròbica com a alternativa de tractament o com a procés previ al compostatge. Quarta Jornada Tècnica sobre la gestió de residus municipals. *Universitat Politècnica de Catalunya*. (in Catalan)
- Flotats, X., Bonmatí, A., Campos, E., Teira, M.R. (2000). El proceso de secado de purines en el marco de gestión integral de residuos ganaderos. *Residuos*. Vol. 53, 40-46. (in Spanish)
- Flotats, X., Campos, E., Palatsi, J. (2004). Concentración de deyecciones ramaderas mediante procesos térmicos. *II Encuentro Internacional Gestión de Residuos Orgánicos*. 28-29 d'octubre de 2004. Pamplona, Spain. (in Spanish)
- Fux, C., Bohler, M., Huber, P., Brunner, I., Siegrist, H. (2002). Biological treatment of ammonium-rich wastewater by partial nitritation and subsequent anaerobic ammonium oxidation (anammox) in a pilot plant. *Journal of Biotechnology*, 99, 295-306.
- Fux, C. (2003). Biological nitrogen elimination of ammonium-rich sludge digester liquids. PhD thesis, *ETH-Zürich*, Switzerland.
- Fux C., Lange K., Faessler A., Huber P., Grueniger B., Siegrist H. (2003) Nitrogen removal from digester supernatant via nitrite - SBR or SHARON? *Wat. Sci. Tech.*, 48(8), 9-18.
- Fux, C., Marchesi, V., Brunner, I., Siegrist, H. (2004). Anaerobic ammonium oxidation of ammonium-rich waste streams in fixed-bed reactors. *Wat. Sci. Tech.*, 49 (11-12), 77-82.
- Fux, C., Siegrist, H. (2004). Nitrogen removal from sludge digester liquids by nitrification/denitrification or partial nitritation/anammox: environmental and economical considerations, *Wat. Sci. Tech.*, 50, 19-26.
- Galí, A., Dosta, J., Mata-Álvarez, J. (2005). Optimisation of a nitrification-denitrification process in a SBR for the treatment of reject water via nitrite. In: *Proceedings of IWA Specialised Conference Nutrient Management in Wastewater Treatment Processes and Recycle Streams*. Krakow, Poland. 925-932.
- Galí, A., Dosta, J., Mata-Álvarez, J. (2006a) Use of hydrolysed primary sludge as external carbon source for denitrification in a SBR treating reject water via nitrite. *Ind. Eng. Chem. Res.* 45, 7661-7666.

- Gali, A., Dosta, J., Van Loosdrecht, M.C.M., Mata-Álvarez, J. (2006b) BNR via nitrite of reject water with a SBR and chemostat SHARON/Denitrification process. *Ind. Eng. Chem. Res.* 45, 7656-7660.
- Gali, A., Dosta, J., Van Loosdrecht, M.C.M., Mata-Álvarez, J. (2007) Two ways to achieve an Anammox influent from reject water treatment: partial SBR nitrification and SHARON process. *Process Biochemistry*, 42(4), 715-720.
- Garbossa, L. H. P., Rodríguez, J. A., Lapa, K. R., Foresti, E. A. (2005) A novel two-module integrated aerobic-anaerobic bioreactor for denitrification using H₂S from biogas. In: *Proceedings of the IWA Specialized Conference Nutrient Management in Wastewater Treatment Processes and Recycle Streams*, IWA Publishing: Krakow, Poland. 347-355.
- Garrido, J.M., van Benthum, W.A.J., van Loosdrecht M.C.M., Heijnen, J.J. (1997). Influence of dissolved oxygen concentration on nitrite accumulation in a biofilm airlift suspension reactor. *Biotechno. Bioeng*; No. 53, 168-178.
- Gernaey, A. K., Petersen, B., Ottoy, J. P., Vanrolleghem, P. (2001) Activated sludge monitoring with combined respirometric titrimetric measurements. *Wat. Sci. Tech.* 35(5) 1280-1294.
- Gernaey, A.K., Petersen, B., Nopens, I., Comeau, Y., Vanrolleghem, P. (2002) Modeling aerobic carbon source degradation using titrimetric data and combined respirometric-titrimetric data: Experimental data and model structure. *Biotechnology and bioengineering*, Vol. 79, No. 7.
- Generalitat de Catalunya (1992) Reglament guia de l'ús i els abocaments d'aigües residuals al clavegueram. *Approved 23th july 1992 by the Consell de Direcció de la Junta de Sanejament del Departament de medi ambient de la Generalitat de Catalunya*. Article 5, chapter 2.
- Ghyoot, W., Vandaele, S., Verstraete, W. (1999) Nitrogen removal from sludge reject water with membrane-assisted bioreactor. *Wat. Res.*, 33, 23-32.
- Gil, K.I., Choi, E. (2004). Nitrogen removal by recycle water nitrification as an attractive alternative for retrofit technologies in municipal wastewater treatment plants. *Wat. Sci. Tech.*, 49(5-6), 39-46.
- Grady Jr., C.P.L., Daigger, G.T., Lim, H.C. (1999) Biological Wastewater Treatment. *Marcel Dekker, Inc.* USA.
- Graja, S., Wilderer, P.A. (2001) Characterization and treatment of the liquid effluents from the anaerobic digestion of biogenic solid waste. *Wat. Sci. Tech.* 43 (3). pp 265-274
- Groeneweg, J., Sellner, B., Tappe, W. (1994) Ammonia oxidation in nitrosomonas at NH₃ concentrations near Km: Effects of pH and temperature. *Wat. Res.*, 28, pp. 2561-2566.
- Grontmij (2004) SHARON N-Removal Over Nitrite For treatment of nitrogen-rich wastewaters. *Grontmij Water & Reststoffen*. De Bilt, 23 February 2004. Available on Line at www.grontmij.nl
- Grunditz, C., Dalhammar, G. (2001) Development of nitrification inhibition assays using pure cultures of Nitrosomonas and Nitrobacter. *Wat. Res.*, 35(2), 433-440.

- Guisasola, A., Jubany, I., Baeza, J. A., Carrera, J., Lafuente, J., 2005. Respiriometric estimation of the oxygen affinity constants for biological ammonium and nitrite oxidation. *J Chem Technol Biotechnol*, 80, 388-396.
- Gujer, W., Henze, M., Mino, T., van Loosdrecht, M. (1999). Activated Sludge Model No. 3. *Wat. Sci. Tech.* 39(1) 183-193.
- Gutiérrez O. (2003) Identificació de paràmetres cinètics i estequiomètrics del procés de depuració de fangs actius mitjançant tècniques respiromètriques. PhD Thesis. *Universitat de Girona*. Spain. (in Catalan).
- Güven, D., Dapena-Mora, A., Kartal, B., Schmid, M.C., Maas, B., van de Pas-Schoonen, K., Sozen, S., Méndez, R., Op den Camp, H.J.M., Jetten, M.S.M., Strous, M., Schmidt, I. (2005) Propionate oxidation by and methanol inhibition of anaerobic ammonium-oxidizing bacteria. *Appl. Env. Microbiol.*, 71(2), 1066-1071.
- Hans, M.J., Helle, F. (1997). Don't reject the idea of treating reject water. *Wat. Sci. Tech*, Vol.35, No.10, 27-34.
- Hao, O.J., Kim, M.H. (1990) Continuous pre-anoxic and aerobic digestion of waste activated sludge. *Journal of Environmental Engineering*, 116, 863-879.
- Hao X., Heijnen J.J., van Loosdrecht M.C.M. (2002). Model-based evaluation of temperature and inflow variations on a partial nitrification-ANAMMOX biofilm process. *Water Reserarch*, 36, 4839-4849.
- Haug RT. The practical handbook of Compost Engineering. Lewis publishers. Boca Ratón. Florida. (1993)
- Hellinga, C., van Loosdrecht, M.C.M., Heijnen, J.J. (1997) Model based design of a novel process for ammonia removal from concentrated flows. *Proc. 2nd Mathmod, TU Vienna Austria*.
- Hellinga, C., Schellen, A.A.J.C., Mulder, J.W. (1998) The SHARON Process: an innovative method for nitrogen removal from ammonium-rich wastewater. *Wat. Sci. Tech.*, 37, (9), 135-142.
- Hellinga, C., Van Loosdrecht, M.C.M., Heijnen, J.J. (1999). Model based design of a novel process for Nitrogen Removal from concentrated flows *Mathematical and Computer Modeling of Dynamical Systems* 5(4), 351-371.
- Henze, M., Grady, C. P. L., Jr, Gujer, W., Marais, G.v.R., Matsuo, T. (1987). Activated Sludge Model No. 1. *IAWPRC Scientific and technical Report No.1*, IAWPRC, London.
- Henze, M. (1992) Characterization of wastewater for modelling of activated sludge processes. *Wat. Sci. Tech.* 25(6) 1-15.
- Henze, M., Gujer, W., Mino, T., Matsuo, T., Wentzel, C., Marais, G.v.R., van Loosdrecht, M.C.M. (1999) Activated Sludge Model No.2d, ASM2D. *Wat. Sci. Tech.* 39(1) pp 165-182
- Henze, M., Gujer, W., Mino, T., van Loosdrecht, MCM (2000) Activated Sludge Models ASM1, ASM2, ASM2d and ASM3. *IWA Publishing*, London.

- Henze, M., Harremoës, P., Jansen, J.C., Arvin, E. (2002) Wastewater treatment: biological and chemical processes. 3rd Edition. Ed. Springer, Berlin.
- Hippen, A., Rosenwinkel, K.H., Baumgarten, G., Seyfried, C.F. (1997) Aerobic deammonification: a new experience in the treatment of wastewater. *Water Sci. Tech.* 35(10), 111-120.
- Hoover, S.R., Porges, N. (1952) Assimilation of dairy wastewater by activated sludge – II. The equations of synthesis and rate of oxygen utilization. *Sew. and Ind. Wastes*, 25(10) 1196
- Hunik, J.H. (1993) Engineering aspects of nitrification with immobilised cells. PhD Thesis, Wageningen Agricultural University.
- Hunik JH; Tramper J; Wijffels RH (1994) A strategy to scale up nitrification processes with immobilized cells of *Nitrosomonas europaea* and *Nitrobacter agilis*. *Bioprocess Eng* 11: 73-82 (1994).
- Hwang, I.S., Min, K.S., Choi, E., Yun, Z. (2005) Nitrogen removal from piggery waste using the combined SHARON and ANAMMOX process. *Wat. Sci. Tech.* 52 (10-11). 487-494.
- Ilies, P., Mavinic, D. (2001). The effect of decreased ambient temperature on the biological nitrification and denitrification of a high ammonia landfill leachate. *Wat. Res.*, 35, 2065-2072.
- Imajo, U., Tokutomi T., Furukawa K. (2004). Granulation of Anammox microorganisms in up-flow reactors, *Wat. Sci. Tech.*, 49, 155-163.
- Insel G., Karahan Gül Ö., Orhon D., Vanrolleghem P.A., Henze M. (2002) Important limitations in the modeling of activated sludge - Biased calibration of the hydrolysis process. *Wat. Sci. Tech.*, 45(12), 23-36.
- Izzet, H.B., Wentzel, M.C., Ekama, G.A. (1991) The effect of thermophilic heat treatment on the anaerobic digestibility of primary sludge. Research report no W76, University of Cape Town, Cape Town South Africa.
- Janus, H.M., van der Roest, H.F. (1997) Do not reject the idea of treating reject water, *Wat. Sci. Tech.* 35 (10). 27–34.
- Jenicek, P., Svehla, P., Zabranska, J. & Dohanyos, M. (2004). Factors affecting nitrogen removal by nitrification/denitrification. *Wat. Sci. Tech.*, 49(5-6), 73-79.
- Jetten M.S.M., Horn S.J., van Loosdrecht M.C.M. (1997). Towards a more sustainable wastewater treatment system. *Wat. Sci. Tech.*, 35(9), 171-179.
- Jetten M.S.M. (1999). New pathways for ammonia conversion in soil and aquatic systems. *Plant & Soil*, 230, 9-19.
- Jetten M.S.M., Strous M., van de Pas-Schoonen K.T., Schalk J., van Dongen U.G.J.M, van de Graaf A.A., Logemann S., Muyzer G., van Loosdrecht M.C.M., Kuenen J.G. (1999) The anaerobic oxidation of ammonium. *FEMS Microbiology Reviews*, 22, 421-437.
- Jokela, J., Kettunen, R., Sormunen, K., Rintal, J. (2002). Biological nitrogen removal from municipal landfill leachate: low-cost nitrification in biofilters and laboratory scale in-situ denitrification. *Wat. Res.*, 36, 4079-4087.

- Kalyuzhnyi, S., Gladchenko, M. (2004). Sequenced anaerobic-aerobic treatment of high strength, strong nitrogenous landfill leachates. *Wat. Sci. Tech.*, **49**(5-6), 301-312.
- Kappeler, J., Gujer, W. (1992). Estimation of kinetic parameters of heterotrophic biomass under aerobic conditions and characterization of wastewater for activated sludge modelling. *Wat. Sci. Tech.*, **25** (6), 125-139.
- Kautz, O., Nelles, M. (1995) Behandlung des Überschusswassers aus der Nassfermentation von Bioabfällen. *Biologische Abfallbehandlung*. K. -J. Thomé-Kosmiensky, EF-Verlag für Energie und Umwelttechnik, 517-546.
- Keller, J., Subramaniam, K., Gösswein, J., Greenfield, P. (1997). Nutrient removal from industrial wastewater using single tank sequencing batch reactors. *Wat. Sci. Tech.*, **35**(6), 137-144.
- Keller, J. (2005) Sequencing Batch Reactor Processes for Biological Nutrient Removal. *Proceedings of the IWA Specialist Conference in Nutrient Management in Wastewater Treatment Processes and Recycle Streams*. Krakow, Poland. September, 18-21. 245-256.
- Ketchum, L.H. (1997) Design and physical features of sequencing batch reactors. *Wat. Sci. Tech.* **35**, (1), 11-18.
- Kim, D.J., Ahn, D.H., Lee, D.I. (2005) Effects of free ammonia and dissolved oxygen on nitrification and nitrite accumulation in a biofilm airlift reactor. *Korean Journal of Chemical Engineering*. **22**. 85-90
- Kleerebezem, R., Méndez, R. (2002) Autotrophic denitrification for combined hydrogen sulphide removal from biogas and post-denitrification. *Wat. Sci. Tech.* **45** (10), 349-356.
- Krishnamoorthy, R., Loer, R.C. (1989) Aerobic sludge stabilization. Factors affecting kinetics. *Journal of Environmental Engineering*, **115** (2), 283-301.
- Kübler H. (1996) Anfall und Reinigung von Abwasser bei der Vergärung von Bioabfall. *Korrespondenz Abwasser*, **5/96**, 796-808.
- Kuypers, M.M.M., Sliemers, A.O., Lavik, G., Schmid, M., Jørgensen, B.B., Kuenen, J.G., Sinninghe Damste, J.S., Strous, M., Jetten, M.S.M. (2003). Anaerobic ammonium oxidation by Anammox bacteria in the Black Sea. *Nature*, **422**, 608-611.
- Laridi, R., Drogui, P., Benmoussa, H., Blais, J., Auclair, J.C. (2005) Removal of Refractory Organic Compounds in Liquid Swine Manure Obtained from a Biofiltration Process Using an Electrochemical Treatment. *J. Envir. Engrg.*, Volume 131, Issue 9, pp. 1302-1310.
- Lence, S. (2005) What can the United States learn from Spain's pork sector? Implications from a comparative Economic Analysis. *MATRIC Research Paper 05-MRP 12*. September, 2005. Available on the web site: www.matric.iastate.edu.
- Lide D.R. (1993). CRC Handbook of chemistry and Physics. *A Ready/Reference Book of Chemical and Physical Data*, 73rd edn. CRC Press, Boca Raton, FL.
- Llabrés-Luengo, P., Mata-Alvarez, J. (1987). Kinetic study of the anaerobic digestion of straw-pig manure mixtures. *Biomass*, **14**(4).

- Loll U. (1998) Sickerwasser aus Kompostierungs. *Und Anaerobalangen*. EP, 7-8, 52-58.
- Macé, S., Mata-Alvarez, J. (2002) Utilization of SBR Technology for wastewater treatment: An overview, *Ind. Eng. Chem. Res.* 41: 5539-5553.
- Macé, S., Dosta, J., Bolzonella, D., Mata-Álvarez, J. (2005a) Full scale implementation of AD technology to treat the organic fraction of municipal solid waste in Spain. In: *Proceedings of the 4th International Symposium of Anaerobic Digestion of Solid Waste*. Copenhagen, Denmark. August 31- September 2, 2005. Vol. 1, pp 409-416
- Macé, S., Dosta, J., Torres, R., Mata-Álvarez, J. (2005b) Characteristics of the residual organic matter removal after AD of the supernatant of the OFMSW: Evolution during aerobic treatment in a SBR. *Proceedings of the 10th Mediterranean Congress on chemical engineering*. Barcelona, Spain. 15-18 November, 2005. p. 359.
- Macé, S., Dosta, J., Baraza, X., Mata-Álvarez, J. (2005c) High COD removals in the supernatant of the OFMSW digestion using a SBR and a coagulation step. In: *Proceedings of X Chemical Engineering Mediterranean Congress*. Barcelona, Spain. 15-18 November, 2005. p. 360.
- Macé, S., Dosta, J., Galí, A., Mata-Álvarez, J. (2006) Optimization of Biological Nitrogen Removal via Nitrite in an SBR treating supernatant from the Anaerobic Digestion of Municipal Solid Wastes. *Ind. Eng. Chem. Res.* 45 (8), 2787-2792.
- Magrí, A., Flotats, X. (2000) Tratamiento de la fracción líquida de purines de cerdo mediante un reactor discontinuo secuencial (SBR). *Residuos* 57, 84-88.
- Magrí, A., Corominas, Ll., López, H., Campos, E., Balaguer, M.D., Colprim, J., Flotats, X. (2007). A Model for the simulation of the SHARON process: pH as a key factor, *Environmental Technology*, 28 , 255-265.
- Marais, G.v.R., Ekama, G.A., 1976. The activated sludge process. Part 1- Steady state behaviour. *Water SA*, 2, 163-199.
- Marsili-Libelli, S., Tabani, F., (2002). Accuracy analysis of a respirometer for activated sludge dynamic modelling. *Wat. Res.*, 36, 1181-1192.
- Mata-Álvarez, J. (2002) Digestió anaeròbica de residus sòlids urbans. *Diputació de Barcelona*, Xarxa de municipis, Area de Medi Ambient. (*In catalan*)
- Metcalf & Eddy, (1991). Wastewater engineering: treatment, disposal and reuse. *McGraw-Hill International Editions, USA*.
- Monod, J. (1942) Recherche sur la Croissance des Cultures Bacteriennes. Paris, France. *Herman et Cie*.
- Mosquera-Corral, A., Campos, J.L., Sánchez, M., Méndez, R., Lema, J.M. (2003). Combined system for biological removal of Nitrogen and Carbon from a fish cannery wastewater. *J. of Environmental Engineering. ASCE*. 129 (9). 826-833.
- Mosquera-Corral, A., González, F., Campos, J.L., Méndez, R. (2005). Partial nitrification in a SHARON reactor in the presence of salts and organic carbon compounds. *Process Biochemistry*. 40 (9), 3109-3118.

- Morgenroth, E., Arvin, E., Vanrolleghem, P. (2002) The use of mathematical models in teaching wastewater treatment engineering. *Wat. Sci. Tech.* 45(6) 229-233.
- Mossakowska, A.; Reinius, L-G.; Hultman, B. (1997) Nitrification reactions in treatment of supernatant from dewatering of digested sludge. *Wat. Env. Res.*, 69, (6), 1128-1133.
- Moussa, MS, Rojas, AR, Hooijmans, CM, Gijzen, HJ, van Loosdrecht, MCM (2004) Model-based evaluation of nitrogen removal in a tannery wastewater treatment plant. *Wat. Sci. Tech.* 50 (6). pp 251-60.
- Mulder, J.W., van Kempen, R. (1997) N-removal by SHARON. *Water Quality International* 2, 30-31.
- Mulder, J.W. van Loosdrecht, M.C.M., Hellinga, C., van Kempen, R. (2001) Full-scale application of the SHARON process for treatment of rejection water of digested sludge dewatering. *Wat. Sci. Tech.* 43 (11) pp. 127-134.
- Müller K. (1999) Anforderungen an die Behandlung von Prozeßabwässern aus der Bioabfallvergärung. Prozeßwasser aus der Bioabfallvergärung, Berichte aus Wassergüte- und Abfallwirtschaft, TUM, Nr. 154. (1999)
- Muller AW, Wentzel MC, Ekama GA. (2004) Experimental determination of the heterotroph anoxic yield in anoxic-aerobic activated sludge systems treating municipal wastewater. *Water SA* 30: pp 7-12.
- Murat, S., Insel, G., Artan, N., Orhon, D. (2003). Performance evaluation of SBR treatment for nitrogen removal from tannery wastewater. In: *IWA Speciality Symposium on Strong Nitrogenous and Agro-Wastewater, volume 2*. Seoul, Korea, June 11-13, 2003, 598-605.
- Musvoto, E.V., Wentzel, M.C., Loewenthal, R.E., Ekama, G.A. (2000a). Integrated chemical-physical processes modelling-I. Development of a kinetic-based model for mixed weak acid/base systems. *Wat. Res.*, 34 (6). pp 1857-1867.
- Musvoto, E.V., Wentzel, M.C., Ekama, G.A. (2000b). Integrated chemical-physical processes modelling-II. Simulating aeration treatment of anaerobic digester supernatants. *Wat. Res.*, 34 (6). pp 1868-1880.
- Nowak, O.; Svardal, K.; Schweighofer, P. (1995) The dynamic behaviour of the nitrifying activated sludge systems influenced by inhibiting wastewater compounds. *Wat. Sci. Tech.* 31(2): 115-124.
- Obaja, D., Macé, S., Costa, J., Sans, C., Mata-Alvarez, J. (2003). Nitrification, denitrification and biological phosphorus removal in piggy wastewater using a sequencing batch reactor. *Bioresource Technology*, 87, 103-111.
- Oles, J., Wilderer, PA. (1991) Computer aided design of sequencing batch reactors based on the IAWPRC Activated Sludge Model. *Wat. Sci. Tech.* 23: 1087-1095
- Orhon, D., Artan, N. (1994). Modelling of activated sludge systems. *Technomic Publishing Co., Inc.*, Pennsylvania, USA. (pp. 397-469)

- Orhon, D., Sözen, S., Artan, N. (1996) The effect of heterotrophic yield on the assessment of the correction factor for anoxic growth. *Wat. Sci. Tech.* 34(5-6), 67-74.
- Piciooreanu, C., van Loosdrecht, M.C.M., Heijnen, J.J. (1997). Modelling the effect of oxygen concentration on nitrite accumulation in a biofilm airlift suspension reactor. *Wat. Sci. Tech.* 36 (1), 147-156.
- Pollice, A., Tandoi, V., Lestingi, C. (2002). Influence of aeration and sludge retention time on ammonium oxidation to nitrite and nitrate, *Wat. Res.*, 36(10), 2541–2546.
- Poo, K., Jun, B., Lee, S., Woo, H. & Kim, C. (2004). Treatment of strong nitrogen swine wastewater at full-scale sequencing batch reactor. *Wat. Sci. Tech.*, 49 (5-6), 315-323.
- Poon, C.S., Chu, C.W. (1999) The use of ferric chloride and anionic polymer I the chemically assisted primary sedimentation process. *Chemosphere*, 39(10), pp. 1573-1582.
- Rostron, W.M., Stuckey, D.C., Young, A.A. (2001). Nitrification of high strength ammonia wastewaters: comparative study of immobilisation media. *Wat. Sci. Tech.*, 35, 1169-1178.
- Rozich, A.F., Gaudy, A.F. Jr. (1992). Design and operation of activated sludge processes using respirometry. *Lewis Publishers, Inc.*, Michigan, USA.
- Ruiz, G., Jeison, D., Chamy, R. (2003). Nitrification with high nitrite accumulation for the treatment of wastewater with high ammonia concentration. *Wat. Res.*, 37, 1371 – 1377.
- Rulkens, W.H., Ten Have, P.J.W. (1994). Central processing pig manure in the Netherlands. *Wat. Sci. Tech.* Vol. 30, No.7, 157-165.
- Rulkens, W.H., Klapwijk, A., Willers, H.C. (1998). Recovery of valuable nitrogen compounds from agricultural liquid wastes: potential possibilities, bottlenecks and future technological challenges. *Environmental Pollution*. No. 102, S1, 727-735.
- Rysgaard, S., Glud, R. N., Risgaard-Petersen, N., Dalsgaard T. (2004) Denitrification and anammox activity in Arctic marine sediments. *Limnology and oceanography*, 49 (5), 1493-1502.
- Salem, S., Berends, D., van Loosdrecht, M.C.M., Heijnen, J.J. (2002) Model-based evaluation of a new upgrading concept for N-removal. *Wat. Sci. Tech.* 45(6), 169-176.
- Schalk, J., De Vries, S., Kunen, J.G., Jetten, M.S.M. (2000) Involvement of a novel hydroxylamine oxidoreductase in anaerobic ammonia oxidation. *Biochemistry* 39(18), 5405-5412.
- Schmidt, I., Hermelink, C., de Pas-Schoonen, K., Strous, M., den Camp, H.J.O., Kuenen, J.G., Jetten, M.S.M. (2002) Anaerobic ammonia oxidation in the presence of nitrogen (NO_x) by two different lithotrophs. *Appl. Env. Microbiol.* 68(11). 5351-5357.
- Schmid, M., Walsh, K., Webb, R., Rijpstra, W.I.C., van de Pas-Schoonen, K.T., Verbruggen, M.J., Hill, T., Moffett, B., Fuerst, J., Schouten, S., Sinnige Damste, J.S., Harris, J., Shaw, P., Jetten, M.S.M., Strous, M. (2003). *Candidatus* “*Scalindua brodae*”, sp. nov., *Candidatus* “*Scalindua wagneri*”, sp. nov., two new species of anaerobic ammonium oxidizing bacteria. *Syst. Appl. Microbiol.*, 26, 529-538.

- Seco, A, Ribes, J, Serralta, J., Ferrer, J. (2004) Biological Nutrient Removal Model No.1 (BNRM1). *Wat. Sci. Tech.* 50: 69-78.
- Serralta, J. (2004) Desarrollo de un algoritmo para el cálculo del pH en los procesos de depuración biológicos de EDARs. Aplicación a la modelación de los procesos de fermentación de fango primario y de eliminación biológica de fósforo. PhD. Departamento de Ingeniería Hidráulica y Medio Ambiente, *Universidad Politécnica de Valencia*. (in Spanish).
- Serralta, J., Ferrer, J., Borrás, L., Seco, A. (2004) An extension of ASM2d including pH calculation. *Wat. Res.* 38. 4029-4038.
- Siegrist, H. (1996). Nitrogen removal from digester supernatant-Comparison of chemical and biological methods. *Wat. Sci. Tech.* Vol. 34 (1-2), 399-406.
- Siegrist H., Rengli, D., Gujer, W. (1993) Mathematical modeling of anaerobic mesophilic sewage sludge treatment. *Wat. Res.*, 27 (2), 26-36.
- Sliekers A.O., Derwort, N., Campos Gómez, J.L., Strous, M., Kuenen, J.G., Jetten M.S.M. (2002). Completely autotrophic ammonia removal over nitrite in one reactor. *Wat. Res.* 36, 2475-2482.
- Sliekers A.O., Tirad K.A., Abma W., Kuenen J.G., Jetten M.S.M. (2003). CANON and Anammox in a gas-lift reactor. *FEMS Microbiology Letters*, 218, 339-344.
- Sollfrank, U., Gujer, W., 1991. Characterization of domestic wastewater for mathematical modelling of the activated sludge process. *Wat. Sci. Tech.* 23, 1057-1066.
- Spanjers, H., Klapwijk, A. (1990) On-line meter for respiration rate and short-term biochemical oxygen demand in the control of the activated sludge process. In: *Advances in Water Pollution Control, Proceedings of 5th IAWPRC Workshop*, 26 July – 3 August, Yokohama and Kyoto, Japan.
- Spanjers, H. (1993) *Respirometry in activated sludge*. PhD thesis, Wageningen Agricultural University, Wageningen, The Netherlands.
- Spanjers, H., Vanrolleghem, P.A. (1995) Respirometry as a tool for rapid characterization of wastewater and activated sludge. *Wat. Sci. Tech.* 31: 105-114.
- Spanjers, H., Vanrolleghem, P.A., Olsson, G., Dold, P.L. (1998). Respirometry in control of the activated sludge process: principles. *IAWQ Scientific and Technical Report No. 7*, London, UK pp. 1-12.
- Sperandio, M., Pambrun, V., Paul, E. (2007) Analysis, modelling and control of partial nitrification in Sequencing batch reactor. In: *Proceedings of the CLONIC Final Workshop'07. Closing the nitrogen cycle from urban landfill leachate by biological nitrogen removal over nitrite and thermal treatment*. pp. 124-133.
- STOWA (1996) One reactor system for ammonia removal via nitrite, *Report no 96-01*. STOWA, Utrecht, The Netherlands. ISBN 90 74476 39 2
- Strous M. (2000). Microbiology of anaerobic ammonium oxidation. PhD Thesis. *TU Delft*. The Netherlands.

- Strous M., Van Gerven E., Zheng P., Gijs Kuenen J., Jetten M.S.M. (1997). Ammonium removal from concentrated waste streams with the anaerobic ammonium oxidation (Anammox) process in different reactor configurations. *Wat. Res.*, 31(8), 1955-1962
- Strous M., Heijnen J.J., Kuenen J.G., Jetten M. (1998). The sequencing batch reactor as a powerful tool for the study of slowly growing anaerobic ammonium-oxidizing microorganisms. *Applied Microbiology and Biotechnology*, 50, 589-596.
- Strous M., Kuenen J.G., Jetten, M.S.M. (1999). Key physiology of Anaerobic Ammonium Oxidation. *Applied and Environmental Microbiology*, 65(7), 3248-3250.
- Strous, M. (2000) Microbiology of anaerobic ammonium oxidation. PhD Thesis, Delft, The Netherlands: *Delft University Press*, ISBN 90-9013621-5.
- Teichgraber, B., Stein, A. (1994) Nitrogen elimination from sludge treatment reject water - Comparison of steam-stripping and denitrification processes. *Wat. Sci. Tech.*, 30(6), 41-51.
- Thayalakumaran, N., Bhamidimarri, R., Bickers, P.O. (2003) Biological nutrient removal from meta processing wastewater using a sequencing batch reactor. *Wat. Sci. Tech.* 47(10) 101-108.
- Tilche, A., Bacilieri, E., Bortone, G., Malaspina, F., Piccinini, S., Stante, L. (1999). Biological phosphorus and nitrogen removal in a full scale sequencing batch reactor treating piggery wastewater. *Wat. Sci. Tech.*, 40(1), 199-206.
- Tilche A, Bortone G, Malaspina F, Piccinini S, Stante L. (2001) Biological nutrient removal in a full-scale SBR treating piggery wastewater: results and modelling. *Wat. Sci Tech.* 43(3) pp 363-71.
- Toh S. K., Webb R. I., Ashbolt N. J. (2002). Enrichment of autotrophic anaerobic ammonium-oxidizing consortia from various wastewaters, *Microbial Ecology*, 43, 154-167.
- Trigo C., Campos J.L., Garrido J.M., Méndez R. (2006). Start-up of the Anammox process in a membrane bioreactor. *Journal of Biotechnology*, 126, 475-487.
- Van de Graaf A.A., de Bruijn P., Robertson L.A., Jetten M.S.M., Kuenen J.G. (1996). Autotrophic growth of anaerobic ammonium-oxidizing micro-organisms in a fluidized bed reactor. *Microbiology (UK)*, 142, 2187-2196.
- Van Dongen U., Jetten M.S.M., Van Loosdrecht M.C.M. (2001). The SHARON-ANAMMOX process for treatment of ammonium rich wastewater. *Wat. Sci. Tech.*, 44 (1), 153-160.
- Van Hulle, S.W.H., Van Den Broeck, S., Maertens, J., Villez, K., Schelstraete, G., Volcke, E.I.P., Vanrolleghem, P.A. (2003) Practical experiences with start-up and operation of a continuously aerated lab-scale SHARON reactor. In: Communications in Applied Biological Sciences 68/2(a), *Proceedings FAB Symposium. Gent, Belgium, September 18-19, 2003*, 77-84.
- Van Hulle, S.W.H., Volcke, E.I.P., López-Teruel, J., Donckels, B., van Loosdrecht, M.C.M., Vanrolleghem, P. (2004). Influence of temperature and pH on the kinetics of the SHARON nitrification process. *Proceedings of the 4th IWA World Water Congress and Exhibition. Marrakech, Morocco, September 19-24, 2004*. (On CD-ROM)

- Van Hulle, S.W.H. (2005) Modelling, simulation and optimization of autotrophic nitrogen removal processes. PhD Thesis. *University of Gent*.
- Van Kempen, R., Mulder, J.W., Uijterlinde, C.A., Van Loosdrecht, M.C.M. (2001) Overview: full scale experience of the SHARON process for treatment of rejection water of digested sludge dewatering. *Wat. Sci. Tech.* 44(1) 145-152
- Van Loosdrecht M.C.M., Salem S. (2006). Biological Treatment of sludge digester liquids. *Wat. Sci. Tech.*, 53(12), 11–20.
- Vandaele, S., Bollen, F., Thoeye, C., November, E., Verachtert, H., van Impe, J.F. (2000). A comparison of SBR and SBBR for nitrogen removal out of ammonia rich sludge liquors and problems encountered. In *Proceedings of the 2nd International Symposium on Sequencing Batch Reactor Technology*; IWA Publishing, London, UK. Vol. 1, 67-74.
- Vanrolleghem, P.A., Spanjers, H., Petersen, B., Ginestet, P., Takacs, I. (1999) Estimating (combinations of) Activated Sludge and components by respirometry. *Wat. Sci. Tech.* 39: 195-214.
- Vázquez-Padín J.R., Figueroa M., Arrojo B., Mosquera-Corral A., Campos J.L., Méndez R. (2006). Why do nitrifying granules accumulate nitrite? *Proceedings of the 2nd Aerobic Granular Sludge Workshop*, Delft, The Netherlands.
- Verstraete, W., Philips, S. (1998) Nitrification-denitrification processes and technologies in new contexts. *Environmental Pollution* 102, S1. pp. 717-726
- Vilar, A., Kennes, C., Veiga, M.C. (2007) Full-scale biological treatment of landfill leachate from urban solid wastes. In: *Proceedings of the CLONIC Final Workshop'07. Closing the nitrogen cycle from urban landfill leachate by biological nitrogen removal over nitrite and thermal treatment*. pp. 156-158
- Wett, B., Rostek, R., Rauch, W., Ingerle, K. (1998) pH-controlled reject-water treatment. *Wat. Sci. Tech.*, 37, (12), 165-172.
- Wett, B., Rauch, W. (2003). The role of inorganic carbon limitation in biological nitrogen removal of extremely ammonia concentrated wastewater. *Wat. Res.*, 37, 1100 – 1110.
- Weatherburn M.W. (1967). Phenol-hypochlorite reaction for determination of ammonia. *Analytical Chemistry*, 28(97), 1-4.
- Winogradsky, S. (1890). *Ann. Inst. Pasteur*, 4.
- Wossink, A., Benson, G. (1999). Animal agriculture and the environment: experiences from northern Europe. *Emerging and Natural Resources Issues in the South, Clearwater*, Florida.
- Wyffels, S. (2004). Feasibility of combined autotrophic nitrogen removal processes for the treatment of highstrength nitrogen wastewaters. PhD thesis, *Ghent University*, Faculty of Applied Biological Sciences.
- Yang Y., Zuo J.E., Shen P., Gu X.S. (2006). Influence of temperature, pH value and organic substance on activity of ANAMMOX sludge. *Huan Jing Ke Xue*, 27(4) 691-695. (in Chinese).

- Zilverentant, A. (1999) Process for the treatment of wastewater containing specific components e.g. ammonia. *Patent PCT/NL99/00462, WO0005177*.
- Zwietering M.H., de Koos J.T., Hasenac, B.E., de Witt J.C. van't Riet K. (1991). Modeling of bacterial growth as a function of temperature. *Applied and Environmental Microbiology*, 57, 1094-1101.

12. Notation.

SYMBOL/ ACRONYM	DESCRIPTION	UNITS
A	Arrhenius constant	(-)
Abs	Absorbance	(-)
AMB	Barcelona Metropolitan Area	(-)
AD	Anaerobic Digestion	(-)
A/D	Analogical to Digital	(-)
ADM	Anaerobic Digestion Model	(-)
ADM1	Anaerobic Digestion Model No.1	(-)
Anammox	Anaerobic Ammonium Oxidation	(-)
ASM	Activated Sludge Model	(-)
ASM1	Activated Sludge Model No.1	(-)
ASM2d	Activated Sludge Model No.2d	(-)
ASM3	Activated Sludge Model No.3	(-)
ATU	Allyl Thiourea	(-)
AUR	Ammonium Uptake Rate	(mg NH ₄ ⁺ -N (L h) ⁻¹)
a	Slope of the pressure increase versus time	(atm day ⁻¹)
b	Specific decay rate	(day ⁻¹)
b _A	Autotrophic specific decay rate	(day ⁻¹)
BABE	Biological Augmentation Batch Enhanced	(-)
b _{AOB}	Autotrophic specific decay rate for AOB	(day ⁻¹)
b _H	Heterotrophic specific decay rate.	(day ⁻¹)
b _H ^{Death-Regeneration}	b _H according to the death regeneration theory	(day ⁻¹)
b _H ^{Lineal death}	b _H according to the lineal death theory	(day ⁻¹)
b _{NOB}	Autotrophic specific decay rate for NOB	(day ⁻¹)
BOD	Biological Oxygen Demand	(mg BOD L ⁻¹)
BOD _{ST}	Biological Oxygen Demand at short time	(mg BOD L ⁻¹)
c	material of a component subject to conservation	(-)
c _i	Concentration of ionic specie i	(mole L ⁻¹)
CANON	Completely Autotrophic Nitrogen Removal Over Nitrite	(-)
CE	Capillary Electrophoresis	(-)
COD	Chemical Oxygen Demand	(mg COD L ⁻¹)

SYMBOL/ ACRONYM	DESCRIPTION	UNITS
Conc.	Concentration	(-)
$C_{\text{sat,CO}_2}$	Saturation concentration of CO ₂ in water	(mole C L ⁻¹)
D/A	Digital to Analogical	(-)
DO	Dissolved Oxygen concentration	(mg O ₂ L ⁻¹)
D_{O_2}	Diffusivity of oxygen	(atm ⁻¹)
D_{CO_2}	Diffusivity of carbon dioxide	(atm ⁻¹)
ϵ	Dielectric constant	(F m ⁻¹)
E_{ACT}	Activation Energy	(J mole ⁻¹)
F_{INH}	Inhibition function	(-)
f_p	Particulated fraction	(-)
F_{pH}	pH dependency function	(-)
f_{SI}	Production of S _I in hydrolysis	(-)
F_T	Temperature dependency function	(-)
f_{XI}	Fraction of inert COD generated in biomass lysis	(-)
GW	Green Waste	(-)
γ_i	Activity coefficient of specie i	(-)
He_{O_2}	Henry's law constant for oxygen	(atm ⁻¹)
He_{CO_2}	Henry's law constant for carbon dioxide	(atm ⁻¹)
He_{NH_3}	Henry's law constant for free ammonia	(atm ⁻¹)
HRT	Hidraulic Retention Time	(days)
η_{fe}	Correction factor for anaerobic hydrolysis	(-)
$\eta_{\text{NO}_2 \rightarrow \text{N}_2}$	Correction factor for reduction of NO ₂ ⁻ -N to N ₂ -N	(-)
η_{NO_3}	Correction factor for denitrification	(-)
$\eta_{\text{NO}_3 \rightarrow \text{NO}_2}$	Correction factor for reduction of NO ₃ ⁻ -N to NO ₂ ⁻ -N	(-)
I	Ionic strength	(mole L ⁻¹)
i	Component considered	(-)
$i_{\text{C},i}$	Content of C in the component i	(mol C (g i) ⁻¹)
$i_{\text{Charge},i}$	Positive charges content in the component i	(mole charge + (g i) ⁻¹)
$i_{\text{COD},i}$	COD content in the component i	(mg COD (mg i) ⁻¹)
$i_{\text{H},i}$	Content of H in the component i	(mole H (mg i) ⁻¹)
$i_{\text{TSS},i}$	TSS content in the component i	(mg TSS (mg i) ⁻¹)
$i_{\text{X},\text{B}}$	Nitrogen content in biomass	mg NH ₄ ⁺ -N (mg COD) ⁻¹
IWA	International Water Association	(-)

SYMBOL/ ACRONYM	DESCRIPTION	UNITS
j	Process considered	(-)
K_A	Half-saturation constant of S_A	(mg COD L ⁻¹)
K_{ALK}	Half-saturation constant of alkalinity	(mole HCO ₃ ⁻ L ⁻¹)
K_F	Half-saturation constant of S_F	(mg COD L ⁻¹)
k_h	Hydrolysis rate constant	(day ⁻¹)
$K_{HNO_2}^{AOB}$	Inhibition constant of HNO ₂ -N for AOB	(mg HNO ₂ -N L ⁻¹)
$K_{HNO_2}^{NOB}$	Inhibition constant of HNO ₂ -N for NOB	(mg HNO ₂ -N L ⁻¹)
K_{LpH}	Inhibition constant for proton concentration	(mole H ⁺ L ⁻¹)
K_{NH}	Half-Saturation constant of NH ₄ ⁺ -N	(mg NH ₄ ⁺ -N L ⁻¹)
K_{NH_3}	Half-Saturation constant of NH ₃ -N	(mg NH ₃ -N L ⁻¹)
$K_{NH_3}^{AOB}$	Inhibition constant of NH ₃ -N for AOB	(mg NH ₃ -N L ⁻¹)
$K_{NH_3}^{NOB}$	Inhibition constant of NH ₃ -N for NOB	(mg NH ₃ -N L ⁻¹)
K_{NO}	Half-saturation constant of NO _x ⁻ -N	(mg NO _x ⁻ -N L ⁻¹)
K_{NO_2}	Half-Saturation constant of NO ₂ ⁻ -N	(mg NO ₂ ⁻ -N L ⁻¹)
K_{La}	Global mass transfer coefficient for oxygen	(min ⁻¹)
K_{LaO_2}	Global mass transfer coefficient for oxygen	(min ⁻¹)
K_{LaCO_2}	Global mass transfer coefficient for carbon dioxide	(min ⁻¹)
K_{LaNH_3}	Global mass transfer coefficient for free ammonia	(min ⁻¹)
K_{OA}	Oxygen affinity constant for autotrophic biomass	(mg O ₂ L ⁻¹)
$K_{O,AOB}$	Oxygen affinity constant for AOB	(mg O ₂ L ⁻¹)
K_{OH}	Oxygen affinity constant for heterotrophic biomass	(mg O ₂ L ⁻¹)
$K_{O,NOB}$	Oxygen affinity constant for NOB	(mg O ₂ L ⁻¹)
K_{pH}	Affinity constant for proton concentration	(mole H ⁺ L ⁻¹)
k_{REF}		(-)
K_S	Half-saturation constant of S_S	(mg COD L ⁻¹)
K_{S1}	Half-saturation constant of limiting substrate 1	(mg L ⁻¹)
K_{S2}	Half-saturation constant of limiting substrate 2	(mg L ⁻¹)
K_X	Saturation coefficient for particulated COD	(g COD g ⁻¹ COD)
λ	Wave length	(nm)
m	Total number of charged species present in solution	(-)
MLSS	Mixed Liquor Suspended Solids	(g SS L ⁻¹)
MLVSS	Mixed Liquor Volatile Suspended Solids	(g VSS L ⁻¹)
M_{N_2}	Molecular weight of Nitrogen	(g N mole ⁻¹)
MSW	Municipal Solid Waste	(-)

SYMBOL/ ACRONYM	DESCRIPTION	UNITS
μ	Actual specific growth rate of biomass	(day ⁻¹)
μ_A	Actual specific growth rate of autotrophic biomass	(day ⁻¹)
μ_{AOB}	Actual specific growth rate of AOB	(day ⁻¹)
μ_H	Actual heterotrophic specific growth rate	(day ⁻¹)
$\mu_{H,DN}$	Actual specific growth rate of denitrifiers	(day ⁻¹)
μ_{max}	Maximum specific growth rate of biomass	(day ⁻¹)
$\mu_{m,A}$	Maximum specific growth rate of autotrophs	(day ⁻¹)
$\mu_{m,AOB}$	Maximum specific growth rate of AOB	(day ⁻¹)
$\mu_{m,H}$	Heterotrophic maximum specific growth rate	(day ⁻¹)
$\mu_{m,H,DN}$	Maximum specific growth rate of denitrifiers	(day ⁻¹)
$\mu_{m,NOB}$	Maximum specific growth rate of NOB	(day ⁻¹)
μ_{NOB}	Actual specific growth rate of NOB	(day ⁻¹)
n	Moles of nitrogen produced per unit of time	(moles N day ⁻¹)
$N_{REJECT\ WATER}$	Total nitrogen of reject water (NH ₄ ⁺ -N + NO ₂ ⁻ -N)	(mg N L ⁻¹)
$N_{PRIMARY\ SLUDGE}$	Total nitrogen of primary sludge (NH ₄ ⁺ -N + NO ₂ ⁻ -N)	(mg N L ⁻¹)
$v_{i,j}$	Stoichiometric coefficient of component i in reaction j	(-)
OC	Oxygen Consumed	(mg O ₂ L ⁻¹)
OFMSW	Organic Fraction of Municipal Solid Waste	(-)
OUR	Oxygen Uptake Rate	(mg O ₂ (L min) ⁻¹)
OUR _{END}	Endogenous Oxygen Uptake Rate	(mg O ₂ (L min) ⁻¹)
OUR _{EX}	Exogenous Oxygen Uptake Rate	(mg O ₂ (L min) ⁻¹)
OUR _{TOT}	Total Oxygen Uptake Rate	(mg O ₂ (L min) ⁻¹)
pH _{OPT}	Optimum pH value	(-)
pK _i ⁰	Acid Base dissociation constant of compound i	(-)
pK _i ⁰ (0°C)	pK _i ⁰ at 0°C	(-)
PLC	Programmable Logic Controller	(-)
P _{P,O2}	Partial pressure of oxygen	(atm)
P _{P,CO2}	Partial pressure of carbon dioxide	(atm)
P _{P,NH3}	Partial pressure of free ammonia	(atm)
Q ₁	Daily influent flowrate of reject water (SHARON/DN)	(L day ⁻¹)
Q ₂	Daily influent flowrate of primary sludge (SHARON/DN)	(L day ⁻¹)
q _F	Maximum rate for fermentation	(day ⁻¹)
Q _{FEED}	Volumetric feeding rate in the SHARON reactor	(L day ⁻¹)

SYMBOL/ ACRONYM	DESCRIPTION	UNITS
θ	temperature coefficient	(-)
ρ_j	Rate equation of reaction j	(mg cellular COD (L h) ⁻¹)
r (pH)	Rate equation at the actual pH value	(mg (L h) ⁻¹)
r (pH _{OPT})	Rate equation at the optimum pH value	(mg (L h) ⁻¹)
r (T)	Rate equation at the actual temperature	(mg (L h) ⁻¹)
$r_{X,A}$	Autotrophic growth rate	(mg COD (L day) ⁻¹)
r (T _{REF})	Rate equation at a reference temperature	(mg (L h) ⁻¹)
R	Ideal gas constant	(atm L (mol K) ⁻¹)
r_i	Transformation rate of component i	(mg i (L h) ⁻¹)
r_j	Transformation rate of reaction j	(mg (L h) ⁻¹)
$r_{i,j}$	Transformation rate of component i in process j	(mg i (L h) ⁻¹)
r_{DECAY}	Biomass decay rate	(mg COD (L day) ⁻¹)
r_S	Substrate (S) removal rate	(mg S (L h) ⁻¹)
r_X	Biomass growth rate	(mg COD (L day) ⁻¹)
SAA	Specific Anammox Activity	(g N (g VSS day) ⁻¹)
sAUR	Specific Ammonium Uptake Rate	(mg NH ₄ ⁺ -N (g VSS h) ⁻¹)
S	Substrate concentration	(mg L ⁻¹)
S ₁	Concentration of limiting substrate 1	(mg L ⁻¹)
S ₂	Concentration of limiting substrate 2	(mg L ⁻¹)
SBR	Sequencing Batch Reactor	(-)
SHARON	Single reactor High Activity ammonia Removal Over Nitrite	(-)
sNUR	Specific Nitrate Uptake Rate	(mg NO ₃ ⁻ -N (g VSS h) ⁻¹)
S/L separator	Solid/Liquid separator	(-)
SRT	Solid Retention Time	(days)
SS	Suspended Solids	(mg SS L ⁻¹)
S _A	Fermentation products.	(mg COD L ⁻¹)
S _{ALK}	Alkalinity	(mole HCO ₃ ⁻ L ⁻¹)
S _{ALK,WW}	Alkalinity of the wastewater	(mole HCO ₃ ⁻ L ⁻¹)
S _C	Concentration of inorganic carbon	(mole C L ⁻¹)
S _{CO2}	Concentration of CO ₂ in the liquid media	(mole CO ₂ L ⁻¹)
S _F	Fermentable, readily biodegradable COD concentration	(mg COD L ⁻¹)
S _H	Concentration of hydrogen	(mole H L ⁻¹)
S _{H+}	Concentration of protons	(mole H ⁺ L ⁻¹)
S _{HNO2}	Nitrous acid nitrogen concentration	(mg HNO ₂ -N L ⁻¹)

SYMBOL/ ACRONYM	DESCRIPTION	UNITS
S_I	Soluble non-biodegradable organic matter concentration	(mg COD L ⁻¹)
S_{N_2}	gaseous nitrogen concentration	(mg N ₂ -N L ⁻¹)
S_{NH}	Ammonium plus ammonia nitrogen concentration	(mg NH ₄ ⁺ -N L ⁻¹)
$S_{NH,EFFLUENT}$	S_{NH} in the effluent	(mg NH ₄ ⁺ -N L ⁻¹)
$S_{NH,PRIMARY}$ SLUDGE	S_{NH} in primary sludge	(mg NH ₄ ⁺ -N L ⁻¹)
$S_{NH,REJECT WATER}$	S_{NH} in reject water	(mg NH ₄ ⁺ -N L ⁻¹)
$S_{NH,WW}$	S_{NH} of the wastewater	(mg NH ₄ ⁺ -N L ⁻¹)
S_{NH_3}	Free ammonia nitrogen concentration	(mg NH ₃ -N L ⁻¹)
S_{NO}	Nitrite plus nitrate nitrogen concentration	(mg NO _x ⁻ -N L ⁻¹)
S_{NO_2}	Nitrite nitrogen concentration	(mg NO ₂ ⁻ -N L ⁻¹)
$S_{NO_2,EFFLUENT}$	S_{NO_2} in the effluent	(mg NO ₂ ⁻ -N L ⁻¹)
$S_{NO_2,PRIMARY SLUDGE}$	S_{NO_2} in primary sludge	(mg NO ₂ ⁻ -N L ⁻¹)
$S_{NO_2,PRODUCED}$	S_{NO_2} produced during the treatment	(mg NO ₂ ⁻ -N L ⁻¹)
$S_{NO_2,REJECT WATER}$	S_{NO_2} in reject water	(mg NO ₂ ⁻ -N L ⁻¹)
$S_{NO_2,WW}$	S_{NO_2} in the wastewater	(mg NO ₂ ⁻ -N L ⁻¹)
S_{NO_3}	nitrate nitrogen concentration	(mg NO ₃ ⁻ -N L ⁻¹)
S_O	Dissolved Oxygen concentration	(mg O ₂ L ⁻¹)
S_O^*	Dissolved Oxygen saturation level	(mg O ₂ L ⁻¹)
S_S	Readily biodegradable COD concentration	(mg COD L ⁻¹)
SVI	Sludge Volumetric Index	(mL g ⁻¹ VSS)
T	Actual temperature	(°C or K)
t_{DN}	Daily denitrification time (SHARON/DN)	(day)
t_N	Daily nitrification time (SHARON/DN)	(day)
t_{N+DN}	Daily nitrification and denitrification time (SHARON/DN)	(day)
T_{REF}	Reference Temperature	(K)
TS	Total Solids	(mg TS L ⁻¹)
V30	Volume of settled sludge after 30 minutes of sedimentation	(mL)
VFA	Volatile Fatty Acids	(mg COD L ⁻¹)
V_G	Volume of the liquid phase	(L)
V_L	Volume of the gas phase	(L)
VSS	Volatile Suspended Solids	(mg VSS L ⁻¹)
VTS	Volatile Total Solids	(mg VTS L ⁻¹)
WW	Wastewater	(-)

SYMBOL/ ACRONYM	DESCRIPTION	UNITS
WWTP	Wastewater Treatment Plant	(-)
X	Biomass concentration	(mg COD L ⁻¹ or g VSS L ⁻¹)
X _{AOB}	Biomass concentration of AOB	(mg COD L ⁻¹)
X _{BA}	Autotrophic biomass concentration	(mg COD L ⁻¹)
X _{BH}	Heterotrophic biomass concentration	(mg cellular COD L ⁻¹)
X _{BH} ⁰	Initial heterotrophic biomass concentration	(mg cellular COD L ⁻¹)
X _{BH,D}	Denitrifying heterotrophic biomass concentration	(mg cellular COD L ⁻¹)
X _{BH,FINAL}	X _{BH} at the end of the experiment	(mg cellular COD L ⁻¹)
X _{BH,TOTAL}	X _{BH} at the beginning of the experiment	(mg cellular COD L ⁻¹)
X _I	inert particulated organic material concentration	(mg COD L ⁻¹)
X _{NOB}	Biomass concentration of NOB	(mg COD L ⁻¹)
X _S	Slowly biodegradable substrate concentration	(mg COD L ⁻¹)
X _{TSS}	Total suspended solids concentration	(mg TSS L ⁻¹)
Y	Yield coefficient	mg COD (mg S _{consumed}) ⁻¹
Y _A	Autotrophic yield coefficient	mg cell COD (mg COD) ⁻¹
Y _{AOB}	Autotrophic yield coefficient for AOB	mg cell COD (mg NH ₄ ⁺ -N) ⁻¹
Y _H	Heterotrophic yield coefficient	mg cell COD (mg COD) ⁻¹
Y _{H,DN}	Heterotrophic yield coefficient during denitrification	mg cell COD (mg COD) ⁻¹
Y _{H,I}	Y _H during the feast phase	mg COD (mg COD) ⁻¹
Y _{H,I+II}	Total Y _H (feast phase and famine phase)	mg COD (mg COD) ⁻¹
Y _{NOB}	Autotrophic yield coefficient for NOB	mg cell COD (mg NO ₂ ⁻ -N) ⁻¹
Z _i	Charge of specie i	(-)

13. Publications.

JOURNAL PUBLICATIONS FROM THIS THESIS

- 1) **Dosta, J.**, Galí, A., Benabdallah El-Hadj, T., Macé, S., Mata-Álvarez, J. (2007) Operation and model description of a sequencing batch reactor treating reject water for Biological Nitrogen Removal via nitrite. *Bioresource Technology*, 98 (11), 2065-2075
- 2) **Dosta, J.**, Galí, A., Macé, S., Mata-Álvarez, J. (2007) Modelling of a SBR to treat the supernatant from anaerobic digestion of the organic fraction of municipal solid waste. *J. Chem. Tech. Biotech.*, 82(2), 158-164.
- 3) **Dosta, J.**, Rovira, J., Galí, A., Macé, S., Mata-Álvarez, J. (2007) Integration of a coagulation/flocculation step in a Biological Sequencing Batch Reactor for COD and nitrogen removal of supernatant of anaerobically digested piggery wastewater. *Bioresource Technology*. Accepted for publication.
- 4) **Dosta, J.**, Galí, A., Benabdallah El-Hadj, T., Mata-Álvarez, J. (2007) Operation of the SHARON-Denitrification process using hydrolysed primary sludge to denitrify. *Wat. Env. Res.* Accepted for publication.
- 5) Galí, A., **Dosta, J.**, Van Loosdrecht, M.C.M., Mata-Álvarez, J. (2007) Two ways to achieve an Anammox influent from reject water treatment: partial SBR nitrification and SHARON process. *Process Biochemistry*, 42(4), 715-720.
- 6) **Dosta, J.**, Fernández, I., Vázquez-Padín, J.R., Mosquera-Corral, A., Campos, J.L., Mata-Álvarez, J., Méndez, R. (2007) Short and long-term effects of temperature on the Anammox process. *Journal of Hazardous Materials*. Accepted for publication

OTHER JOURNAL PUBLICATIONS

- 1) Galí, A., **Dosta, J.**, van Loosdrecht, MCM, Mata-Álvarez, J. (2006) BNR via nitrite of reject water with a SBR and chemostat SHARON/Denitrification process. *Ind. Eng. Chem. Res.*, 45, 7656-7660.
- 2) Macé, S., **Dosta, J.**, Galí, A., Mata-Álvarez, J. (2006) Optimisation of the nitrogen removal in a Sequencing Batch Reactor treating supernatant from the anaerobic digestion of Municipal Solid Wastes. *Ind. Eng. Chem. Res.*, 45, 2787-2792.
- 3) Benabdallah El-Hadj, T., **Dosta, J.**, Mata-Álvarez, J. (2006) Biodegradation of PAH and DEHP micropollutants in mesophilic and thermophilic anaerobic digestion. *Wat. Sci. Tech*, 53 (8), 99-107.

- 4) Benabdallah El-Hadj, T., **Dosta, J.**, Márquez-Serrano, R., Mata-Álvarez, J. (2007) Effect of ultrasound pre-treatment in mesophilic and thermophilic anaerobic digestion with emphasis on naphthalene and pyrene removal. *Water Research*, 41(1), 87-94.

COMUNICATIONS IN INTERNATIONAL CONGRESSES

- 1) **Dosta, J.**, Galí, A., Macé, S., Mata-Álvarez, J. (2006) Modelling of a SBR to treat the supernatant from anaerobic digestion of the organic fraction of municipal solid waste. In: *Proceedings of ORBIT 2006. Biological Waste Management - From local to global. 5th International Conference*. (ISBN 3-935974-09-4). 779-787
- 2) Benabdallah, T., **Dosta, J.**, Torres, R., Mata-Álvarez, J. (2006) PCB and AOX removal in mesophilic and thermophilic anaerobic sewage sludge digestion. In: *Proceedings of ORBIT 2006. Biological Waste Management - From local to global. 5th International Conference*. (ISBN 3-935974-09-4) 601-606
- 3) **Dosta, J.**, Galí, A., Mata-Álvarez, J. (2006) Modelling of partial nitrification in a SHARON chemostat and in a sequencing batch reactor to achieve an appropriate influent to the Anammox process. In: *Proceedings of the First Mediterranean Congress: Chemical Engineering for environment*. 625-627
- 4) Galí, A., **Dosta, J.**, Mata-Álvarez, J. (2006) Optimisation of nitrification-denitrification process in a SBR for the treatment of reject water via nitrite. In: *Proceedings of the IWA Specialised Conference Nutrient Management in Wastewater Treatment Processes and Recycle Streams*. 925-932 (ISBN 83-921140-1-9)
- 5) **Dosta, J.**, Galí, A., Macé, S. and Mata-Álvarez, J. (2005) *Calibration of an extended Activated Sludge Model considering the influence of pH and Temperature*. In: *Proceedings of the IWA Specialised Conference Nutrient Management in Wastewater Treatment Processes and Recycle Streams*. 1363-1367. (ISBN 83-921140-1-9)
- 6) Benabdallah El-Hadj, T., **Dosta, J.**, Mata-Álvarez, J. (2005) Biodegradation of PAH and DEHP micropollutants in mesophilic and thermophilic anaerobic digestion. In: *Proceedings of the IWA 4th International Symposium on anaerobic Digestion of Solid Waste*. 340-347.
- 7) Macé, S., **Dosta, J.**, Bolzonella, D., Mata-Álvarez, J. (2005) Full-scale implementation of AD technology to treat the organic fraction of municipal solid waste in Spain. In: *Proceedings of the IWA 4th International Symposium on anaerobic Digestion of Solid Waste*. 409 – 416.

14. Resum en Català.

La legislació és cada vegada més estricta per tal de reduir el contingut de nutrients (entre els que destaca el nitrogen) en l'efluent de les plantes de tractament d'aigües residuals, la qual cosa estimula la recerca per tal de millorar aquest aspecte en les plantes ja existents. La tendència actual és cercar aquelles corrents riques en contaminant per aplicar un tractament específic sobre elles.

En aquesta tesi s'ha treballat amb diferents aigües residuals d'alt contingut en nitrogen amoniacal en provenir d'un tractament de digestió anaeròbica de materials fortament proteics: sobrenedant de digestió anaeròbica de fangs d'Estacions Depuradores d'Aigües Residuals (EDAR) municipals, sobrenedant de digestió anaeròbica de la Fracció Orgànica de Residus Municipals (FORM) i sobrenedant de digestió anaeròbica de purins de porc. Entre les possibles alternatives de tractament d'aquestes aigües residuals, el tractament biològic acostuma a ser el més recomanable, en base a l'eficiència del tractament i els costos d'instal·lació i operació.

Per tal de tractar aquestes aigües residuals s'ha fet un estudi d'operació i modelització de diferents tractaments avançats d'eliminació biològica de nitrogen: En primer lloc, la utilització d'un reactor discontinu seqüencial en el qual es realitza un procés de nitrificació/desnitrificació via nitrit, la qual cosa suposa un estalvi, respecte els tractaments biològics convencionals, del 25% dels costos d'aireig i del 40% de matèria orgànica externa per desnitrificar. Per altra banda, s'ha experimentat el tractament biològic de nitrogen en un reactor SHARON/Desnitrificació, el qual suposa una reducció de costos similar a la obtinguda en un reactor seqüencial per càrregues. Finalment, s'ha estudiat la utilització d'un sistema combinat de nitrificació parcial i Anammox. Respecte el tractament convencional, aquesta tecnologia evita la necessitat d'emprar matèria orgànica per desnitrificar i condueix a un estalvi del 65% dels costos d'aireig, produint molt poca quantitat de fangs. Tot i així, els punts febles del procés de Nitrificació parcial/Anammox són els requeriments de calor, el lent creixement dels microorganismes Anammox i la seva baixa resistència a inhibidors.

14.1 INTRODUCCIÓ.

Existeixen diferents processos pel tractament d'aigües residuals amb un elevat contingut en nitrogen amoniacal, essent els més destacats el procés MAP, el *stripping* amb aire, el *stripping* amb vapor d'aigua i el procés d'eliminació biològica de nitrogen. El procés MAP és un tractament físico-químic que consisteix en la recuperació del nitrogen amoniacal contingut en l'aigua en forma de $MgNH_4PO_4$. El procés de *stripping* amb aire consisteix en la recuperació del nitrogen amoniacal present en l'aigua residual en forma d'amoniac lliure, transferint aquest compost volàtil a un corrent d'aire. Posteriorment, aquest amoniac lliure es condensa en una solució d'àcid sulfúric per formar $(NH_4)_2SO_4$. El procés de *stripping* amb vapor d'aigua és equivalent al de *stripping* amb aire però emprant un corrent de vapor d'aigua enlloc d'aire per tal d'extreure el nitrogen amoniacal de l'aigua residual. Finalment, el procés d'eliminació biològica de nitrogen consisteix en una primera oxidació del nitrogen amoniacal a nitrit o nitrat per l'acció de microorganismes autotròfics i una posterior reducció d'aquest nitrit o nitrat a nitrogen gas per part de microorganismes desnitrificants.

Recentment, diversos estudis tècnic-econòmics (STOWA, 1996; van Loosdrecht i Salem, 2006) han demostrat que l'aplicació d'un procés d'eliminació biològica de nitrogen pel tractament d'aigües residuals amb elevat contingut en nitrogen amoniacal ($100\text{-}5.000\text{ mg N-NH}_4^+ \text{ L}^{-1}$) és preferible en comparació amb altres processos físico-químics (veure Figura 14.1).

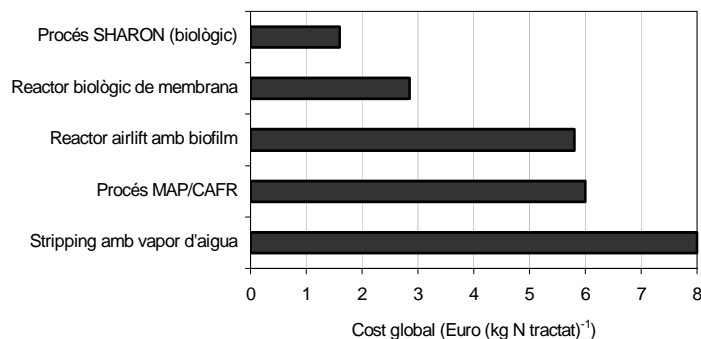


Figura 14.1 – Comparació de costos entre diferents processos físico-químics i biològics pel tractament de sobrenedant de digestió anaeròbica de fangs d'EDAR després d'un estudi a nivell de planta pilot (STOWA, 1996; van Loosdrecht i Salem, 2006)

de les AOB (Wett i Rauch, 2003). En canvi, aquesta relació s'inverteix per elevades temperatures (Hunik, 1993).



De l'expressió 14.3 es dedueix que es consumeixen 2 mols d'alcalinitat per cada mol de N-NH₄⁺ nitrificat. En aquells casos en què l'aigua residual no posseeixi suficient alcalinitat, caldrà un control de pH. De no realitzar-se aquest control, es podrien assolir valors de pH suficientment baixos com per reduir fortament el creixement dels microorganismes, tot deteriorant el funcionament global del sistema.

Els principals *factors que afecten al procés de nitrificació* són:

Concentració d'amoni i d'oxigen dissolt. Aquests nutrients són necessaris pel correcte desenvolupament de les bactèries autotròfiques ja que representen el donant i l'acceptador d'electrons, respectivament. La seva influència pot ser descrita matemàticament mitjançant una cinètica de Monod tal com mostra l'equació 14.4 (veure nomenclatura). L'afinitat per a l'oxigen de les bactèries AOB és superior a la de les NOB, de manera que sota condicions de limitació d'oxigen, les AOB es veuen afavorides front les NOB.

$$r_{X,A} = \mu_{m,A} \frac{S_{NH}}{K_{NH} + S_{NH}} \frac{S_O}{K_{O,A} + S_O} X_{B,A} \quad (14.4)$$

Concentració d'amoniac i àcid nítrós al medi. Per concentracions elevades d'amoniac s'ha experimentat una inhibició del procés de nitrificació (Hellinga *et al.*, 1999; Wett i Rauch, 2003). Tanmateix, aquesta inhibició afecta de manera diferent a les bactèries AOB i NOB. A la Figura 14.3 es presenten les zones d'inhibició de la nitrificació en funció del pH i la concentració de nitrogen (Anthonisen *et al.*, 1976). Tal i com es pot comprovar, a partir de valors de 1,0 mg N-NH₃ L⁻¹ es produeix una inhibició de la reacció de nitratació. Si aquest valor és superior a 150 mg N-NH₃ L⁻¹ la inhibició afecta a ambdues reaccions de nitrificació. Per tant, sota determinades condicions d'elevada càrrega amoniacal i pH

bàsic, es produeix una acumulació de nitrits al medi. Una altra substància que inhibeix el procés de nitrificació és l'àcid nítric (HNO_2), que exerceix una inhibició sobre les bacteries NOB per concentracions superiors a $2.8 \text{ mg HNO}_2 \text{ L}^{-1}$.

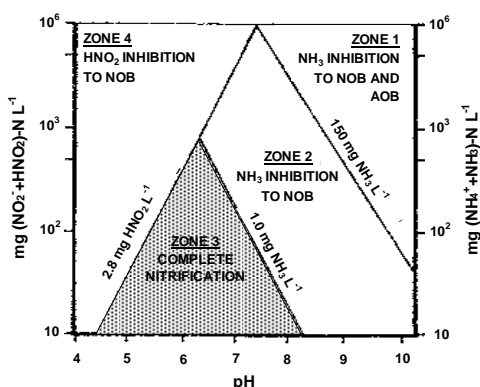


Figura 14.3 – Condicions ambientals d'inhibició per a les bacteries nitrificants (Antonishen *et al.*, 1976)

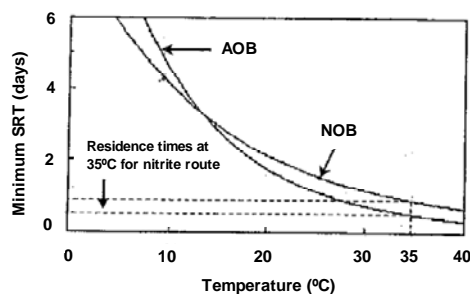


Figura 14.4 - Influència del temps de residència cel·lular i la temperatura sobre l'activitat de les bacteries autotròfiques. (Hellings *et al.*, 1999)

Temperatura: El procés de nitrificació és extremadament sensible a la temperatura, obtenint l'òptim d'operació al voltant de $35\text{-}40^\circ\text{C}$ (Grunditz i Dalhammar, 2002).

pH: L'interval òptim de condicions de pH és estret, entre 7.5 i 8.6 (Metcalf i Eddy, 1991; Grunditz i Dalhammar, 2002).

Temps de retenció cel·lular: Es defineix el temps de residència cel·lular (TRC) com el temps mig de residència dels microorganismes dins el reactor. Aquest paràmetre és de gran importància en el disseny de sistemes de fangs actius, ja que determina el rendiment en l'eliminació de nutrients i la quantitat d'oxigen necessària en el procés. La Figura 14.4 mostra l'edat mínima de fangs perquè les bacteries amonioxidants i nitritoxidants puguin desenvolupar la seva activitat. Com es pot comprovar, per temperatures relativament elevades i seleccionant amb cura el TRC, es pot anular el desenvolupament dels bacteris NOB, mantenint els AOB dins el reactor. Aquest és precisament el principi bàsic del procés SHARON, que regulant el TRC i la temperatura evita la formació de nitrats i, per tant, un estalvi en costos d'aireig.

14.1.3 – Desnitrificació

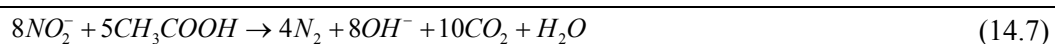
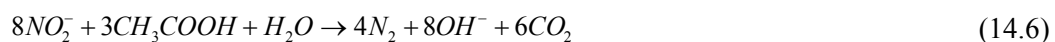
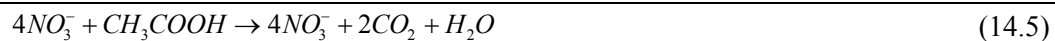
La desnitrificació és la segona etapa de l'eliminació biològica de nitrogen. Mitjançant aquest procés, els microorganismes transformen el nitrit o nitrat a nitrogen gas que passa a l'atmosfera. En el present treball s'han estudiat dos processos de desnitrificació: la

desnitrificació heterotròfica convencional i la desnitrificació autotròfica Anammox. A continuació es detallen aquests processos i la seva dependència amb els paràmetres d'operació.

14.1.3.1– Desnitrificació heterotròfica

El procés de desnitrificació heterotròfica és similar al procés d'oxidació de la matèria orgànica en condicions aeròbiques, essent el N-NO_x l'acceptador d'electrons enlloc de l'oxigen. De fet, les bactèries heterotròfiques facultatives responsables del procés de desnitrificació són capaces, en condicions aeròbiques, d'oxidar la matèria orgànica utilitzant l'oxigen com acceptador d'electrons. Aquesta diferència en l'acceptador d'electrons es tradueix en una menor producció de biomassa per unitat de substrat consumit. És a dir, el rendiment de les bactèries heterotròfiques facultatives utilitzant nitrit o nitrat com a acceptador d'electrons és menor que utilitzant oxigen (Orhon *et al.*, 1996).

El major rendiment de les bactèries responsables del procés de desnitrificació utilitzant l'oxigen com a acceptador d'electrons provoca que, quan ambdós acceptadors d'electrons hi són presents, les bactèries tendeixin a utilitzar l'oxigen. Per aquest motiu, cal que el procés de desnitrificació es porti a terme sota condicions anòxiques. Les reaccions de reducció del nitrit i el nitrat a nitrogen gas mitjançant àcid acètic es presenten a les expressions 14.5 i 14.6, respectivament. Tal i com es comprova, el procés de desnitrificació suposa la producció de 1 mol d'alcalinitat per cada mol de N-NO₃⁻ desnitrificat. Per tant, el procés de desnitrificació suposa la recuperació de la meitat de l'alcalinitat consumida en el procés de nitrificació.



Els principals *factors que influeixen sobre el procés de desnitrificació* són:

Tipus i concentració de substrat orgànic. La desnitrificació heterotròfica requereix la presència d'un substrat orgànic com a donador d'electrons. La cinètica de desnitrificació dependrà de la biodegradabilitat d'aquest substrat. Per altra banda, la velocitat del procés es modela mitjançant la corresponent funció de Monod pel substrat orgànic.

Concentració de nitrats i/o nitrats: Degut a que els N-NO_x representen l'acceptador d'electrons durant el procés de desnitrificació, la seva presència és essencial pel seu correcte funcionament. Per altra banda, Abeling i Seyfreid (1992) van observar que concentracions elevades d'àcid nítric suposaven una disminució de l'activitat desnitrificant.

Temperatura. L'efecte de la temperatura sobre la velocitat del procés presenta un valor òptim al voltant de 40°C (Orhon i Artan, 1994).

pH. Les bacteries heterotròfiques tenen un ampli rang de pH pròxim a la neutralitat (7-8,5) dins el qual l'activitat d'aquesta biomassa es pot considerar constant. En sistemes on es treballi fora d'aquest interval, la influència del pH sí ha de ser considerada.

Concentració d'oxigen dissolt. La presència d'oxigen dissolt inhibeix el procés de desnitrificació perquè les bacteries heterotròfiques desnitrificants tendeixen a utilitzar l'oxigen com a acceptador d'electrons degut al major rendiment que n'obtenen. Per tasques de modelització, aquesta inhibició es sol incloure en l'expressió cinètica amb una funció d'inhibició no competitiva (Henze *et al.*, 2000).

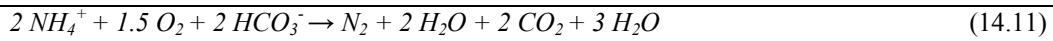
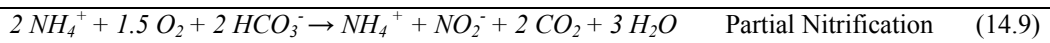
L'expressió 14.8 mostra l'expressió cinètica utilitzada per representar la velocitat del procés de creixement de les bacteries heterotròfiques utilitzant N-NO_x com a acceptador d'electrons. L'expressió contempla una cinètica de primer ordre corregida per diverses funcions que permeten establir l'efecte de les concentracions de substrat orgànic, nitrat i oxigen dissolt (veure nomenclatura).

$$r_{X, DN} = \mu_{m, H, DN} \frac{S_S}{K_S + S_S} \frac{S_{NO}}{K_{NO} + S_{NO}} \frac{K_{OH}}{K_{OH} + S_O} X_{BH, DN} \quad (14.8)$$

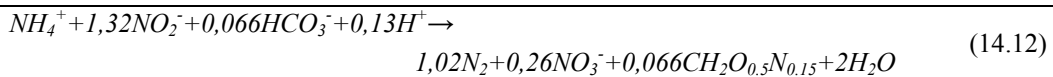
14.1.3.2– Anammox

El process Anammox (de l'anglès, ANaerobic AMMonium OXidation) consisteix en la oxidació d'amoni utilitzant nitrit com a acceptador terminal d'electrons. És necessari, per tant, que aquest procés vingui precedit per una unitat de nitrificació parcial, on aproximadament el 50% de l'amoni és oxidat a nitrit per acció de bacteris AOB (veure Equació 14.9). Seguidament, el procés Anammox converteix l'amoni i el nitrit directament a nitrogen gasós sota condicions d'absència d'oxigen (veure Equació 14.10). La reacció global de nitrificació parcial / Anammox es presenta a la Equació 14.11. Com

es pot observar, aquest procés evita totalment la utilització d'una font de carboni biodegradable per desnitrificar, implica un estalvi del 65% dels costos d'aireig i produeix molt poc fang (Fux *et al.*, 2002).



L'expressió 14.12 mostra la reacció Anammox que considera el creixement cel·lular i la producció de nitrat (Jetten, 1999; van Dongen *et al.*, 2001; Mosquera-Corral *et al.*, 2005). Com es pot comprovar, el procés Anammox té una relació estequiomètrica real entre el N-NH₄⁺ i el N-NO₂⁻ de 1,32 i produeix una petita quantitat d'alcalinitat.



Els principals *factors que afecten el procés Anammox* són:

Temperatura. Strous *et al.* (1999) van estudiar la dependència de la biomassa Anammox front la temperatura, trobant una eliminació òptima de nitrit a 40±3 °C. Tanmateix, Rysgaard *et al.* (2004) van analitzar l'activitat Anammox en sediments permanentment freds (de -1.7 a 4 °C), trobant una temperatura òptima pel seu desenvolupament de 12 °C. Per tant, sembla que en sediments marins, les bactèries Anammox es troben adaptades a baixes temperatures.

pH. Strouss (2000) va analitzar la influència del pH sobre l'activitat Anammox a 33 °C, trobant un valor òptim a pH 8,0.

Efecte de substrats (NH₄⁺-N and NO₂⁻-N) i productes (NO₃⁻-N). Segons Van Hulle (2005), el procés Anammox no es veu perjudicat per concentracions de N-NH₄⁺ o N-NO₃⁻ inferiors a 1 g N L⁻¹. En canvi, el nitrit representa un inhibidor molt fort per aquesta biomassa. Fux (2003) va observar una inactivació total dels microorganismes Anammox en mantenir una concentració de 40 mg N-NO₂⁻ L⁻¹ durant un període de pocs dies.

Oxigen dissolt. Van de Graaf *et al.* (1996) va demostrar que una concentració d'oxigen dissolt superior a 0,01 mg O₂ L⁻¹ representa una inhibició completa del procés Anammox.

Matèria Orgànica i llum. En períodes prolongats de temps, la presència de fonts de carboni (tals com l'acetat, la glucosa o el piruvat) en el licor mesclat té un impacte negatiu sobre el procés Anammox, ja que afavoreix el creixement de biomassa heterotròfica. Per altra banda, Van der Graaf *et al.* (1996) van detectar que la llum visible provoca un descens en l'activitat Anammox entre un 30-50 %.

14.1.4 – Modelització de tractaments biològics. Respirimetria.

La modelització de tractaments d'aigües residuals suposa els següents avantatges:

- *Ajuda a entendre el comportament real del sistema.*
- *Ofereix la possibilitat de comparar resultats obtinguts per a diferents alternatives que es puguin plantejar.*
- *Permet dissenyar estratègies d'operació i sistemes de control del procés.*

Els models de fangs activats de la International Water Association (Henze *et al.*, 2000) esdevenen els models més emprats a l'hora de simular processos biològics d'eliminació de nutrients. El Model de fangs actius No. 1 (Activated Sludge Model No.1; ASM1) considera dos tipus de bacteres (heterotròfiques i autotròfiques) i els 8 processos principals associats a elles. Per altra banda, el model ASM2d el model ASM3 van ser posteriorment desenvolupats per modelitzar el tractament de desfosfatació i l'acumulació intracel·lular de substrat orgànic, respectivament. Aquests models, però, estan pensats per modelitzar els tractaments d'aigües residuals municipals i han de ser convenientment modificats per modelitzar altres tractaments similars.

Una de les tècniques més emprades per tal de calibrar aquests models és la respirometria que es basa en l'anàlisi de l'oxigen consumit pels microorganismes involucrats en els processos d'oxidació biològica de nutrients (Rozich i Gaudy, 1992).

14.1.5 – Problemàtica dels sobrenedants de digestió anaeròbica de residus orgànics.

En aquest treball s'ha estudiat el tractament biològic de tres aigües residuals provinents d'un tractament de digestió anaeròbica de materials fortament proteics: sobrenedant de digestió anaeròbica de fangs d'Estacions Depuradores d'Aigües Residuals (EDAR) municipals, sobrenedant de digestió anaeròbica de la Fracció Orgànica de Residus Municipals (FORM) i sobrenedant de digestió anaeròbica de purins de porc

La Figura 14.5 mostra d'una forma esquematitzada el procés de digestió anaeròbica de residus orgànics. Tal com es pot comprovar, en formar-se biogàs a partir de la DQO

biodegradable del residu orgànic, el sobrenedant del digestor anaerobi queda molt enriquit en nitrogen amoniacal procedent del nitrogen orgànic associat a aquesta DQO (de l'ordre de 0.4-3,5 g N-NH₄⁺ L⁻¹, depenent del tipus i origen del residu). Si l'eficiència de la digestió anaeròbica és bona, la DQO continguda en l'aigua de sobrenedant serà principalment refractària.

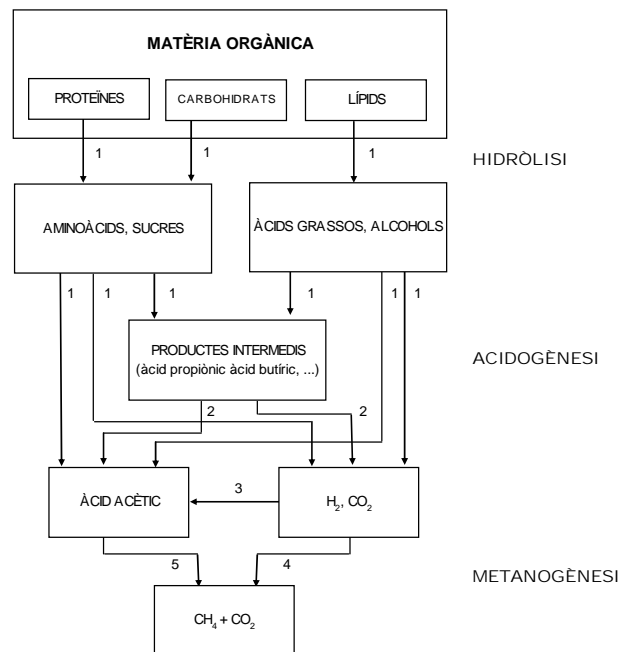


Figura 14.5 – Diagrama del procés de digestió anaeròbica i poblacions microbianes responsables dels processos (1 - Bacteris hidrolíticoacidogènics; 2 - Bacteris acetogènics; 3 - Bacteris homoacetogènics; 4 - Bacteris metanogènics hidrogenòfils; 5 - Bacteris metanogènics acetoclàstics). (Flotats, 2000)

14.1.6 – Tractaments d'eliminació biològica de nitrogen en els sobrenedants de digestió anaeròbica

Per tal de tractar el N-NH₄⁺ present en els sobrenedants de digestió anaeròbica de residus orgànics altament proteics es pot implantar un sistema de tractament biològic intensiu, ja que proporciona bons rendiments en l'eliminació i no suposa un cost econòmic d'inversió i operació tant elevat com els possibles tractament físico-químics. Tanmateix, és necessari que el sistema proposat sigui capaç d'absorbir fluctuacions substancials en la composició i cabal de l'aigua a tractar i que esdevingui un tractament compacte, donades les habituals limitacions d'espai en les plantes de depuració.

Entre els possibles tractaments biològics en destaquen tres, els quals han estat objecte d'estudi d'aquesta tesi:

- El tractament en un **reactor seqüencial discontinu SBR**, que consisteix en un digestor on s'alternen diferents operacions d'ompliment, reacció aeròbica, reacció anòxica/anaeròbica, sedimentació i purga. En aquest SBR es pot realitzar l'eliminació biològica de nitrogen via nitrit, amb el conseqüent estalvi del 40% de carboni orgànic per desnitrificar i del 25% d'oxigen a aportar respecte el procés via nitrat.
- El tractament en un **reactor SHARON/Desnitrificació (SHARON/DN)** que consisteix en un reactor alimentat contínuament i sense retenció de fangs, que assegura la proliferació de biomassa AOB, sense permetre el desenvolupament de la biomassa NOB. D'aquesta manera s'evita la oxidació de nitrit a nitrat. En el reactor SHARON/Desnitrificació s'alternen períodes aeròbics i anòxics (amb aportació de carboni orgànic biodegradable) aconseguint d'aquesta manera l'eliminació biològica de nitrogen via nitrit.
- El tractament en un **sistema combinat de nitrificació parcial / Anammox**. En aquest tractament es realitza la conversió del 50% de $N-NH_4^+$ a $N-NO_2^-$ en un primer digestor, l'efluent del qual representa l'entrada a un segon reactor biològic on es duu a terme una desnitrificació autotròfica Anammox. En comparació amb un tractament convencional d'eliminació biològica via nitrat, el tractament nitrificació parcial / Anammox suposa un estalvi del 65% d'oxigen a aportar i del 100% del carboni orgànic necessari, així com una reduïda producció de fangs.

14.2 JUSTIFICACIÓ I OBJECTIUS.

En aquest treball s'ha abordat el tractament biològic de diferents sobrenedants de digestió anaeròbica de residus orgànics (concretament, fangs d'EDAR, FORM i purins de porc). Per depurar aquestes aigües residuals d'alt contingut en nitrogen, s'han emprat tractaments d'eliminació biològica de nitrogen que condueixen a minimitzar els costos d'aireig, el requeriment de matèria orgànica biodegradable i la generació de fangs. Concretament, els tractaments estudiats han estat el procés d'eliminació biològica de nitrogen via nitrit en un SBR, el procés SHARON/Desnitrificació i el procés combinat nitrificació parcial / Anammox.

Tanmateix, aquests processos han estat analitzats des d'una perspectiva de modelització. Donat que els models de fangs actius de la IWA (Henze *et al.*, 2000) estan pensats pel tractament d'aigües residuals urbanes, aquests s'han de modificar convenientment per descriure els processos i inhibicions d'altres tractaments, com els descrits en aquesta tesi.

Concretament, els *objectius d'aquest treball* són:

Optimitzar el tractament dels sobrenedants estudiats en aquesta tesi en un reactor SBR. En cas de no satisfer els límits legals en matèria de DQO, insertar en el cicle operatiu una etapa de Coagulació/Floculació.

Introduir les extensions necessàries en els models de fangs actius de la IWA (Henze *et al.*, 2000) per tal de modelitzar aquests processos. Implementar aquest model en el programa Mathematica 4.1.

Construir i posar a punt un respiròmetre per estimar experimentalment els coeficients cinètics i estequiomètrics del model. Establir una metodologia de calibratge.

Operar un reactor SHARON/DN per tractar sobrenedant de digestió anaeròbica de fangs d'EDAR emprant metanol i fang primari com a agents desnitrificants.

Operar i modelitzar dos tractaments de nitrificació parcial (SBR i SHARON) com a pas previ a un reactor Anammox.

Estudiar la influència de la temperatura sobre un reactor Anammox pel tractament d'aigües residuals amb alt contingut en nitrogen.

14.3 MATERIALS I MÈTODES.

A continuació es detallen les instal·lacions i tècniques emprades per satisfer els objectius proposats.

14.3.1 – Reactors biològics a escala de laboratori

S'han utilitzat tres tipus d'instal·lacions a escala de laboratori: un reactor SBR (3L), un reactor SHARON (4L) i un reactor Anammox (1L). Aquests reactors es mostren a la Figura 14.6. En tots ells, les operacions d'alimentació i purga es duen a terme mitjançant bombes peristàltiques. Tots els reactors es troben encamisats i connectats a banys termostàtics per tal de controlar la temperatura. A més, estan dotats d'agitadors mecànics per tal d'assegurar una bona mescla en el seu interior. En els reactors on es requereix aireig, aquest es realitza mitjançant compressors d'aire connectats a pedres poroses. Pel reactor Anammox, que s'ha de trobar en condicions d'absència absoluta d'oxigen, totes les canonades i connexions són de neoprè i s'afegeix de manera continuada un petit cabal d'argó (95%) i CO₂(5%) en el capçal del reactor.

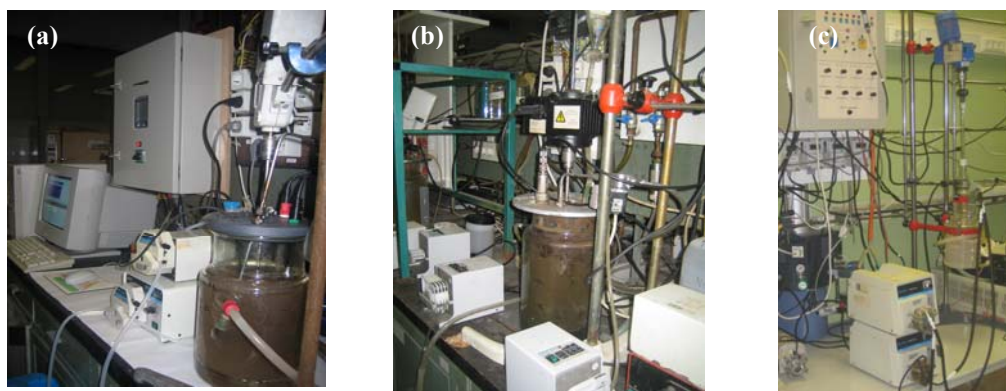


Figura 14.6 – Reactors de laboratori emprats en aquest estudi
(a: reactor SBR; b: reactor SHARON; c: reactor Anammox)

14.3.2 – Respiròmetre tancat seqüencial

Per tal de poder realitzar les tasques de modelització s'ha construït un respiròmetre. Entre els proposats a la bibliografia (Spanjers *et al.*, 1998) s'ha optat per instal·lar un respiròmetre tancat seqüencial degut, principalment, a la seva senzillesa i fiabilitat (Marsilli-Libelli i Tabani, 2002; Gutiérrez, 2003).

El respiròmetre utilitzat es mostra a la Figura 14.7 i consisteix en una cambra d'aireig (3 L) i una cambra tancada i estanca de respiració (0.250 L). El sistema està dotat d'agitadors mecànics i d'un sistema de control de pH i de temperatura. La cambra de respiració està equipada amb una sonda d'oxigen dissolt (Oxi 340i, WTW) i el pH de la cambra d'aireig es mesura mitjançant un elèctrode Crison pH 28. Les dues cambres estan connectades mitjançant una bomba peristàltica (Watson Marlow 323) que funciona intermitentment. Quan el nivell d'oxigen a la cambra de respiració disminueix per sota de $2 \text{ mg O}_2 \text{ L}^{-1}$ o el temps de mesura dura més de 300 s, el seu contingut es renova per bombeig del líquid de la cambra d'aireig durant un temps suficient per desplaçar tres vegades el contingut de la cambra de mesura.



Figura 14.7 – Respiròmetre utilitzat en aquest estudi.

Els valors d'oxigen dissolt i pH s'enregistren en un ordinador equipat amb el programa Advantech Genie. La Figura 14.8 mostra el perfil d'oxigen enregistrat en un experiment de respirometria. Els diferents augments d'oxigen dissolt en aquest perfil corresponen als espais de temps en què es renova el contingut de la cambra de respiració. El pendent de les caigudes d'oxigen dissolt representa la mesura de la velocitat de consum d'oxigen a cada moment, que es coneix com OUR (Oxygen Uptake Rate) i és proporcional a la velocitat de consum de qualsevol tipus de substrat en condicions aeròbiques. Les dades enregistrades pel programa s'exporten a una plantilla d'Excel on s'obté automàticament el perfil d'OUR amb el temps (respirograma) tal com es mostra a la Figura 14.8b.

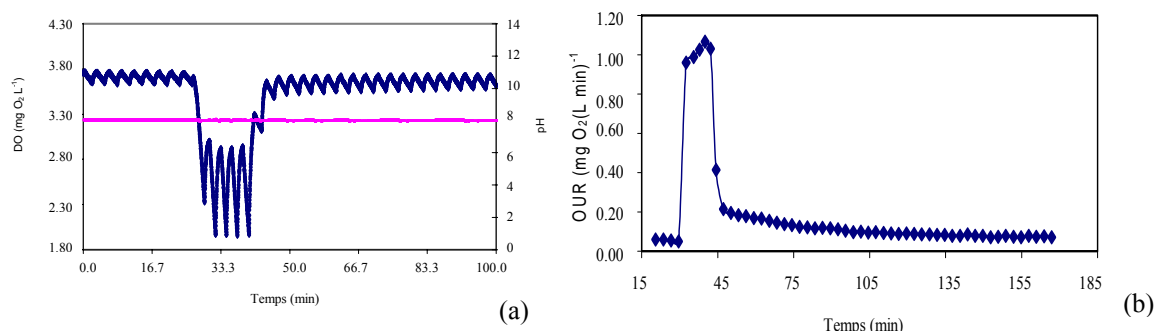


Figura 14.8 - Perfil d'oxigen dissolt (a) enregistrat en un assaig respirometric i el seu corresponent respirograma (b). (DO (—), pH (—) i OUR (◆))

14.3.3 – Test d'activitat Anammox

L'activitat específica màxima de la biomassa Anammox es va analitzar emprant la metodologia establerta per Dapena-Mora *et al.* (2007), que es basa en l'enregistrament de l'increment de pressió degut a la producció de nitrogen en vials tancats sota condicions d'absència total d'oxigen. Aquests experiments es van realitzar dins un agitador orbital amb control de temperatura (New Brunswick Scientific, C24 Incubator).

14.3.4 – Jar Tests

Els tests de Coagulació/Floculació es van dur a terme en un dispositiu de Jar-Test (Flocculator 2000, KEMIRA Kemwater) amb els següents períodes i temporització: mescla vigorosa (30 s), mescla lenta (15 min) i decantació (20 min). Tant l'agent coagulant com el floculant es van addicionar a l'inici de la mescla vigorosa. L'eficiència d'aquest procés es realitza en base al percentatge d'eliminació de DQO i de sòlids suspesos.

14.3.5 – Modelització de processos biològics

Les tasques de simulació van ser realitzades mitjançant un programa propi, implementat en Mathematica 4.1. Per a determinar cadascun dels paràmetres del model es van fer experiments individuals en els que es potencia la influència de cadascun d'ells. L'estimació dels paràmetres del model es va dur a terme minimitzant la suma d'errors al quadrat entre els resultats simulats i les dades mesurades experimentalment.

14.3.6 – Substrat i inòcul

Els sobrenedants de digestió anaeròbica estudiats en aquesta tesi es van obtenir de digestors anaeròbics mesofílics de plantes de Catalunya. Aquests corrents es van recollir i mantenir a 4°C en el laboratori fins el seu tractament. Els microorganismes utilitzats per inocular els reactors van esser extrets de purgues cel·lulars del reactor biològic secundari d'una EDAR de l'Àrea metropolitana de Barcelona i se'ls va enriquir en biomassa nitrificant. Per altra banda, el reactor Anammox es va inocular amb 7,4 g SSV L⁻¹ de biomassa Anammox (en forma de biofilm sobre una zeolita) procedent d'un reactor Anammox que tractava aigua sintètica (Fernández *et al.*, 2006).

14.3.7 – Mètodes analítics

Les anàlisis de DQO, DBO₅, NH₄⁺-N, NO₂⁻-N, NO₃⁻-N, àcids grassos volàtils (AGV), alcalinitat, sòlids totals (ST), sòlids totals volàtils (STV), sòlids suspesos (SS) i sòlids suspesos volàtils (SSV) es van realitzar d'acord amb els *Standard Methods* (APHA, 1998).

14.4 DISCUSSIÓ DE RESULTATS I CONCLUSIONS

A nivell global, en aquest treball s'han estudiat tres tipus de tractaments avançats d'eliminació biològica de nitrogen en aigües residuals amb alt contingut d'amoni, com els sobrenedants de digestió anaeròbica de residus orgànics rics en proteïnes. Concretament, els processos estudiats han estat l'eliminació biològica via nitrit en un reactor seqüencial per càrregues (SBR), el procés SHARON/Desnitricació i el procés nitrificació parcial/Anammox.

En aquest apartat s'inclourà una petita descripció de cada tractament estudiat i se'n destacaran les principals conclusions.

14.4.1 – Eliminació biològica de nitrogen via nitrit en un reactor SBR

En els capítols 4, 5 i 6, s'ha operat i analitzat mitjançant models matemàtics el tractament biològic de nitrogen en un reactor SBR dels sobrenedants de digestió anaeròbica de fangs d'EDAR(capítol 4), de FORM (capítol 5) i de purins de porc (capítol 6).

La Taula 14.1 recull els principals paràmetres d'operació de cadascun dels processos SBR proposats en aquest estudi. Tal com es pot comprovar, en totes les estratègies es van assolir alts valors de càrrega tractada de nitrogen. La temperatura de treball es va mantenir al voltant de 30-32 °C, ja que l'aigua residual a tractar prové d'una digestió anaeròbica mesofílica (35-37 °C). També es va treballar amb cicles de 8h en base a experiments previs al laboratori que justificaven aquesta durada de cicle com a òptima. L'edat de fangs o temps de retenció cel·lular (TRC) es va mantenir a 12 dies. Un valor de TRC molt més petit contribuiria a disposar d'una biomassa molt jove i una gran producció de fangs, mentre que un TRC molt major implicaria disposar d'una població microbiana molt envellida que consumiria gran part de l'oxigen aportat per dur a terme processos de lisi.

Tanmateix, durant la fase de reacció de tots els cicles SBR es van anar alternant etapes aeròbiques (on es duu a terme la nitrificació) amb etapes anòxiques (desnitricació). D'aquesta manera s'aconsegueix prevenir l'acumulació de nitrits que pot esdevenir tòxica pel procés d'eliminació biològica de nitrogen, així com acotar el valor de pH al voltant del valor òptim per la biomassa activa (entorn de 8.0) Totes les aigües residuals amb les que s'ha treballat posseeixen molt poca quantitat de DQO fàcilment biodegradable en

provenir d'un procés de digestió anaeròbica on la major part de la DQO biodegradable s'ha convertit en biogàs. Per aquesta raó, es va addicionar una font externa de carboni orgànic biodegradable (acetat, àcid acètic o metanol) durant els períodes anòxics per desnitrificar. El procés d'eliminació biològica de nitrogen es va realitzar via nitrit, amb la qual cosa es va aconseguir l'estalvi del 25% de costos d'aireig i del 40% de la font externa de carboni orgànic respecte el procés de nitrificació/desnitrificació via nitrat. Per altra banda, en el cas del procés SBR per tractar sobrenedant de digestió anaeròbica de purins de porc, es va incloure una etapa de coagulació/floculació durant els darrers 30 minuts (en període anòxic) del cicle operatiu per tal de satisfer els límits d'evacuació de DQO a clavegueram públic. Es va fer un estudi d'optimització d'aquesta etapa, obtenint que una dosi òptima de 800 mg FeCl₃ L⁻¹ conduïa a una reducció de la DQO de l'efluent per sota dels límits legals, sense perjudicar el procés d'eliminació biològica de nitrogen.

Taula 14.1 – Principals característiques dels processos SBR estudiats en aquest treball.

	Sobrenedant de DA de fangs d'EDAR	Sobrenedant de DA de FORM	Sobrenedant de DA de purins de porc
<i>Nitrogen tractat (kg (m³ dia)⁻¹)</i>	0,87	0,36	0,87
<i>TRH (dies)</i>	1	3	2,7
<i>Durada del cicle (h)</i>	8	8	8
<i>Temperatura (°C)</i>	30	30	32
<i>TRC (dies)</i>	11	12	12
<i>Nivell d'O₂ dissolt (mg O₂ L⁻¹)</i>	< 1,0	< 1,5	< 1,0
<i>Control extern de pH</i>	NO	NO	NO

Per altra banda, es va desenvolupar un model matemàtic per tal de descriure el funcionament dels reactors SBR. Aquest model es va realitzar a partir dels models de fangs actius de la IWA (Henze *et al.*, 2000), tot programant-lo en Mathematica 4.1. Les principals extensions sobre els models de la IWA que es van proposar en aquest treball van ser el fet de definir el procés de nitrificació/desnitrificació com un procés de 4 etapes amb les possibles inhibicions per NH₃ i HNO₂ i el fet de considerar la influència del pH i el seu càlcul al llarg del cicle operatiu del reactor SBR. Aquestes modificacions es van realitzar prenent com a referència els treballs de Wett i Rauch (2003) i Serralta *et al.* (2004).

Tanmateix, es va emprar el respiròmetre construït en aquest treball (veure apartat 14.3.2) per tal de calibrar el model proposat. Es va desenvolupar un protocol de calibratge per determinar aquells paràmetres cinètics i estequiòmètrics més rellevants d'una manera relativament ràpida i senzilla. L'anàlisi d'aquests paràmetres i la posterior modelització dels processos de tractament van permetre identificar la concentració de NH_3 i, en menor mesura, de l'oxigen dissolt dins el digestor com els principals paràmetres d'operació responsables d'inhibir l'oxidació de nitrit a nitrat, contribuint d'aquesta manera a un estalvi considerable en els costos d'aireig, de subministrament de carboni orgànic i de generació de biomassa.

Les principals conclusions que es poden extreure dels tractaments en SBR són:

- ✓ La tecnologia SBR es pot emprar de manera efectiva per tractar el nitrogen present en els sobrenedants de digestió anaeròbica de fangs d'EDAR, FORM o purins de porc, mitjançant el procés d'eliminació biològica via nitrit. Aquests sobrenedants es caracteritzen per un baix contingut en DQO fàcilment biodegradable de manera que és necessari el subministrament de carboni orgànic durant les etapes de desnitrificació.
- ✓ Durant el cicle operatiu, és recomanable alternar períodes de nitrificació i desnitrificació, per tal de prevenir l'acumulació de nitrit i mantenir el pH acotat dins un rang òptim sense l'addició de reactius externs.
- ✓ Bona part de la DQO present en els sobrenedants de digestió anaeròbica acostuma a ser refractària. En cas de que la DQO en l'efluent del tractament biològic en SBR no sigui prou reduïda, es pot incorporar al cicle operatiu una etapa de coagulació/floculació emprant FeCl_3 com a agent coagulant. Aquesta etapa es pot realitzar durant el darrer període de desnitrificació.
- ✓ Per tal de modelitzar el procés d'eliminació biològica de nitrogen via nitrit, cal modificar convenientment els models de fangs actius de la IWA, incorporant la definició de la nitrificació com un procés de dues etapes i les possibles inhibicions per part de NH_3 i HNO_2 , així com el càlcul i influència del pH.
- ✓ Es pot utilitzar un respiròmetre tancat seqüencial per tal de calibrar els models de fangs actius d'una manera ràpida i senzilla. Tanmateix, aquest instrument es pot

emprar per determinar l'efecte d'inhibidors o reactius externs sobre la biomassa desenvolupada en un reactor biològic.

- ✓ El model proposat en aquest treball, prèviament calibrat mitjançant respirometria, proporciona excel·lents resultats i esdevé una eina útil per obtenir un millor enteniment dels processos i inhibicions que tenen lloc dins un tractament determinat. Pels casos estudiats, es va comprovar que les condicions operacionals que conduïen a la inhibició del procés d'oxidació de nitrit eren la concentració d'amoniac lliure dins el reactor i, en menor mesura, el nivell d'oxigen dissolt.

14.4.2 – Eliminació biològica de nitrogen via nitrit en un reactor SHARON/DN

El procés SHARON/Desnitricació es va analitzar en el capítol 7 per a tractar sobrenedant de digestió anaeròbica de fangs d'EDAR. Aquest procés consisteix en un reactor en continu sense retenció de fangs, que treballa a una temperatura suficientment elevada (en aquest cas, 33°C) i sota un temps de retenció hidràulic (TRH) suficientment baix (en aquest cas 2,1 dies) com per afavorir el desenvolupament de biomassa amonioxidant impedit el creixement de la biomassa nitritoxidant. A més, en aquest reactor es van alternar períodes amb aireig (1h) amb períodes anòxics (1h) amb l'addició de carboni orgànic per desnitricar.

En el cas estudiat, es va realitzar un primer estudi emprant metanol com a font externa per desnitricar, obtenint una bona eficiència d'eliminació de nitrogen. La Taula 14.2 mostra la composició del sobrenedant d'entrada i la composició d'aquesta aigua residual a la sortida, on es pot comprovar que es va obtenir una eficiència d'eliminació de nitrogen superior al 85%.

Taula 14.2 – Caracterització de l'aigua residual en l'influent i l'efluent del reactor SHARON/Desnitricació emprant metanol i fang primari com a font de carboni extern.					
	SS (g SS L ⁻¹)	SSV (g SSV L ⁻¹)	N-NH ₄ ⁺ (mg N L ⁻¹)	N-NO ₂ ⁻ (mg N L ⁻¹)	N-NO ₃ ⁻ (g N L ⁻¹)
<i>Sobrenedant de digestió anaeròbica de fangs d'EDAR</i>	0,76 ± 0,07	0,65 ± 0,04	699 ± 47	n.d.	n.d.
<i>SHARON-DN emprant metanol</i>	1,19 ± 0,07	1,09 ± 0,22	60,2 ± 17,6	28,5 ± 14,4	n.d.
<i>SHARON-DN emprant fang primari</i>	1,83 ± 0,12	1,35 ± 0,21	9,6 ± 3,8	20,2 ± 10,2	n.d.

Posteriorment, es va realitzar un estudi de diferents corrents interns d'una EDAR municipal per tal de substituir el metanol. Mitjançant les anàlisis de DQO fàcilment biodegradable es va detectar que la fracció líquida de fang primari hidrolitzat podia esdevenir una bona font de carboni orgànic per desnitrificar. Per tant, es van mantenir totes les condicions en el reactor SHARON/Desnitrificació però substituint el metanol per fang primari. La caracterització de l'efluent obtingut es presenta a la Taula 14.2, on s'observa que l'eficiència del tractament va millorar sensiblement en emprar aquesta nova font de carboni orgànic, donada l'alcalinitat d'aquest corrent residual.

Les principals conclusions que s'extreuen d'aquest estudi són:

- ✓ L'aplicació de la tecnologia SHARON/Desnitrificació per tractar sobrenedant de digestió anaeròbica de fangs d'EDAR pot reduir el seu contingut en nitrogen amoniacal en més del 85%.
- ✓ La utilització generalitzada de metanol per desnitrificar en el reactor SHARON/Desnitrificació es pot evitar utilitzant la fracció líquida de fang primari hidrolitzat, ja que conté una quantitat considerable de DQO fàcilment biodegradable.
- ✓ En el cas estudiat, l'eficiència d'eliminació biològica de nitrogen va augmentar notablement en utilitzar fang primari hidrolitzat per desnitrificar, ja que l'alcalinitat present en aquest corrent va tamponar el licor mesclat dins un interval de pH òptim (7,5-8,5).

14.4.3 – Nitrificació parcial en un reactor SBR i un reactor SHARON

En aquest treball s'han estudiat dues estratègies de nitrificació parcial per obtenir un efluent adequat per a ser alimentat a un reactor Anammox: el tractament de nitrificació parcial en un SBR i el tractament mitjançant el procés SHARON. Tanmateix, ambdós tractaments s'han modelitzat mitjançant el model de fangs actius plantejat als capítols 4 i 5. Amdós processos són adequats per nitrificar aproximadament el 50% del $N-NH_4^+$ a $N-NO_2^-$. La inhibició de la biomassa nitritoxidant en el reactor SBR és deguda a la concentració d'amoníac lliure amb què es treballa al reactor, mentre que en el reactor SHARON no es permet el desenvolupament de biomassa nitritoxidant degut a l'efecte combinat del reduït TRC de treball juntament amb la temperatura d'operació (35°C)

Les principals conclusions que es poden extreure en aquest capítol són:

- ✓ Per tal de generar un influent adequat per un reactor Anammox, dues alternatives eficients són la utilització d'un reactor SBR (amb inhibició total de biomassa nitrítoxidant a través de les concentracions d'amoniac lliure) i la utilització d'un reactor continu SHARON (eliminació de biomassa nitrítoxidant mitjançant el TRC i la temperatura de treball).
- ✓ El tractament en SBR és capaç de tractar una major càrrega de nitrogen (en aquest treball, $2,2 \text{ kg N-NH}_4^+ (\text{m}^3 \text{ dia})^{-1}$) que no pas el tractament mitjançant un procés SHARON (en aquest treball, $0,7 \text{ kg N-NH}_4^+ (\text{m}^3 \text{ dia})^{-1}$). Aquest fet és degut a la major retenció de biomassa obtinguda en el reactor SBR.
- ✓ Ambdós processos s'han modelitzat mitjançant un model de fangs actius amb les pertinents modificacions per predir l'eliminació biològica de nitrogen via nitrit. El model es va calibrar mitjançant assajos discontinus de respirometria. Els resultats simulats obtinguts concorden amb els valors obtinguts experimentalment, la qual cosa permet tenir una explicació teòrica dels processos i inhibicions que tenen lloc dins aquests digestors.

14.4.4 – Eliminació biològica de nitrogen en un reactor Anammox

En el capítol 9, es va realitzar un estudi del procés Anammox per tal de tractar aigües residuals amb un elevat contingut en nitrogen amoniacal a baixes temperatures. A fi i efecte de tenir una referència de la influència a curt termini de la temperatura sobre la biomassa Anammox, es van realitzar diferents assajos d'activitat desnitrificant (Dapena-Mora *et al.*, 2007) a diferents temperatures. La Figura 14.9 mostra els resultats obtinguts juntament amb l'ajust dels models matemàtics d'Arrhenius i de Ratkowsky.

En base a aquests resultats, es va inocular un reactor SBR a escala de laboratori (1L) i es va analitzar la influència a llarg termini de la temperatura sobre el procés Anammox, trobant una baixa adaptació d'aquesta biomassa a baixes temperatures i un canvi considerable en l'estequiometria del procés.

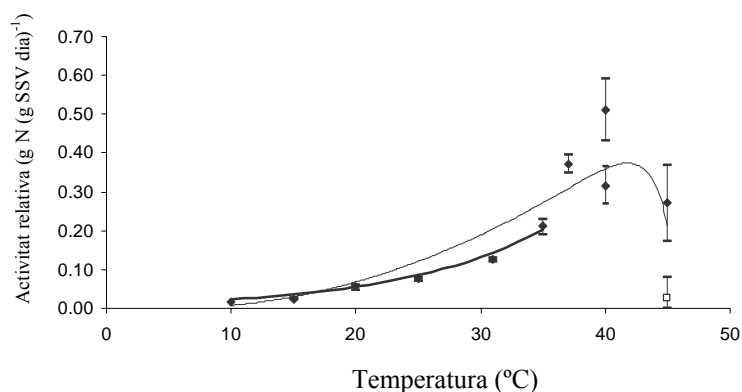


Figura 14.9 – Perfils de dependència de temperatura per biomassa Anammox en forma granulada. (Activitat específica durant la primera injecció de substrat ●; Activitat específica durant la segona injecció de substrat ○; Model d'Arrhenius —; Model de Ratkowsky —).

Les principals conclusions extretes en aquest estudi es llisten a continuació:

- ✓ Un reactor SBR amb biomassa Anammox pot tractar aigües residuals amb elevat contingut en nitrogen (amb una relació $\text{N-NH}_4^+/\text{N-NO}_2^-$ de 1.0) a baixes temperatures (18°C).
- ✓ La dependència de l'activitat Anammox amb la temperatura es pot avaluar de manera ràpida i senzilla mitjançant els assajos de desnitrificació proposats per Dapena-Mora *et al.* (2007). En aquest treball, l'activitat màxima es va detectar a 40°C. A partir de 45 °C es va observar un descens de l'activitat Anammox i una transferència del citocrom des de la biomassa fins al medi líquid.
- ✓ L'estratègia emprada en un reactor Anammox ha d'assegurar una elevada retenció de fangs, especialment en treballar a baixes temperatures. En aquest treball, es van assolir TRC molt elevats mitjançant el tipus de biomassa emprat (en forma de biopel·lícula sobre una zeolita) i realitzant un període d'agitació sense alimentació d'aigua residual durant els darrers 30 minuts del cicle operatiu, afavorint d'aquesta manera l'exhauriment total de nitrit i la completa desorció de les bombolles de nitrogen gas.
- ✓ S'ha observat que l'estequiometria del procés Anammox depèn de manera molt pronunciada de la temperatura d'operació. A 30°C, la relació $\text{N-NO}_2^-/\text{N-NH}_4^+$ observada va ser 1,38, mentre que a 18 °C es va observar una relació $\text{N-NO}_2^-/\text{N-NH}_4^+$ de 1,04.

14.5 RECOMANACIONS

Per futures investigacions, es proposen les següents recomanacions:

Dispositius experimentals.

- Enregistrar en els reactors biològics lectures d'altres variables d'estat com el potencial redox o la conductivitat.
- En el respiròmetre tancat seqüencial, l'addició d'àcid o base es podria realitzar mitjançant bombes peristàltiques tot enregistant la quantitat de reactiu afegit.

Experiments de laboratori

- Per tal d'avaluar els perfils de N-NH_4^+ i N-NO_2^- durant el procés SHARON/Desnitricació, s'hauria de dur a terme el procés en un reactor de majors dimensions. D'aquesta manera, el cabal d'alimentació d'aigua residual seria major i, per tant, es podria fer un anàlisi intensiu de mostres i no només analitzar una mostra integrada com en aquest treball.
- El procés d'eliminació biològica via nitrit es podria dur a terme en reactors granulars, tal com descriuen Arrojo *et al.* (2004) o Vázquez-Padín *et al.* (2006). Aquest tipus de tractament resulta molt eficient, produeix poca biomassa i es minimitzen els temps de sedimentació.
- Es podria avaluar el tractament de sobrenedant de digestió anaeròbica de FORM o purins de porc mitjançant un sistema combinat de nitrificació parcial i Anammox.
- Altres tractaments d'eliminació biològica de nitrogen, alternatius als proposats en aquest treball, com la desnitricació autotròfica amb sulfid, el procés CANON o el procés BABE, podrien ser analitzats a escala de laboratori.

Modelització de tractaments biològics

- En aquest treball, l'activitat màxima de cada població bacteriana s'ha mesurat mitjançant la combinació de paràmetres μX . Caldria trobar alguna metodologia per tal de poder separar aquests dos paràmetres del model, de manera que es pugui tenir més informació dels sistemes biològics estudiats.
- Recentment han aparegut treballs (De Gracia *et al.*, 2006; Magrí *et al.*, 2007) en els quals el pH s'introdueix en el model de fangs actius com una variable d'estat. Aquest fet simplifica molt la programació del model i, per tant, seria convenient aplicar-ho al model proposat en aquest treball.
- La desnitrificació s'ha modelitzat considerant la conversió de nitrat a nitrit i d'aquest a N_2 gas. Tot i així, existeixen altres intermedis de la reacció que podrien produir-se (NO, N_2O). Podria resultar interessant investigar les causes que poden conduir a la formació de NO o N_2O enlloc de nitrogen gas.

14.6 REFERÈNCIES

- Abeling, U., Seyfried, C.F. (1992). Anaerobic-aerobic treatment of high-strength ammonium wastewater - nitrogen removal via nitrite. *Wat. Sci. Tech.*, 26, 1007– 1015.
- Anthonisen, A.C., Loehr, R.C., Prakasam, T.B.S., Srinath, E.G. (1976). Inhibition of nitrification by ammonia and nitrous acid. *Journal WPCF*, 48, 835-852.
- APHA (1998). Standard methods for the examination of water and wastewater, 20th edn, *American Public Health Association*, Washington DC, USA.
- Arrojo, B., Mosquera-Corral, A., Garrido, J.M., Méndez, R. (2004). Aerobic granulation with industrial wastewater in sequencing batch reactors. *Wat. Res.*, 38, 3389-3399.
- Dapena-Mora, A., (2007). Wastewater treatment by anammox process: A short-circuit in the natural nitrogen cycle. PhD. *University of Santiago de Compostela (USC)*, Spain.
- Dapena-Mora, A., Fernández, I., Campos, J.L., Mosquera-Corral, A., Méndez, R., Jetten, M.S.M. (2007). Evaluation of activity and inhibition effects on Anammox process by batch tests based on the nitrogen gas production. *Enzyme and Microbial Technology*, 40 (4), 859-865.
- De Gracia, M., Sancho, L., García-Heras, J.L., Vanrolleghem, P., Ayesa, E. (2006) Mass and charge conservation check in dynamic models: Application to the new ADM1 model. *Wat. Sci. Tech.*, 53(1) 225-334.
- Fernández, I., Vázquez-Padín, J.R., Mosquera-Corral, A., Campos, J.L., Méndez, R. (2006). Biofilm and granular systems to improve Anammox biomass retention, 7th *IWA Specialty Conference on Small Water and Wastewater Systems*, Mexico City, Mexico.
- Flotats, X. (2000) La digestió anaeròbica com a alternativa de tractament o com a procés previ al compostatge. Quarta Jornada Tècnica sobre la gestió de residus municipals. *Universitat Politècnica de Catalunya*.
- Fux, C., Boehler, M., Huber, P., Brunner, I., Siegrist, H. (2002). Biological treatment of ammonium-rich wastewater by partial nitrification and subsequent anaerobic ammonium oxidation (anammox) in a pilot plant. *Journal of Biotechnology*, 99, 295-306.
- Grunditz, C., Dalhammar, G. (2001) Development of nitrification inhibition assays using pure cultures of *Nitrosomonas* and *Nitrobacter*. *Wat. Res.*, 35(2), 433-440.
- Gutiérrez O. (2003) Identificació de paràmetres cinètics i estequiòmètrics del procés de depuració de fangs actius mitjançant tècniques respiromètriques. PhD Thesis. *Universitat de Girona*. Spain.
- Hellinga, C., Van Loosdrecht, M.C.M., Heijnen, J.J. (1999). Model based design of a novel process for Nitrogen Removal from concentrated flows *Mathematical and Computer Modeling of Dynamical Systems* 5(4), 351-371.
- Henze, M., Gujer, W., Mino, T., van Loosdrecht, MCM (2000) Activated Sludge Models ASM1, ASM2, ASM2d and ASM3. *IWA Publishing*, London.
- Hunik, J.H. (1993) Engineering aspects of nitrification with immobilised cells. PhD Thesis, *Wageningen Agricultural University*.
- Jetten M.S.M. (1999). New pathways for ammonia conversion in soil and aquatic systems. *Plant & Soil*, 230, 9-19.

- Magrí, A., Corominas, Ll., López, H., Campos, E., Balaguer, M.D., Colprim, J., Flotats, X. (2007). A Model for the simulation of the SHARON process: pH as a key factor, *Environmental Technology*, 28, 255-265.
- Marsili-Libelli, S., Tabani, F., (2002). Accuracy analysis of a respirometer for activated sludge dynamic modelling. *Wat. Res.*, 36, 1181-1192.
- Metcalf & Eddy, (1991). Wastewater engineering: treatment, disposal and reuse. *McGraw-Hill International Editions, USA*.
- Mosquera-Corral, A., González, F., Campos, J.L., Méndez, R. (2005). Partial nitrification in a SHARON reactor in the presence of salts and organic carbon compounds. *Process Biochemistry*. 40 (9), 3109-3118.
- Orhon, D., Artan, N. (1994). Modelling of activated sludge systems. *Technomic Publishing Co., Inc.*, Pennsylvania, USA. (pp. 397-469)
- Orhon, D., Sözen, S., Artan, N. (1996) The effect of heterotrophic yield on the assessment of the correction factor for anoxic growth. *Wat. Sci. Tech.* 34(5-6), 67-74.
- Rysgaard, S., Glud, R. N., Risgaard-Petersen, N., Dalsgaard T. (2004) Denitrification and anammox activity in Arctic marine sediments. *Limnology and oceanography*, 49 (5), 1493-1502.
- Serralta, J., Ferrer, J., Borrás, L., Seco, A. (2004) An extension of ASM2d including pH calculation. *Wat. Res.* 38. 4029-4038.
- Spanjers, H., Vanrolleghem, P.A., Olsson, G., Dold, P.L. (1998). Respirometry in control of the activated sludge process: principles. *IAWQ Scientific and Technical Report No. 7*, London, UK pp. 1-12.
- STOWA (1996) One reactor system for ammonia removal via nitrite, *Report no 96-01*. STOWA, Utrecht, The Netherlands. ISBN 90 74476 39 2
- Strous M., Kuenen J.G., Jetten, M.S.M. (1999). Key physiology of Anaerobic Ammonium Oxidation. *Applied and Environmental Microbiology*, 65(7), 3248-3250.
- Van de Graaf A.A., de Bruijn P., Robertson L.A., Jetten M.S.M., Kuenen J.G. (1996). Autotrophic growth of anaerobic ammonium-oxidizing micro-organisms in a fluidized bed reactor. *Microbiology (UK)*, 142, 2187-2196.
- Van Loosdrecht M.C.M., Salem S. (2006). Biological Treatment of sludge digester liquids. *Wat. Sci. Tech.*, 53(12), 11-20.
- Van Dongen U., Jetten M.S.M., Van Loosdrecht M.C.M. (2001). The SHARON-ANAMMOX process for treatment of ammonium rich wastewater. *Wat. Sci. Tech.*, 44 (1), 153-160.
- Vázquez-Padín J.R., Figueroa M., Arrojo B., Mosquera-Corral A., Campos J.L., Méndez R. (2006). Why do nitrifying granules accumulate nitrite? *Proceedings of the 2nd Aerobic Granular Sludge Workshop*, Delft, The Netherlands.
- Wett, B., Rauch, W. (2003). The role of inorganic carbon limitation in biological nitrogen removal of extremely ammonia concentrated wastewater. *Wat. Res.*, 37, 1100 – 1110.

NOMENCLATURA.

SIMBOL O ACRÒNIM	DESCRIPCIÓ	UNITATS
A/D	Analògic / Digital	(-)
Anammox	Anaerobic Ammonium Oxidation	(-)
AOB	Biomassa amonioxidant	(-)
ASM	Activated Sludge Model	(-)
BABE	Biological Augmentation Batch Enhanced	(-)
CANON	Completely Autotrophic Nitrogen Removal Over Nitrite	(-)
DA	Digestió anaeròbica	(-)
D/A	Digital / Analògic	(-)
DBO	Demanda biològica d'Oxigen	(mg DBO L ⁻¹)
DQO	Demanda Química d'Oxigen	(mg DQO L ⁻¹)
EDAR	Estació Depuradora d'Aigües Residuals	(-)
FORM	Fracció Orgànica de Residus Municipals	(-)
IWA	International Water Association	(-)
K _{NH}	Constant d'afinitat per N-NH ₄ ⁺ dels bacteris nitrificants	(mg N-NH ₄ ⁺ L ⁻¹)
K _{NO}	Constant d'afinitat per N-NO _x ⁻ dels bacteris desnitrificants	(mg N-NO _x ⁻ L ⁻¹)
K _{OH}	Constant d'inhibició per OD dels bacteris desnitrificants	(mg O ₂ L ⁻¹)
K _{O,A}	Constant d'afinitat per l'OD dels bacteris nitrificants	(mg O ₂ L ⁻¹)
K _S	Constant d'afinitat per la DQO fàcilment biodegradable	(mg DQO L ⁻¹)
μ	Constant màxima específica de creixement de bacteris	(dia ⁻¹)
μ _{m,A}	Constant màxima específica de creixement de nitrificants	(dia ⁻¹)
μ _{m,H,DN}	Constant màxima específica de creixement de desnitrificants	(dia ⁻¹)
NOB	Biomassa nitritoxidant	(-)
OD	Oxigen dissolt	(-)
OUR	Taxa de consum d'oxigen	(mg O ₂ (L min) ⁻¹)
r _{X,A}	Taxa de creixement de bacteris nitrificants	(mg DQO (L dia) ⁻¹)
r _{X,DN}	Taxa de creixement de bacteris desnitrificants	(mg DQO (L dia) ⁻¹)
S _{NH}	Concentració de nitrogen amoniacal	(mg N-NH ₄ ⁺ L ⁻¹)
S _{NO}	Concentració de nitrogen nitrit o nitrat	(mg N-NO _x ⁻ L ⁻¹)
S _O	Concentració d'oxigen dissolt	(mg O ₂ L ⁻¹)
S _S	Concentració de DQO fàcilment biodegradable	(mg DQO L ⁻¹)
SS	Sòlids Suspesos	(mg SS L ⁻¹)
SSV	Sòlids Suspesos Volàtils	(mg SSV L ⁻¹)

SIMBOL O ACRÒNIM	DESCRIPCIÓ	UNITATS
ST	Sòlids Totals	(mg ST L ⁻¹)
STV	Sòlids Totals Volàtils	(mg STV L ⁻¹)
TRC	Temps de retenció cel·lular	(dies)
TRH	Temps de retenció hidràulic	(dies)
X	Concentració de biomassa activa	(mg DQO L ⁻¹)
X _{BA}	Concentració de biomassa activa nitrificant	(mg DQO L ⁻¹)
X _{BH,DN}	Concentració de biomassa activa desnitrificant	(mg DQO L ⁻¹)